PROGRAM SUMMARY

Task A1

In 1994 we will focus on data acquisition and analysis of run 1b of the DØ detector, which is expected to yield about 70 pb^{-1} of data. Our special projects will be: (i) the search for top quark pairs decaying to dileptons and (ii) the measurement of the magnetic moment of the W-boson through the study of $W\gamma$ production. The coming three years will see an expanding effort on campus in the development of silicon microstrip trackers for the DØ detector upgrade and for SDC at SSC.

Task A2

Experimental tests of the electroweak theory with the OPAL experiment at LEP will continue to be the main effort of Task A2. The OPAL Collaboration, with a data sample of over one million Z decays, has published papers on a wide range of topics, particularly studies of Z resonance parameters, QCD effect, and particle searches. By the end of 1994, with five times the statistics, we will be able to carry out tests of the Standard Model with unprecedented precision. The exploitation of physics at energies above the W boson pair production threshold will begin in the latter part of 1995. The RD5 experiment at the SPS, in which we also participate, provides technical inputs for the design of detector elements for CMS at LHC.

High Energy Physics
at
UC Riverside

High Energy Physics at UC Riverside

Table of Contents

I. Physics Research

Task A1

1. Task A1 : Hadron Collider Physics

Contents

1.1 Task A1 : Overview/Personnel/Talks/Publications

1.1.1 Task A1 : Overview

The DØ detector moved into the Tevatron ring in February 1992. Detector commissioning was successfully completed during the May–July Tevatron engineering run. During the subsequent run (Run 1a) from August '92 to May '93, a total of 16.7 pb^{-1} data was recorded. An integrated luminosity in the range 60–80 pb^{-1} is projected for Run 1b, scheduled to begin November 1993. In the coming three years, we will concentrate on the analysis of DØ data and on designing and building a Silicon Tracker for the DØ detector upgrade. We will also, in parallel, carry out R&D for the SDC Silicon Tracker. (In this proposal we are assuming continuation of the SSC project.)

UC Riverside joined the DØ Collaboration in fall 1986. Our contributions to the present detector include design and implementation of the DØ high voltage system and the Level 1 muon trigger and we have also been active in the areas of online and offline software for the muon system. Our emphasis has now shifted to data analysis. Professor S. Wimpenny, who has been on-site at Fermilab since June 1992, is leading the DØ team which is seeking evidence of top quark production via decay into the dilepton channels. He has developed the analysis strategy and the software package for this project. While Wimpenny concentrates on the e–μ channel, graduate student R. Hall is analyzing the dimuon channel as his Ph.D. thesis research. Postdoctoral researcher K. Bazizi, who led the team which developed the Level 1 muon trigger, is now coordinating the analysis of inclusive muon production. As part of this effort, graduate student T. Huehn is studying events recorded with a muon-jet trigger, in order to measure the b-quark production cross-section. Professor J. Ellison has played a leading role in initiating the study of the trilinear vector boson couplings using DØ data. Together with postdoctoral researcher B. Choudhary, he is responsible for the analysis of $W\gamma$ production in the $W \rightarrow \mu\nu$ channel. Invited talks on the top quark search and the b-quark cross-section have been presented by Wimpenny, Bazizi and Choudhary in recent months (see section 1.1.3).

Over the last four years, our group has developed a well-equipped silicon detector facility at UCR. The initial planning for a Silicon Tracker for the DØ detector upgrade was done jointly by Fermilab, LBL and UCR. As described in section 1.2.7, we continue to lead in many aspects of design, prototyping and project management. In particular, we have sole responsibility for the novel double-sided wedge detectors. This activity is the responsibility of J. Ellison, research faculty A. Heinson, and postdoctoral researcher C. Boswell. A. Heinson gave an invited presentation on the DØ Silicon Tracker at the 1992 DPF meeting and J. Ellison was invited to talk on the wedge detectors at the International Symposium on Semiconductor Tracking at Hiroshima, Japan in May 1993.

J. Ellison is also leading the UCR effort on the SDC Silicon Tracker which is concentrated in three areas: (a) radiation damage studies, (b) design of an automated laser module tester and (c) wedge detector R&D for the forward silicon disks. We recently received funding of $90K per year from the Texas National Research Commission Laboratory to recruit two postdoctoral researchers for this program.

Current personnel are listed in section 1.1.2. These include: three faculty, Ellison, Kernan and Wimpenny, one research faculty, Heinson, five postdoctoral researchers and four graduate students. Three of the postdocs, Bazizi, Boswell and Choudhary, work on DØ, while Bischoff and Gill, who are supported by TNRCL, work on SDC. Bazizi will be replaced at the end of 1993. During 1994, we plan to have two postdocs, Bazizi's replacement and Choudhary, on site at Fermilab along with two graduate students. S. Wimpenny will also spend the spring and summer quarters continuously at Fermilab. Work on the DØ and SDC Silicon Trackers will be based at UCR.

J. Ellison was named a DOE Junior Investigator in Spring 1993. The funds awarded are being used for equipment and student support. A. Kernan joined the URA Board of Overseers of SSC in April 1993. A. Heinson was recently appointed as a member of the DØ search committee to select a successor to spokesperson P. Grannis.

The increase in the 1994/95 budget over the preceding year reflects:

(i) an increase in the indirect cost rate from 21% to 25.4%,

(ii) mandatory increases in salary and benefits for graduate students,

(iii) equipment/computer needs, in particular for the DØ silicon tracker,

(iv) general support for the two additional postdoctoral researchers (Bischoff, Gill) whose salaries are provided by TNRCL.

University contributions to this project in academic year 1992/93 included fall and winter quarter salary for S. Wimpenny while on leave at Fermilab, and $25K in startup funds for J. Ellison. Ellison will receive two further installments of startup funds: $125K and $50K in academic years 93/94 and 94/95 respectively. In addition, the university will pay Ellison's summer salary in 1994. The startup funds are being used primarily to expand and upgrade our infrastructure for silicon microstrip R&D. The university is also providing approximately $3K annually for miscellaneous expenses.

The performance of the DØ detector in 1993 surpassed all expectations. We look forward to a very exciting year in 1994 with the possibility of finally sighting the elusive top quark.

1.1.2 Task A1 : Personnel (as of Sept. 1993)

Faculty

John Ellison	Assistant Professor	DØ	SDC
Anne Kernan	Professor	DØ	
Stephen Wimpenny	Associate Professor	DØ	SDC

Research Faculty

Ann Heinson	Assistant Research Physicist	DØ	SDC

Postdoctoral Researchers

Kamel Bazizi	Postgraduate Researcher	DØ	
Andreas Bischoff	Postgraduate Researcher		SDC
Christopher Boswell	Postgraduate Researcher	DØ	
Brajesh Choudhary	Postgraduate Researcher	DØ	
Karl Gill	Postgraduate Researcher		SDC

Graduate Students

Raymond Hall	DØ	
Thorsten Huehn	DØ	
Armik Khachatourian	DØ	
Yungryel Ryu	DØ	

Undergraduate Students

Douglas Chapin	DØ	SDC
Patrick Gartung	DØ	SDC
Martin Mason	DØ	SDC

1.1.3 Task A1 : Invited and Contributed Talks, 8/92 – 8/93

Invited Talks

1. "Double Pomeron Exchange in $p\bar{p}$ Interactions at 0.63 TeV",
   A. Kernan,
   Workshop on Small-x and Diffractive Physics at the Tevatron, Fermilab, Sept. 1992.

2. "Inclusive Single Muons at DØ",
   K. Bazizi,
   APS, Division of Particles and Fields Meeting, Fermilab, November 1992.

3. "The DØ Upgrade Silicon Tracker",
   A.P. Heinson,
   APS, Division of Particles and Fields Meeting, Fermilab, November 1992.

4. "Status of Top Search at DØ",
   S.J. Wimpenny,
   Aspen Winter Conference, January 1993.

5. "A Silicon Tracker for the DØ Detector",
   A.P. Heinson,
   High Energy Physics seminar, University of California, Los Angeles, February 1993.

6. "A Silicon Tracker for the DØ Detector",
   A.P. Heinson,
   High Energy Physics seminar, University of California, Irvine, February 1993.

7. "Flavors and Colors",
   B. Choudhary,
   High Energy Physics seminar, Institute of Physics, Bhubaneshwar, India, March 1993.

8. "QCD, Electroweak and Top Physics with DØ Detector at Fermilab",
   B. Choudhary,
   High Energy Physics seminar, Delhi University, India, March 1993.

9. "Silicon Microstrip Wedge Detectors for the DØ Silicon Tracker",
   J. Ellison,
   International Symposium on Development and Application of Semiconductor Tracking Detectors, Hiroshima, Japan, May 1993.

10. "The Search for the Top Quark at DØ",
    S.J. Wimpenny,
    High Energy Physics seminar, University of California, Los Angeles, May 1993.

11. "B Physics at DØ",
    K. Bazizi,
    Workshop on Physics at Current Accelerators and Supercolliders, Argonne National Lab, June 1993.

Task A1 : Invited Talks (continued)

12. "B Production at DØ",
B. Choudhary,
Workshop on B Physics at Hadron Colliders, Snowmass, June 1993.

13. "Measurement of Single Muon and J/ψ Cross Sections at DØ",
K. Bazizi,
International EuroPhysics Conference on High Energy Physics, Marseille, France, July 1993.

Contributed Talks, 8/92 – 8/93

1. "The Search for Top in the *ee* and $\mu\mu$ Channels at DØ",
R. Hall,
APS Annual Meeting, Washington, DC, April 1993.

2. "A Study of $p\bar{p} \rightarrow \mu\, jet + X$ at $\sqrt{S}$ = 1.8 TeV at DØ",
T. Huehn,
APS Annual Meeting, Washington, DC, April 1993.

1.1.4 Task A1 : Publications, 8/92 – 8/93

1. "Muoproduction of J/ψ and the Gluon Distribution of the Nucleon",
S.J. Wimpenny and the European Muon Collaboration, Z. Phys., **C56**, 21-28, (1992).

2. "A Comparison of CF_4 + Hydrocarbon Fast Gases for Drift Chambers and Straw Tubes",
A.P. Heinson and D. Rowe, Nucl. Instr. Meth. **A321**, 165-171 (1992).

3. "Temperature Effects on Radiation Damage to Silicon Detectors",
J. Ellison, J.K. Fleming, S. Jerger, D. Joyce, C. Lietzke, E. Reed, S.J. Wimpenny and members of the SDC Silicon Tracker group, Nucl. Instr. Meth. **A326**, 373-380 (1993).

4. "Beam Tests of the DØ Uranium Liquid Argon End Calorimeters",
K. Bazizi, J. Ellison, R. Hall, T. Huehn, A. Kernan, A. Klatchko, D. Smith, S.J. Wimpenny, J.-J. Yang and DØ Collaboration, Nucl. Instr. Meth. **A324**, 53-76 (1993).

5. "A Measurement of the Ratio of the Nucleon Structure Function in Copper and Deuterium",
S.J. Wimpenny and the European Muon Collaboration, Z. Phys. **C57**, 211-218 (1993).

6. "Double Pomeron Exchange Studies in $p\bar{p}$ Interactions at 0.63 TeV",
D. Joyce, A. Kernan, M. Lindgren, B.C. Shen, D. Smith, S.J. Wimpenny, M.G. Albrow, B. Denby, and G. Grayer, Phys. Rev. **D**, August 1993 (in press).

7. "The DØ Upgrade Silicon Tracker",
A.P. Heinson for the DØ Collaboration, Proceedings of the American Physical Society Division of Particles and Fields Meeting, November 1992, (World Scientific Publishing), Vol. 2, p. 1731–3 (1993).

8. "Inclusive Single Muons at DØ",
K. Bazizi for the DØ Collaboration, Proceedings of the American Physical Society Division of Particles and Fields Meeting, November 1992, (World Scientific Publishing), Vol .1, p. 750–2 (1993).

9. "Inclusive χ_c Production in $p\bar{p}$ Collisions at $\sqrt{S}$ = 1.8 TeV",
C. Boswell for the CDF Collaboration, Proceedings of the American Physical Society Division of Particles and Fields Meeting, November 1992, (World Scientific Publishing), Vol .1, p. 768–70 (1993).

10. "Improved Upper Limit on the Branching Ratio $B(K_L \rightarrow \mu\, e)$",
A.P. Heinson and BNL E791 Collaboration, Phys. Rev. Lett. **70**, No. 8 (1993).

11. "Temperature Dependence of Radiation Damage and its Annealing in Silicon Detectors",
J. Ellison, J.K. Fleming, S. Jerger, D. Joyce, C. Lietzke, E. Reed, S.J. Wimpenny, accepted for publication in IEEE Trans. Nucl. Sci., 1993.

12. "Study of Four-Jet Events and Evidence for Double Parton Interactions in $p\bar{p}$ Collisions at $\sqrt{S}$ = 1.8 TeV",
C. Boswell et al. (CDF Collaboration), Phys. Rev. **D47**, p4857, 1993.

Task A1 : Publications (continued)

13. "Measurement of the Cross-Section for the Production of Two Isolated Prompt Photons in $p\bar{p}$ Collisions at $\sqrt{S}$ = 1.8 TeV",
C. Boswell et al. (CDF Collaboration), Phys. Rev. Lett. **70**, p2232-6, 1993.

14. Search for $\Lambda_b \rightarrow J/\psi\ \Lambda_0$ in $p\bar{p}$ Collisions at $\sqrt{S}$ = 1.8 TeV",
C. Boswell et al. (CDF Collaboration), Phys. Rev. **D47**, p2639-43, 1993.

1.1.5 Task A1 : Technical Notes, 8/92 – 8/93

1. "The Muon Trigger "MTRG" Bank Description",
K. Bazizi, DØ Note 1451, UCR/DØ/92–06.

2. "Cosmic Rejection: Some Thoughts and Studies",
B. Choudhary, A. Klatchko, DØ Note 1505, UCR/DØ/92–07.

3. "Top Triggers",
R. Hall and 6 authors from the DØ Collaboration, DØ Note 1476, UCR/DØ/93–01.

4. "Using Muons Embeded in Jets for Calibration",
A. Klatchko (UC Riverside) and H. Xu (Brown Univ.), DØ Note 1541, UCR/DØ/93–02.

5. "The DØ Upgrade Silicon Tracker",
A.P. Heinson, for the DØ Collaboration, DØ Note 1542, UCR/DØ/93–03.

6. "Inclusive Single Muons at DØ",
K. Bazizi, for the DØ Collaboration, DØ Note 1539, UCR/DØ/93–04.

7. "$W \rightarrow \mu + \nu$ Study",
B. Choudhary, DØ Note 1590, UCR/DØ/93–05.

8. "Top Search Status at DØ",
S.J. Wimpenny, DØ Note 1609, UCR/DØ/93–06.

9. "Level 1.0 and Level 1.5 Muon Trigger Efficiencies for Single Tracks",
K. Bazizi, DØ Note 1618, UCR/DØ/93–07.

10. "The Top Leptons Analysis Package",
S.J. Wimpenny, DØ Note 1690, UCR/DØ/93–08.

11. "Description of the Muon Trigger Data in the TRGR Bank",
K. Bazizi, DØ Note 1587, UCR/DØ/93–10.

12. "Muon Trigger Words in the PMUO Bank",
K. Bazizi, DØ Note 1591, UCR/DØ/93–11.

13. "E823 (DØ Upgrade) $D\emptyset_\beta$",
The DØ Collaboration, DØ Note 1733.

1.2 DØ : Proton–Antiproton Interactions at 2 TeV

UC Riverside joined the DØ Collaboration in the fall of 1986. Since then, we have made substantial contributions to both the detector hardware and the data analysis. The hardware areas include design and implementation of the DØ high voltage system and Level 1 muon trigger system for the current detector, and the design of the Silicon Tracker for the upgraded detector. We are active in the areas of online and offline software for the muon system, and we are playing leading roles in the search for the top quark via its dilepton decay modes, in measuring the *b*-quark cross-section and in $WW\gamma$ analysis. The Riverside group has four to five physicists stationed at Fermilab.

1.2.1 The DØ Detector

The DØ detector is one of two large experiments at the Fermilab Tevatron Collider. Its non-magnetic design is complementary to the older CDF detector and is optimized for charged lepton and jet identification over most of the 4π solid angle [1]. Figure 1 shows a schematic of the detector and its three principal components: the inner tracking system, the three calorimeters and the muon system.

The inner tracking system, shown in Figure 2, consists of four drift chamber sections. These are the vertex chamber (VTX) which surrounds the beam pipe, the central drift chamber (CDC) which provides tracking in the central region and two packages of forward drift chambers (FDC), one at each end of the tracking region. The chambers together cover the pseudorapidity range $|\eta| < 3.1$ and give resolutions ~ 2 mm along the beam (z) axis and 60, 180 and 200 μm in the transverse plane for the VTX, CDC and FDC respectively. In addition to the position information, each detector provides dE/dx measurements for particle identification. This is supplemented by the Transition Radiation Detector (TRD) which covers the central region and lies between the VTX and CDC chambers.

The tracking system is surrounded by three uranium–liquid argon calorimeters (Central Calorimeter (CC), End Cap North (ECN), End Cap South (ECS)), shown in Figure 3. The calorimeters combine to cover the pseudorapidity interval out to 4.2. The calorimetry is compensating, with an electron–hadron response close to unity and a linearity of better than 0.5% [2]. The measured energy resolution is $0.003 \oplus 15\% /\sqrt{E}$ for electrons and $0.04 \oplus 50\% /\sqrt{E}$ for hadrons, for all the calorimeter modules. The mechanical structure of the calorimeters is uniform over the full rapidity range, with up to 9 depth samplings (4 electromagnetic + 5 hadronic) and a

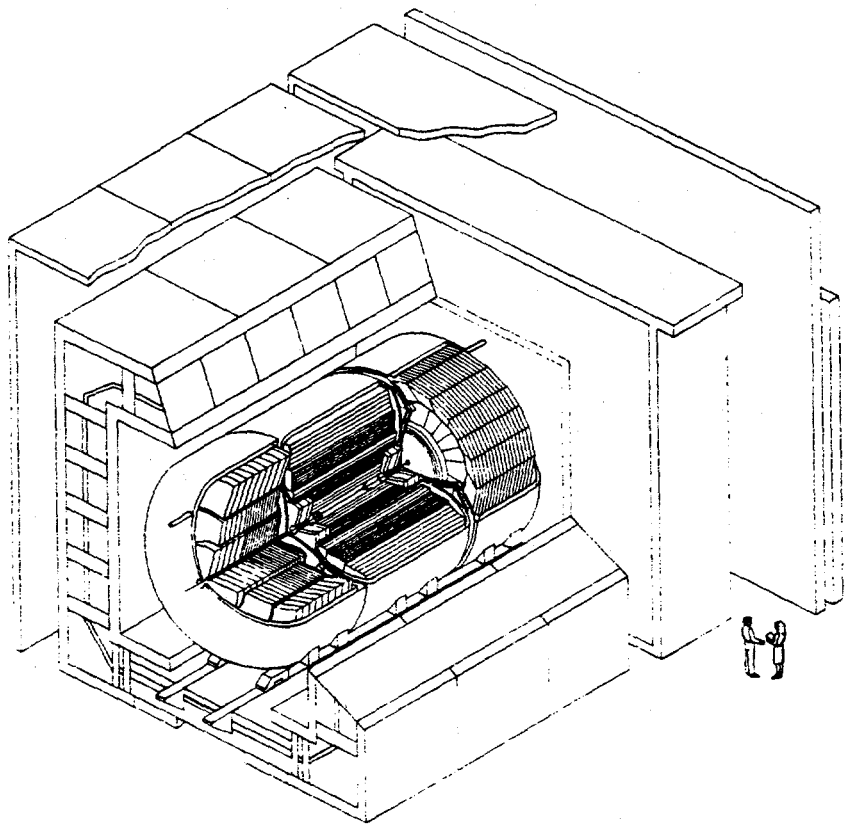

Fig. 1 The DØ Detector, showing the tracking system, calorimeters and outer muon system.

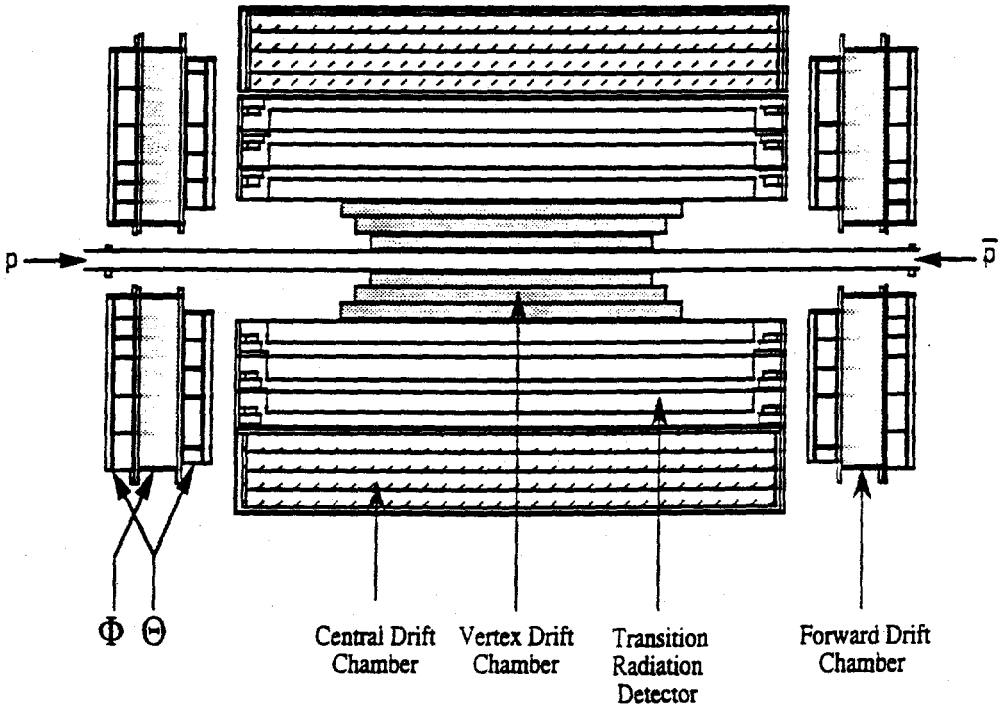

Fig. 2 A close-up of the DØ tracking system, showing the vertex detector, transition radiation detector, central drift chamber and forward drift chambers.

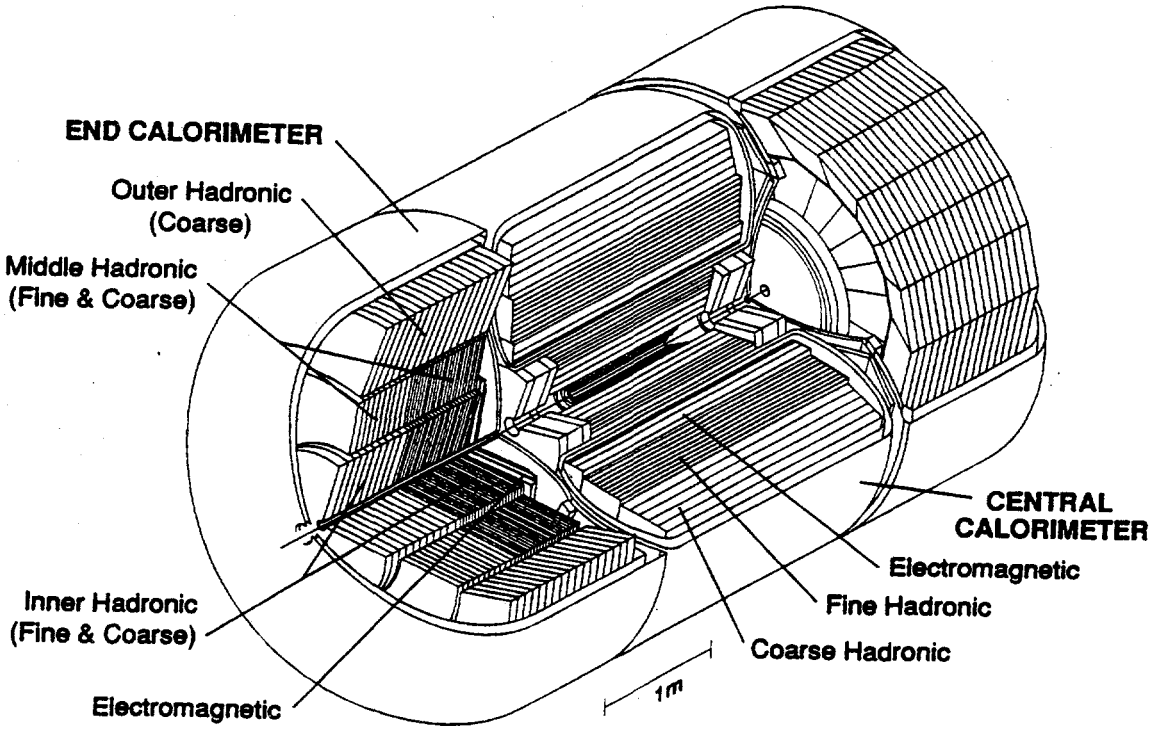

Fig. 3 A close-up of the DØ calorimeters, showing the central calorimeter, and two end caps. Each module is divided into an inner electromagnetic region, and outer fine and coarse hadronic regions.

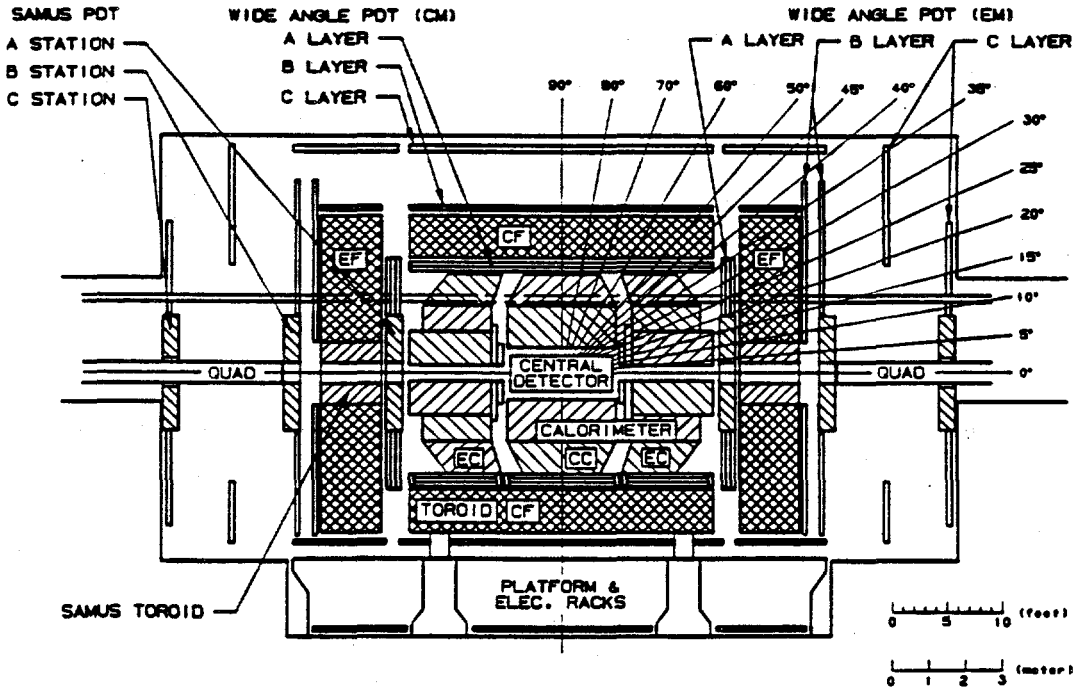

Fig. 4 The DØ muon system, showing the central and endcap toroids (CF, EF), the three layers of proportional drift tubes (PDT layers A, B and C), and the small angle muon system very close to the beamline.

lateral segmentation of 0.1×0.1 in $\Delta\eta \times \Delta\phi$ (with 0.05×0.05 at the electromagnetic shower maximum).

The outer part of the detector is the muon system, which consists of a 156 module, wide angle spectrometer (WAMUS) and two 9 module small angle spectrometers (SAMUS), shown in Figure 4. The WAMUS and SAMUS detectors provide between 10 and 16 measurement points along muon trajectories, down to 3° to the beam axis ($|\eta| = 3.64$). These two systems of chambers, combined with five 2 T toriodal magnets, provide a momentum resolution of ~ 30% for muons with momentum up to 40 GeV/c. The iron in the toroids, combined with the material of the calorimeter, provide between 13 and 18 interaction lengths over the full detector coverage. The probability of hadronic punchthrough is therefore ~ 10^{-5}.

The completed DØ detector was moved into the Tevatron ring on February 14th 1992 and first collisions were observed shortly after the collider turn-on on May 12th. Detector commissioning was successfully completed during theTevatron engineering run between May 12th and July 20th and the detector was fully operational at the start of Collider Run 1a on 21st August. Data-taking continued steadily through the run and by time the machine was turned off at the end of May 1993, 16.7 pb^{-1} of data had been recorded.

(a) *References*

1 S. Abachi et al., (DØ Collaboration), "The DØ Detector", submitted to Nucl. Inst. Meth., July 1993, Fermilab PUB 93/179.
S. Aronson et al., (DØ Collaboration), "The DØ Experiment at the Fermilab Antiproton-Proton Collider", DØ Design Report (1984).

2 M. Abolins et al., (DØ Collaboration), "Hadron and Electron Response of Uranium Liquid Argon Calorimeter Modules for the DØ Detector", Nucl. Inst. Meth. A280, 36 (1989).

1.2.2 Search for the Top Quark in the Dilepton Channels

One of the primary objectives for DØ is the search for the top quark and study of its properties. The CDF Collaboration has established that the top quark mass exceeds 91 GeV/c^2 [1], while theoretical considerations set an upper bound of around 220 GeV/c^2 [2]. Therefore, with such a high mass, a standard model top quark will decay via a real W boson and a b-quark:

$$\begin{aligned} t \;&\rightarrow\; W + b \\ &\quad\;\; | \\ &\rightarrow\; l + \nu \qquad (l = e,\, \mu,\, \tau) \\ &\rightarrow\; q + \bar{q} \end{aligned}$$

The final states of a $t\bar{t}$ decay will be characterized by multiple leptons and/or jets with a large amount of missing energy. DØ is ideally suited for such studies, since it is hermetic and has precise and uniform muon, electron and jet capabilities covering almost 4π of the solid angle.

To date, no group has been able to reliably tag W boson decays into quark final states. The W decay to $\tau\,\nu$ has been observed, but is difficult to tag with high efficiency. Therefore, the most promising lepton plus neutrino decays are $e\nu$ and $\mu\nu$. A $\bar{t}t$ event can be tagged using either one or both of the daughter W decays into a high transverse momentum (P_T) electron or muon, and missing energy. The primary signatures are:

- two high P_T leptons ($e^+ e^-$, $\mu^+ \mu^-$, $e^+\mu^-$, $e^- \mu^+$), missing energy and jets
- one high P_T lepton (e or μ), missing energy and jets

Each channel has a different admixture of conventional backgrounds, so to establish a top quark discovery, it is necessary to understand each of these in detail and to find a signal in at least two decay channels.

(a) *The UCR Role in the Top Analysis*

The UC Riverside group has concentrated its efforts on the dilepton decay modes, and is playing a major role in the data analysis. S.J.Wimpenny, is leading the DØ team of about 12 people working on dilepton channels and has been responsible for the development of the analysis strategy and the design and implementation of a software package [3] used for most of the data analysis. In addition, while Wimpenny has concentrated on the e–μ channel, graduate

student R.Hall has been responsible for the analysis of the dimuon channel, and this will constitute his PhD thesis.

Preliminary results based on data from the first half of Run 1a (7.5 pb^{-1}) have been presented at Aspen [4], Moriond [5], Washington [6], McGill [7] and Marseille [8]. Analysis of the full Run 1a dataset of 16 pb^{-1} is well advanced and results will be available soon. An initial paper, based on the e–μ and e–e analyses, is in preparation. An overview of the preliminary results from the dilepton channels is given here.

(b) *Event Selection*

From the data collected between September 1992 and March 1993, all events were selected which contain at least two isolated lepton candidates with $P_T > 15$ GeV/c. The integrated luminosities and remaining event samples are:

	$\mu\,\mu$	$e\,e$	$e\,\mu$
$L\,dt$ [pb^{-1}]	7.7	7.2	7.5
Events	29	1159	27

The dielectron channel contains a substantial background from Z^0 decays, as shown in Figure 5. The dimuon channel does not, since the $Z^0 \rightarrow \mu\,\mu$ background is heavily suppressed at the trigger level by the use of online jet and missing energy cuts [6].

Dimuon Channel

For the top search in the dimuon channel, we require that the opening angle between the muons in the transverve plane $\phi < 160°$, to suppress residual $Z^0 \rightarrow \mu\,\mu$ and $Z^0 \rightarrow \tau\,\tau \rightarrow \mu\,\mu$ decays, leaving 9 events. With the additional requirement of two hadronic jets of transverse energy $E_T > 12.5$ and 10 GeV, the data sample reduces to 2 events. To compute the expected background and signal yield, we have used the ISAJET event generator [9] and the GEANT detector simulation package [10]. For the current set of selection cuts, we expect 2.6 ± 1.0 background events, mainly from Z^0 decays, and 0.27 ± 0.08 events from top with a mass of 120 GeV/c^2. Given the current sensitivity, it is not possible to conclude anything other than that the observed number of events and predicted yields from background processes are in good agreement. Ongoing studies of the use of cuts on missing energy and muon pair transverse momentum will significantly increase the sensitivity to top events and will permit the use of less restrictive trigger conditions.

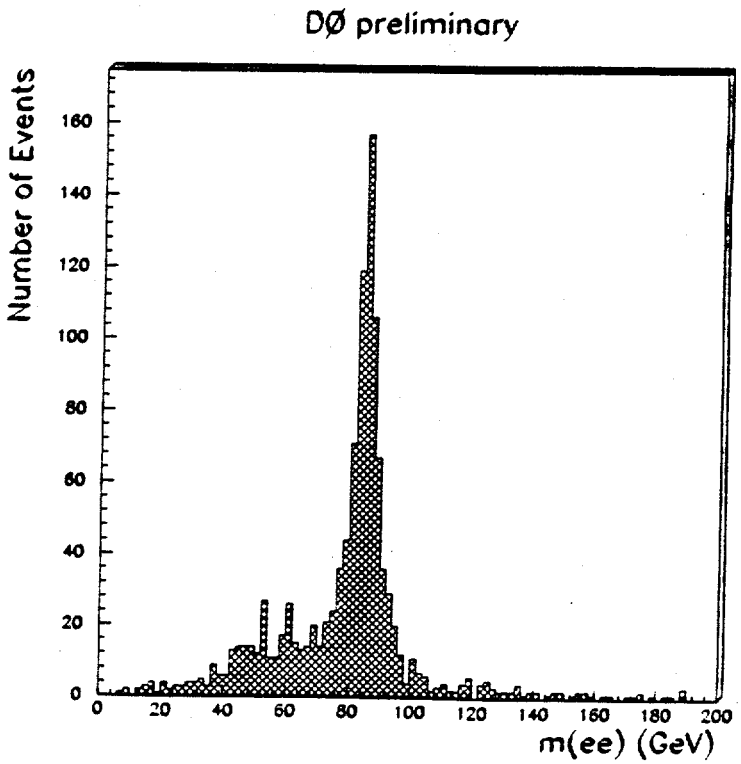

Fig. 5 Dielectron event sample, after preliminary selection cuts. Some electrons from $Z^0 \rightarrow e\ e$ are still present.

Dielectron Channel

Starting with the 1159 event dielectron sample, the next step in the search is to apply the two jet cut described above. Figure 6 shows the resulting dielectron pair missing energy versus invariant mass for (a) data and (b) $t\bar{t} \rightarrow e\ e$ Monte Carlo events with $M_{top} = 140\ GeV/c^2$. The Monte Carlo events correspond to an integrated luminosity of 2660 pb^{-1}. There is still a clear enhancement in the data in the region of the Z^0 mass. This is removed by rejecting events within $\pm$ 14 GeV/c^2 of the Z^0 mass peak. Lastly, to discriminate against $Z^0 \rightarrow \tau\ \tau$, *WW*, Drell Yan and QCD backgrounds, we require that the missing energy be greater than 20 GeV. No events survive these selection criteria.

Electron–Muon Channel

The e–μ channel is essentially free from the large Drell-Yan backgrounds which affect the e–e and μ–μ channels. In order to suppress backgrounds due to radiative $W \rightarrow \mu\ \nu$ and $Z^0 \rightarrow \mu\ \mu$, we require that the minimum separation between the electron and muon tracks be at least 0.25 in ΔR, where $\Delta R = ((\Delta\phi)^2 + (\Delta\eta)^2\ )^{1/2}$. In Figure 7, we compare the muon P_T versus the electron E_T for (a) surviving events and (b) $t\bar{t} \rightarrow e\ \mu$ Monte Carlo events, subject to the same cuts. The Monte Carlo sample corresponds to an integrated luminsity of 1184 pb^{-1}. As with the dielectron analysis, we then apply cuts of 20 GeV on the missing energy and require at least two jets with $E_T >$ 12.5 and 10 GeV, to suppress residual $Z^0 \rightarrow \tau\ \tau$, *WW* and QCD backgrounds. One event survives the selection criteria in this channel.

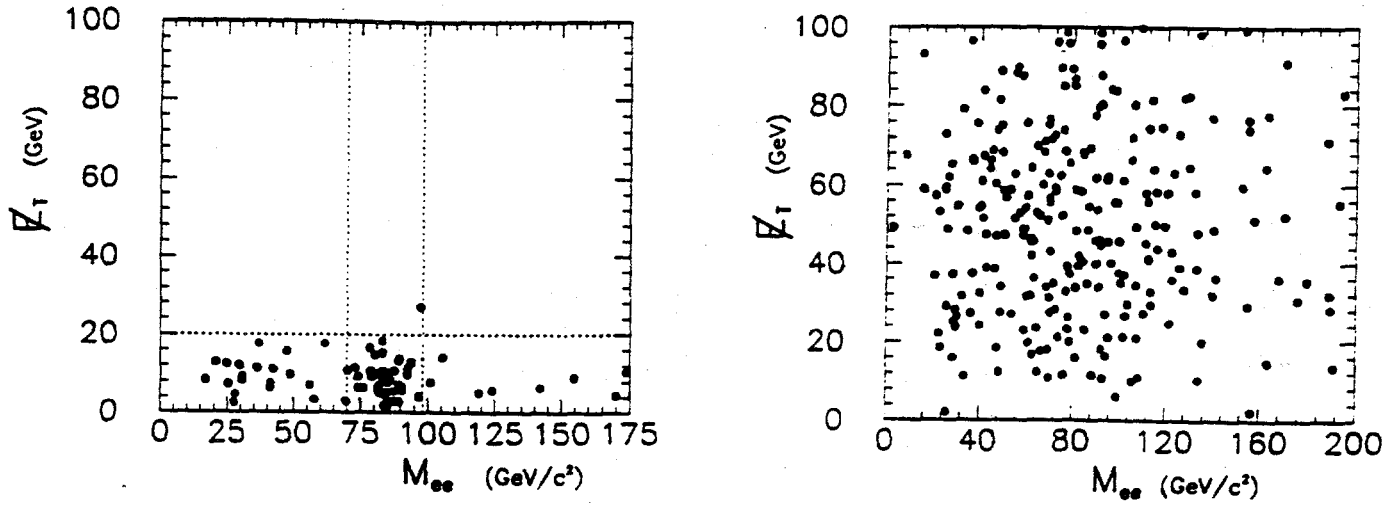

Fig. 6 Missing energy versus invariant mass for (a) the dielectron event sample, and (b) $t\bar{t} \rightarrow e\,e$ Monte Carlo events with M_{top} = 140 GeV/c^2. The dotted lines in plot (a) show the cuts for minimum missing energy required, and for eliminating electrons from Z^0 decays.

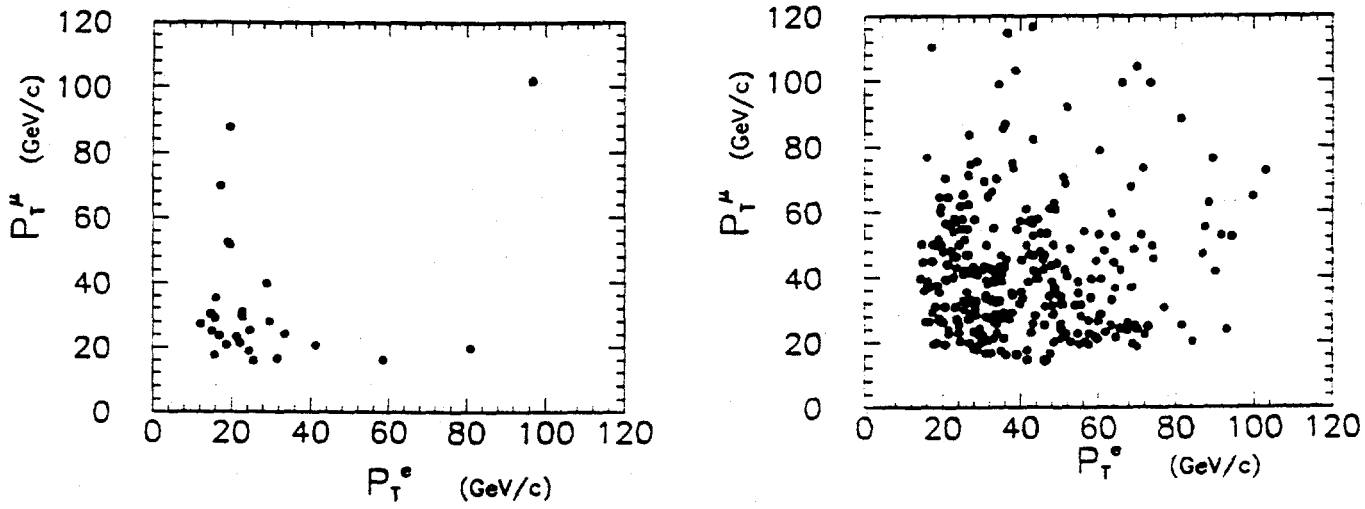

Fig. 7 Muon transverse momentum versus electron transverse energy for (a) the e–μ event sample, and (b) $t\bar{t} \rightarrow e\,\mu$ Monte Carlo events with M_{top} = 140 GeV/c^2.

(c) *Acceptance Calculations*

In order to determine the acceptance for the signal from top decays in the e–e and e–μ analyses, we have generated $t\,\bar{t} \rightarrow e\,e$ and $t\,\bar{t} \rightarrow e\,\mu$ events at five different top masses, M_{top} = 80, 100, 120, 140 and 160 GeV/c^2, using the ISAJET generator and full GEANT detector simulation. These events were then processed through a simulation of the online trigger and were fully reconstructed. Using the cuts described above, we find an acceptance which varies between 11% (9%) and 33% (27%) as M_{top} varies from 80 to 160 GeV/c^2 for the e–e (e–μ) analyses. We estimate the systematic uncertainty on these numbers to be 15% (23%) for the e–e (e–μ) channels. Combining this with the top production cross-section calculations of Berends, Tausk and Giele [11] leads to an estimated signal yield of between 3.7 (6.1) and 0.5 (1.0) events over the same M_{top} range for the e–e (e–μ) channels.

(d) *Background Studies*

We have studied the backgrounds to the e–e and e–μ channels from QCD multijets, $Z^0 \rightarrow e\,e$, $Z^0 \rightarrow \tau\,\tau$, $Z^0 \rightarrow b\bar{b}$, $Z^0 \rightarrow c\bar{c}$, $W + jets$, WW, WZ and radiative $W \rightarrow \mu\,\nu$ and $Z^0 \rightarrow \mu\,\mu$ decays using Monte Carlo events generated with ISAJET and processed through full detector simulation. Additionally, we have also considered the instrumental backgrounds which result from particle mismeasurement and/or misidentification. We have studied backgrounds which result from mismeasured missing energy, from in-flight π / $K \rightarrow \mu$ decays, from cosmic rays and from fake electrons from charged and neutral pion overlaps. Combining the direct and instrumental background calculations gives a total background estimate of 0.22 (0.65) events for the e–e (e–μ) channels, where the dominant contributions come from QCD and $W + jet$ backgrounds.

(e) *Top Quark Mass Limit*

Combining the acceptance for $t\bar{t}$ events with the observed event in the e–μ channel, provides an upper limit on the top production cross-section at the 95% confidence level, as shown in Figure 8. When combined with the cross-section of reference [11], this leads to a lower limit on M_{top} of 103 GeV/c^2 with background subtraction, and 99 GeV/c^2 when the conservative assumption of no background is made.

The $e-\mu$ event which passes all the event selection criteria merits further discussion. Both leptons are well isolated with E_T (e) = 96.9 ± 2.0 GeV, P_T (μ) = 110 GeV/c (> 43 GeV/c at the 90% C.L.). Though the uncertainty in the muon momentum is quite large, it should be noted that it is still 5σ above the 15 GeV/c cut imposed during event selection. Since the missing energy vector is perpendicular to both the electron and muon tracks, the missing energy is not sensitive to the value of the muon momentum and we find a missing energy of 74 GeV (> 66 GeV at 95% C.L.). The event contains three hadronic jets with E_T's of 29.5 ± 5.3, 27.6 ± 5.0 and 13.6 ± 2.4 GeV. If one makes the hypothesis that this event is a $t\bar{t}$ decay and interprets the two leading jets as b-jets, then a mass analysis of the kind proposed by Dalitz and Goldstein [12] implies 130 < M_{top} < 170 GeV/c^2 at the 90% C.L..

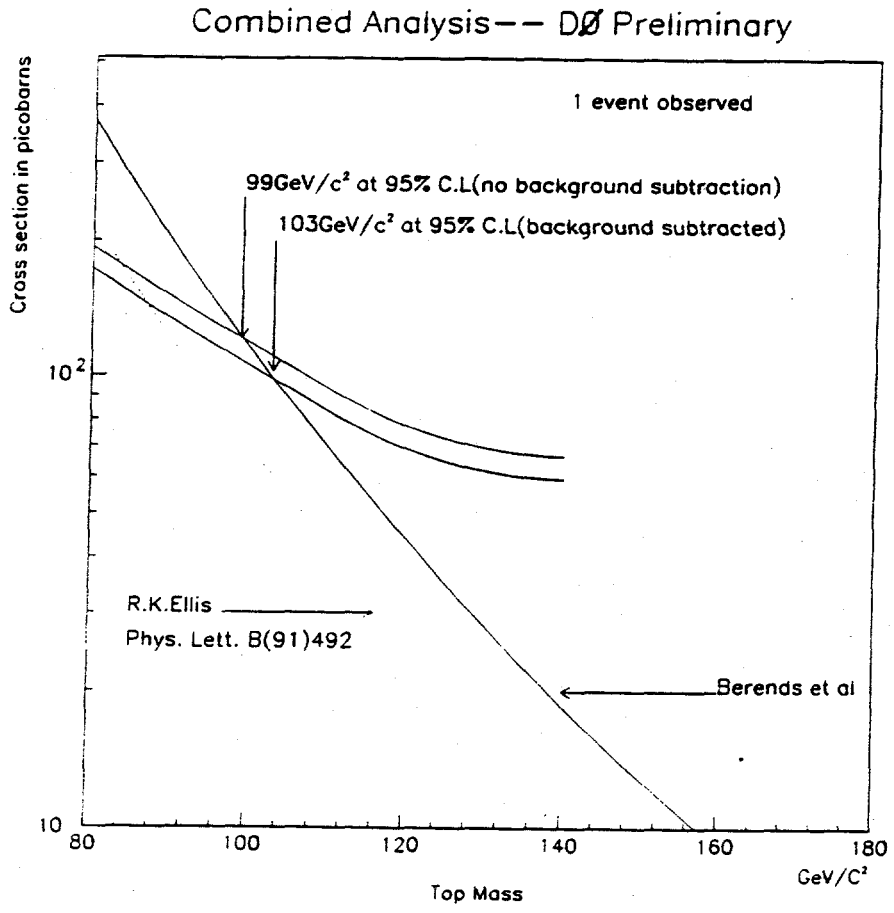

Fig. 8 Preliminary DØ measurement of the upper limit on the top quark production cross-section at the 95% C.L.. Also shown are two theoretical calculations of the cross-section.

(f) *Future Plans*

Over the next few months, we will calculate a final mass limit by incorporating measurements from each of the $t\bar{t}$ decay channels from the full Run 1a dataset. The first step towards this will be completion of the analyses in the three dilepton channels (e–e, e–μ and μ -μ). This requires a more sophisticated and complete simulation of the detector acceptance and response functions, which are actively being pursued. We plan to update the top acceptance and background calculations by the late summer. Where possible, these are being derived directly from the data so as to minimise the dependence on details of the Monte Carlo and detector modelling. For some channels however, no experimental data exist (eg. W^+W^- production) and here we must rely on Monte Carlo calculations for the production cross-sections and decay mechanisms.

We are actively developing more advanced analysis techniques using multi-dimensional likelihood and neural net methods to exploit the correlation between kinematic parameters in the optimization of signal to background ratios. While still in the early stages of development, these look quite promising and will lead to increased signal sensitivity compared to the conventional anayses discussed above. Preliminary results from these analyses will not be available before the fall and much of the work is currently aimed at analysis of the data from the next collider run.

The two lepton + jet channels (e + *jets*, μ + *jets*) are more difficult to analyze because of large backgrounds from W production with three or more jets. These can be significantly reduced by using any additional non-isolated leptons (e, μ) to tag b-quark decays in the $t\bar{t}$ events. This type of analysis, using a muon b-tag, is well suited to DØ because of the relative cleanness of the muon system (low probability of hadron punchthrough or of finding muons from π/K in-flight decays) which gives good acceptance for muons of momentum above 5 GeV/c.

By combining the dilepton and lepton + jet analyses, we estimate that we will reach a mass limit sensitivity at the 95% C.L. in the region of 120 to 130 GeV/c^2. Since the combination of analyses with differing backgrounds and systematic uncertainties must be done with considerable care, we are pursuing a variety of algorithms to determine which is the most reliable. This, like the background studies, is heavily reliant on accurate models of the detector response and requires that this be well understood.

In preparation for Run 1b, which is scheduled to begin in November, the Level 1 and 2 triggers need some re-optimization to cope with the projected increase in peak instantaneous luminosity to over 10^{31} cm^{-2}s^{-1} (the higest level reached during Run 1a was 8.8×10^{30}). Although the data acquisition system will be upgraded to increase the bandwidth, more restrictive trigger configurations will still be needed for both the Level 1 and Level 2 triggers.

With projected integrated luminosities of between 60 and 80 pb^{-1} from Run 1b, the analyses will be sensitive to top masses of up to 160 GeV/c^2. Because of the small cross-sections at these

masses, it is essntial that the triggers are optimised for maximum top acceptance while still passing sufficient background events to allow precise estimations of the competing non-top backgrounds. To this end, a series of trigger optimization studies are planned for the fall.

(g) *References*

1 F. Abe et al. (CDF Collaboration), "A Lower Limit on the Top Quark Mass from Events with Two Leptons in $p\bar{p}$ Collisions at $\sqrt{S}$ = 1.8 TeV", Phys.Rev.Lett. 68,447 (1992).

2 G. Abrams et al. (Mark 2 Collaboration), "Measurements of Z Boson Resonance Parameters in e^+e^- Annhilation", Phys.Lett. 63, 2173 (1989),
D. Decamp et al. (ALEPH Collaboration), "Determination of the Number of Light Neutrino Species", Phys.Lett. B231, 519 (1989),
P. Aarino et al. (DELPHI Collaboration), "Measurement of the Mass and Width of the Z^0 Particle from Multi-Hadronic Final States Produced in e^+e^- Annhilations"Phys Lett B231, 539 (1989),
B. Adeva et al. (L3 Collaboration), "A Determination of the Properties of the Neutral Intermediate Vector Boson Z^0", Phys.Lett. B231, 509 (1989),
M. Akrawy et al. (Opal Collaboration), "Measurement of the Z^0 Mass and Width with the Opal Detector at LEP", Phys Lett. B231, 530 (1989).

3 S.J. Wimpenny, "The TOP_LEPTONS Analysis Package", DØ Note 1690, May 1993.

4 S.J. Wimpenny, Proceedings of the Aspen Winter Conference in Particle Physics, January 1993.

5 M. Narain, Proceedings of the XXVIII th Rencontres de Moriond, Les Arcs, March 1993,
S. Protopescu, Proceedings of the XXVIII th Rencontres de Moriond, Les Arcs, March 1993.

6 J. Cochran, American Physical Society Meeting, Washington, April 1993,
R.E. Hall, APS Meeting, Washington, April 1993,
S. Snyder, APS Meeting, Washington, Aprill 1993.

7 S. Abachi, Proceedings of the 5th. International Symposium on Heavy Flavour Physics, McGill, July 1993.

8 M. Strovink, Proceedings of the European Physical Society Conference on High Energy Physics, Marseille, July 1993.

9 F. Paige and S. Protopopescu, "ISAJET 5.30 : A Monte Carlo Event generator for pp and $p\bar{p}$ Interactions", Brookhaven Report No. BNL38774.

10 R. Brun et al., "GEANT 3.10 User's Guide", CERN Report, CERN DD-EE-84-1, (1984).

11 E. Laenen, J. Smith, W.van Neervan, "All Order Resummation of Soft Gluon Contributions to Heavy Quark Production in Hadron-Hadron Collisions", Nucl. Phys. B369, 543 (1992),
F.A. Berends, B. Tausk, W.T. Giele, "Top Search in Multi-Jet Signals", Phys. Rev. D47 : 2746 (1993).

12 R.H. Dalitz and G.R. Goldstein, "The Decay and Polarization Properties of the Top Quark", Phys.Rev. D45, 1531 (1992),
R.H. Dalitz and G.R. Goldstein, "The Analysis of Top–AntiTop Production and Dilepton Decay Events and the Top Quark Mass", Phys. Lett. B287 : 225 (1992),
G.R. Goldstein, K. Sliwa and R.H. Dalitz, "On Observing Top Quark Production at the Tevatron", TUFTS-TH-92-G01, May 1992, 15pp.

1.2.3 The Muon Trigger System

The DØ trigger has four levels: 0, 1, 1.5 and 2. The sequence of steps in the acquisition of an event begins with the Level 0 trigger which uses scintillation counters to determine if one or more beam-beam interactions occurred during a beam crossing. The Level 1 muon trigger requires the presence of coarse track-like hit distributions in the muon drift chamber, along with a scintillator roof which rejects cosmic rays more than ±40 ns out of time. Level 0 and 1 decisions are made in the 3.5 μsec between bunch crossings. The Level 1.5 muon trigger utilizes a finer grained processing of candidate tracks in the muon drift chambers. The Level 2 muon filter is a subset of the offline muon identification code, including special cosmic ray rejection tests.

Over the last year, K. Bazizi has served as the coordinator of the DØ muon trigger group of 20 people. This group has been responsible for the installation, maintenance and operation of the Level 1 and Level 1.5 muon trigger frameworks [1] throughout the detector commissioning and Run 1a. The UCR team, consisting of Bazizi and graduate students R.Hall and T.Huehn, was responsible for the implementation, maintenance and repair of the Level 1 trigger logic throughout the run [2].

The Level 1 muon trigger is a fast hardware trigger which signals a track traversing the muon detector. At the start of Run 1a, trigger coverage was restricted to the central pseudorapidity region, $|\eta| < 1$. Studies of the trigger backgrounds from the main ring and from cosmic rays enabled the development of cleaner trigger algorithms at Levels 1, 1.5 and 2. This required several mid-run upgrades of both the trigger hardware and control logic, for which the UCR group took responsibility. These upgrades were successfully implemented so that the muon trigger was fully active out to its maximum coverage of $|\eta| < 3.3$ by the end of the run.

In addition to trigger hardware, the UCR group has also developed the online monitoring software for the Level 1 framework and the offline simulator which is used to optimize the trigger logic in studies of trigger efficiencies. This package, coupled to the Run 1a data, is now being used to re-optimized the trigger logic for Run 1b, which starts in November 1993.

(a) *References*

1 K. Bazizi, "Level 1 and Level 1.5 Muon Trigger Efficiencies for Single Tracks", DØ Note 1618, February 1993.
K. Bazizi, "Description of the Muon Trigger Data in the TRGR Bank", DØ Note 1587, January 1993.
K. Bazizi, "Muon Trigger Words in the PMUO Bank", DØ Note 1591, January 1993.

2 K. Bazizi, R.E. Hall, "Muon Module Address Card (MAC) Description", DØ Note 1143, September 1991.
R.E. Hall. "Update History of Muon MAC Card", forthcoming DØ Note.

1.2.4 Muon Software

The UCR group has devoted consideragble effort to developing and testing algorithms for identifying cosmic ray muons during online (Level 2) and offline muon reconstruction [1]. S. Wimpenny has developed the offline software package "CLEANMU" used for muon identification in DØ.

CLEANMU takes the raw muon track candidates from the offline reconstruction program and performs a series of quality and matching tests. These tests establish track quality and give strong rejection against combinatoric and cosmic ray backgrounds, which can fake isolated muon signatures in the detector.

The algorithm used in CLEANMU starts with a track segment from the muon detector and then matches it to the information from the remainder of the detector. To define a good muon track, the muon segment must be cleanly reconstructed in the outer muon chambers and central tracking chambers and have a matching energy deposition in the calorimeter, consistent with that of a minimum ionizing particle (MIP). Cosmic ray muons are eliminated by further requiring that the track point to the reconstructed vertex position and that there be no back-to-back track in the central tracking system or MIP trace in the calorimetry.

While CLEANMU provides the standard muon track definition, it is also simple to re-optimize for specific muon topologies for which the backgrounds may be considerably different. This is achieved by controlling the package with a Run Control Parameter (RCP) file, through which the user can trivially enable, disable or vary the track quality cuts.

(c) *References*

1 B. Choudhary and A. Klatchko, "Cosmic Rejection: Some Thoughts and Studies", DØ Note 1505, October 1992.

2 S.J. Wimpenny, "The CLEANMU Offline Muon ID Package", forthcoming DØ Note.

1.2.5 Inclusive Muon Production and the *b*-Quark Cross-Section

(a) *Inclusive Muon Production*

Many processes contribute to muon production in $p\bar{p}$ collisions at high energies. These include Drell Yan, J/ψ, and Υ production, W and Z^0 decays and semileptonic decays of b- and c-hadrons. All of these processes give rise to "prompt" muon production. In addition, non-prompt muons from the in-flight decays of π's and K's contribute strongly to the muon spectrum at low transverse momentum, P_T.

The DØ detector is well equipped for muon studies since the muon coverage extends to within 3° of the beamline ($|\eta| = 3.64$). The calorimeter and magnetized toroids provide between 12 and 18 interaction lengths of material over all η and ϕ. Thus DØ can reliably measure μ's within a jet with negligible background from hadron punch-through.

During Run 1a a total of 16.7 pb^{-1} of data were recorded with a variety of muon trigger configurations. This dataset covers the pseudorapidity inteval $|\eta| < 3.2$ and will be used to obtain the inclusive muon production cross-section $d^3\sigma/dy\, dP_T^2$. K. Bazizi is coordinating this measurement by a group of physicists and graduate students from Riverside, Arizona and CBPF (Brazil) [1]. Since the combinatoric backgrounds and those due to cosmic rays are both trigger and rapidity dependent, the analysis is divided up according to trigger and rapidity range. Figure 9 shows preliminary results for a) the central and b) forward regions of the Wide Angle Muon Spectrometer (WAMUS); this data presented by B. Choudhary at the 1993 Snowmass Workshop on B- Physics [2]. The dotted lines in fig. 9 show Monte Carlo calculations of the major components expected to contribute to muon production below P_T of 25 GeV. A definitive measurement of inclusive muon production will require:

i) extension of the analysis to include the Small Angle Muon Spectrometer (SAMUS) data at $1.7 < |\eta| < 3.2$,
ii) more extensive Monte Carlo calculations,
iii) refinement of efficiency and background studies, especially at forward angles.

b) *b-Quark Cross-Section*

Graduate student T. Huehn is measuring the b-quark production cross-section as his Ph.D. thesis project. A dedicated run of 0.3 pb^{-1} of data was recorded with a muon · jet trigger [$P_T(\mu) > 3$ GeV; $E_T(\text{jet}) > 10$ GeV] for this measurement. The jet condition reduces cosmic ray

triggers and enhances the data sample in b- and c-quark muonic decays which have a muon-in-jet configuration.

A preliminary measurement of the muon P_T spectrum from b/c quark production was presented by T. Huehn at the April 1993 Washington APS meeting [3]. This was based on 1442 muon events coming from 14,139 triggers, (49 nb^{-1}). The sample is restricted to the central muon detector, $|\eta| < 1$, for which systematics are now well understood.

Processing of the complete data sample (300 nb^{-1}) is nearing completion. Remaining tasks include:

i) large scale Monte Carlo simulations of $b\bar{b}/c\bar{c}$ production to evaluate efficiencies,

ii) a more precise estimate of π/K decay-in-flight contamination and

iii) measurement of the $b\bar{b}/c\bar{c}$ ratio.

Finally, the muon P_T spectrum, after subtraction of the decay-in-flight and $c\bar{c}$ components, will be translated into $d\sigma/dP_T$ for b-quarks. This thesis project will be completed in 1994.

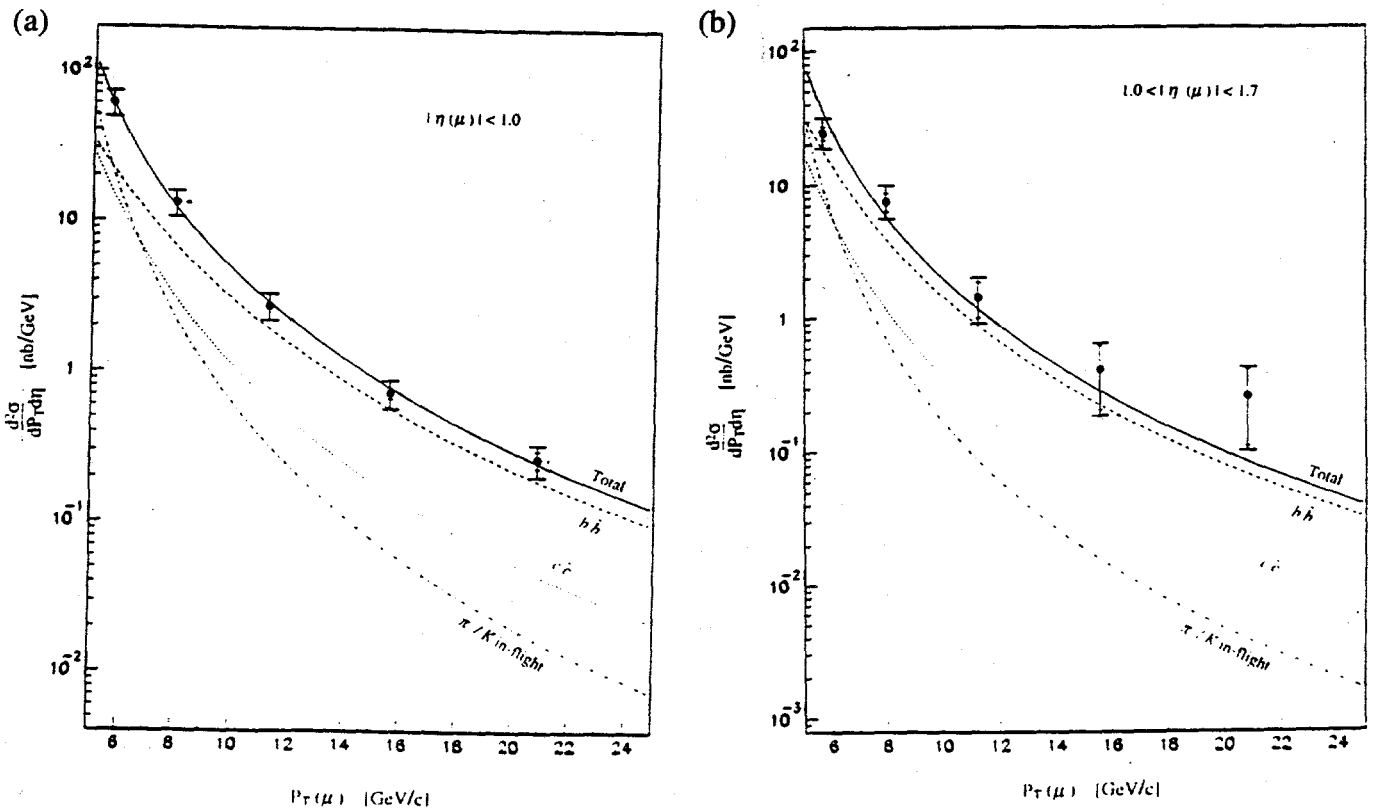

Fig. 9 Differential cross-sections for inclusive muon production for (a) $|\eta| < 1.0$ and (b) $1.0 < |\eta| < 1.7$. The points show measurements from data, with the smaller error bars for statistical errors and the larger ones for statistical plus systematic errors, added in quadrature.

(c) *References*

1 K. Bazizi, "Inclusive Single Muons at DØ", Proceedings of the 7th Meeting of the APS , Division of Particles and Fields, Fermilab, November 1992, (World Scientific 1993), p. 750-2.

2. B. Choudhary, "Inclusive Single Muons at DØ", Proceedings of the Snowmass Workshop of B-physics, Snowmass, June (1993), (in press).

3. T. Huehn, "A Study of $p\bar{p} \rightarrow \mu + jet + X$ at $\sqrt{S}$ = 1.8 TeV at DØ", Contributed talk at the APS Annual Meeting, Washington DC, April (1993).

1.2.6 Study of the $WW\gamma$ coupling

The UCR group is playing a leading role in the study of the trilinear vector boson couplings in DØ. We are responsible for analysis of $W\gamma$ production with decay of the W into the muon channel. Since the successful completion of the first DØ physics run, considerable progress has been made and a preliminary analysis using the Run 1a data has been completed. The UCR personnel working on this topic are B. Choudhary and J. Ellison. The $W\gamma$ production analysis was presented by B. Choudhary at the DØ workshop at Stony Brook, June 93 [1] and will be presented by J. Ellison at the Workshop on $p\bar{p}$ Collider Physics, Tsukuba, Japan, October 1993.

(a) *Introduction*

At the Tevatron, the process $p\bar{p} \rightarrow W^{\pm}\gamma$ provides an opportunity to measure directly the three vector boson coupling $WW\gamma$. In the Standard Model (SM) at the tree level, the trilinear $WW\gamma$ coupling is completely fixed by the gauge theory structure of the model. Experimental observation of the $WW\gamma$ coupling is therefore a crucial test of the SM, and has so far been measured only by UA2 [2]. In Runs 1a and 1b of the DØ experiment, we expect to collect a data sample of about 75 pb^{-1} and make a much more sensitive measurement.

At the parton level, the principal processes are:

$$q + \bar{q}' \rightarrow \gamma + W^- \; (W^- \rightarrow l^- + \bar{\nu}) \qquad \text{"production"}$$
$$q + \bar{q}' \rightarrow W^- \rightarrow \gamma + l^- + \bar{\nu} \qquad \text{"decay"}$$

The general $WW\gamma$ coupling can be described by four free parameters and is given by the effective Lagrangian:

$$L_{WW\gamma} = -ie[\,(W^{\dagger}_{\mu\nu}W^{\mu}A^{\nu} - W^{\dagger}_{\mu}A_{\nu}W^{\mu\nu}) + \kappa W^{\dagger}_{\mu}W_{\nu}F^{\mu\nu} + \frac{\lambda}{m_W^2}W^{\dagger}_{\lambda\nu}W^{\mu}_{\nu}\tilde{F}^{\nu\lambda} + \tilde{\kappa}W^{\dagger}_{\mu}W_{\nu}\tilde{F}^{\mu\nu} + \frac{\tilde{\lambda}}{m_W^2}W^{\dagger}_{\lambda\nu}W^{\mu}_{\nu}\tilde{F}^{\nu\lambda}\,]$$

where A_μ is the photon field W_μ is the W^- field, $W_{\mu\nu} = \partial_\mu W_\nu \partial_\nu W_\mu$, $F_{\mu\nu} = \partial_\mu A_\nu - \partial_\nu A_\mu$, and $\tilde{F}_{\mu\nu} = \frac{1}{2}\varepsilon_{\mu\nu\rho\sigma}F^{\rho\sigma}$.

The first term in the equation for the Lagrangian is the so-called "minimal" coupling term, and the second coefficient κ is conventionally called the "anomalous" magnetic moment of the W. This term and the third coefficient λ are related to the magnetic dipole moment μ_W and the electric quadrupole moment Q_W of the W by

$$\mu_W = \frac{e}{2m_W}(1+\kappa+\lambda)$$

$$Q_W = \frac{e}{m_W^2}(\kappa-\lambda)$$

While κ and λ do not violate any discrete symmetries, the $\tilde{\kappa}$ and $\tilde{\lambda}$ terms are P odd and CP violating. They are related to the electric dipole moment d_W and the magnetic quadrupole moment $\tilde{Q}_W$ of the W by

$$d_w = \frac{e}{2m_W}(\tilde{\kappa}+\tilde{\lambda})$$

$$\tilde{Q}_W = \frac{e}{m_W^2}(\tilde{\kappa}-\tilde{\lambda})$$

In the SM at tree level, $\kappa = 1$, $\lambda = 0$, $\tilde{\kappa} = 0$ and $\tilde{\lambda} = 0$. The consequences of deviations of these parameters from their SM values are:

- The cross-section for the process $p\bar{p} \rightarrow W^{\pm}\gamma$ increases, and thus any excess of events measured will be an indication for physics beyond the SM.

- The differential distributions for some kinematical variables depend strongly on κ, λ, $\tilde{\kappa}$ and $\tilde{\lambda}$. Such variables are, for example, the transverse momentum of the photon ($P_T(\gamma)$), the invariant mass of the $W\gamma$ system ($M_{W\gamma}$) and the angular distribution of the photon in the partonic center of mass system ($\cos\theta^*$).

(b) *Event Selection*

A first pass analysis of the full Run 1a data is in progress. Candidate $W\gamma$ events were selected from the "expressline" data with a total integrated luminosity of 16.6 ± 2.0 pb^{-1}. The $W\gamma$ muon channel candidates were derived from a trigger which required at least one EM cluster with $E_T > 7$ GeV and at least one muon with $P_T > 5$ GeV/c.

The offline muon selection code requirements were: (a) minimum path length through the magnetized iron toroid of $\int \boldsymbol{B} \cdot d\boldsymbol{l} > 2.0$ Tm, corresponding to a P_T kick of 0.6 GeV/c, (b) muon pointing to primary vertex, (c) track match between muon detector and central drift chamber, (d) minimum ionizing signal in the calorimeter and (e) no jet activity in the calorimeter within $\Delta R < 0.5$ around the muon. The muon was restricted to the region $|\eta| < 1.7$ and $P_T > 15$ GeV/c. The events were also required to have missing transverse energy $\not\!\!E_T > 15$ GeV.

Photon selection code requirements were (a) EM/total energy > 0.9, (b) shower shape χ^2 cut, (c) isolation in a cone of $\Delta R < 0.4$ and (d) no track pointing to an EM cluster within $\Delta\eta \times \Delta\phi = 0.1 \times 0.1$. The photon was required to be within $|\eta| < 3.2$ and have $P_T > 10$ GeV/c.

Fiducial cuts were imposed to remove the tracks through cracks and known inefficient parts of the detector. All the selected events were finally scanned to ensure the quality of the muon and photon and to remove cosmic ray background.

Efficiencies were studied separately for the trigger, and for the muon and photon selection. The combined efficiency for the trigger (including geometric acceptance) and the offline selection is 13.4 ± 4.3 %.

(c) *Backgrounds*

The major source of background comes from $W + jet$ events, where a jet fakes a photon. This background was calculated by folding the $W + jets$ cross-section from the data with the calculated probability that a jet fakes a photon. The latter was estimated from QCD events. Another main source of background is $Z^0 \rightarrow \tau\ \tau$ where one tau decays into a muon and the other tau decays into an electron which is misidentified as a photon. This background was estimated using Monte Carlo. The other sources of backgrounds that we have simulated are firstly a 140 GeV/c^2 mass top quark decaying into an electron and a muon where the electron is misidentified as a photon, secondly dibosons decaying into an electron and muon where again the electron is misidentified as a photon and thirdly QCD background. The total estimated background is 2.0 ± 0.6 events.

(d) *Results*

With the event selection described above, we are left with 9 $W\gamma$ candidate events. Using the background estimate, this yields 7.0 ± 2.8 signal events. In Figure 10, we plot (a) muon transverse momentum and (b) photon transverse energy for the $W\gamma$ candidate events. The shaded histograms show the distributions obtained using the Baur Monte Carlo and the DØ detector resolutions. Figure 11 shows the distributions of (a) separation between the muon and photon in ΔR space, and (b) transverse cluster mass M_T (μ, γ, $\not\!\!E_T$). Production events, which are more sensitive to the anomalous couplings, can be separated from decay events by a transverse cluster mass cut, M_T (μ, γ, $\not\!\!E_T$) > 90 GeV/c^2.

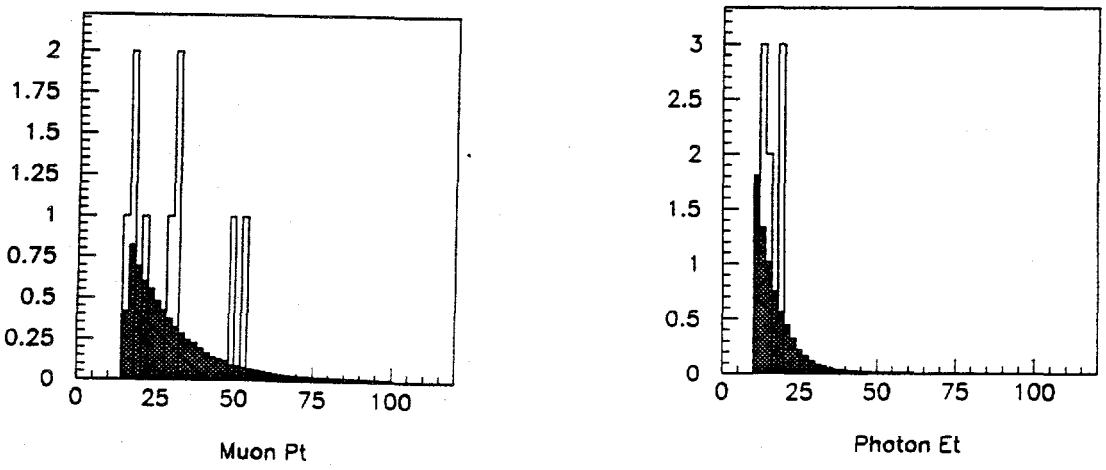

Fig. 10 For the 9 $W\gamma$ candidate events, (a) P_T (μ) distribution, (b) E_T (γ) distribution. Shaded histograms are Monte Carlo distributions.

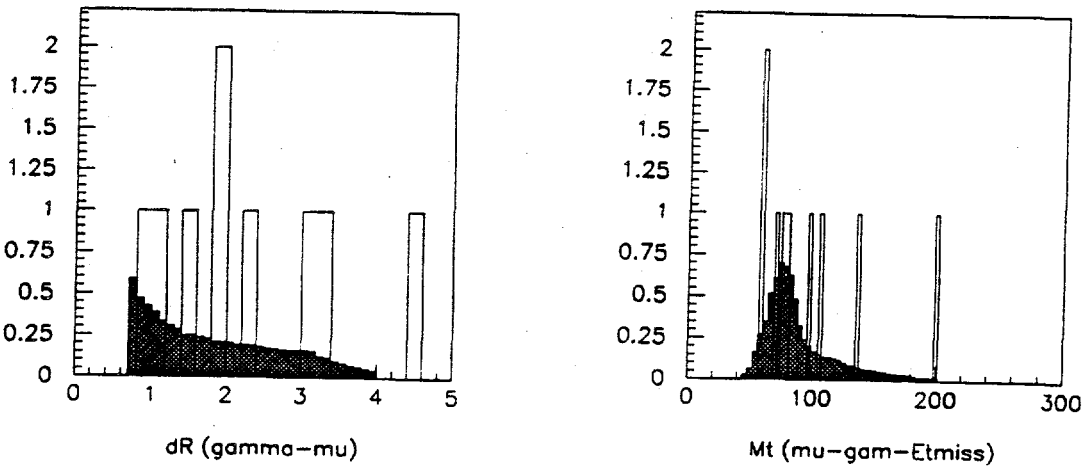

Fig. 11 For the 9 $W\gamma$ candidate events, (a) ΔR between muon and photon, (b) M_T (μ, γ, $\not\!\!E_T$).

(e) *Theoretical Predictions*

The Baur Monte Carlo [2] was used to generate $W\gamma$ events and to calculate the cross-section. The Monte Carlo included smearing to simulate the detector resolutions. Using the fiducial volume and kinematic cuts required for event selection, the cross-section was found to be 3.73 ± 0.02(stat) pb. We are currently studying the systematic errors on this theoretical prediction.

Figure 12 shows plots of the Monte Carlo calculation of the cross-section as a function of (a) λ and (b) $\Delta\kappa$, where $\Delta\kappa = \kappa - 1$. The data point is the cross-section calculated in this analysis. The shaded band corresponds to one standard deviation. Note that the systematic error on the theory is not shown, since it is still under study.

We conclude that our data are in agreement with the Standard Model within the sensitivity of the measurement. In the near future we will be able to set competitive limits on the anomalous couplings $\Delta\kappa$ and λ.

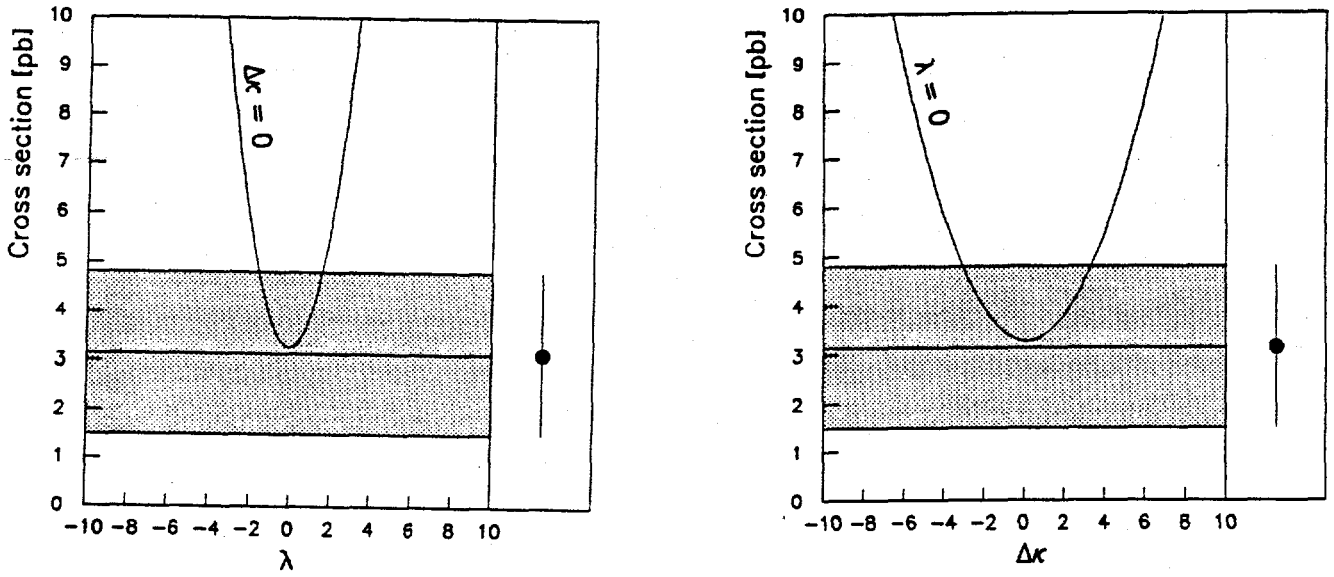

Fig. 12 The Baur Monte Carlo calculation of the $WW\gamma$ cross-section, and the preliminary cross-section measured from the DØ data from Run 1a for (a) variation of λ and (b) variation of $\Delta\kappa$.

(f) *Future Plans*

In the next year we plan to bring this analysis to completion and publish our results. We will also start work on the analysis of the data from Run 1b. During the summer of 1993, we will be refitting our whole Run 1a dataset with a new and final version of the reconstruction, which will incorporate a better understanding of the calibration constants. We hope to have the final analysis well underway by the end of the summer and plan to present our results at the Workshop on $p\,\bar{p}$ Collider Physics in Tsukuba in October 1993.

A detailed study of the probability that a jet fakes a photon in DØ will be undertaken. This is crucial for calculating the $W + jets$ background. In particular we plan to study the P_T and trigger dependence of this probability. We need to calculate our muon and photon detection efficiencies with better statistics than we have done so far. We expect the efficiencies to improve once the new reconstruction code is implemented. The photon efficiency will be calculated separately for the central and endcap calorimeters.

For the comparison with the SM, we need to estimate the systematic error on the theoretical cross-section. This will be done by incorporating next-to-leading order effects into the calculations and studying the results of varying the structure function and the Q^2 scale. Events generated using the Baur program will also be passed through the DØ detector simulation, to fully incorporate the effects of the detector response. This work will require a significant amount of computer CPU time and we will be fully utilizing our SGI and VAX clusters on campus.

We will also study improved analysis strategies for obtaining tighter limits on the anomalous couplings. These include the use of a likelihood analysis using kinematic variables such as the photon P_T, the invariant mass of the $W\gamma$ system, and the angular distribution of the photon in the partonic center of mass system.

On the time scale of the next couple of years, we will improve the analysis by combining data from the muon and electron channels and by combining the Run 1a and 1b data. We are also pursuing the analysis of $Z\gamma$ events to probe the $ZZ\gamma$ coupling.

(g) *References*

1 B. Choudhary, Transparencies from the DØ Stony Brook Workshop, June 1993, forthcoming DØ note.

2 J. Alitti et al. (UA2 Collaboration), "Direct Measurement of the $W\gamma$ Coupling at the CERN $\bar{p}\,p$ Collider", Phys. Lett. B277, p. 194 (1992).

3 U. Baur and E.L. Berger, "Probing the $WW\gamma$ Vertex at the Fermilab Tevatron Collider", Phys. Rev. D 41, No. 5, p. 1476 (1990).

1.2.7 The DØ Upgrade

The DØ detector will undergo a major upgrade over the next few years, to enable it to run when the Tevatron luminosity is increased to ten times its present level and the time between bunch crossings is reduced from 3.5 μs to 132 ns. A 2 T solenoid magnet will be added to extend the physics reach of the experiment, and the entire existing tracking system of gaseous wire chambers will be replaced with an extensive high resolution silicon strip tracking system and a scintillating fiber outer tracker. The upgrades will be installed during 1996, ready for Tevatron Run 2 at the beginning of 1997. The tracking upgrade will allow DØ to measure the momenta of charged particles, to separate electrons from positrons, to tag b-jets from top decays using secondary vertex impact parameter measurements within jets, to separate multiple interactions in one beam crossing more effectively, and to reduce conversion backgrounds using pulse height information from the silicon.

(a) *The DØ Silicon Tracker*

The Silicon Tracker consists of barrels made of silicon ladders, and of disks made of silicon wedge-shaped wafers. It will provide high resolution tracking for $|\eta| < 3.2$. An r-z view of the full upgrade DØ tracking system is shown in Figure 31 and a cross-section in the r-ϕ plane of the original design Silicon Tracker is shown in Figure 14. The small disks are double-sided and the large disks and barrels are single-sided. Extensive GEANT simulations have been made, which show that the new tracking system is almost 100% efficient at reconstructing tracks within its geometric acceptance, with virtually no ghost tracks [1]. A. Heinson has made several presentations describing the geometry and performance of the Silicon Tracker, including an invited paper at the Fermilab DPF meeting in November 1992 [2,3].

(b) *The UCR Role in the DØ Upgrade*

The original group working on the hardware for the Silicon Tracker consisted of physicists and engineers from Fermilab, LBL and UC Riverside. The software and hardware activities now include over 60 people from Moscow State, Northeastern, Northwestern, Notre Dame and Rice Universities and the Brazilian Center for Physics Research.

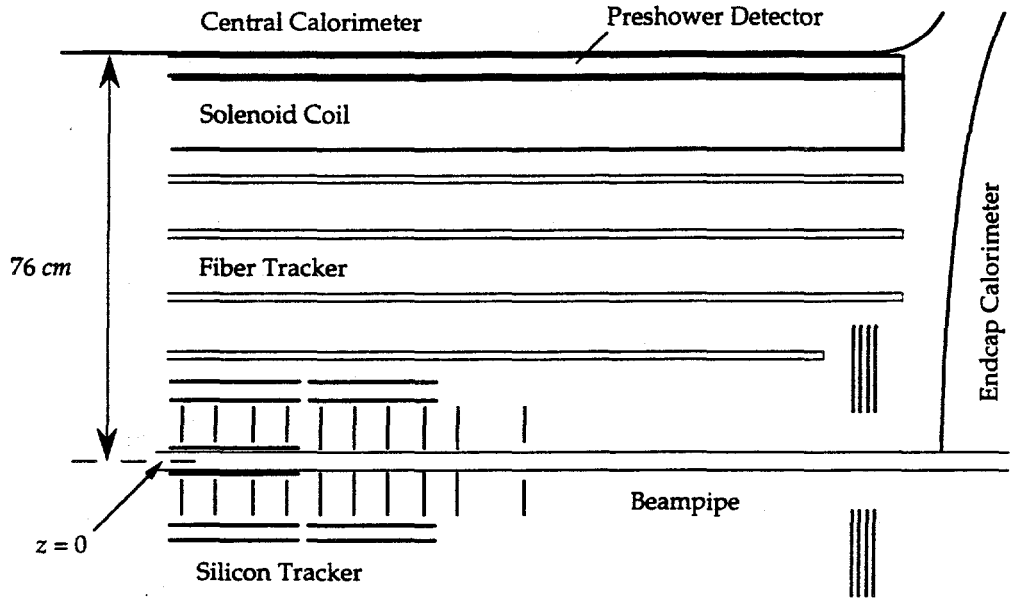

Fig. 13 The baseline DØ Upgrade Tracking System, showing the 2 T magnet, scintillating fiber tracker and silicon tracker, with 3 barrel layers, 20 double-sided disks (10 shown) and 8 large single-sided disks (4 shown).

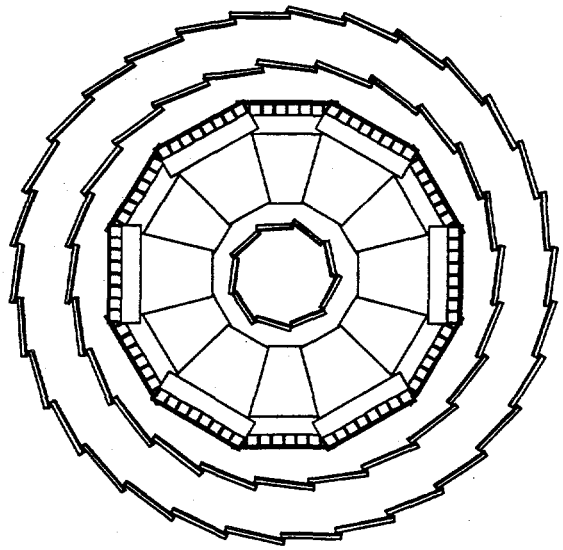

Fig. 14 A cross-section through the baseline Step 2 Silicon Tracker, showing three barrel layers and an E-disk made of wedge-shaped silicon wafers, with readout mounts and chips at the outer radius of the wedges. The radius of the outer barrel is ~ 15 cm.

UC Riverside has taken a major role in the Silicon Tracker since its inception by members of this group [4], and continues to lead many aspects of the designing, prototyping and project management. Work undertaken by members of the UCR group over the last year on the Silicon Tracker includes:

- Design of the E-disk and F-disk silicon wedge detectors
- Procurement of F-disk prototype wedge detectors
- Preliminary evaluation of prototype F-disk detectors
- Setting up a laser test system for evaluating the silicon detectors
- Design of the readout mount, for attaching chips to the silicon wafers
- Studying and optimizing the geometry of the Silicon Tracker
- Setting up a database for all parameters of the Silicon Tracker and its materials
- Producing schedules for construction of the full Tracker

The members of the UCR high energy physics group who are actively working on the DØ upgrade are John Ellison, Ann Heinson, Christopher Boswell and two undergraduate students. Chris Boswell is a recently appointed postdoc who has extensive silicon detector experience from working on the CDF silcon vertex detector.

Details of work by the UCR group are presented below.

(c) *Design of Silicon Detectors for the Disks*

The double-sided wedge detectors which form the disks of the tracker are among the largest such devices in the world. They are extremely ambitious detectors with an unusual geometry, and a very large number of steps are involved in their fabrication. The UCR group has the sole responsibility for these detectors. We have chosen two manufacturers to work with on the development of prototypes, so that we can compare their different detector technologies and production quality, and then choose the best vendor for mass production on the basis of their performance. The manufacturers are Micron Semiconductor in England [5] and SINTEF SI in Norway [6]. The UCR group received $141k from Fermilab to procure the detectors. We placed initial orders in March 1992 and received the first detectors in May 1993. It took five months to complete the mask designs. The wedge detector is designed to fit on the 4" diameter silicon wafer, shown in Figure 15. Three wedge detectors with readout mounts attached are shown in Figure 16.

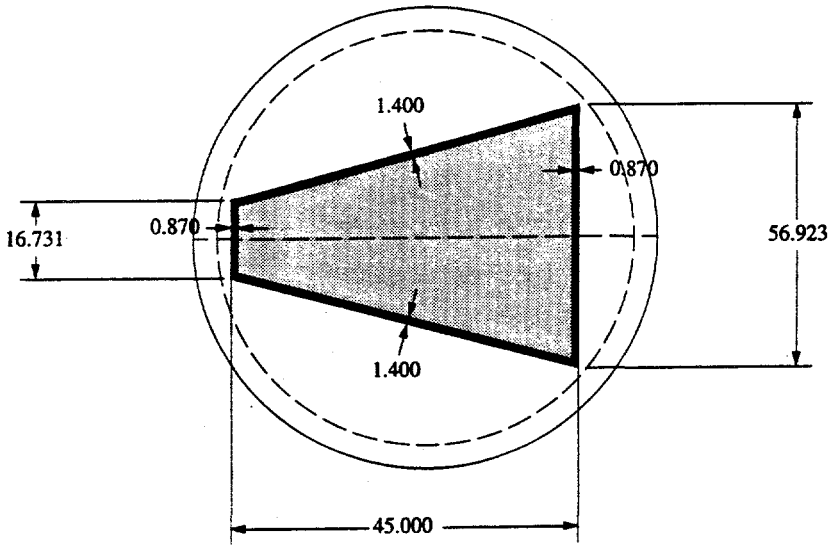

Fig. 15 Wedge detector layout on a 4" wafer. The lighter shaded area is the active part and the darker shaded area is the inactive region, used for guard rings, bias lines and fiducial alignment marks.

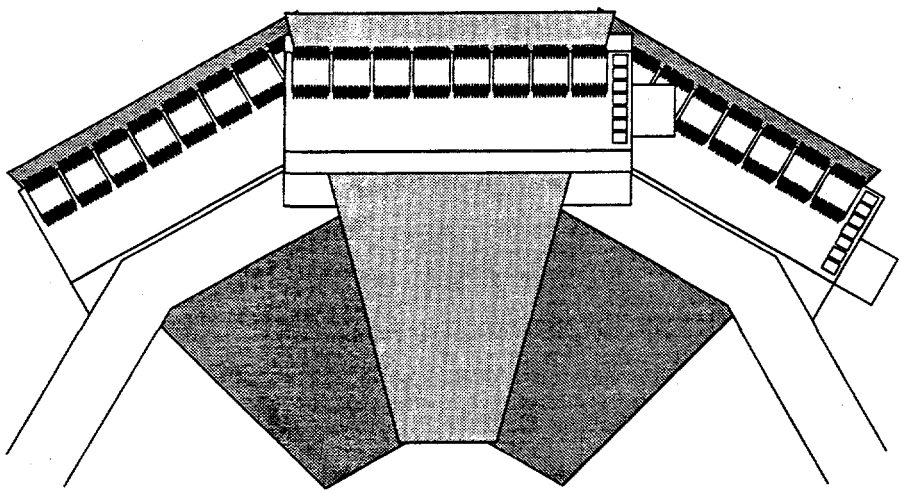

Fig. 16 Three wedge detectors, showing the position of the readout mounts and cooling pipe.

Specifications for the DØ F-Disk Silicon Detectors			
Dimensions		Bias Resistor	
Wafer Size	4 inch	Polysilicon [7, 8]	2.0 ± 0.4 MΩ
Thickness	300 μm		
Flatness	< 25 μm	Coupling Capacitor	
Detector Shape	Trapezoidal	Micron	SiO_2 : 200 nm
Height	75.000 mm	SINTEF SI	SiO_2 220nm+Si_3N_4 100nm
Base Width	56.923 mm		
Top Width	16.731 mm	n^+ Strip Isolation	
Active Area	24.46 cm^2	Micron	Intermediate p^+ Strips
Dead Region at Sides	1.40 mm	SINTEF SI	Aluminum Gate
Dead Region at Base, Top	1.45 mm		
Stereo Angle	± 15°		
Readout Strip Pitch	50 μm		
Bond Pad Pitch	51.8 μm		
Strip Width	10 μm		
Number of Readout Strips	1024 per side		
Overlap Between Wedges	707 μm		

Figure 17 shows a schematic of the p-side of the wedge detector mask layout. Both Micron and SINTEF SI detectors have intermediate p^+ strips on the p-side of the detector at a 25 μm pitch, to improve the resolution. Two sets of bond pads, offset by 2 mm, are provided to allow support directly under the bond pads during ultrasonic wire bonding. The nominal implant strip width for the readout strips on the p-side and n-side is 10 μm, chosen to give a small interstrip capacitance and a reasonably large value for the coupling capacitance.

The coupling capacitors were formed by growing a 200 nm silicon dioxide layer over the strip or by combining a 220 nm SiO_2 layer plus a 100 nm silicon nitride layer. The double layer of dielectric increases the breakdown voltage and minimizes the number of pinholes.

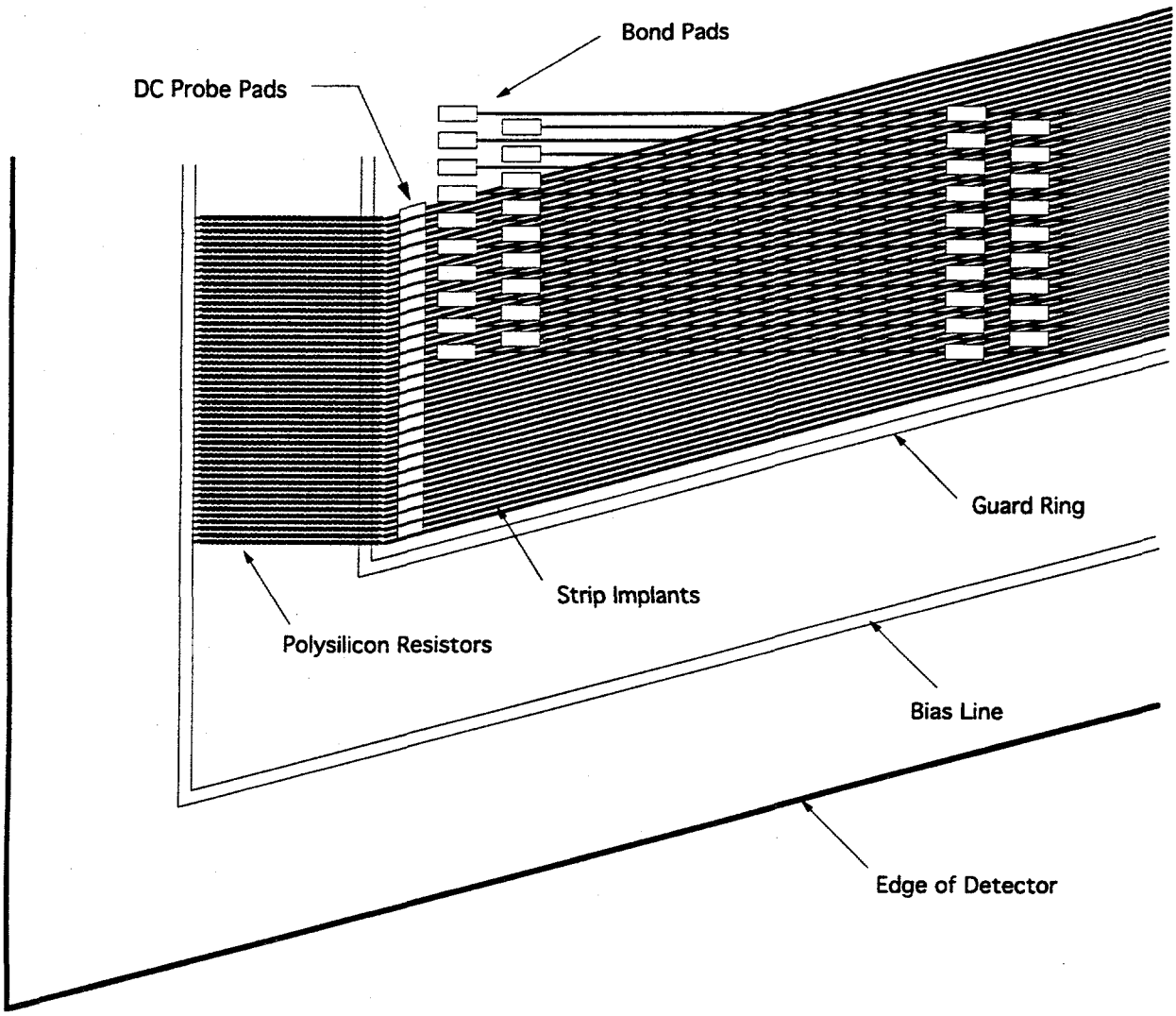

Fig. 17 Schematic of a corner of the wedge detector layout, showing the polysilicon bias resistors and dual rows of ac-coupled bond pads, for the p-side of the detector.

The two prototypes differ principally in the method used for isolation of neighboring n^+ strips on the n-side. For n-type bulk silicon, the positive fixed oxide charge can create an accumulation layer at the silicon surface, causing a very low impedance path between neighboring n^+ strips. To circumvent this, p^+ isolation implants have been introduced between the n^+ strips in the prototypes fabricated by Micron. The width of this implant, 24 μm, was chosen to be as wide as possible to achieve a low interstrip capacitance [9]. An alternative method, using an aluminum gate, biased so that the silicon surface is driven into inversion (forming a field-induced junction), was used in the SINTEF SI devices. Figure 18 shows a schematic cross-section through the silicon wafer for both designs.

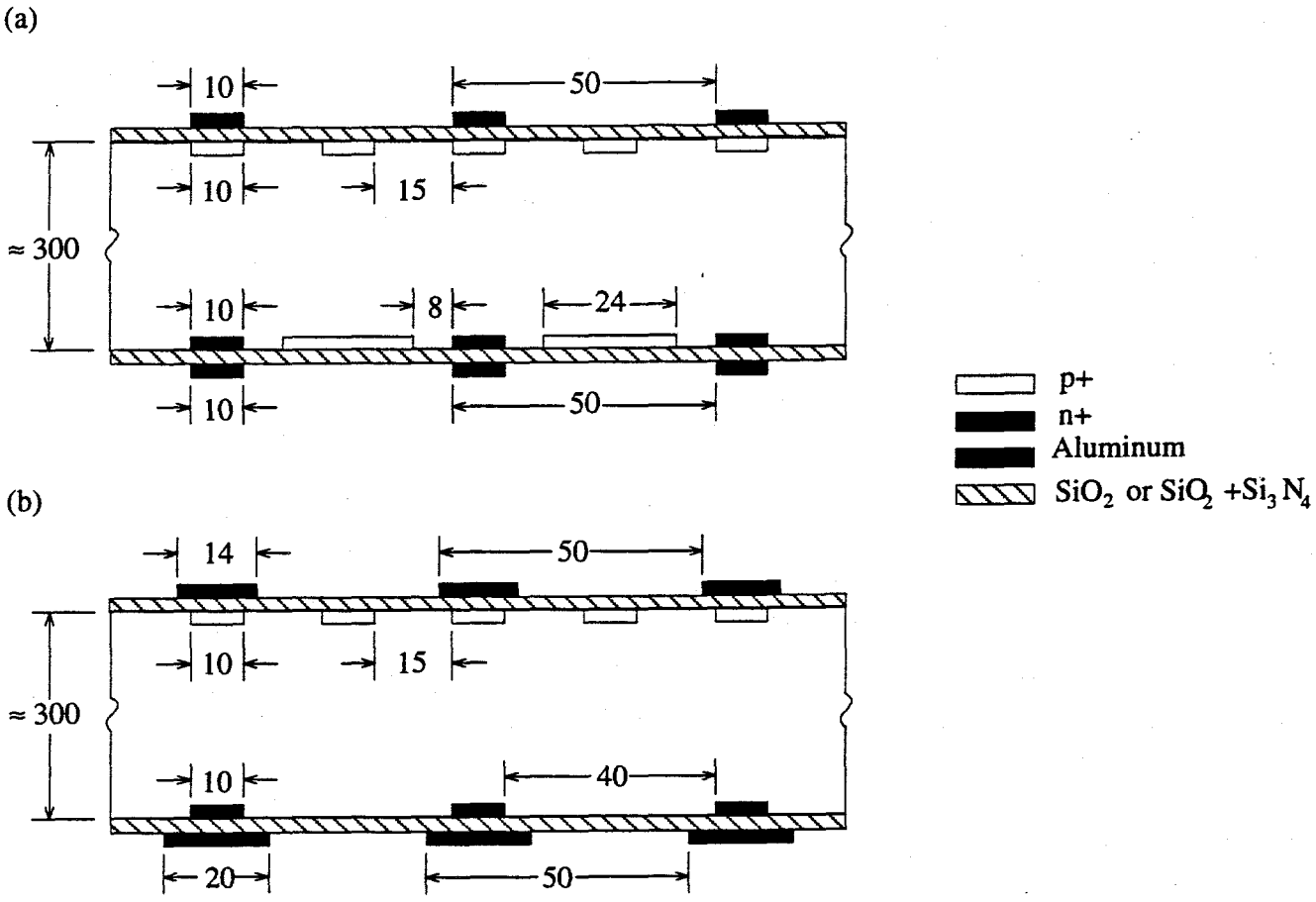

Fig. 18 Cross-sections through the double-sided detectors, showing two different methods of strip isolation on the n-side : (a) intermediate p+ strip isolation (Micron) and (b) aluminum gate isolation (SINTEF SI). All dimension are in microns.

(d) *Testing of Prototype Silicon Detectors for the Disks*

We have received 12 prototype wedge detectors from SINTEF SI and 4 from Micron. Measurements on these detectors are in progress. We have developed techniques for handling double-sided irregular geometry detectors, and have made preliminary probe station measurements of the leakage currents, breakdown voltages, coupling capacitances and interstrip resistances. J. Ellison presented these results by invitation at the International Symposium on Development and Application of Semiconductor Tracking Detectors, May 1993, Hiroshima, Japan [10].

CV Characteristics and Leakage Currents

The capacitance versus voltage characteristics were measured by biasing a detector and measuring the capacitance between the p-side and n-side bias lines using an LCR meter. Figure 19 shows the CV characteristics of one of the SI detectors measured at several frequencies. The frequency dependence is probably due to the finite implant resistance and the polysilicon bias resistors. At low frequencies, the measured capacitance at full depletion approaches that of the true detector capacitance, since the impedance of these resistances becomes relatively small. From this measurement we obtain a full depletion voltage of approximately 18 V, which agrees well with the value measured using a test structure from the same wafer.

Leakage currents of good detectors were less than 2 μA for a total active area of 24.5 cm^2 and a detector thickness of 297 μm. Figure 20 shows the IV curve for one of the Micron wedge detectors. At the full deletion voltage (18 V) the total leakage current was 298 nA and at 40 V it was 450 nA. These leakage currents are very low and so this detector design will be suitable for use in a high rate environment such as that found at the Tevatron.

Coupling Capacitors and Polysilicon Resistors

The capacitance of the coupling capacitors was measured by connecting one probe to the aluminum strip and another probe to the dc contact hole which connects to the strip implantation. The capacitance is shown as a function of measurement frequency in Figure 21. The decline of the measured capacitance as the frequency increases is due to the finite resistance of the strip implantation [11]. At low frequencies, the effect of this resistance is small and the measured capacitance is about 160 pF. This value is about 20% higher than the expected value. Two effects may explain this – the uncertainty in the strip width and dielectric thickness, and the capacitance to neighboring strips.

The breakdown voltage of the coupling capacitors is an important parameter, since if it is too low it will limit the maximum operating voltage. The coupling capacitor leakage current as a function of applied voltage was measured for capacitors fabricated using a 200 nm SiO_2 layer and for capacitors using 220 nm SiO_2 + 100 nm Si_3N_4. A current limit of 50 nA was imposed to avoid damage to the capacitors. Typical leakage current curves are shown in Figure 22. The breakdown voltage for the capacitors with only 200 nm of SiO_2 is ~ 85 V. For capacitors using the double layer of dielectric material, the breakdown voltage is ~ 185 V.

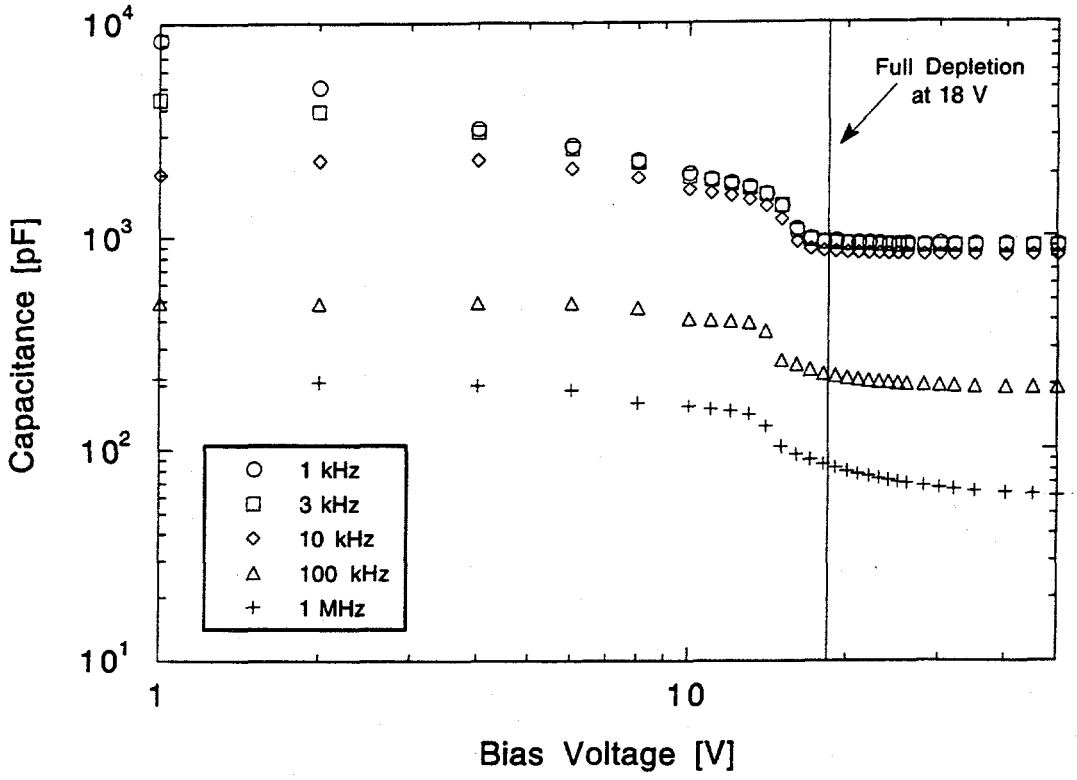

Fig. 19 Capacitance - Voltage characteristics for a double-sided wedge detector.

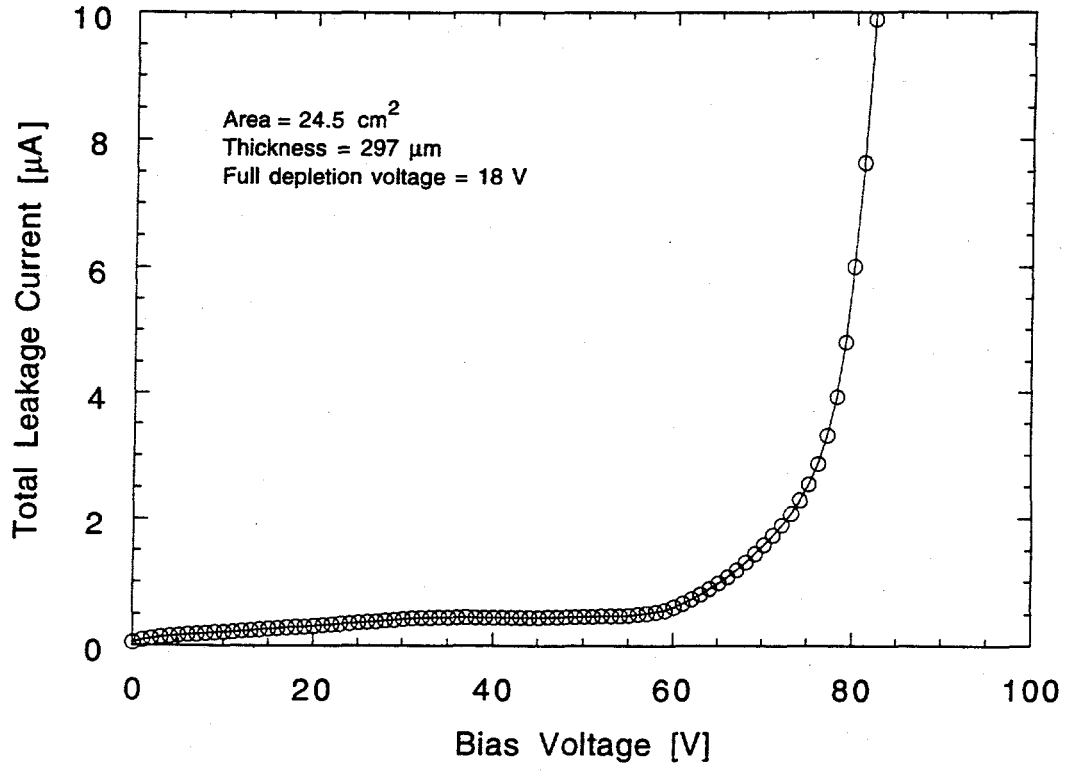

Fig. 20 Leakage current versus bias voltage for a double-sided wedge detector. The active area is 24.5 cm^2.

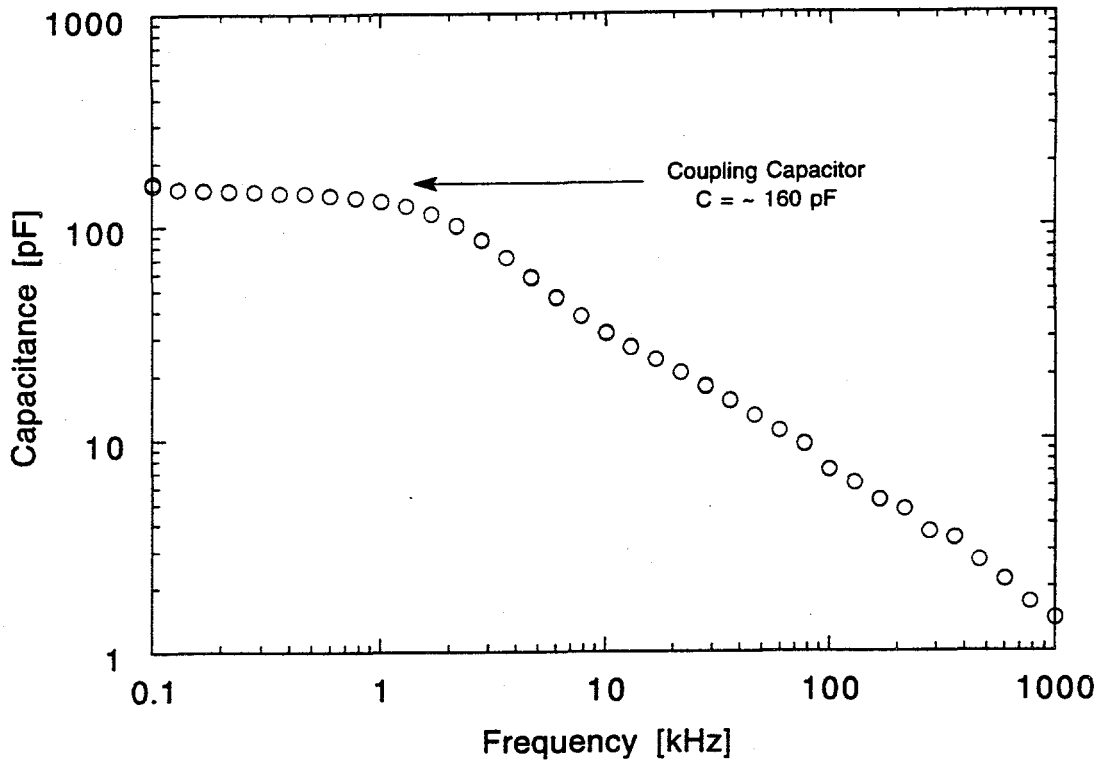

Fig. 21 Capacitance of a coupling capacitor versus measurement frequency.

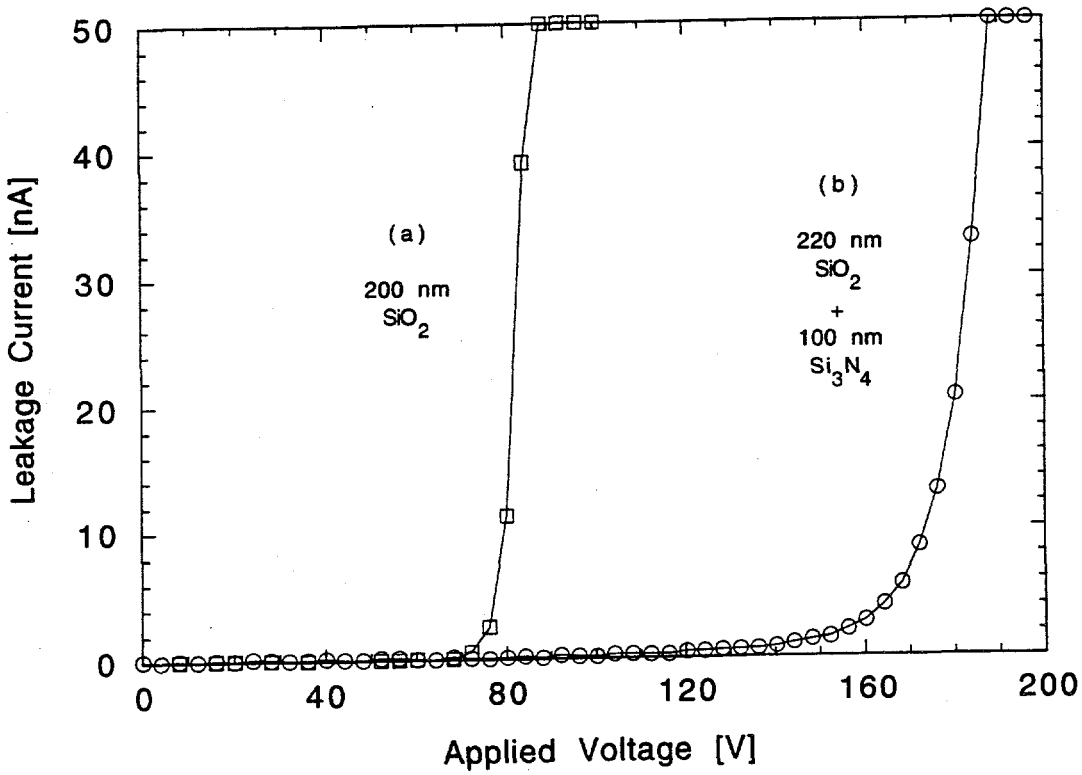

Fig. 22 Coupling capacitor leakage current versus applied voltage for (a) 220 nm SiO_2 dielectric layer and (b) 220 nm SiO_2 layer plus a 100 nm Si_3N_4 layer. The extra layer increases the coupling capacitance and decreases the chances of pinholes occurring.

Over the next few months, we will complete our detailed evaluation of the two detector designs. We will then place an order with one of the companies for sufficient detectors for the new tracker geometry. We will redesign the mask layouts at UC Riverside, using AutoCAD on a Silicon Graphics workstation. By the time the final detectors arrive, we will have set up an automated probe station test stand, using a Macintosh to control BPIB semiconductor test equipment with LabVIEW. This testing procedure will be adopted at Fermilab and at LBL, so that all wafers for the barrels and disks are uniformly tested and assessed in preparation for assembly.

We will be using a 1064 nm laser and x-y translation tables to evaluate the silicon wedge detectors once they have been wire-bonded to readout chips. We are setting up this system and integrating it into our CAMAC-based readout system. This readout system is designed for the front-end SVX chips used by CDF on their silicon vertex detector. By the end of the calendar year, we hope to have the first prototype SVX II digital readout chips, which will be read out using a VME-based system. Over the next year, we will develop a standard method for testing every channel of large numbers of detectors, for adoption at Fermilab, where the ladders for the barrels will be tested, as well as for use at UCR in testing the silicon wedge detectors. This system will probably be implemented using LabVIEW on a Macintosh, which will also control the VME readout system. The laser test system will be similar to the system we are setting up for the SDC Silicon Tracker (see section 1.3.3 (b) and Figure 28).

(e) *Design of the Readout Mount*

Over the past year, work has been done by the UCR group on the design of the readout mount for the Silicon Tracker. The readout mount includes all the material between the readout chips and the silicon detector, and a cross-section is shown in Figure 23. It provides mechanical mounting for the chips, which have to be wire-bonded to the readout strips on the detector. It also provides mechanical support for the ladders or wedges onto the cooling pipe. The original plan was to mount the detector modules with the cooling pipe directly on the surface of the readout chips. However, this was shown by the UCR group to be a very high-risk design, with the possibility of large-scale chip failure [12]. The mounting method was replaced with an improved off-chip design. The readout mount provides a thermal path for the heat from the readout chips to the cooling pipe, via a 300 μm thick layer of beryllium, on each side of the detector. The beryllium also provides shielding of the 53 MHz clock signals from the detector, to prevent crosstalk.

Work was done by the UCR group on the materials used in the high density interface circuit (HDI) [13]. It was found that it is not easy to wire bond to a kapton circuit, since it is not sufficiently rigid, and absorbs much of the ultrasonic energy needed to form the bond. The HDI will now be made of adhesiveless kapton, where the layers of copper for the circuitry traces are produced directly on the kapton surface, without intermediate layers of epoxy. This reduces the mass of the HDI considerably, and improves the prospects for successful wire-bonding by reducing the step height and increasing the rigidity of the structure. Cross-sections through the old and new HDI's are shown in Figure 24.

(f) *Evolution of the Silicon Tracker Design and Geometry*

In January 1993, the Silicon Tracker group held a three day workshop at LBL, which resulted in a provisional Technical Design Report [14]. This was presented to the full DØ upgrade group by A. Heinson [15]. In March, an internal DØ Technical Review gave their approval to the design [16, 17].

Fermilab budget cuts are now mandating a redesign of the entire Upgrade tracking system. We have to reduce the cost of the Silicon Tracker by over 50%. This redesign is still in progress. Final approval of the scaled-back Upgrade tracking system is expected from the Fermilab PAC in November 1993.

A. Heinson has taken the initiative to explore possible redesign options. The UCR group is concerned to maintain the acceptance of the Silicon Tracker, especially in the central region with $|\eta| < 2$, where most $t\bar{t}$ events are expected. The interaction region at the Tevatron is very long, with $\sigma(z) = 22$ cm. Therefore, long central barrels are needed. Acceptance calculations have included the length of the central barrel, the number of barrel layers, the number and positions of disks, the effect of cracks on the acceptance, the lever arm needed for high resolution impact parameter measurement, and the implications of z measurement in the barrel region. The effect of the detector geometry on the acceptance for $t\bar{t}$ events is shown in Figure 25 [18]. The silicon geometry used for Figure 25 has a central barrel region only. Each barrel segment is 24 cm long, giving a total barrel length of 72 cm or 96 cm, which may be compared with the length of the CDF SVX II barrels of 102 cm.

Silicon detectors are not as efficient as more traditional tracking systems such as wire chambers. The probability of getting 3 hits from a particle traversing 3 layers of silicon is only ~ 87%. This assumes an efficiency in good parts of the silicon of 97% and that 1.5% of the silicon channels are dead [19], giving an efficiency per layer of 95.5%. The efficiency has not been included in the geometrical acceptances shown in Figure 25.

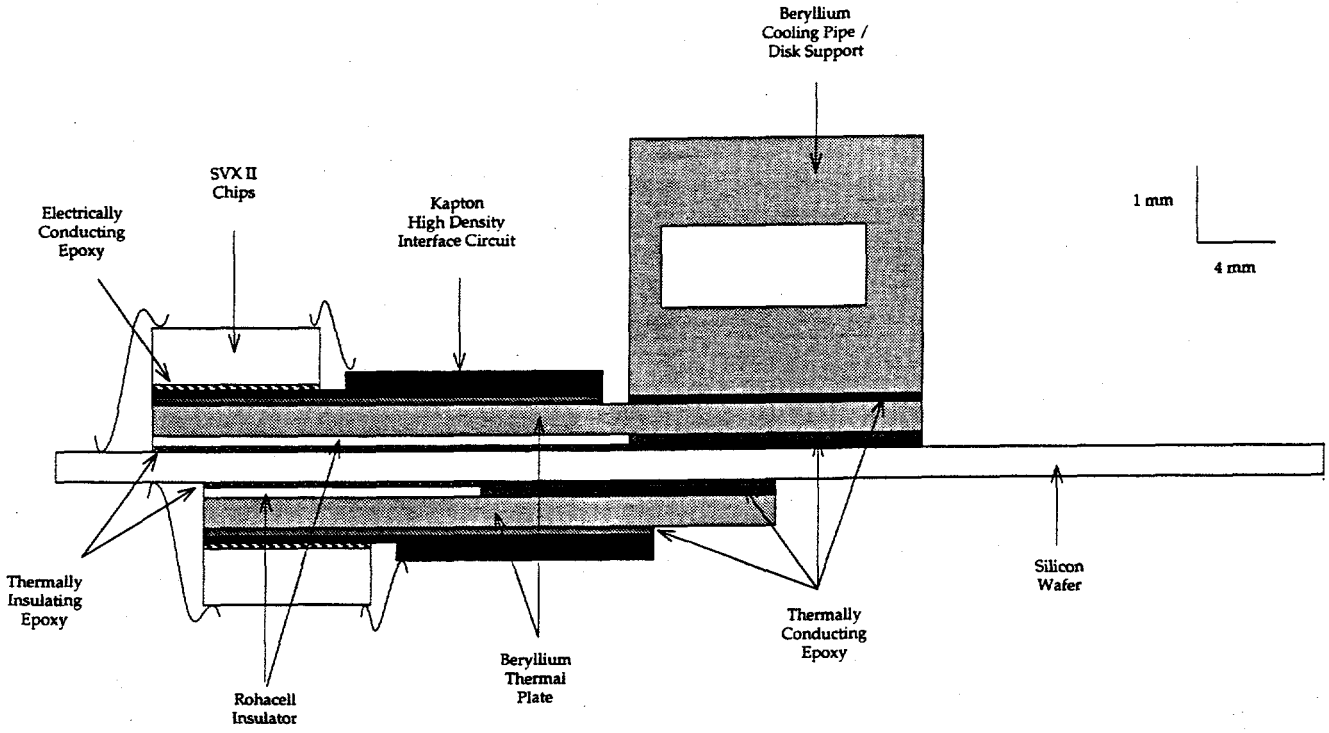

Fig. 23 A cross-section through the readout mount at the edge of a double-sided wedge detector. The beryllium cooling pipe is approximately thermally equidistant from each of the rows of readout chips.

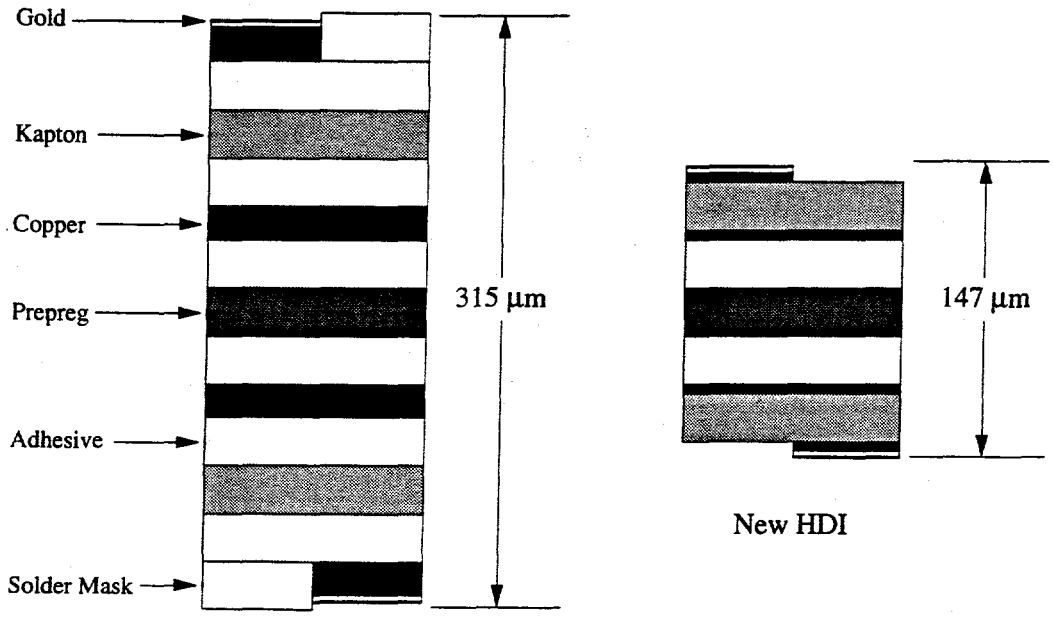

Fig. 24 Cross-sections through the Kapton sandwiches of the old and new High Density Interface circuits, showing the reduction in material obtained by using adhesiveless material, thinning the copper and omitting the solder masks.

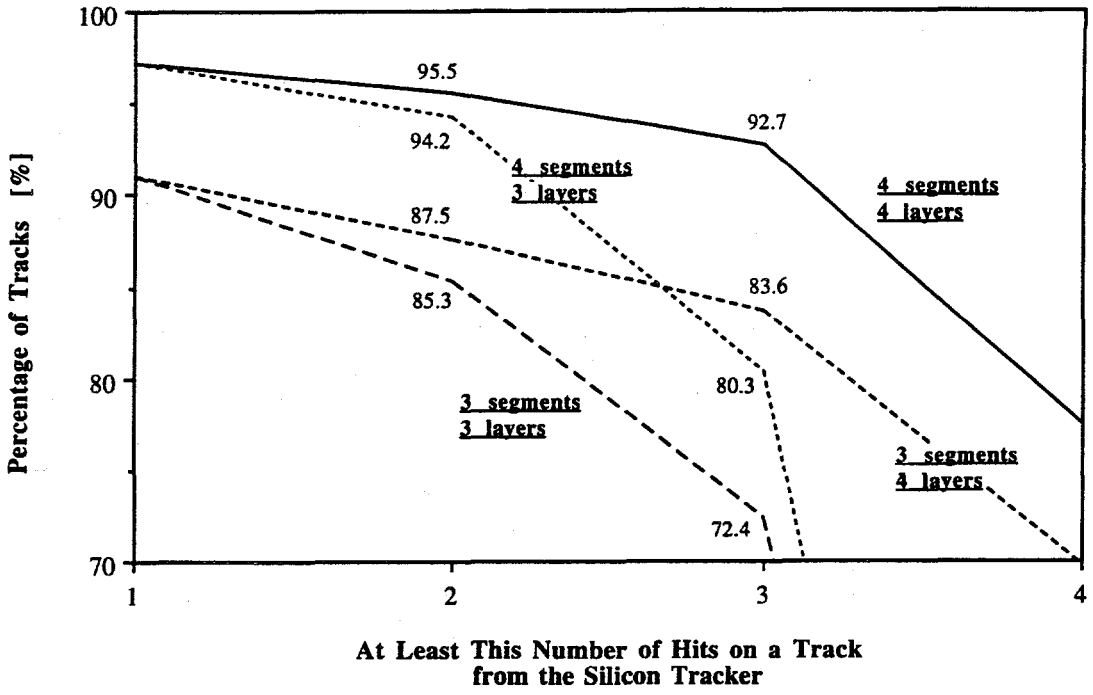

Fig. 25 The effect of changing the number of barrel layers and of changing the length of the Silicon Tracker on the acceptance for $t\bar{t} \rightarrow W/b \rightarrow \mu/e$, with $\sigma(z) = 22$ cm, and $M_{top} = 120$ GeV/c^2.

(g) *Conclusions*

Our group has played a major and expanding role in this project since its inception. We have complete responsibility for the design and production of the silicon wedge detectors for the disks, which are one of the most technically challenging parts of the system. We have taken the initiative in organizing the silicon group and its schedules, and are leading the group through the difficult task of redesigning the tracker. We plan to continue this level of involvement over the next few years until the Silicon Tracker is installed and running in DØ and we are using it to make world class physics measurements.

(h) *References*

1 E823 (DØ Upgrade) DØβ, The DØ Collaboration, May 1993, DØ note 1733.

2 A.P. Heinson, for the DØ Collaboration, "The DØ Upgrade Silicon Tracker", Proceedings of the 7th Meeting of the American Physical Society Division of Particles and Fields, Fermilab, November 1992, (World Scientific 1993), p. 1731–3. Also DØ note 1542, 27 pages.

3 A.P. Heinson, "A Silicon Tracker for the DØ Detector", presented at UC Irvine and UCLA in February 1993.

4 J. Ellison, A. Kernan and D. Smith, "Simulation of *b*-jet identification in a non-magnetic detector", Nucl. Instr. Meth. A302 (1991) 227-240.

5 Micron Semiconductor, 1, Royal Buildings, Marlborough Road, Churhill Industrial Estate, Lancing, Sussex, BN15 8UN, England.

6 SINTEF SI, P.O. Box 124 Blindern, 0314 Oslo 3, Norway.

7 J. Ellison et al., "Study of Radiation Effects on AC-Coupled Silicon Strip Detectors", Proceedings of the 2nd Conference on Advanced Technology and Particle Physics, Como, Italy (1990), Nucl. Phys. B (Proc. Sppl.) 23A (1991) 340.

8 J. Ellison, S. Jerger, C. Lietzke, S.J. Wimpenny et al., "Tests of the Radiation Hardness of VLSI Integrated Circuits and Silicon Strip Detectors for the SSC Under Neutron, Proton and Gamma Irradiation", IEEE Trans. Nucl. Sci. NS-38 (1991) 269-276.

9 K. Yamamoto et al., "A Study on the Interstrip Capacitance of Double-Sided Silicon Strip Detectors", Proceedings of the 6th European Symposium on Semiconductor Detectors, Milan, Italy (1992), Nucl. Instr. Meth. A326, 222-227.

10 J. Ellison, for the DØ Collaboration, "Silicon Microstrip Wedge Detectors for the DØ Silicon Tracker", submitted to Nucl. Instr. Meth., June 1993, for the proceedings of the International Symposium on Development and Application of Semiconductor Tracking Detectors, May 1993, Hiroshima, Japan. Preprint number UCR/DØ/93–09.

11 H.F.-W. Sadrozinski, "Capacitances in Silicon Microstrip Detectors", presented at the International Symposium on Development and Application of Semiconductor Tracking Detectors, May 1993, Hiroshima, Japan.

12 A.P. Heinson, "Mounting the Cooling Pipe / Support Frame on the SVX Chips", presented at the LBL DØ Silicon Tracker meeting, September 1992.

13 A.P. Heinson, "Bonding to Kapton", presented at the LBL DØ Silicon Tracker meeting, September 1992.
The HDI has been designed by N. Roe and an engineering team at LBL.

14 "E823 (DØ Upgrade), Step 1 Silicon Tracker Design Report", March 1993, draft, 74 pages.

15 A.P. Heinson, "Design Decisions from the Silicon Tracker Workshop at LBL", January 1993, part of DØ note 1615, 29 pages.

16 "DØ Upgrade Silicon Step 1 Tracker Review", J. Sculli, March 1993, DØ note 1708.

17 "Internal Review of the Upgrade Step 1 Silicon Tracker", April 1993, DØ note 1669.

18 Simulations studies were made using a program based on a program by N. Roe.

19 O. Schneider, for the CDF Collaboration, "Performance of the CDF Silicon Vertex Detector", Proceedings of the 7th Meeting of the American Physical Society Division of Particles and Fields, Fermilab, November 1992, (World Scientific 1993), p. 1743–5.
Similar results have been reported at meetings for SDC Silicon Tracker prototype detectors and for Moscow State University prototype detectors for DØ.

1.3 SDC : Proton–Proton Interactions at 40 TeV

1.3.1 *Introduction*

The Solenoidal Detector Collaboration (SDC) will build one of two major detectors for the 40 TeV Superconducting Super Collider in Texas. UC Riverside joined SDC in mid 1989, and has taken an increasing role over the past four years. Our efforts are focussed through the Silicon Tracker group on designing and building the world's largest silicon detector, to be completed by 1998. This year the UCR hadron collider group has obtained funding of $90,000 per year from the Texas National Research Commission Laboratory, which will considerably strengthen our SDC silicon tracker research program. The funds will be used to support two postdoctoral researchers and will result in a major increase in our activities. Two outstanding researchers have been recruited, both with expertise in silicon detector development. They will join our group in the coming months. We will also receive $30,000 this year from SDC to purchase equipment needed for the project.

1.3.2 *The SDC Silicon Tracker*

The design of the SDC detector for the SSC [1,2,3] calls for a very large silicon tracking system [4,5] which will form the basis of the charged particle tracking at radii between 9 and 36 cm from the beam (Figure 26). The total area of silicon is about 17 m^2 and the system contains about 6×10^6 electronics readout channels. The design represents a significant step beyond any of the present generation of collider experiment silicon detectors. In March 1992, the Silicon Tracking Conceptual Design Report was released, which contains very detailed specifications of the performance goals for the system, and of the physical design of the detector and its readout system [6]. The design is also summarized in the SDC Technical Design Report [4]. There are 122 physicists and engineers associated with this project, from 27 universities and laboratories in the United States, Japan, Italy, Great Britain and the Former Soviet Union. The group at UC Riverside is working very closely with the group at UC Santa Cruz, from where the whole project is coordinated and led.

The tracker consists of 300 μm thick double-sided detectors with axial strips on one side and stereo strips on the other side. Pairs of such detectors with opposite stereo pitch are arranged in superlayers in a cylindrical barrel section and also in planar endcaps. The superlayers allow local hit association into segments that are then further associated into tracks. The intermediate angle

detectors are spaced along the beam out to a distance of 2.58 m from the interaction point to allow good momentum measurement out to a pseudorapidity of $|\eta| \leq 2.5$.

(a)

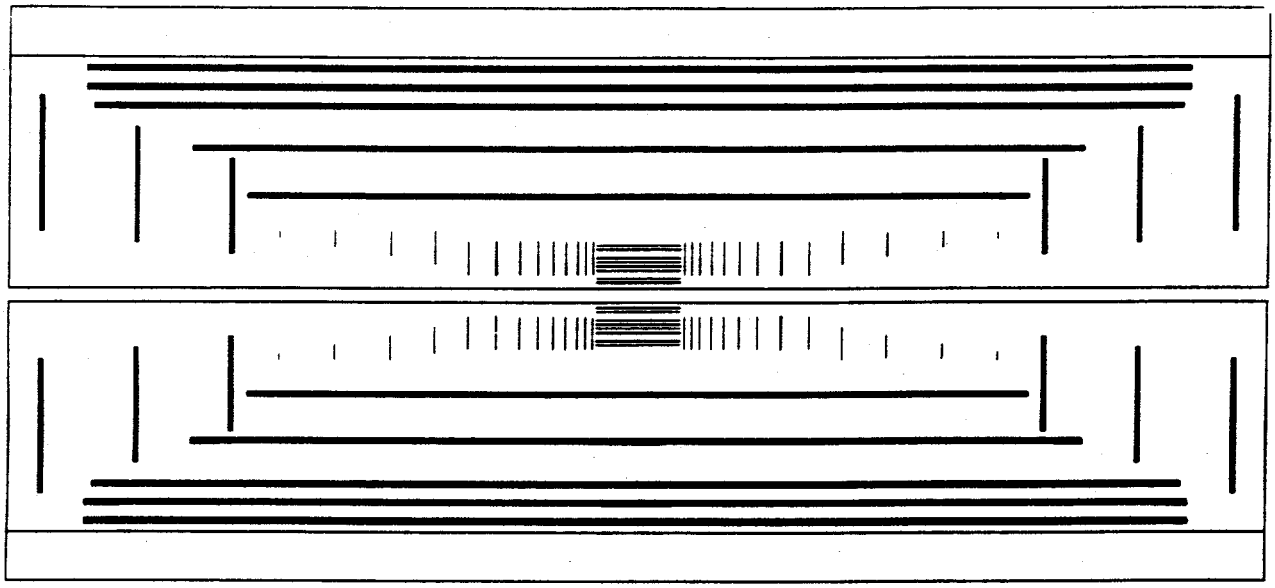

(b)

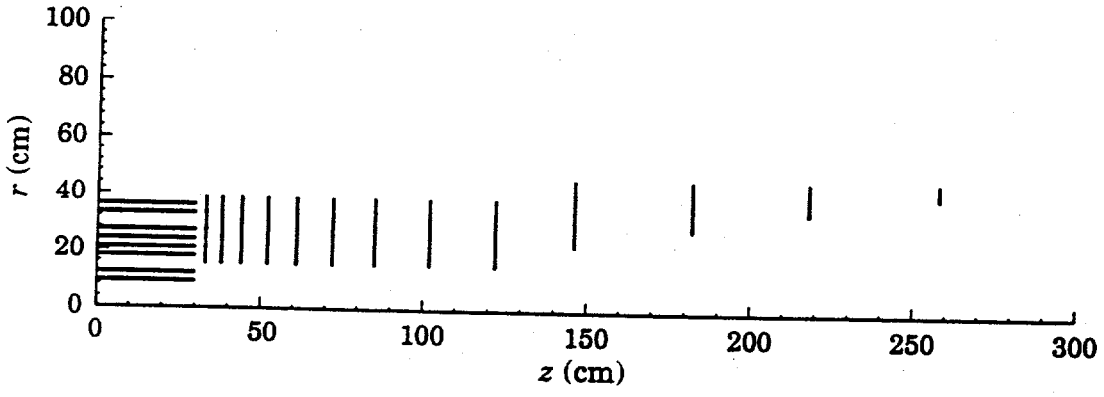

Fig. 26 (a) Full SDC tracking system, including inner silicon layers, outer straw-tube superlayers and forward gas microstrip detectors. (b) Silicon tracker design.

1.3.3 *Detector R&D at UCR*

The following section gives details of the UCR contribution to the SDC Silicon Tracker to date, and presents proposals of what we plan to do over the next few years.

The silicon detector laboratory at Riverside was set up in 1989 using UCR funding, with the purpose of studying silicon detectors and readout for trackers in the hadron collider environment. Since this time the facility has been continually evolving and has now doubled in size. It is equipped with a semiconductor probe station for testing prototype detectors, a clean room containing an ultrasonic wire bonder, and various test and readout systems for evaluating the behavior of prototype detectors and the effects of radiation damage. Recently we have procured a 1064 nm wavelength laser which will simulate a charged particle track in the silicon detectors and enable automated testing of large numbers of silicon detector modules.

Our SDC effort is concentrated in three main areas: (a) radiation damage studies, (b) design of an automated laser module tester and (c) wedge detector R&D for the forward silicon disks.

(a) *Radiation Damage Studies*

We have carried out systematic studies of the effects of radiation damage on silicon detectors for SSC use, with the aim of determining the limit on the lifetime of silicon detectors at the SSC. This has resulted in the identification of a radiation hard detector biasing technology and enabled us to predict detector operating lifetimes at the SSC [6–10]

Work on radiation damage studies has made rapid progress over the past two years. Beam tests were done in September 1991 and in September 1992 in collaboration with UC Santa Cruz and Los Alamos. The UCR contribution consisted of preparations for exposures, pre-irradiation measurements at UCR, setting up and running during irradiation at the LAMPF proton beam and post-irradiation measurements and data analysis at UCR. The main results are summarized below:

- We have measured the capacitance of the ac-coupling capacitors as a function of fluence. We found no change after neutron and proton fluences of 1×10^{14} cm^{-2}. The capacitor breakdown voltages were > 150 V after exposure, well above the expected maximum operation voltage.

- Exposure of polysilicon resistors to 8×10^{14} protons cm^{-2} and 3×10^{13} neutrons cm^{-2} resulted in changes of less than 10% in the value of the resistors. These resistors are used to bias the strips on ac-coupled detectors and the observed changes are not a problem for

detector performance. Therefore, this biasing method has been chosen for the SDC detectors.

- The increase in leakage current due to 650 MeV proton irradiation was measured and resulted in a damage constant (including annealing effects) of $\alpha = 3 \times 10^{-8}$ nA cm^{-1} at 26°C and $\alpha = 0.6 \times 10^{-8}$ nA cm^{-1} at 0°C. The damage constant is an important parameter in determining detector lifetime, since the leakage current fluctuations are an additional noise source.

- The change in doping concentration of the bulk silicon was measured. Values for the acceptor creation rate of $\beta = 0.02$ cm^{-1} at 26°C and $\beta = 0.045$ cm^{-1} at 0°C were obtained. A dramatic 'anti-annealing' behavior was observed for detectors annealed at room temperature, while this was not observed for 0°C annealing. This is shown in the plots of full depletion voltage versus time in Figure 27. The consequences are that the Silicon Tracker must be operated at a temperature of $\leq$ 0°C and that during shutdown periods this temperature must be maintained.

The above measurements demonstrate that double-sided silicon detectors will function up to doses of 10^{14} particles cm^{-2}, implying 15 years of lifetime at a radius of 10 cm for the SSC design luminosity. These results were presented by J. Ellison in invited talks at the 1992 European Symposium on Semiconductor Detectors and at the 1990 London Conference on Position Sensistive Detectors.

Over the next few years, we will continue these studies and plan to measure the radiation damage effects on detector pulse height, pulse shape, and interstrip resistance and capacitance. We will make the transition between irradiating simple detectors with no readout electronics to using full prototype detector modules. This will allow a detailed understanding of how detectors will behave during running at the SSC.

(b) *Detector Module Testing and Calibration*

Another important area of research at UCR is directed towards the development of an automated calibration and laser test station for silicon detector module testing (a "module tester"). To build a successful large array will require the testing and integration of very large numbers of detectors and electronics chips. The development of suitable testing equipment and a quality asurance program will be very challenging. The ultimate goal is to arrive at a system that

(a)

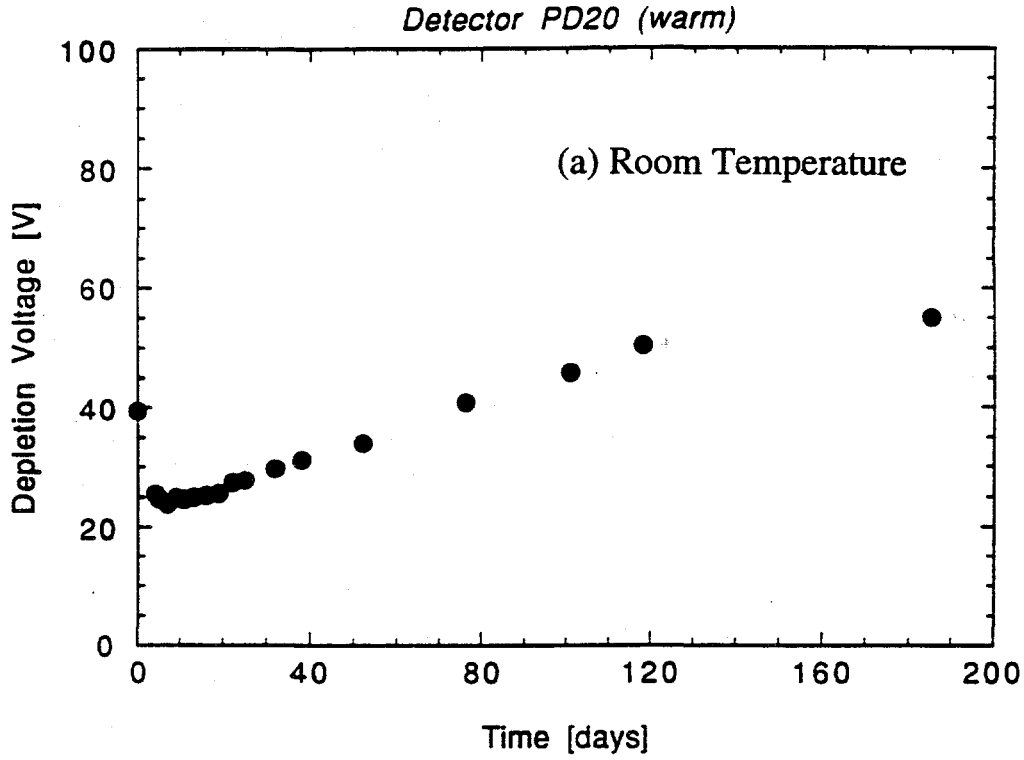

(b)

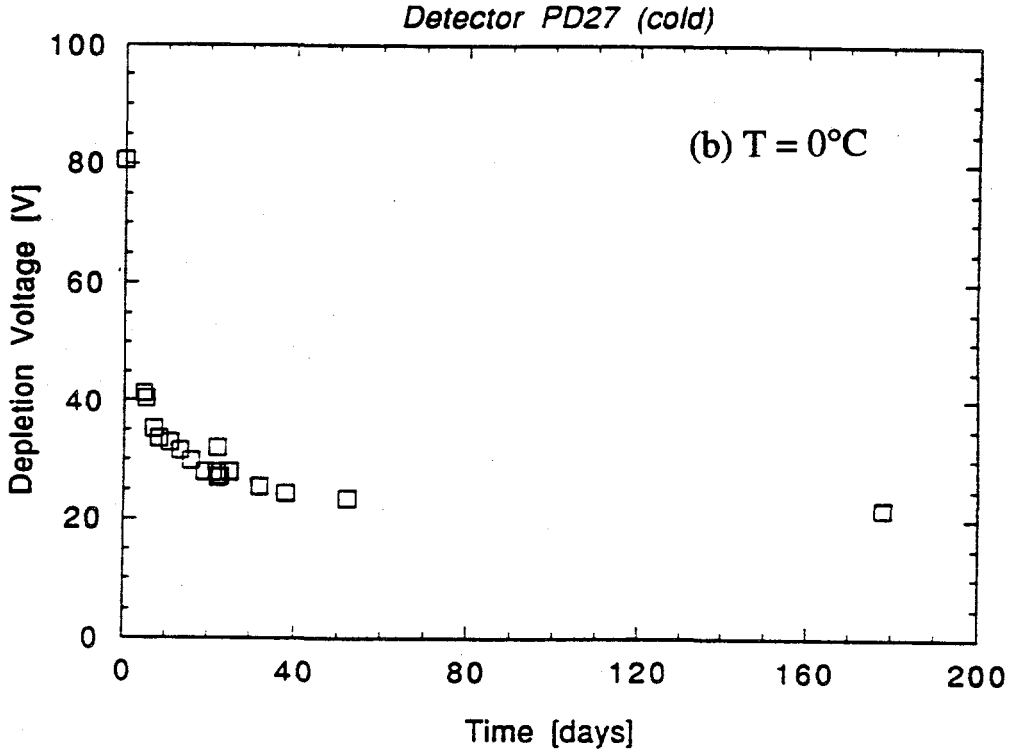

Fig. 27 Detector full depletion voltage versus annealing time at (a) room temperature and (b) T = 0°C. The fluence was $\Phi = 8.5 \times 10^{13}$ protons cm^{-2}.

can be used for testing and calibration of over several thousand detector modules in approximately a one-year time period.

Calibration and testing of the readout electronics chain will be very challenging because the front-end is essentially a "hit / no-hit" system and therefore only limited signal diagnostics are available. The total number of channels is more than a factor 10 higher than previous systems and understanding the effects of variations in gain, shaping time, noise, and thresholds will be critical.

Module testing will be done using an automated laser test station. A laser of the correct wavelength and power can simulate fairly closely the ionization profile of a minimum ionizing particle. Using a precision x–y translation stage, the laser can be directed at a single strip of the detector and can be stepped from strip to strip very quickly with 1 μm precision. By controlling the x–y stage and the data acquisition system by computer, every channel of the module can be tested automatically. This will immensely speed up the testing of modules compared with more conventional test methods such as test beams, cosmic rays or radioactive sources. We have recently procured the 1064 nm laser and a computer-controlled x–y translation stage and are studying various optical configurations for producing the very small laser spot size required (about 5–10 μm diameter).

We have prepared a detailed set of specifications for the module tester. We will build the module tester at UCR and develop the calibration and testing procedures. It will then be replicated at other Universities and Labs, so that testing of the final modules for SDC can be distributed among several groups. A schematic of the module tester is shown in Figure 28. The setup consists of the following main components:

- A pulsed laser of wavelength 1064 nm, with a pulse width of appproximately 1 ns. The wavelength is chosen to give a roughly uniform distribution of e–h pair creation as a function of silicon depth, thereby simulating closely the ionization deposition of a minimum ionizing particle.

- A collimation and optics system that will focus the laser beam to a diameter of about 5 μm and keep the beam perpendicular to the detector module.

- A precision x–y translation stage on which the detector modules are mounted. This will have a resolution of 1 μm and be connected to a GPIB bus to enable computer control.

- A VME-based data acquisition system running at 63 MHz. This will provide control for the front end electronics and will record the chip ID and channel address of strips with hits above threshold.

- A Macintosh for control, data acquisition and analysis.

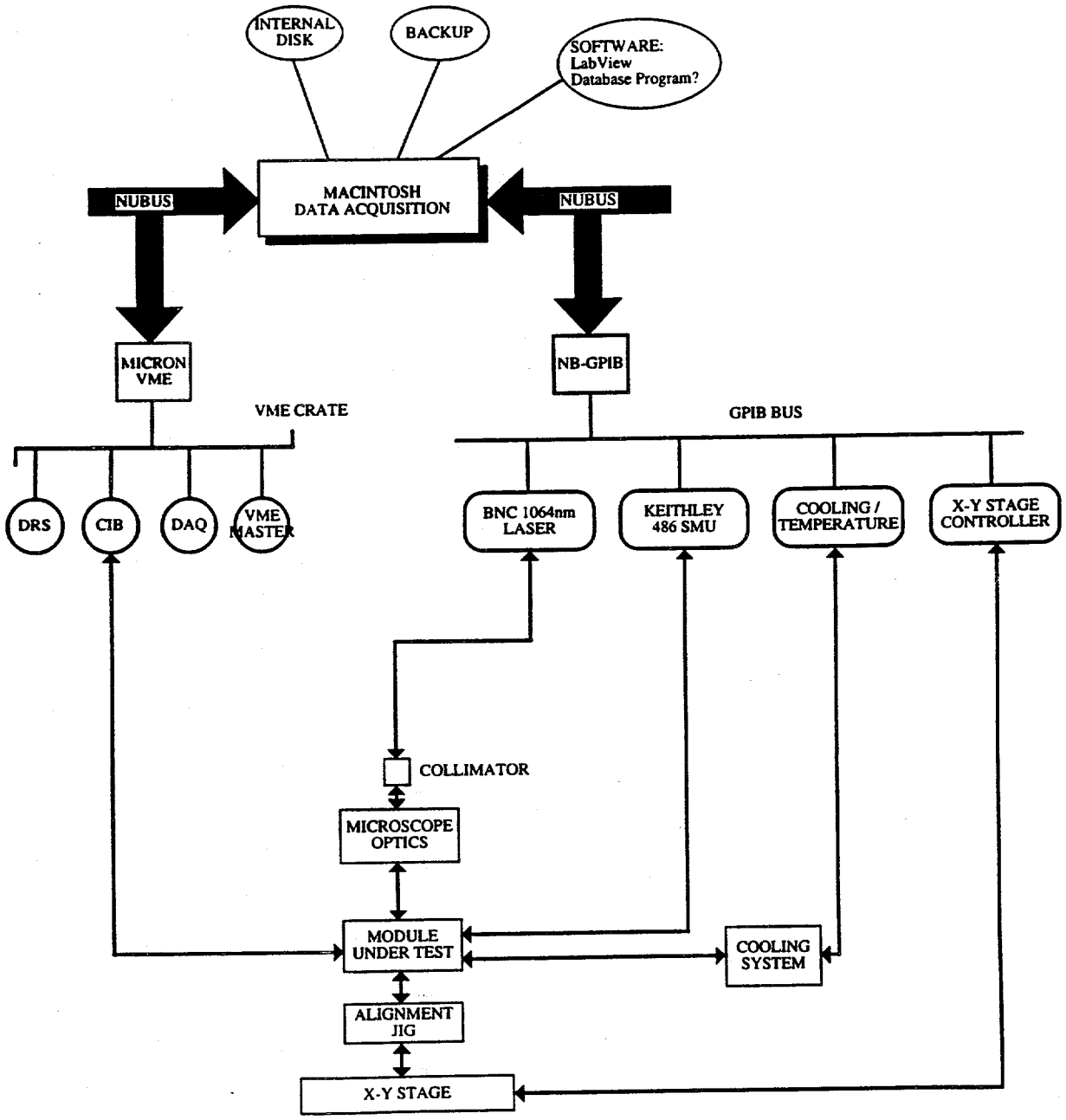

Fig. 28 Schematic diagram of the SDC silicon detector module tester.

(c) *Wedge Detector Design and Testing*

The group at UCR is working on the design and testing of the forward disks for the SDC tracker. Single-sided test structures are being fabricated at Hamamatsu Corp. and will be used to optimize the wedge detector designs. We are collaborating with other universities to design the masks for the double-sided ac-coupled wedge detectors, and then to evaluate the prototypes produced. There will be 8 different detector designs for the disks of the final detector, and once these designs are finalized, production will begin. With the addition of two TNRLC funded postdocs, we will be able to make a significant contribution to this work.

1.3.4 *References*

1 J. Ellison, S.J. Wimpenny et al., "Solenoidal Detector Collaboration Expression of Interest to Construct and Operate a Detector at the Superconducting Super Collider", May 24th 1990.

2 J. Ellison, S.J. Wimpenny et al., "Letter of Intent by the Solenoidal Detector Collaboration to Construct and Operate a Detector at the Superconducting Super Collider", November 30th 1990.

3 J. Ellison, A. Heinson, S.J. Wimpenny et al., "SDC Technical Design Report", April 1, 1992, SDC-92-201, SSCL-SR-1215.

4 J. Ellison, S.J. Wimpenny et al., "SSC Detector Subsystem Proposal: Subsystem R&D Proposal to Develop a Silicon Tracking System", 1989.

5 J. Ellison, S.J. Wimpenny et al. "Subsystem R&D Proposal to Develop a Silicon Tracking System", 1990.

6 J. Ellison, D. Joyce, C. Lietzke, S.J. Wimpenny et al., "SDC Silicon Tracking Conceptual Design Report", SDC-91-133.

7 J. Ellison, S.J. Wimpenny et al., "Study of Radiation Effects on AC-Coupled Silicon Strip Detectors", Proceedings of 2nd Conference on Advanced Technology and Particle Physics, Como, Italy, 1990. Nucl. Phys. B (Proc. Suppl.) 23A (1991) 340.

8 J. Ellison, S. Jerger, C. Lietzke, S.J. Wimpenny et al., "Tests of Radiation Hardness of VLSI Integrated Circuits and Silicon Strip Detectors for the SSC Under Neutron, Proton and Gamma Irradiation", IEEE Trans. Nucl. Sci. NS38 (1991) 269.

9 J. Ellison et al., "Radiation Hard Frontend Electronics and Silicon Microstrip Detectors", Proceedings of the Symposium on Detector Research and Development for the SSC, Fort Worth, TX, October 15-18, 1990. World Scientific Publishing, Singapore, p. 166.

10 J.A. Ellison, J.K. Fleming, E. Reed, S.J. Wimpenny et al., "Temperature Effects on Radiation Damage to Silicon Detectors", Nucl. Instr. and Meth. A326 (1993) 373.

11 J.A. Ellison, J.K. Fleming, S. Jerger, E. Reed, S.J. Wimpenny et al., "Temperature Dependence of Radiation Damage and its Annealing in Silicon Detectors", submitted to IEEE Trans. Nucl. Sci.

1.4 Task A1 : Computing Facilities

1.4.1 *Introduction*

This section describes the existing computing facilities for the hadron collider group at UC Riverside, and our aniticipated needs over the next three years. The present configuration is the result of a substantial modernization of the computer facilities, funded by a $300k DOE Computing Infrastructure Award. The DOE and the University each provided half of the money. The department system now consists of a 12 node VAX/VMS cluster and a 5 node UNIX cluster, which are very heavily used by the Hadron and e^+e^- Collider groups.

Following the start of DØ running in May 1992, our data processing needs have increased enormously. With 17 pb^{-1} of data from the first collider run and preparations being made for the start of the second run in the late fall, there is an enormous need for large volume Monte Carlo generation, both for data analysis and for detector upgrade design. For example, the UCR group is playing a leading role in the top search and is using the two UCR clusters for generating high statistics Monte Carlo datasets. At present levels, this corresponds to a processing rate of around 300 events per day with full detector simulation, which is a major contribution to the DØ analysis effort. In addition, UCR physicists working on the upgrade Silicon Tracker design and the $WW\gamma$ and inclusive muon analyses are also consuming large amounts of processor time. While the upgraded VAX and UNIX systems are adequate for our current needs, we are moving very rapidly towards saturation and may need to request some upgrades such as memory in the near future.

In addition to the VAX and UNIX computing facilities, the hadron collider group also makes extensive use of Macintosh computers for data acquisition and analysis and instrument control in the laboratory. These machines are vital to the detector design and development for the DØ and SDC upgrade tracking systems. We have recently upgraded the system to cope with our increased work load. Macintosh's are also extensively used for word processing and report preparation.

1.4.2 *Vax and Unix Systems*

Figure 29 shows the Vax and Unix systems that are running on the UC Riverside campus. We have four Vax processors and every member of the group has an X-terminal and about 1 Gbyte of hard disk space for analysis files. There is also disk space for the entire DØ and SDC libraries. Backups are made using high density 8 mm tape drives. We have one Silicon Graphics Indigo

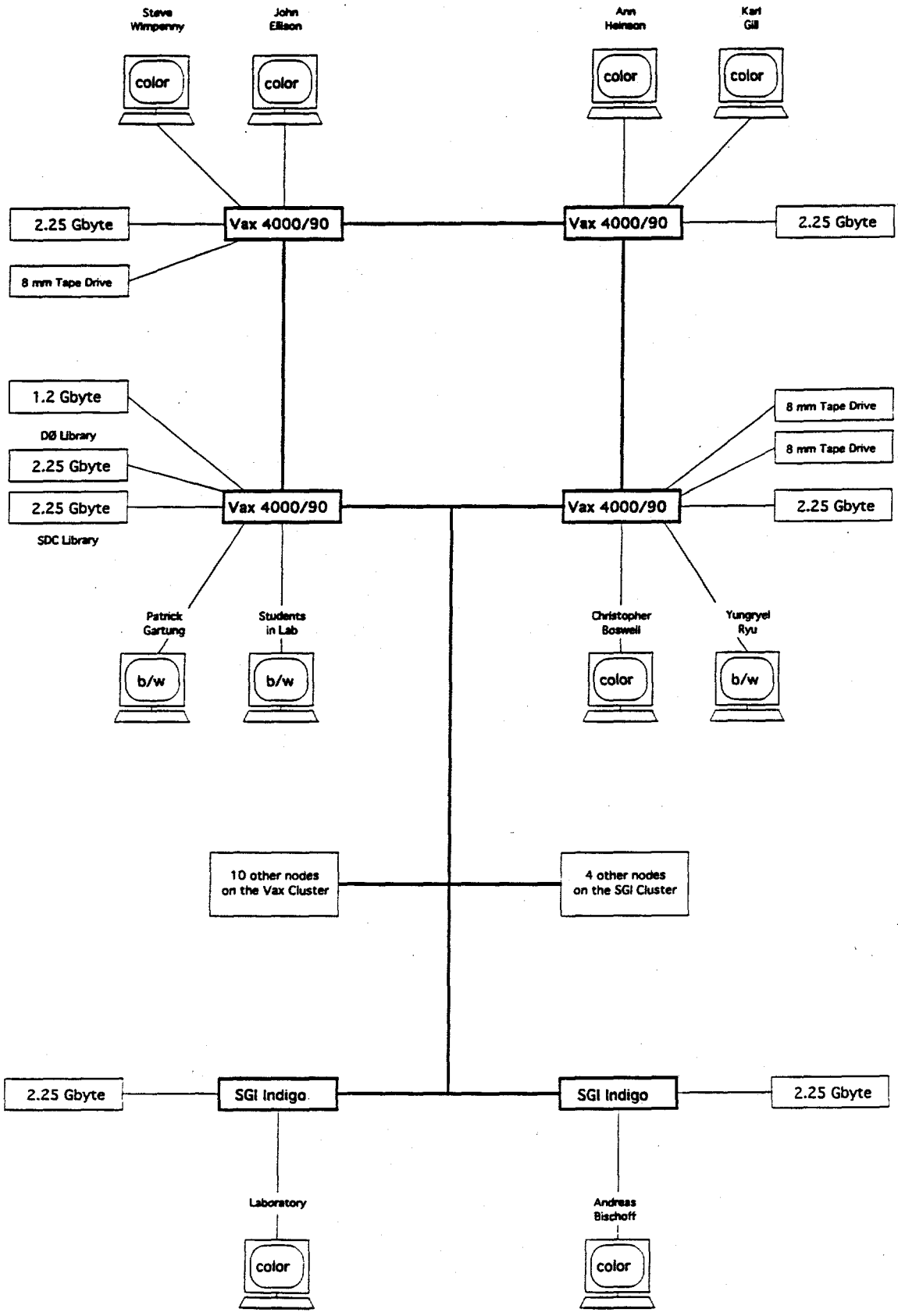

Fig. 29 UC Riverside hadron collider group computing facilities on campus.

workstation at present, and may purchase a second very soon, since user demand is continuing tc increase. We run AutoCAD on the SGI, for silicon detector mask design (see the section in this report on the DØ Upgrade), and will soon run TOSCA, PISCES II and SPICE to simulate measurements from the prototype detectors and to optimize their design for DØ.

Within the next couple of years, we will need to expand our Unix system, as the most cost-effective way of providing large amounts of computing power. We anticipate that we will need two Silicon Graphics Crimson machines, in order to continue to contribute significantly to the DØ analyses of data from Runs 1a and 1b, and to prepare adequately for Run 2, with the upgraded tracking system.

Figure 30 shows the UC Riverside $p\bar{p}$ group computing facilities at Fermilab. It includes a Vax Alpha, as part of a move by DØ to make extensive use of these machines, since they provide very large amounts of processing power relative to their cost. The Alpha needs much more disk space and memory than a 4000/60, as its system is significantly different. DØ code has been converted to run under the new operating system. These three machines are part of an extensive DØ Vax cluster, with over 90 other nodes. We anticipate that we will need to add two additional Vax Alphas to this group, to enable us to fulfil our commitments to the DØ analysis, with color x-terminals for event displays, and extra disk drives .

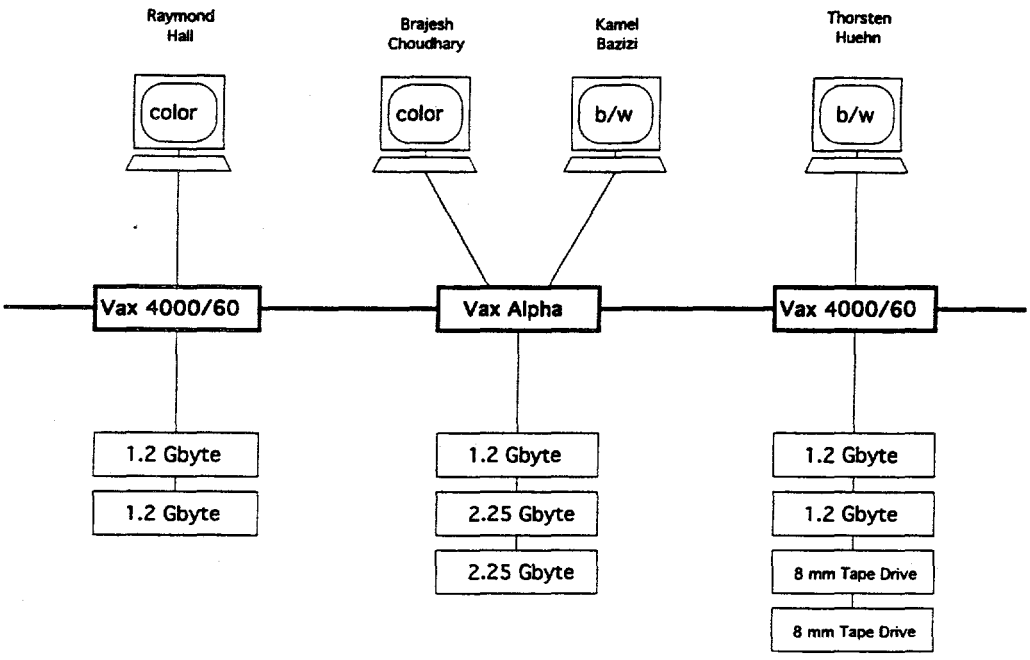

Fig. 30 UC Riverside $p\bar{p}$ group computing facilities at Fermilab.

1.4.3 *Macintosh Systems*

Figure 31 shows the Macintosh system that the hadron collider group has on the UCR campus. The system is very heavily used, for many purposes. The following list shows a few of the current and immediate future tasks performed with this system :

- Preparation of papers for publication
- Preparation of work for DØ and SDC notes
- Preparation of presentations for conferences, seminars and meetings
- Electrical and Mechanical CAD designing
- DØ upgrade design and project management
- Data acquisition for silicon detector readout
- Probe station control and video imaging
- Laser test system control
- Radiation damage measurements and data analysis
- Group administration

It is important to be able to make public presentations in color, and much data analysis also benefits from the use of color. Color is essential for our detector design CAD package due to the complexity of the multilayer mask designs. We have invested in sufficient input and output facilities to make this work possible. Backups are made onto optical disks, which offer large amounts of space on a flexible and reliable medium.

In the silicon laboratory, we are moving much of the data acquisition and instrument control onto Macintoshes, using the LabVIEW package from National Instruments. This package is being widely adopted throughout the scientific and engineering research communities, including Fermilab for DØ and Los Alamos for SDC. LabVIEW is a graphical programming language, containing an extensive plotting and fitting package. It replaces the need to write code in verbal languages such as FORTRAN, PASCAL or C. Instead, pictoral representations of the data acquisition are made, and virtual instruments are created, such as oscilloscopes, which may then be used on the Macintosh to view signals, and perform signal processing such as fast Fourier Transforms. It is much easier and faster to write new packages and to modify them as needs change.

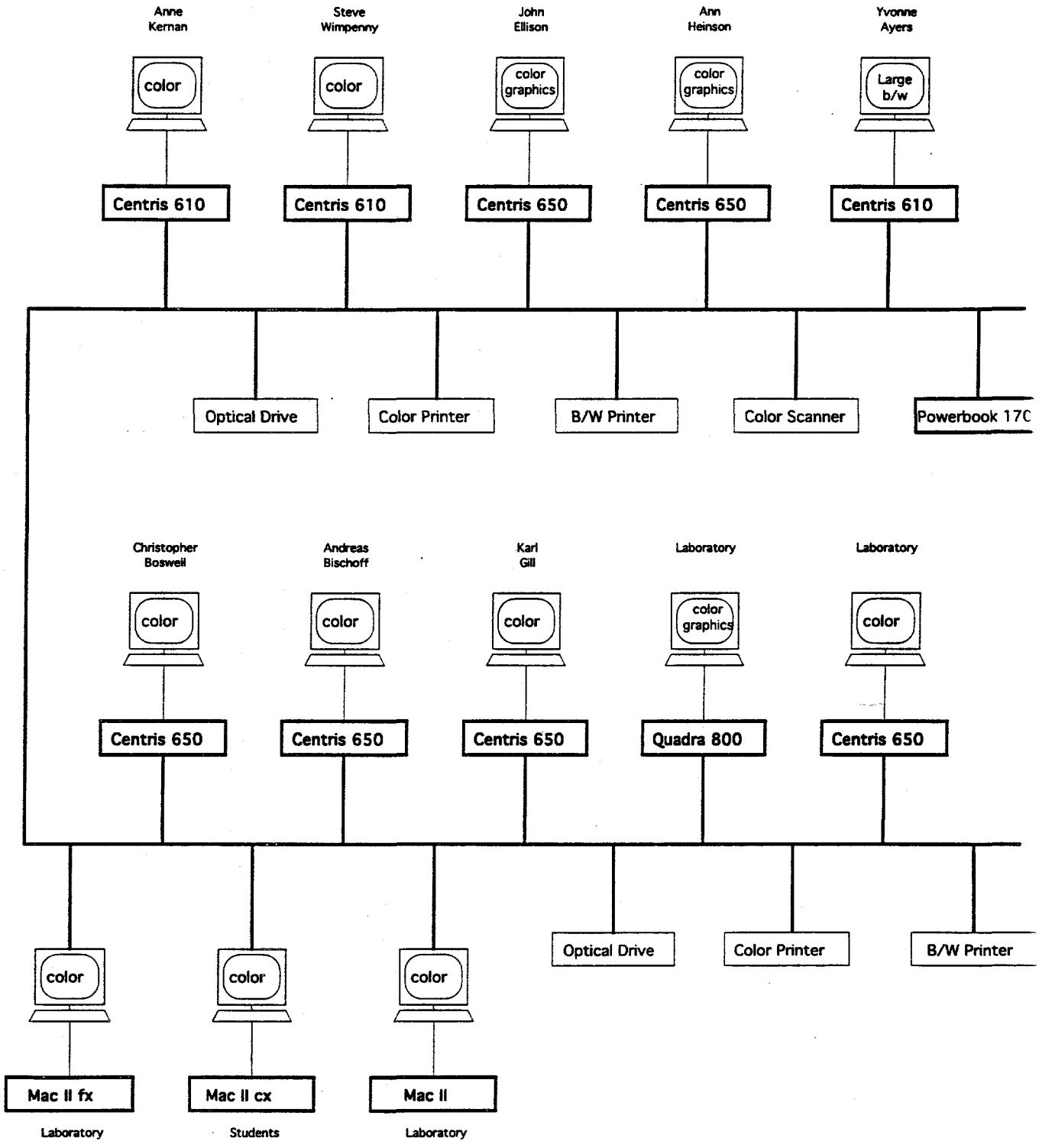

Fig. 31 UC Riverside $p\bar{p}$ group Macintosh facilities on campus.

Over the next couple of years, we will outgrow the number of Macintoshes in the Laboratory. The Mac II fx, Mac IIcx and Mac II are very old machines will probably not last very long. We will need to invest in approximately four more machines, probably two Quadra 800's and two Centris 650's or equivalent. For DØ, there will be one Mac used for the probe station, and one for the laser test system and readout system. SDC will have two similar parallel setups using different technology standards. The fifth and sixth machines will be used for the radiation damage studies, for general data analysis, and by our students. We will need to buy several more optical drives, as CAD design files and video images of silicon detectors from the probe stations are very large and will need to be stored externally.

1.5 Task A1 : Equipment Needs

The equipment required for development and construction work on the DØ and SDC Silicon Trackers is listed below.

For 1994–5, we need to test many prototype DØ detectors in our labs. Probe station testing of detectors will require an anti-vibration table for the probe station and custom-built probe cards in order to test large numbers of channels. We are also setting up the laser test system, which needs an anti-vibration table to ensure stability of the whole system. A Macintosh Quadra with a VME interface is needed to control the integrated SVX II readout system and laser test system.

During 1995–6, we will be testing over 100 wedge detectors for the DØ Silicon Tracker. The detectors have to be kept inside a clean room throughout the probe testing, assembly and laser testing process. We are requesting $10,000 to enable us to extend our clean room, so that it it possible to undertake such a large part of the detector production on the UC Riverside campus. An optical disk system will be used to record measurements from tests of the wedges in a database. We will be setting up a second laser test system, so that DØ and SDC detector testing can occur in parallel. The laser system will need an x–y translation table with control interface, an antivibration table and a Macintosh computer for instrument control, data acquisition and analysis.

By 1996–7, work in our campus laboratories will be fully directed towards the SDC Silicon Tracker. Our existing Macintosh II, IIfx and IIcx will not be repairable by then, and we request two new Macintosh computers to replace them. They will be used to control the laser test and readout systems and to control one of the probe stations. We will need to probe SDC silicon detectors, for which we request a Hewlett Packard source monitor unit and power supply, for measuring leakage currents, and new probe cards for the new detector geometries.

Our computing needs will be met with four workstations, spread out over three years. A Silicon Graphics workstation is needed in 1994–5, to run DØGEANT and DØRECO, and a DEC Alpha workstation is needed for DØ data analysis. This will enable us to meet our obligations for Runs 1a and 1b. For 1995–6, we will need a Silicon Graphics workstation to allow us to fully participate in the design of the SDC Silicon Tracker. In 1996–7, the DØ Silicon Tracker will be running at the Tevatron, and we will need additional processing power at Fermilab to enable us to perform offline calibrations, for channel gain and alignment. For this, we are requesting a DEC Alpha workstation, so that our additional responsibilities do not interfere with the data analysis in progress on other machines.

Equipment 1994–95

2	Kinetic Systems anti-vibration tables	4716
2	Probe station picoprobes	5000
3	Probe cards (100 probes)	4500
1	Macintosh Centris 650 computer	6222
1	VME crate	1600
1	VME interface for Macintosh (National Instruments VME-NB2040)	3000
1	Silicon Graphics workstation	12000
1	DEC Alpha workstation	12000

Total 1994–95 **49038**

Equipment 1995–96

1	Clean room extension	10000
2	Low profile translation stages	466
2	Actuators	2960
1	2-axis motion controller with GPIB interface	3450
1	Hewlett-Packard fast preamplifier HP8447D	1700
1	Kinetic Systems anti-vibration table	2358
1	Macintosh Quadra 800 computer	8869
1	Optical disk drive	1500
10	Optical disks	600
1	Silicon Graphics workstation	12000

Total 1995–96 **43903**

Equipment 1996–97

1	Macintosh Quadra 800 computer	8869
1	Macintosh Centris 650 computer	6222
1	Hewlett-Packard programmable power supply HP 6628A	4850
1	Hewlett-Packard Source Monitor Unit	5000
6	Probe card (100 probes)	9000
1	DEC Alpha workstation	12000

Total 1996–97 **45941**

1.6 Task A1 : Budget Notes

We are requesting support for a leave of absence for S. Wimpenny during the Spring Quarter 1994. This will enable him to spend Spring, Summer 1994 on-site at Fermilab in order to complete the search for top decaying to dileptons in Runs 1a and 1b data. Note that the University will provide Summer salary for J. Ellison in Summer 1994.

The salaries of Postgraduate researchers A. Bischoff and K. Gill will be paid from a three-year grant of $90K annually from the Texas National Research Commission Laboratory. Postgraduate Researcher no. 8 is a replacement for K. Bazizi who will leave our group in December 1993.

Graduate student salaries have increased due to the change, effective July 1994, from the Research Assistant title to the Graduate Student Researcher appointment. This change has been mandated by the UCR administration in line with most other UC campuses. The university also requires that the funding source for graduate student researchers pay for the following benefits: (i) Graduate Student Health Insurance Plan (GSHIP), (ii) fee increases (Partial Fee Remission, PFR) and (iii) tuition, which only applies to students who are not California residents, (Non Resident Tuition, NRT).

Justification for the equipment requests are detailed in sections 1.5 (Task A1: Equipment Needs) and 1.4 (Task A1: Computing Facilities). Students who are heavily involved in equipment development are included in the equipment category. As noted in the introductory overview the university will be contributing $125K in 1994 towards equipment/student support in the form of faculty initial complement.

Task A2

2. Task A2

Contents

2.1 Task A2

2.1.1 Overview

The physics program of Task A2 has been the systematic study of leptons and hadrons. From the mid-1970s to the early 1980s, the TPC/2γ experiment at PEP focussed on e^+e^- annihilation and two-photon processes. Since 1984 we have been working on the OPAL experiment at LEP, the high energy e^+e^- collider at CERN. The OPAL detector at LEP began taking data in 1989 and has now accumulated over a million Z^0 decays. Publications by the Collaboration cover a broad spectrum of physics:

- the precision measurement of electroweak parameters,
- the first direct determination of the number of light neutrino generations by the method of single photon counting,
- the measurement of the running coupling constant of the strong interaction by several independent methods,
- the differences between quark and gluon jets,
- the extension of the mass limit of the Higgs and other new particles,
- topics in heavy quark and tau physics.

The continued exploitation of the rich physics potential of LEP and LEP200 will form the core of the UCR effort for the coming several years.

In our continuing effort to test the validity of the Standard Model and to search for new physics, we have begun participating in a new experimental program. Since 1990 the UCR group has been part of an international collaboration which proposes to build the Compact Muon Solenoid (CMS), a detector designed to exploit the physics at the Large Hadron Collider at CERN. The CMS Letter of Intent was submitted on October 1, 1992. The CERN Research Board has given its approval for CMS to proceed with a Technical Proposal. We have also been participating in the RD5 experiment at the CERN SPS which studies muon triggering and momentum reconstruction in a strong magnetic field, issues of great importance in the design of the CMS detector. First results from RD5 have been reported recently.

Several members of our group are also participating in an ongoing neutrino oscillation program LSND at Los Alamos which will begin to take data in the Fall of 1993.

2.1.2 Personnel

Ph.D. Physicists

J.W. Gary	Assistant Professor
P. Giacomelli	Postgraduate Researcher
W. Gorn	Staff Research Associate
C.C.H. Jui	Postgraduate Researcher
J.G. Layter	Adjunct Professor
B.C. Shen	Professor
P. Schenk	Postgraduate Researcher
G.J. VanDalen	Professor
G.W. Wilson	Postgraduate Researcher

Graduate Students

S.L. Chu
E.G. Heflin
J.R. Letts
W. Strossman

Summer Student

C. Ju
K.L. Wang

Invited Talks 1992-1993

1992

1. J.G. Layter, "LEP Physics from the OPAL Vantage Point"
   University of California at Davis, seminar; February 10, 1992

2. B.C. Shen, "Z^0 Physics and the Number of Families"
   California State University, Long Beach, Colloquium; February 1992

3. J.G. Layter, Exclusive Production Session Chairman, Convener
   Photon-Photon '92 Conference, San Diego; March 24, 1992

4. G.J. VanDalen, "Low Energy Neutrino Experiments - Doing TeV Physics with MeV Neutrinos"
   California State University, Long Beach, Colloquium; April 27, 1992

5. M. Dittmar, "A Measurement of Photon Radiation in Lepton Pair Events from Z Decays," University of Montreal; April 28, 1992

6. H. Oh, "New Particle Searches at OPAL"
   University of California at Irvine, Seminar; April 28, 1992

7. J.W. Gary, "QCD at LEP"
   American Physical Society Meeting, Washington D. C., Plenary talk; April 1992

8. B.C. Shen, "Some Aspects of LEP Physics, Present and Future"
   Columbia University, Colloquium; April 1992

9. M. Dittmar, "Search for Rare Exotic Z Decays"
   International Workshop on the Search for New Particles: Status and Prospects, ICTP, Trieste; May 20, 1992

10. M. Dittmar, "Measurement of Strange Baryon Production in Hadronic Z Decays," University of Trieste; May 21, 1992

11. B.C. Shen, "Strange Baryon Production in e^+e^- Collisions"
    22^{nd} International Symposium on Multiparticle Dynamics, Santiago de Compostela, Spain; July 13, 1992

12. J.G. Layter, "Measurements of gamma-gamma Collisions with the OPAL Detector at LEP and Comparison with QCD Models," XXVI International Conference on High Energy Physics, Dallas, Texas; August 6, 1992

13. M. Dittmar, "Searching for Rare Exotic Z^0 Decays," 4th Hellenic School on Elementary Particle Physics, Corfu, Greece; September 7, 1992

14. J. Letts, "Some Recent Results from OPAL"
CERN School of Physics, Monschau, Germany; September 17, 1992

15. M. Dittmar, "Strange Baryon Production in e^+e^- annihilation"
ETH-Zurich, Switzerland; September 21, 1992

16. B.C. Shen, "The Study of Strange Baryon Production in e^+e^- Collisions at LEP," Physics Institute, Academica Sinica, Taiwan; October 24, 1992

17. B.C. Shen, "The Search for New Physics in High Energy Collisions"
National Central University, Taiwan; October 27, 1992

18. B.C. Shen, "Particle Physics"
National Normal University, Taiwan; October 28, 1992

19. B.C. Shen, "Tau Physics at LEP"
National Taiwan University, Taiwan; October 29, 1992

20. M. Dittmar, "Measurement of Strange Baryon Production in Hadronic Z^0 Decays"
DPF 92 Conference Fermilab; November 10–14, 1992

21. M. Dittmar, "Strange Baryon Production in e^+e^- Annihilation"
University of California, Riverside, Seminar; November 16, 1992

22. M. Dittmar, "Strange Baryon Production in e^+e^- Annihilation"
UCLA, Physics Seminar; November 18, 1992

23. M. Dittmar, "Strange Baryon Production in e^+e^- Annihilation"
Los Alamos national Lab, MP Division Seminar; November 23, 1992

1993

24. P. Schenk, "The OPAL Monte Carlo Production System"
International Conference on Monte Carlo Simulation in High Energy and Nuclear Physics; February 22-26, 1993

25. J.G. Layter, "Physics at Future Hadron Colliders"
University of California, Riverside, Departmental Colloquium; April 15, 1993

26. J. Letts, "A Study of Quark-Gluon Jet Differences Using Vertex Tagging of Quark Jets," APS General Meeting, Washington DC; April 15, 1993

27. J. Letts, "Evidence for Chain-Like Production of Strange Baryons in Jets"
APS General Meeting, Washington DC; April 15, 1993

28. G.W. Wilson, "Search for Anomalous Production of High Mass Photon Pairs in e^+e^- Collisions," PPE Seminar, CERN; May 3, 1993

29. J.W. Gary, "A study of Quark-Gluon Jet Differences Using Vertex Tagging of Quark Jets," California Institute of Technology; May 10, 1993

30. M. Dittmar, "Exotic Z^0 Decays, New Results"
Glasgow University, UK; June 3, 1993

31. M. Dittmar, "Baryon Production in Hadronic Z^0 Decays"
Glasgow University, UK; June 3, 1993

32. M. Dittmar, "Baryon Production in Hadronic Z^0 Decays"
Rutherford Laboratory, UK; June 7, 1993

33. M. Dittmar, "Baryon Production in Hadronic Z^0 Decays"
Oxford University, UK; June 8, 1993

34. M. Dittmar, "Baryon Production in Hadronic Z^0 Decays"
Imperial College, London, UK; June 9, 1993

35. J.W. Gary, "A New Study of Quark and Gluon Jet Properties Using Vertex Tagging," UCLA, Seminar; June 9, 1993

36. J. Letts, "Strange Baryon Production and Correlations in Hadronic Z0 Decays," Particles and Nuclei XIII International Conference, Perugia, Italy, 28 Jun - 2 July 1993

37. G.W. Wilson, "High Mass Photon Pairs at LEP," International Europhysics Conference on High Energy Physics, Marseilles; July 23, 1993

Other Talks 1992 - 1993

1992

1. M. Dittmar, "Detailed Studies of Strange Baryon Production"
   OPAL Weekly Meeting, CERN; February 6, 1992

2. J. Letts, "A Measurement of Inclusive Strange Baryon Production in Hadronic Z0 Decays," OPAL Weekly Meeting, CERN; February 6, 1992

3. J. Letts, "A Measurement of Inclusive Strange Baryon Production in Hadronic Z0 Decays, Update," OPAL Weekly Meeting, CERN; April 9, 1992

4. J. Letts, "Strange Baryon Production in Hadronic Z0 Decays"
   APS Meeting, Washington D.C.; April 20, 1992

5. J.G. Layter, "Muon Chamber Status"
   RD5 Group Meeting, CERN; May 9, 1992

6. G.W. Wilson, "Proposal for a highly efficient TOF trigger based on single–ended logic," OPAL Trigger Group Meeting, CERN; May 22, 1992

7. C.C.H. Jui, "The Status of the OPAL HPUX Cluster"
   OPAL Plenary Meeting, CERN; June 22, 1992

8. G.W. Wilson, "Developments in the single photon analysis"
   OPAL Plenary Week, CERN; June 23, 1992

9. M. Dittmar, "Update of the Radiative Lepton Pair Paper Using 1990 and 1991 Data," OPAL Plenary Week, CERN; June 23, 1992

10. J. Letts, "A Measurement of Inclusive Strange Baryon Production in Hadronic Z0 Decays, Update," OPAL Plenary Week, CERN; June 25, 1992

11. C.C.H. Jui, "OPAL's Experience with HPUX Cluster"
    EAGLE Collaboration Meeting, CERN; July 2, 1992

12. G.J. VanDalen, "How Many Types of Matter are There?"
    Expanding Horizons Summer Student Program, UC Riverside; July 13, 1992

13. G.J. VanDalen, "OffLine Analysis Progress"
    LSND Collaboration Meeting, Los Alamos, NM; July 16, 1992

14. J.W. Gary, "Data quality checks for QCD"
    OPAL Thursday meeting; September 9, 1992

15. J.W. Gary, "Quark-Gluon Jet Differences Using Leptons"
OPAL QCD workshop, OPAL week; September 23, 1992

16. J.W. Gary, "Quark-Gluon Jet Differences Using Lepton tagging"
OPAL Thursday meeting, CERN; October 22, 1992

17. J. Letts, "Strange Baryon Production: Preliminary results Using the 1992 Data"
OPAL Thursday Meeting, CERN; October 29, 1992

18. J.W. Gary, "Quark-Gluon Jet Differences Using Silicon for Vertex Tagging"
OPAL QCD working group meeting, CERN; November 4, 1992

19. J.W. Gary, "Quark-Gluon Jet Differences Using Vertex Tagging"
OPAL Thursday meeting, CERN; November 19, 1992

20. J. Letts, "Correlations in Strange Baryon Pairs and a 1992 Update on Baryon Signals," Inclusives/Fragmentation WG meeting of the OPAL plenary week, CERN; December 7, 1992

21. J.W. Gary, "Quark-Gluon Jet Differences Using Vertex Tagging"
Physics session, OPAL week, CERN; December 10, 1992

1993

22. J. Letts, "Strange Baryons"
Charm/Light Flavour WG meeting of the OPAL plenary week, CERN; March 15, 1993

23. J. Letts, "Xi- Lepton Correlations"
Exclusives Working Group meeting of the OPAL plenary week, CERN; June 14, 1993

24. J. Letts, "Flavour Composition in High x Lambda Events"
Charm/Light Flavour WG meeting of the OPAL plenary week, CERN; June 14, 1993

25. J. Letts, "Lambda Production in the 1993 PASS1 Data"
reROPE preparations meeting, CERN; July 9, 1993

Publications 1992 - 1993

1992

1. M. Dittmar, J.W. Gary, W. Gorn, E.G. Heflin, C. Ho, W.J. Larson, J.G. Layter, J. Letts, B.P. O'Neill, H. Oh, K. Riles, B.C. Shen, G.J. VanDalen, Y. Yang *et al.* (OPAL Collaboration), *"Properties of Multihadronic Events with a Final State Photon at $\sqrt{s} = M_{Z^0}$,"* Zeitschrift für Physik, **C54**, (1992) 193-209.

2. M. Dittmar, J.W. Gary, W. Gorn, E.G. Heflin, C. Ho, W.J. Larson, J.G. Layter, J. Letts, B.P. O'Neill, H. Oh, K. Riles, B.C. Shen, G.J. VanDalen, Y. Yang *et al.* (OPAL Collaboration), *"Measurement of the Average B Hadron lifetime in Z^0 Decays,"* Phys. Lett. **B274** (1992) 513-525.

3. M. Dittmar, J.W. Gary, W. Gorn, E.G. Heflin, C. Ho, W.J. Larson, J.G. Layter, J. Letts, B.P. O'Neill, H. Oh, K. Riles, B.C. Shen, G.J. VanDalen, Y. Yang *et al.* (OPAL Collaboration), *"Measurement of B^0-$\overline{B^0}$ Mixing in Hadronic Z^0 Decays,"* Phys. Lett. **B276** (1992) 379-392.

4. M. Dittmar, J.W. Gary, W. Gorn, E.G. Heflin, C. Ho, W.J. Larson, J.G. Layter, J. Letts, B.P. O'Neill, H. Oh, K. Riles, B.C. Shen, G.J. VanDalen, Y. Yang *et al.* (OPAL Collaboration), *"An Improved Measurement of $\alpha_s(M_{Z^0})$ Using Energy Correlations with the OPAL Detector at LEP ,"* Phys. Lett. **B276** (1992) 547-564.

5. M. Dittmar, J.W. Gary, W. Gorn, E.G. Heflin, C. Ho, W.J. Larson, J.G. Layter, J. Letts, B.P. O'Neill, H. Oh, K. Riles, B.C. Shen, G.J. VanDalen, Y. Yang *et al.* (OPAL Collaboration), *"A Search for Free Gluons in Hadronic Z^0 Decays,"* Phys. Lett. **B278** (1992) 485-494.

6. M. Dittmar, J.W. Gary, W. Gorn, E.G. Heflin, C. Ho, W.J. Larson, J.G. Layter, J. Letts, B.P. O'Neill, H. Oh, K. Riles, B.C. Shen, G.J. VanDalen, Y. Yang *et al.* (OPAL Collaboration), *"Test of CP Invariance in $e^+e^- \rightarrow Z^0 \rightarrow \tau^+\tau^-$ and a Limit on the Weak Dipole Moment of the τ Lepton,"* Phys. Lett. **B281** (1992) 405-415.

7. M. Dittmar, J.W. Gary, W. Gorn, E.G. Heflin, C. Ho, W.J. Larson, J.G. Layter, J. Letts, B.P. O'Neill, H. Oh, K. Riles, B.C. Shen, G.J. VanDalen, Y. Yang *et al.* (OPAL Collaboration), *"Evidence for b-flavoured Baryon Production in Z^0 Decays at LEP,"* Phys. Lett. **B281** (1992) 394-404.

8. M. Dittmar, W. Gorn, C. Ho, W.J. Larson, J.G. Layter, B.P. O'Neill, H. Oh, K. Riles, B.C. Shen, G.J. VanDalen, Y. Yang the LEP Collaborations: Aleph, Del-

phi, L3, OPAL, *"Electroweak Parameters of the Z^0 Resonance and the Standard Model,"* Phys. Lett. **B276**, 247-253 (1992).

9. B.C. Shen, *"Photon Emission and Gluon Emission Processes at the Z^0,"* Proceedings of the XXI International Symposium on Multiparticle Dynamics, Wuhan, China; September 23-27, 1992; Y. Wu and L. Liu (Eds.), 26-41.

10. M. Dittmar, J.W. Gary, W. Gorn, E. Heflin, C. Ho, W.J. Larson, J.G. Layter, J. Letts, B.P. O'Neill, H. Oh. K. Riles, B.C. Shen, G.J. VanDalen, Y. Yang *et al.* (OPAL Collaboration) *"A Global Determination of $\alpha_S(M_{Z^0})$ at LEP,"* Z. Phys. **C55**, 1-24 (1992).

11. M. Dittmar, J.W. Gary, W. Gorn, E. Heflin, C. Ho, W.J. Larson, J.G. Layter, J. Letts, B. P. O'Neill, H. Oh, K. Riles, B.C. Shen, G.J. VanDalen, Y. Yang *et al.* (OPAL Collaboration) *"A Measurement of Electron Production in Hadronic Z^0 Decays and a Determination of $\Gamma(Z^0 \to b\bar{b})$,"* Z. Phys. **C55**, 191-207 (1992).

12. M. Dittmar, J.W. Gary, W. Gorn, E. Heflin, J.G. Layter, J. Letts, H. Oh, K. Riles, B.C. Shen, G.J. VanDalen *et al.* (OPAL Collaboration) *"A Test of Higher Order Electroweak Theory in Z^0 Decays to Two Leptons with an Associated Pair of Charged Particles,"* Phys. Lett. **B287**, 389-400 (1992).

13. M. Dittmar, J.W. Gary, W. Gorn, E. Heflin, J.G. Layter, J. Letts, H. Oh, K. Riles, B.C. Shen, G.J. VanDalen *et al.* (OPAL Collaboration) *"A Measurement of the τ Topological Branching Ratios at LEP,"* Phys. Lett. **B288**, 373-385 (1992).

14. M. Dittmar, J.W. Gary, W. Gorn, E. Heflin, J.G. Layter, J. Letts, H. Oh, K. Riles, B.C. Shen, G.J. VanDalen *et al.* (OPAL Collaboration) *"A Study of Two-Particle Momentum Correlations in Hadronic Z^0 Decays,"* Phys. Lett. **B287**, 401-412 (1992).

15. M. Dittmar, J.W. Gary, W. Gorn, E. Heflin, C. Jui, J.G. Layter, J. Letts, H. Oh, B.C. Shen, G.J. VanDalen, G.W. Wilson *et al.* (OPAL Collaboration) *"A Measurement of Strange Baryon Production in Hadronic Z^0 Decays,"* Phys. Lett. **B291**, 503-518 (1992).

16. M. Dittmar, J.W. Gary, W. Gorn, E. Heflin, C. Jui, J.G. Layter, J. Letts, H. Oh, B.C. Shen, G.J. VanDalen, G.W. Wilson *et al.* (OPAL Collaboration) *"A Measurement of the Forward-Backward Asymmetry in Hadronic Decays of the Z^0,"* Phys. Lett. **B294**, 436-450 (1992).

17. M. Dittmar, J.W. Gary, W. Gorn, E. Heflin, C. Jui, J.G. Layter, J. Letts, H. Oh, B.C. Shen, G.J. VanDalen, G.W. Wilson *et al.* (OPAL Collaboration)

"Inclusive Neutral Vector Meson Production in Hadronic Z^0 Decays.," Z. Phys. **C56**, 521-535 (1992).

18. M. Dittmar, J.W. Gary, W. Gorn, E. Heflin, C. Jui, J.G. Layter, J. Letts, H. Oh, B.C. Shen, G.J. VanDalen, G.W. Wilson *et al.* (OPAL Collaboration) *"A Search for Doubly-Charged Higgs Production in Z^0 Decays,"* Phys. Lett. **B295**, 347-356 (1992).

19. M. Dittmar, J.W. Gary, W. Gorn, E. Heflin, C. Jui, J.G. Layter, J. Letts, H. Oh, B.C. Shen, G.J. VanDalen, G.W. Wilson *et al.* (OPAL Collaboration) *"Evidence for the Existence of the b-flavour Meson B_S^0 in Z^0 Decays,"* Phys. Lett. **B295**, 357-370 (1992).

20. G.J. VanDalen, D. Beavis, S. Y. Fung, W. Gorn, R. T. Poe and 25 authors from Los Alamos National Laboratory, UCLA, University of Iowa, University of New Mexico, Temple University, Valparaiso University, *"Muon-neutrino Carbon Charged-Current Interaction Near the Muon Threshold,"* Phys. Rev. **C46**, 2554-2566 (1992)

21. G. Anderson, I. Cohen, B. Homann, D. Smith, W. Strossman, G.J. VanDalen, L.S. Weaver, D. Evans, W. Vernon, A. Band, R. Burman, T. Chang, F. Federspiel, W. Forman, S. Gomulka, G. Hart, T. Kozlowski, W.C. Louis, J. Margulies, A. Nuanes, V. Sandberg, T.N. Thompson, D.H. White, D. Whitehouse, *"Data Acquisition System for the Large Scintillating Neutrino Detector at Los Alamos,"* Proceedings of the International Conference on Computing in High Energy Physics 92, Annecy, france, 21-25 September 1992, 301-304 (1992).

22. M. Dittmar, M. Arignon *et al.*, *"The Trigger System of the OPAL Experiment at LEP,"* Nucl. Instr. and Meth., **A313** (1992) 103-125.

23. M. Dittmar, J.W. Gary, J.G. Layter, E. Riles, G.J. VanDalen and 61 authors from the OPAL Collaboration, *"The Detector Simulation Program for the OPAL Experiment at LEP,"* Nucl. Instrum. Methods **A317**, 47-74 (1992).

24. S.A. Abel, M. Dittmar, H. Dreiner, *"Testing Locality at Colliders via Bell's Inequality?,"* Phys. Lett. **B280** (1992) 304-312.

25. M. Dittmar, J.W. Gary, W. Gorn, C.C.H. Jui, J.G. Layter, B.C. Shen, G.J. VanDalen, G.W. Wilson, *et al.* (CMS Collaboration), *"Letter of Intent by the CMS Collaboration for a General Purpose Detector at the LHC,"* CERN/LHCC 92-3 (1 October 1992).

1993

26. M. Dittmar, J.W. Gary, W. Gorn, E. Heflin, C. Jui, J.G. Layter, J. Letts, H. Oh, B.C. Shen, G.J. VanDalen, G.W. Wilson *et al.* (OPAL Collaboration) *"A Study of $K^0_S K^0_S$ Bose-Einstein Correlations in Hadronic Z^0 Decays,"* Phys. Lett. **B298**, 456-468 (1993).

27. M. Dittmar, J.W. Gary, W. Gorn, E. Heflin, C. Jui, J.G. Layter, J. Letts, H. Oh, B.C. Shen, G.J. VanDalen, G.W. Wilson *et al.* (OPAL Collaboration) *"A Measurement of $K^{*\pm}(892)$ Production in Hadronic Z^0 Decays,"* Phys. Lett. **B305**, 407-414 (1993).

28. S.L. Chu, M. Dittmar, J.W. Gary, W. Gorn, E. Heflin, C. Jui, J.G. Layter, J. Letts, P. Schenk, B.C. Shen, G.J. VanDalen, G.W. Wilson *et al.* (OPAL Collaboration) *"A Study of the Electric Charge Distributions of Quark and Gluon Jets in Hadronic Z^0 Decays,"* Phys. Lett. **B302**, 523-532 (1993).

29. S.L. Chu, M. Dittmar, J.W. Gary, W. Gorn, E. Heflin, C. Jui, J.G. Layter, J. Letts, P. Schenk, B.C. Shen, G.J. VanDalen, G.W. Wilson *et al.* (OPAL Collaboration) *"QCD Coherence Studies Using Two Particle Azimuthal Correlations,"* Z. Phys. **C58**, 207-217 (1993).

30. S.L. Chu, M. Dittmar, J.W. Gary, W. Gorn, E. Heflin, C. Jui, J.G. Layter, J. Letts, P. Schenk, B.C. Shen, G.J. VanDalen, G.W. Wilson *et al.* (OPAL Collaboration) *"Precision Measurements of the Neutral Current from Hadron and Lepton Production at LEP,"* Z. Phys. **C58**, 219-237 (1993).

31. S.L. Chu, M. Dittmar, J.W. Gary, W. Gorn, E. Heflin, C. Jui, J.G. Layter, J. Letts, P. Schenk, B.C. Shen, G.J. VanDalen, G.W. Wilson *et al.* (OPAL Collaboration) *"Evidence for Chain-Like Production of Strange Baryon Pairs in Jets,"* Phys. Lett. **B305**, 415-427 (1993).

32. S.L. Chu, M. Dittmar, J.W. Gary, W. Gorn, E. Heflin, C. Jui, J.G. Layter, J. Letts, P. Schenk, B.C. Shen, G.J. VanDalen, G.W. Wilson *et al.* (OPAL Collaboration) *"Studies of the Strong and Electroweak Interactions Using Final State Photon Emission in Hadronic Z^0 Decays,"* Z. Phys. **C58**, 405-418 (1993).

33. S.L. Chu, M. Dittmar, J.W. Gary, W. Gorn, E. Heflin, C. Jui, J.G. Layter, J. Letts, P. Schenk, B.C. Shen, G.J. VanDalen, G.W. Wilson *et al.* (OPAL Collaboration) *"A Study of the Differences Between Quark and Gluon Jets Using Vertex Tagging of Quark Jets,"* Z. Phys. **C58**, 219-237 (1993).

34. S.L. Chu, M. Dittmar, J.W. Gary, W. Gorn, E. Heflin, C. Jui, J.G. Layter, J. Letts, P. Schenk, B.C. Shen, G.J. VanDalen, G.W. Wilson *et al.* (OPAL

Collaboration) *"Measurement of the B^0 and B^+ Lifetimes,"* Phys. Lett. **B307**, 247-261 (1993).

35. S.L. Chu, M. Dittmar, J.W. Gary, W. Gorn, E. Heflin, C. Jui, J.G. Layter, J. Letts, P. Schenk, B.C. Shen, G.J. VanDalen, G.W. Wilson and many authors from the LEP Energy Group, and the Aleph, Delphi, L3 and OPAL Collaborations , *"Measurement of the Mass of the Z Boson and the Energy Calibration of LEP,"* Phys. Lett. **B307**, 187-193 (1993).

36. S.L. Chu, M. Dittmar, J.W. Gary, W. Gorn, E. Heflin, C. Jui, J.G. Layter, J. Letts, P. Schenk, B.C. Shen, G.J. VanDalen, G.W. Wilson *et al.* (OPAL Collaboration) *"Measurement of $\Gamma(Z^0 \rightarrow b\bar{b})/\Gamma(Z^0 \rightarrow hadrons)$ Using Leptons,"* Z. Phys. **C58** 523-539 (1993).

37. W. Gorn, B.P. O'Neill, J. Baines *et al.*, *"The Data Acquisition System of the OPAL Detector at LEP,"* Nucl. Instrum. Meth. **A325** (1993) 271-293.

38. M. Daoudi, J.G. Layter, W.T. Lin, B.C. Shen, D.A. Bauer *et al.* (TPC/Two-Gamma Collaboration) *"Study of χ_{c2} production in photon–photon collisions,"* Phys. Lett. **B302** 345-350 (1993).

39. J.G. Layter, *" Measurements of gamma-gamma Collisions with the OPAL Detector at LEP and Comparison with QCD Models,"* Proceedings of the XXVI International Conference on High Energy Physics, August 6-12, 1992; Dallas, Texas; James R. Sanford (ed.) Vol. I, pp 812-816.

Publications Submitted

1. S.L. Chu, M. Dittmar, J.W. Gary, W. Gorn, E. Heflin, C. Jui, J.G. Layter, J. Letts, P. Schenk, B.C. Shen, G.J. VanDalen, G.W. Wilson *et al.* (OPAL Collaboration) *"Measurement of the Tau Lifetime,"* CERN-PPE/93-09 (15 January 1993), submitted to Z. Phys.

2. S.L. Chu, M. Dittmar, J.W. Gary, W. Gorn, E. Heflin, C. Jui, J.G. Layter, J. Letts, P. Schenk, B.C. Shen, G.J. VanDalen, G.W. Wilson *et al.* (OPAL Collaboration) *"A Determination of $\alpha_S(M_{Z^0})$ at LEP Using Resummed QCD Calculations,"* CERN-PPE/93-38 (3 March 1993), submitted to Z. Phys.

3. S.L. Chu, M. Dittmar, J.W. Gary, W. Gorn, E. Heflin, C. Jui, J.G. Layter, J. Letts, P. Schenk, B.C. Shen, G.J. VanDalen, G.W. Wilson *et al.* (OPAL Collaboration) *"Search for Anomalous Production of High Mass Photon pairs in e^+e^- Collisions,"* CERN-PPE/93-67 (30 April 1993), submitted to Phys. Lett. B.

4. S.L. Chu, M. Dittmar, J.W. Gary, W. Gorn, E. Heflin, C. Jui, J.G. Layter, J. Letts, P. Schenk, B.C. Shen, G.J. VanDalen, G.W. Wilson *et al.* (OPAL Collaboration) *"The Forward Backward Asymmetry of $e^+e^- \to b\bar{b}$ and $e^+e^- \to c\bar{c}$ Using Leptons in Hadronic Z^0 Decays,"* CERN-PPE/93-78 (10 May 1993), submitted to Z. Phys.

5. S.L. Chu, M. Dittmar, J.W. Gary, W. Gorn, E. Heflin, C. Jui, J.G. Layter, J. Letts, P. Schenk, B.C. Shen, G.J. VanDalen, G.W. Wilson *et al.* (OPAL Collaboration) *"A Measurement of $\Gamma(Z^0 \to b\bar{b})/\Gamma(Z^0 \to hadrons)$ Using an Impact Parameter Technique,"* CERN-PPE/93-79 (12 May 1993), submitted to Z. Phys.

6. S.L. Chu, M. Dittmar, J.W. Gary, W. Gorn, E. Heflin, C. Jui, J.G. Layter, J. Letts, P. Schenk, B.C. Shen, G.J. VanDalen, G.W. Wilson *et al.* (OPAL Collaboration) *"Search for Massive, Unstable Photinos that Violate R Parity,"* CERN-PPE/93-91 (4 June 1993), submitted to Phys. Lett. B.

7. S.L. Chu, M. Dittmar, J.W. Gary, W. Gorn, E. Heflin, C. Jui, J.G. Layter, J. Letts, P. Schenk, B.C. Shen, G.J. VanDalen, G.W. Wilson *et al.* (OPAL Collaboration) *"Measurement of the Average b Hadron Lifetime in Z^0 Decays,"* CERN-PPE/93-92 (4 June 1993), submitted to Z. Phys.

8. S.L. Chu, M. Dittmar, J.W. Gary, W. Gorn, E. Heflin, C. Jui, J.G. Layter, J. Letts, P. Schenk, B.C. Shen, G.J. VanDalen, G.W. Wilson *et al.* (OPAL Collaboration) *"Measurement of the B_S^0 Lifetime,"* CERN-PPE/93-95 (14 June 1993), submitted to Phys. Lett. B.

9. S.L. Chu, M. Dittmar, J.W. Gary, W. Gorn, E. Heflin, C. Jui, J.G. Layter, J. Letts, P. Schenk, B.C. Shen, G.J. VanDalen, G.W. Wilson *et al.* (OPAL Collaboration) *"Measurements of $B_0 - \overline{B}_0$ Mixing, $\Gamma(Z^0 \to b\bar{b})$ and Semileptonic Branching Ratios for b-flavoured Hadrons in Hadronic Z^0 Decays,"* CERN-PPE/93-106 (21 June 1993), submitted to Z. Phys.

10. S.L. Chu, M. Dittmar, J.W. Gary, W. Gorn, E. Heflin, C. Jui, J.G. Layter, J. Letts, P. Schenk, B.C. Shen, G.J. VanDalen, G.W. Wilson *et al.* (OPAL Collaboration) *"A Test of the Flavour Independence of the Strong Interaction for Five Flavours,"* CERN-PPE/93-118 (9 July 1993), submitted to Z. Phys.

11. G.W. Wilson, M. Arignon *et al.*, *"The Pretrigger System of the OPAL Experiment at LEP,"* CERN-PPE/93-48 (March 1993), submitted to Nucl. Instrum. Meth.

12. W. Gorn, J.G. Layter, B.C. Shen, M. Aalste *et al.* (RD5 Collaboration) *"Measurement of Hadron Shower Punchthrough in Iron,"* CERN-PPE/93-71 (March 1993), submitted to Z. Phys.

13. M. Daoudi, J.G. Layter, W.T. Lin, B.C. Shen, D.A. Bauer *et al.* (TPC/Two-Gamma Collaboration) *"Evidence for Spin One Resonance Production in the Reaction* $\gamma\gamma^* \rightarrow \pi^+\pi^-\pi^0\pi^0$*,"* SLAC-PUB-6094 (March 1993).

14. J. Letts, *"A Measurement of Strange Baryon Production with the OPAL Detector,"* OPAL-CR115 (Mar 2, 1993), to be published in the Proceedings of the CERN School of Physics, 1992.

15. M. Dittmar, *"Testing the Tau Lepton,"* to appear in the Proceedings of the 26^{th} Rencontres de Moriond, Electroweak and Unified Theories, Les Arcs, France, 10-17 March 1991.

16. M. Dittmar, *"A Measurement of Photon Radiation in Lepton Pair Events from* Z^0 *Decays,"* to appear in the Proceedings of the International Meeting on Physics Beyond the Standard Model, Valencia, Spain, October 2-5 (1992).

17. M. Dittmar, *"Searching for Rare Exotic* Z^0 *Decays,"* CERN-PPE/92-177 (12 October 1992) to appear in the Proceedings of the International Workshop on Search for New Elementary Particles, ICTP, Trieste, May 20-22 (1992).

18. P. Schenk, *"The OPAL Monte Carlo Production System,"* to appear in the Proceedings of the International Conference on Monte Carlo Simulation in High Energy and Nuclear Physics, Feb. 22-26.

2.2 OPAL at LEP

UCR's participation in the OPAL experiment at LEP started in 1984 and was the continuation of our effort in the study of leptons and quarks in e^+e^- collisions begun at PEP. Our group's work in OPAL has spanned the full range of particle physics: detector construction, data acquisition, and physics analysis. The excellent results obtained by OPAL so far have contributed immensely to our understanding of the physics of leptons and quarks. The operation of LEP at the Z^0 mass peak in the next two years will continue to probe the Standard Model with unprecedented precision.

As the energy of the collider is increased to about 200 GeV in the LEP200 era, we will be able to extend our studies in a number of areas, among them the search for the Higgs boson and other new particles to much higher masses, the measurement of the mass of the W boson to an accuracy of about 50 MeV, and the determination of the triple boson coupling from W pair production as a further test of the Standard Model.

In this section of the report, we present the progress made in the operation of LEP, the improvements to the OPAL detector, and some of the principal OPAL physics results to which our group has contributed significantly.

2.2.1 LEP Performance

LEP performance in 1992 continued its steady, if unspectacular, upward climb. While the goal of a "million Z's per year" proclaimed two years ago has not yet been achieved, it is within reach in 1993; and all four experiments already have "million Z" data samples to work with. Operation with eight bunches became routine during the year, as did the energy calibration using the method of resonance depolarization.

Luminosity

LEP achieved a significant increase in integrated luminosity during 1992, 28.6 pb^{-1}, compared to 18.651 pb^{-1} in 1991. The data samples obtained by the four experiments during 1992, and their accumulated totals, are given in Table 2.1.

In 1993 little time was lost experimenting with different "operating points" for the machine, and 8-on-8 bunch running began early on. By mid-August nearly 18.5 pb^{-1} had been delivered. Figure 2.1 presents the integrated luminosity obtained since 1991 and shows the markedly improved performance in the current year. LEP is now running in scan mode, dividing luminosity equally between the peak and the two off-peak points at ± 2 GeV. Energy calibration is taking place ordinarily at all scan points. Initial luminosities seen by the experiments have been around 1.3×10^{31} $cm^{-2}sec^{-1}$, and beam lifetimes have been in excess of 15 hours. During one fill the OPAL detector accumulated 12,399 multihadron events. The running efficiency of the OPAL detector

		ALEPH	DELPHI	L3	OPAL	LEP
$q\bar{q}$	'90-'91	451	365	423	454	1693
	'92	686	695	677	714	2772
	total	1137	1060	1100	1168	4465
$\ell^+\ell^-$	'90-'91	55	37	40	58	190
	'92	82	76	58	89	305
	total	137	113	98	147	495

Table 2.1: The LEP statistics in units of 10^3 events used for the analysis of the Z^0 line shape and lepton forward-backward asymmetries.

is stable at around 85%. It is estimated that the delivered luminosity should be in excess of 50 pb^{-1} on the peak, which should produce the long awaited "million Z's."

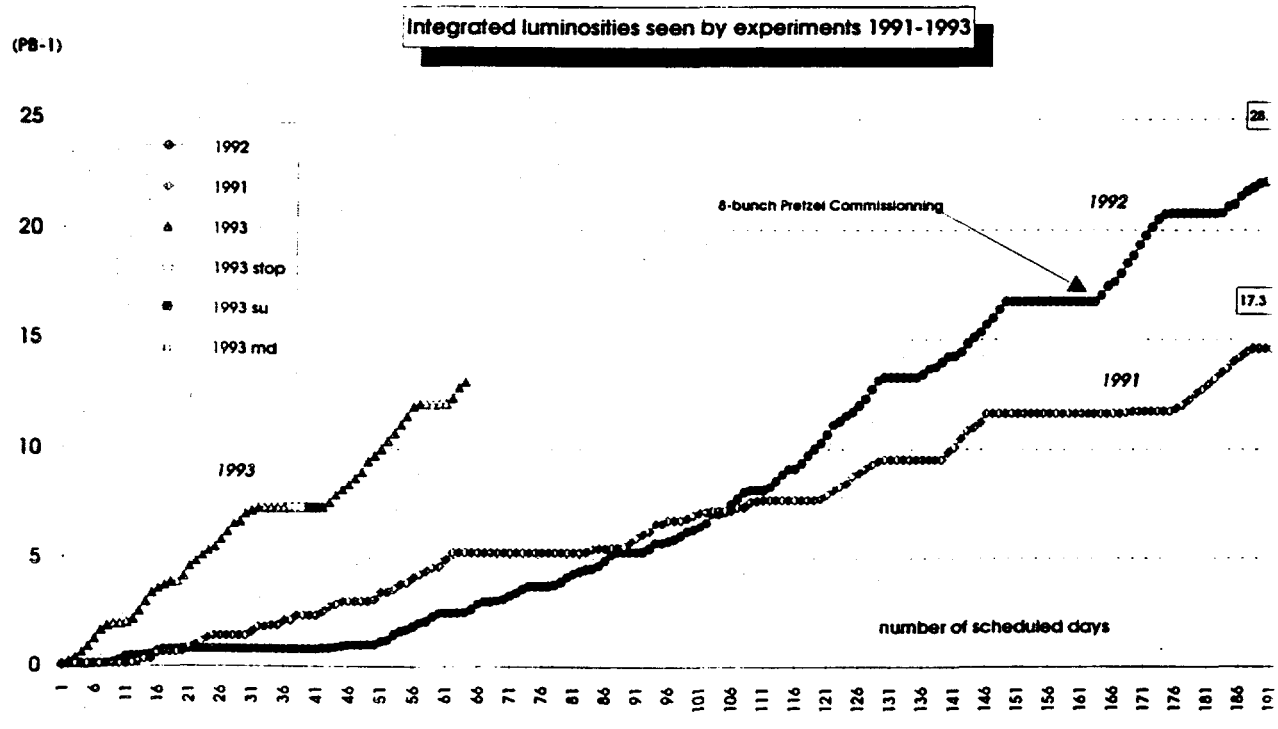

Figure 2.1: Integrated LEP luminosity day by day from 1991 to 1993

LEP Running Plans

One of the ideas being considered for increasing luminosity is that of introducing "bunch trains" into LEP. This means that instead of one beam consisting of four or eight bunches equally spaced around the ring as has been the case up to now, LEP would operate with some number of trains of bunches, where the bunches would be spaced a small number of RF wavelengths apart within a train, giving a spacing of 28 meters or 85 nsec, and the trains would be equally spaced as the bunches are now. The number of bunches in a train should not exceed 5 if higher-order mode problems are to be avoided, nor is it likely that the number of trains will exceed 8, so that existing trigger schemes could still be used. To avoid unwanted crossing points, one would arrange to collide the beams at a small (0.5 mrad) crossing angle.

Tests done in machine development runs show that the background is still tolerable under these conditions. Clearly several beam crossings would take place within the 340 nsec train length currently being proposed. Additional work must be done to determine how well the experiments can cope with this situation, and in particular if they are able to identify which bunches of a train have collided. A decision on whether to pursue this scheme, rather than simply increasing the number of bunches, should be made by the end of this year.

Toward the end of next year, LEP will begin concentrated machine development work leading to the LEP 200 era. According to one scenario [1], 12 additional superconducting accelerating cavities will be installed in a six week shutdown in September. Together with cavities already installed, this should be enough to reach W-pair threshold. Alternatively, all the installation would be done during the $94-95$ shutdown, and the first part of 1995 would be spent mostly in necessary commissioning work, with some running for the experiments near the end of that year. The first full year of running above the W threshold will be 1996. The goal for the luminosity is $5 \times 10^{31}\,\mathrm{cm}^{-2}\mathrm{sec}^{-1}$ and the integrated luminosity should be 100 pb^{-1} per year. If money is available to replace most of the warm, i.e., non-superconducting, cavities with superconducting ones, the machine impedance is drastically reduced and the luminosity improved. Although progress on LHC will have an impact, it is generally assumed that LEP 200 running will last four years.

2.2.2 The OPAL Detector

As the table in the previous section shows, OPAL again surpassed all the other LEP detectors in number of Z^0s collected during the 1992 run period, logging some 714,000 multihadron events. OPAL's continued high running efficiency, between 85 and 90%, comes from careful attention to deadtime sources, vigilance in monitoring background levels, and high standards in detector maintenance.

During the 1992-93 shutdown, the silicon-tungsten luminosity monitor was installed in the forward regions of the detector, and a new improved version of the silicon strip vertex detector was implemented. Additional upgrades were made to the online data acquisition system, in particular to the filter processor. The "Riverside Snake Farm" a Hewlett-Packard based farm designed to provide extensive Monte Carlo capacity, entered into regular production. Improvements previously made in the hadron calorimeter electronics and monitoring devices paid dividends in trouble free running.

During the past year the group has published or submitted for publication a number of articles on various aspects of the detector. We list these here and will discuss them only briefly or not at all.

- pretrigger system [2]
- central jet chamber performance [3]
- data acquisition system [4]
- filter processor [5]
- MAW data analysis system [6]
- laser calibration of the central jet chamber [7]

Disaster Averted

Near the end of the 1992 running period, it became evident that moisture was accumulating inside the central detector. A decision was made that the detector would have to be opened at the end of the run, even though this entailed a large amount of effort. Once the insides of the detector were accessible, it was apparent that the moisture was coming from coil cooling hoses which were deteriorating in the gas environment, and that only good fortune had prevented a disastrous rupture in one or more of these high pressure hoses. During the shutdown, all the hoses were replaced with material known to be more resistant to the central detector gas.

Si-W Luminosity Monitor

The motivation for the silicon-tungsten luminosity monitor, approved for construction at the end of 1991 by the LEP Committee and the CERN Research Board, was the desire to determine the luminosity with a precision on the 0.1% level, to match the statistical precision of data samples of one million Z^0s per year. The only way to reach this precision was to place a detector at a smaller radius to collect a greater portion of the forward bhabha cross section. Its fiducial region lies between 25 and 60 milliradians, and consequently it sees a cross section of 70 nb, sufficient to achieve the desired precision.

The Si-W detector, whose innermost radius is only 6 cm from the beam, consists of 19 layers of silicon wafers interleaving precisely machined tungsten slabs for a total of 22 radiation lengths. The wafers in each layer are divided into 32 azimuthal sectors, each of which is further divided into 32 radial segments, for a total of 38,912 channels. Readout makes use the AMPLEX chip, developed at CERN. To obtain 0.1% precision on the luminosity, the limit of the inner acceptance must be known to 25 microns. Construction of the silicon wafers made use of printed circuit techniques which could readily maintain an accuracy of 3 microns. Effects of translation and rotation during installation, as well as temperature variations, can be tracked to 10 microns. Reconstruction of hits on the curved pad boundaries has been shown to contribute an uncertainty of less than 6 microns in test beam data. Consequently there is confidence that the required precision can be maintained.

As with any new detector, commissioning and shakedown have occupied a good part of this year's early running. Problems of heat buildup have been dealt with, but the radiation sensitivity of the detector is high, requiring careful monitoring of background conditions. A problem of a different sort is that of large data volume. Work is under way to compress the Si-W data structure, but inevitably more offline storage will be required. Energy resolution is currently $\Delta E/E \approx 24\%/\sqrt{E}$, and the design goal is $21\%/\sqrt{E}$. Figure 2.2 shows a typical luminosity event in the detector.

Current Luminosity Precision

Data from the Si-W monitor was not available for the 1992 analysis. However, further reductions in the overall experimental uncertainty of the luminosity determination coming from the original OPAL luminosity monitor were achieved during the past year. A comparison of the level of the systematic errors from all sources is presented in Table 2.2 for 1991 and 1992.

Silicon Strip Vertex Detector

The first phase of the OPAL silicon strip vertex detector was installed during the 1990-1991 shutdown and became fully operational by June of 1991. This version has two layers of single-sided strips giving information in the r-ϕ plane. The second phase was

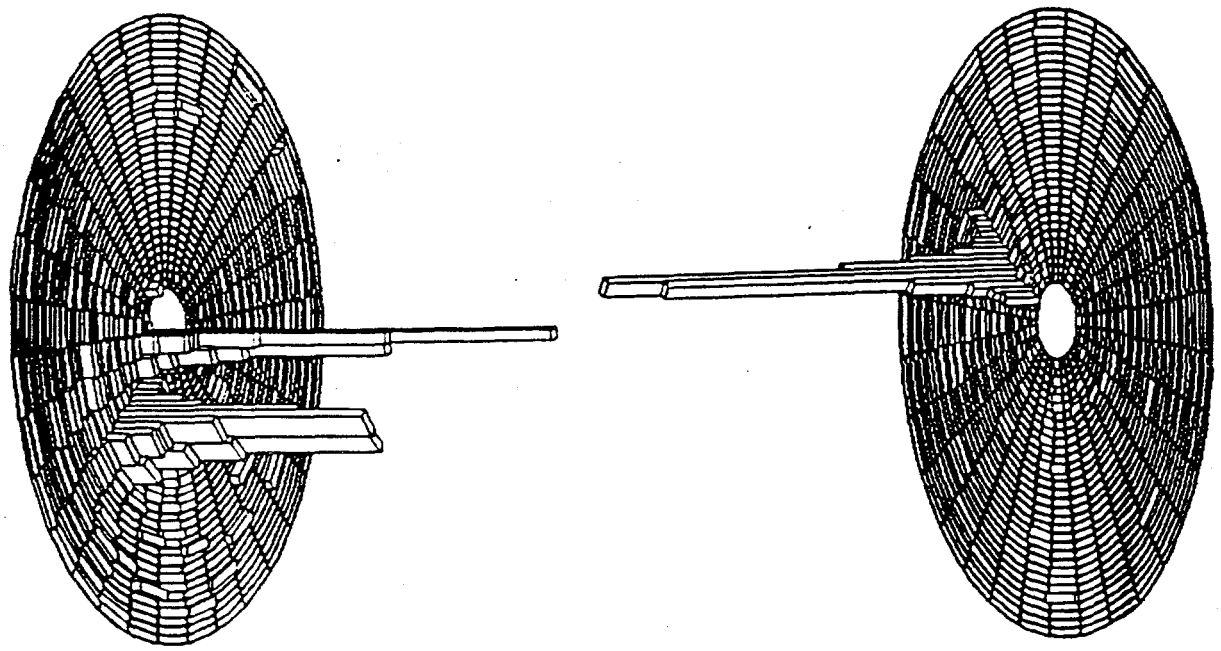

Figure 2.2: A radiative Bhabha event in the Si-W luminosity monitor

installed during this past shutdown and adds more precise z coordinate information for the vertex. This new version is not strictly a "double sided" detector in the nomenclature of the trade, but rather a "back-to-back" type, in which two single-sided strips are simply glued together. A novel feature of the detector construction is the use of a printed circuit on glass to daisy chain the z-coordinate readout of the three detector elements making up the "ladder" structure of the device and fan it into the multiplexing readout electronics at the end of the ladder.

The multiplexor chip is the MX7, a further evolution of the "Foxfet" chips developed by Micron Corporation that were used in the phase one version of the detector. [8] The high voltage system for the phase two detector is a suitably modified version of the original system manufactured in Italy under the supervision of Dr. William Gorn of UCR. Since the detector was completely rebuilt, the large initial calibration effort to correct for gravitational sag and torques applied during insertion over the beampipe that was necessary for the phase one version had to be repeated for the new one. Resolution in the r-ϕ plane is now 6 microns, approaching what had been obtained previously after two years running, while the resolution in the r-z plane is 13 microns, a factor of 50 improvement over what was previously available from the stereo readout of the gaseous vertex detector.

The Collaboration is discussing plans for an "extended Si vertex detector," which would be a true double sided detector and would have increased polar angle coverage and overlapping azimuthal coverage. Current plans are to install such a detector

Source of Uncertainty	1991 [%]	1992 [%]
Inhomogeneity in tube chambers	0.30	0.30
Pitch of tubes	0.08	0.07
Survey (with drift chambers)	0.21	0.21
Locations of drift wires	0.10	0.08
Calorimeter coordinates	0.04	0.02
Distance to interaction point	0.04	0.04
Using 1992 survey for 1991	0.06	n.a.
Trigger efficiency	< 0.02	< 0.02
Reconstruction inefficiency	< 0.01	< 0.01
Accidental background	< 0.01	< 0.01
Data statistics	0.32	0.19
Monte Carlo statistics	0.24	0.16
Overall	0.60	0.52

Table 2.2: Comparison of experimental uncertainties in the published 1991 and the preliminary 1992 absolute luminosity analysis

in 1995. It would thus benefit from continued improvement in double sided wafer technology and in readout chips. This proposal will be presented to the LEPC in November with the hope that construction can begin early in 1994. The extended vertex detector would be adequate into the LEP 200 era.

Data Acquisition and Reconstruction

The OPAL Event Filter, having once shaken off the confines of VME 68000 boards when it moved to the Apollo DN10K machine for last year's running, continued to expand its capabilities by migrating to a three-processor HP747/742, which has nearly 3.5 times the capacity of the Apollo. The function of the filter is to verify the hardware trigger and to classify the events into physics categories such as multihadronic or leptonic. The existence of such a process in the acquisition chain makes it possible to use loose hardware triggers with high and easily measurable efficiencies, but which also contain relatively high background levels. The filter is able to reject such backgrounds, and with current trigger implementations, approximately 35% of the

triggered events are rejected at this level. Recently the filter began active rejection of events, after extensive testing showed that filter-flagged events were inevitably rejected in subsequent analysis.

The SHIFT project, started jointly by OPAL and the CERN CN division, has become a general CERN computing facility and has replaced the IBM mainframe for large scale data analysis. Upgrades currently proposed for this system will bring its computing power from 96 CERN units (IBM 370/168 units) to 208 units, while the disk storage space will increase from 180 to 280 Gbytes.

The Hewlett Packard Workstation Farm

A farm of Hewlett Packard (HP) 9000 series workstations has been in operation at OPAL since the spring of 1992. At the time of this report, there are 29 workstations in all. Since the start, the UCR group has been the main contributor to this farm. Firstly, 10 of the 29 machines are provided by UCR, purchased with funds from the University. Secondly, nearly all of the initial setup of the farm, as well as the conversion of existing OPAL software libraries were done by UCR personnel. Lastly, the entire farm has always been, and continues to be, managed solely by two UCR research associates.

The original motivation for the purchase of the HP 9000 systems was two-fold. First, at a price of about $10,000, each 9000 series computer combines impressive processing power of approximately 45 million instructions per second (MIPs), with a 19 inch, 8-bit-plane high-resolution color display, and roughly 800 Megabytes of disk space. This highly competitive performance-to-price comparison makes them ideal as replacements for the aging, and increasingly troublesome, Apollo/DOMAIN and MicroVAX systems as general-purpose, personal workstations for OPAL physicists. Second, the spare CPU power on these machines can be utilized to generate large samples of Monte Carlo events, which are needed for the analysis of the nearly 2,000,000 Z^0 events produced at LEP. Those workstations belonging to UCR were purchased primarily for the latter use.

In the past year, the HP 9000 farm has performed extremely well in both roles described above. It was far more reliable than either the Apollo farm or the VAX cluster. The response of the HP-UX operating system on the 9000's is also consistently faster than either DOMAIN-OS on the Apollo's or VMS on the VAX systems, even if the HP workstations were running the OPAL detector Monte Carlo program in the background.

UCR played a key role in setting up a very simple but extremely efficient system for the generation of Monte Carlo events. A subset of 13 systems, including 8 of the 10 UCR CPU's, were fitted with extra disk space reserved for Monte Carlo production use. These special stations form the so-called "Riverside Snake Farm" (RSF) and have been used, in tandem with the "Central Snake Farm" (CSF) at CERN, as OPAL's main production platform for Monte Carlo simulation. (The initials "SF" really stand

for "Simulation Facility." "Snake Farm" is the popular designation.) After startup, each job runs locally on the designated CPU, immune to network problems, until the required number of events have been generated. The produced "data" file is then automatically spooled to an IBM cartridge, entered into the CERN on-line tape catalogue (FATMEN), and immediately made available to any member of OPAL. Since September, 1992, more than 1,500,000 simulated hadronic Z^0 decays have been produced, along with many hundreds of thousands of events of other types. It is estimated that the total output of RSF to date is equivalent to that of a VAX 780 running at 100% efficiency for 300 years.

Indeed, the production program on RSF has been so successful that it has led to unforeseen congestion in tape-handling at the CERN computing center, resulting from the great number of requests to read the now very large sample of Monte Carlo events. This observation has led to further development within the UCR group to extend the usefulness of the HP workstations. Despite their superior CPU power, the 9000 systems were not originally intended for batch processing of OPAL data summary tapes (DST's). That role has been adequately served by SHIFT, a cluster of Silicon Graphics RISC CPU's connected by the expensive but very fast ULTRANET, in contrast to the low-cost, slow thin-wire ETHERNET inhabited by the HP systems.

However, in view of the recent saturation of tape-staging on SHIFT, the UCR group has begun to evaluate the possibility of using an HP workstation, equipped with a digital-audio-tape (DAT) auto-changing drive ("stacker"), to analyze Monte Carlo DST's. A stacker that handles up to eight DAT cartridges has been ordered to set up a prototype system. It is estimated that an I/O-bound analysis job can run, without human intervention, through a sequence of eight tapes in a little under 24 hours, so that it would take merely three days to make a single pass through the DST files for a million simulated hadronic Z^0 decays. This task would currently require more than a month of real time on SHIFT or on the CERN IBM mainframe (CERNVM). It is envisioned that all of the Monte Carlo DST's currently available to OPAL can be fitted onto 40 to 50 DAT cartridges, which can in turn be placed in 6 to 8 stackers. At approximately $5,000 per stacker, this scheme would make available automatic access to some 80 gigabytes of simulated DST's for under $50,000.

2.2.3 OPAL Physics at the Z^0 – an Overview

Within the framework of the Standard Model, M_Z, the mass of the Z^0 boson, the massive neutral carrier of the electroweak field, is a fundamental parameter. Its precise determination, in conjunction with the knowledge of the fine structure constant α and the Fermi coupling constant G_F leads to well defined predictions for the couplings of the Z^0 to all fermions. Since these couplings, as well as the mass of the Z^0, are measured to high precision at LEP, comparison with predictions provides a stringent test of the Standard Model and places bounds on the allowed ranges of M_t and M_H.

The data recorded by the four LEP experiments until the end of 1992 correspond to approximately $5 \cdot 10^6$ Z^0 decays into hadrons and charged leptons. Various published and preliminary electroweak results from the four LEP collaborations were available at the time of the Europhysics Conference on High Energy Physics, Marseille, July 22–28 1993. These include the measurement of hadronic and leptonic cross sections, the leptonic forward-backward asymmetries, the τ polarization asymmetries, the $b\bar{b}$ and $c\bar{c}$ partial widths and forward-backward asymmetries, and the $q\bar{q}$ charge asymmetry. A preliminary combined result is now being circulated among the LEP collaborations. To demonstrate the sensitivity of the data, this combined set of electroweak measurements is used to constrain the parameters of the Standard Model.

Previously a procedure was proposed for combining the results from the LEP experiments for hadronic and leptonic cross sections and the leptonic forward-backward asymmetries [9, 10]. This procedure has introduced certain standards in the presentation of results among the four LEP experiments and is now well established. Details of the individual analyses can be found in [11, 12, 13, 14]. The results are based on the final results from two energy scans in 1990 and 1991 with center-of-mass energies in a range $\sqrt{s} = M_Z \pm 3$ GeV, and the preliminary high statistics data collected at the Z^0 peak in 1992. The total statistics for the four experiments have been presented in the section on LEP. An important aspect of the lineshape analysis is a precise knowledge of the LEP center-of-mass energies. The treatment of the LEP center-of-mass energies by the four LEP experiments is based on [15].

Z^0 Lineshape and Lepton Forward-Backward Asymmetries

For the averaging of results the LEP experiments provide a standard set of 9 parameters describing the information contained in hadronic and leptonic cross-sections and leptonic forward-backward asymmetries:

- The mass of the Z^0, M_Z, and the total width, Γ_Z, where the definition is based on the Breit Wigner denominator $(s - M_Z^2 + is\Gamma_Z/M_Z)$.

- The hadronic pole cross section:

$$\sigma_{\rm had}^{\rm pole} \equiv \frac{12\pi}{M_{\rm Z}^2}\frac{\Gamma_{ee}\Gamma_{\rm had}}{\Gamma_{\rm Z}^2}\,.$$

  Here Γ_{ee} and $\Gamma_{\rm had}$ are the partial widths of the Z^0 for decays into electrons and hadrons.

- The ratios:

$$R_{\rm e} \equiv \Gamma_{\rm had}/\Gamma_{ee} \qquad R_\mu \equiv \Gamma_{\rm had}/\Gamma_{\mu\mu} \qquad R_\tau \equiv \Gamma_{\rm had}/\Gamma_{\tau\tau}\,.$$

  Here $\Gamma_{\mu\mu}$ and $\Gamma_{\tau\tau}$ are the partial widths of the Z^0 for the decays $Z^0 \to \mu^+\mu^-$ and $Z^0 \to \tau^+\tau^-$.

- The pole asymmetries, $A_{\rm FB}^{0,f}$, for the processes $e^+e^- \to e^+e^-$, $e^+e^- \to \mu^+\mu^-$, $e^+e^- \to \tau^+\tau^-$:

$$A_{\rm FB}^{0,f} \equiv 3\frac{\hat{g}_{\rm e}^{\rm v}\,\hat{g}_{\rm e}^{\rm a}}{\hat{g}_{\rm e}^{\rm v\,2} + \hat{g}_{\rm e}^{\rm a\,2}}\frac{g_{\rm V_f}g_{\rm A_f}}{g_{\rm V_f}^2 + g_{\rm A_f}^2} \qquad {\rm f} = {\rm e},\ \mu,\ \tau\,.$$

  Here g_{V_f} and g_{A_f} are the effective vector and axial-vector neutral current couplings to fermions.

The four sets of 9 parameters provided by the LEP experiments from fits to the data taken until the end of 1992 are presented in Table 2.3.

	ALEPH	DELPHI	L3	OPAL
$M_{\rm Z}$(GeV)	91.187±0.009	91.187±0.009	91.195±0.009	91.182±0.009
$\Gamma_{\rm Z}$(GeV)	2.501±0.011	2.482±0.012	2.493±0.010	2.483±0.012
$\sigma_{\rm had}^{\rm pole}$(nb)	41.61±0.16	41.02±0.27	41.33±0.26	41.57±0.26
R_e	20.58±0.15	20.70±0.18	20.90±0.16	20.85±0.17
R_μ	20.82±0.15	20.48±0.15	21.02±0.16	20.79±0.12
R_τ	20.62±0.17	20.88±0.20	20.78±0.20	21.01±0.16
$A_{\rm FB}^{0,e}$	0.0185±0.0059	0.0237±0.0092	0.0135±0.0078	0.0057±0.0086
$A_{\rm FB}^{0,\mu}$	0.0147±0.0047	0.0143±0.0050	0.0167±0.0064	0.0100±0.0052
$A_{\rm FB}^{0,\tau}$	0.0182±0.0053	0.0213±0.0068	0.0257±0.0089	0.0211±0.0062

Table 2.3: Line shape and asymmetry parameters from 9-parameter fits to the data of the four LEP experiments.

The procedure used for the averaging the LEP results is described briefly below. A fuller description was presented at last year's Dallas meeting. [10]. Each of the

experiments provided a correlation matrix for their parameters, and also a matrix including only the uncertainties introduced by the LEP energy calibrations. In addition the theoretical uncertainty for the calculation of the small angle Bhabha cross-section, which is assumed to be fully correlated among the experiments, has been taken into account. The information above is used to construct the full covariance matrix of the input parameters. Then a combined parameter set is obtained by minimizing $\chi^2 = \Delta^T \mathcal{V}^{-1} \Delta$, where Δ denotes the vector of residuals of the combined parameter set to the results of the individual experiments. The combined parameter set is given in Table 2.4

Parameter	Average Value
M_Z(GeV)	91.187±0.007
Γ_Z(GeV)	2.489±0.007
σ_{had}^{pole}(nb)	41.55±0.14
R_e	20.746±0.081
R_μ	20.772±0.071
R_τ	20.829±0.090
$A_{FB}^{0,e}$	0.0156±0.0038
$A_{FB}^{0,\mu}$	0.0136±0.0028
$A_{FB}^{0,\tau}$	0.0205±0.0034

Table 2.4: Average line shape and asymmetry parameters from the data of the four LEP experiments, without assumption of lepton universality. The χ^2 of the average is $\chi^2/(\text{d.o.f.}) = 26/27$.

The parameters given in this table make no assumption on lepton universality. Lepton universality means that the gauge couplings of the three known lepton doublets are assumed to be equal. The assumption of lepton universality can be used to reduce the set of nine parameters given above to a set of five parameters. Due to mass corrections to $\Gamma_{\tau\tau}$ we expect, however, a small (0.2%) difference between the values for R_e and R_μ and the value for R_τ. The procedure as to how to take into account these mass terms, when specifying a single partial width, $\Gamma_{\ell^+\ell^-}$, for the decay of the Z^0 into leptons is not unambiguous and has to be defined. At present $\Gamma_{\ell^+\ell^-}$ is defined as the partial Z^0 width of a massless charged lepton. In terms of effective couplings $\Gamma_{\ell^+\ell^-}$ can be written as:

$$\Gamma_{\ell^+\ell^-} = \frac{G_F M_Z^3}{6\pi\sqrt{2}} (\hat{g}_l^{v\,2} + \hat{g}_l^{a\,2})(1 + \delta_{QED}),$$

where $\delta_{QED} = 3\alpha/(4\pi)$ accounts for final state photonic corrections.

The data are consistent with lepton universality. Table 2.5 provides the five parameters, M_Z, Γ_Z, σ_{had}^{pole}, R_ℓ and $A_{FB}^{0,\ell}$, based on this assumption. These are obtained

from a parameter transformation of the LEP average for the 9 parameter fit (Table 2.4), which has an unambiguous treatment of mass terms.

The parameter R_ℓ can be used to determine the strong coupling constant α_S. For $M_{\rm Z} = 91.187 \pm 0.007$, $M_{\rm top} = 150$ GeV and $M_{\rm H} = 300$ GeV we obtain from $R_\ell = 20.766 \pm 0.049$:

$$\alpha_S(M_{\rm Z}^2) = 0.124 \pm 0.008\,.$$

The uncertainty introduced by a variation of $M_{\rm top}$ and $M_{\rm H}$ is still negligible compared to the experimental precision.

The parameters $M_{\rm Z}$, $\Gamma_{\rm Z}$, $\sigma_{\rm had}^{\rm pole}$, R_ℓ and $A_{\rm FB}^{0,\ell}$ are convenient for fitting and averaging since they have minimal correlations among them. However a number of other parameters, which can be derived from the previous set, are of physical importance. Table 2.6 gives a number of these commonly used parameters derived from the results of the 9-parameter (Table 2.4), and the 5-parameter fit (Table 2.5).

Among these parameters we quote $\sin^2\theta_{eff}^{\rm lept}$ which is defined as:

$$\sin^2\theta_{eff}^{\rm lept} \equiv \frac{1}{4}(1 - \hat{g}_{\rm l}^v \,/\, \hat{g}_{\rm l}^a)\,.$$

As an indication of the power of these new data we use them to derive the number of light neutrino species. Using the results of Table 2.5 we find:

$$\Gamma_{\rm inv}/\Gamma_{\ell^+\ell^-} = 5.940 \pm 0.054\,.$$

Taking the Standard Model value for the ratio of the partial widths to neutrinos and charged leptons:

$$\Gamma_\nu/\Gamma_l = 1.993 \pm 0.002$$

we find:

$$N_\nu = 2.980 \pm 0.027\,.$$

The τ Polarization

The τ polarization $\mathcal{P}_\tau$ is determined by measuring the longitudinal polarization of τ pairs produced in $\rm Z^0$ decays. It is defined as

$$\mathcal{P}_\tau = \frac{\sigma_{\mathcal{R}} - \sigma_{\mathcal{L}}}{\sigma_{\mathcal{R}} + \sigma_{\mathcal{L}}}$$

where σ_R and σ_L are the cross-sections for production of a right-handed and left-handed τ^-, respectively.

Correcting for small QED effects due to photon exchange and interference, and initial state radiation the angular dependence of $\mathcal{P}_\tau$, as a function of the angle θ between the e^- and the τ^-, is given by:

$$\mathcal{P}_\tau(\cos\theta) = -\frac{\mathcal{A}_\tau + \mathcal{A}_{\rm e}\frac{2\cos\theta}{1+\cos^2\theta}}{1 + \mathcal{A}_\tau\mathcal{A}_{\rm e}\frac{2\cos\theta}{1+\cos^2\theta}}\,.$$

Parameter	Average Value
M_Z(GeV)	91.187±0.007
Γ_Z(GeV)	2.489±0.007
σ^{pole}_{had}(nb)	41.55±0.14
R_ℓ	20.766±0.049
$A^{0,\ell}_{FB}$	0.0161±0.0019

Table 2.5: Average line shape and asymmetry parameters from the data of the four LEP experiments. The χ^2 of the average is χ^2/(d.o.f.) = 30/31.

Without Lepton Universality:	
Γ_{ee}(MeV)	83.83±0.31
$\Gamma_{\mu\mu}$(MeV)	83.75±0.41
$\Gamma_{\tau\tau}$(MeV)	83.50±0.46
With Lepton Universality:	
Γ_l(MeV)	83.79±0.28
Γ_{had}(MeV)	1740.2±6.0
Γ_{inv}(MeV)	497.6±4.3
$g^2_{V_l}$	0.00137±0.00017
$g^2_{A_l}$	0.25074±0.00085
$\sin^2\theta^{lept}_{eff}$	0.2315±0.0012

Table 2.6: Average values of some derived parameters.

Correcting for small QED effects due to photon exchange and interference, and initial state radiation the angular dependence of $\mathcal{P}_\tau$, as a function of the angle θ between the e^- and the τ^-, is given by:

$$\mathcal{P}_\tau(\cos\theta) = -\frac{\mathcal{A}_\tau + \mathcal{A}_e \frac{2\cos\theta}{1+\cos^2\theta}}{1 + \mathcal{A}_\tau \mathcal{A}_e \frac{2\cos\theta}{1+\cos^2\theta}}.$$

When averaged on all production angles $\mathcal{P}_\tau$ is a measurement of $\mathcal{A}_\tau$, while as a function of $\cos\theta$, $\mathcal{P}_\tau(\cos\theta)$ provides nearly independent determinations of $\mathcal{A}_\tau$ and $\mathcal{A}_e$, allowing thus a test of the universality of the couplings of the Z^0 to e and τ. The values of $\mathcal{A}_\tau$ and $\mathcal{A}_e$ at the peak are directly related to the ratio of the vector and axial vector couplings for τ and e:

$$\mathcal{A}_f = \frac{2 g_{V_f} g_{A_f}}{(g_{V_f}^2 + g_{A_f}^2)}.$$

The results for $\mathcal{A}_\tau$ and $\mathcal{A}_e$ respectively obtained by the four experiments [16, 17, 18, 19] are

$$\begin{aligned} \mathcal{A}_\tau &= 0.139 \pm 0.014 \\ \mathcal{A}_e &= 0.130 \pm 0.025 \end{aligned}$$

Only OPAL and ALEPH have so far provided a measurement of $\mathcal{A}_e$.

The partial widths of the Z^0 into leptons, the lepton forward-backward asymmetries, the τ polarization and the τ polarization asymmetry can all be combined to determine the vector and axial vector couplings for e, μ and τ. The asymmetries determine the ratio $\hat{g}_l^v$ / $\hat{g}_l^a$, while the axial vector coupling squared is derived from the leptonic partial width. The corresponding results for the effective lepton couplings are given in Table 2.7. Figure 2.3 shows the one standard deviation contours in the $\hat{g}_l^a$-$\hat{g}_l^v$ plane.

$\hat{g}_e^v$	-0.0382 ± 0.0032	$\hat{g}_e^a$	-0.5008 ± 0.0009
g_{V_μ}	-0.0289 ± 0.0065	g_{A_μ}	-0.5011 ± 0.0013
g_{V_τ}	-0.0350 ± 0.0032	g_{A_τ}	-0.5006 ± 0.0014
$\hat{g}_l^v$	-0.0360 ± 0.0019	$\hat{g}_l^a$	-0.5008 ± 0.0009

Table 2.7: Results for the leptonic vector and axial vector couplings without and with the assumption of lepton universality.

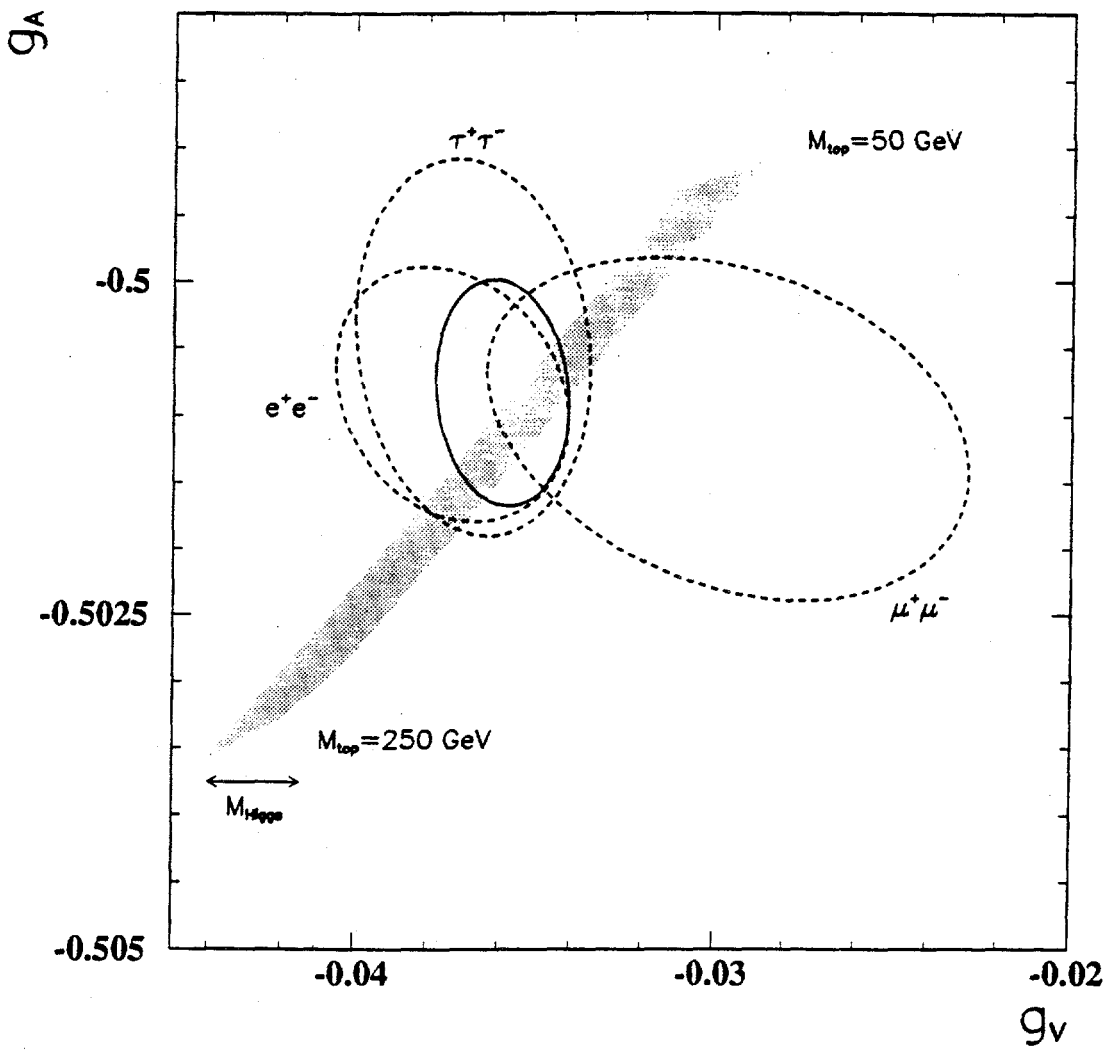

Figure 2.3: One standard deviation contours (39% probability) in the $\hat{g}_l^v$-$\hat{g}_l^a$ plane. The shaded band represents the Standard Model prediction.

In addition, the measured ratios of the e, μ and τ couplings provide a test of universality:

$$g_{A_\mu}/\,\hat{g}^a_e = 1.0005 \pm 0.0027\ ,\ g_{A_\tau}/\,\hat{g}^a_e = 0.9995 \pm 0.0029\ ,$$

$$g_{V_\mu}/\,\hat{g}^v_e = 0.76 \pm 0.20\ ,\qquad g_{V_\tau}/\,\hat{g}^v_e = 0.92 \pm 0.12\ .$$

Electroweak Results with b and c Quarks

The measurements of $\Gamma_{b\bar{b}}/\Gamma_{had}$ are divided into three categories: lepton tagging [20, 21, 22, 23], for which the LEP average is

$$\Gamma_{b\bar{b}}/\Gamma_{had} = 0.221 \pm 0.003 \pm 0.002 \pm 0.005$$

event shapes [24, 25, 26] with average value

$$\Gamma_{b\bar{b}}/\Gamma_{had} = 0.226 \pm 0.002 \pm 0.003 \pm 0.004$$

and lifetime tagging [27, 28, 29]. where the average is

$$\Gamma_{b\bar{b}}/\Gamma_{had} = 0.2169 \pm 0.0018 \pm 0.0015 \pm 0.0027$$

Where three errors are quoted for the LEP averages, the first is statistical, the second from uncorrelated systematic errors, i.e., those specific to a given experiment, and the third from systematic errors common to all four experiments. The Boosted Sphericity Product results were neglected because the overall errors from this method, and in particular the systematic uncertainty due to the light quarks, are very large.

To compute the overall average of all the results of LEP, the results from the three methods were assumed to be entirely uncorrelated. This is not exact, as there are statistical correlations between the results using different methods by the same experiment (for example the mixed lepton/lifetime result of DELPHI). In addition there are some sources of common systematic error, for example due to b quark fragmentation. However, the different measurements consider different aspects of the fragmentation process, and the correlations are difficult to extract. These correlations are expected to have a negligible effect on the overall average, which is:

$$\Gamma_{b\bar{b}}/\Gamma_{had}(\text{LEP Average}) = 0.2200 \pm 0.0027.$$

The values for $\Gamma_{c\bar{c}}/\Gamma_{had}$ are unchanged since the Montreal conference[30, 20, 31, 32]. The LEP average value quoted is a simple weighted average assuming no common errors.

$$\Gamma_{c\bar{c}}/\Gamma_{had} = 0.171 \pm 0.014$$

Measurements of $A_{FB}^{b\bar{b}}$ and $A_{FB}^{c\bar{c}}$ using a lepton tag, a lifetime tag in combination with a jet charge measurement and a D^* tag are available [20, 34, 35, 36, 37]. The

lepton tag values for $A_{FB}^{b\bar{b}}$ are corrected for mixing using $\chi = 0.115 \pm 0.009 \pm 0.006$, where the second error is due to the semileptonic decay model uncertainty [33]. In general no other corrections are made, in particular no QCD corrections. As above, the systematic errors are divided into an uncorrelated part, for example due to backgrounds, lepton identification, detector effects, and a correlated part. The combined result is

$$A_{FB}^{b\bar{b}} = (9.4 \pm 0.5 \pm 0.2 \pm 0.3)\% \ (\chi^2/(\text{d.o.f.}) = 4.0/5).$$

For the measurements of $A_{FB}^{c\bar{c}}$, no corrections are applied to the experimental values. The covariance matrix was calculated as before but dividing the correlated errors into six slightly different categories: Semileptonic decay model,semileptonic branching ratios, fragmentation, $\Gamma_{b\bar{b}}$ and $\Gamma_{c\bar{c}}$, $A_{FB}^{b\bar{b}}$, D^* branching ratios. In this case the average result is:

$$A_{FB}^{c\bar{c}} = (6.6 \pm 1.1 \pm 0.8 \pm 0.6)\% \ (\chi^2/(\text{d.o.f.}) = 4.5/5)$$

with the errors divided up as before.

In order to derive the pole asymmetries, $A_{FB}^{0,b}$ and $A_{FB}^{0,c}$ (defined in an analogous way as for leptons) certain corrections should be applied: A QED shift mainly due to initial state radiation, a QCD correction calculated using a k-factor of 0.75 ± 0.25, reflecting the range of explicit or implicit event selection criteria of the experimental methods which biases the relative fractions of 2- and 3-jet events, and a correction due to the shift in centre-of-mass energy. The pole asymmetries are therefore

$$\begin{aligned} A_{FB}^{0,b} &= 0.098 \pm 0.006 \quad \text{and} \\ A_{FB}^{0,c} &= 0.075 \pm 0.015 \end{aligned}$$

for b and c quarks, respectively.

Determination of $\sin^2\theta_{eff}^{lept}$ from the Hadronic Charge Asymmetry

ALEPH [38], DELPHI [39], and OPAL [40] have published measurements of the charge asymmetry in the inclusive hadronic event sample, based on the data including 1991. ALEPH [41] has given a preliminary number including 1992 data and an improved technique. Within the $SU(2) \times U(1)$ structure the quark asymmetries are determined by one unique value of the effective mixing angle, $\sin^2\theta_{eff}^{lept}$, up to small fermion dependent vertex corrections which are small and assigned to their Standard Model values. The analyses differ somewhat, ALEPH and DELPHI using an integrated charge average, OPAL and DELPHI using a charge assignment on event by event basis using different combinations of tracks. The intermediate quantities given in the papers, the average forward-backward charge asymmetry $\langle Q_{FB} \rangle$, or the hadronic forward backward asymmetry A_h, cannot be directly compared as they include detector dependent effects, acceptances and detector efficiencies. It is therefore reasonable to use $\sin^2\theta_{eff}^{lept}$ as a means of combining these results.

The present average, being dominated by the preliminary result of one experiment, is not very sensitive to the treatment of common uncertainties. More attention in the combination procedure will certainly be needed when all experiments quote a comparable error.

Exp.	data	s/u	Sph. cut?	$\sin^2\theta^{\rm lept}_{eff}$
ALEPH	89-90 publ. +89-92 prel.	0.315±0.045	NO	0.2317±0.0013±0.0011
DELPHI	90-91 publ.	0.315±0.045	NO	0.2345±0.0030±0.0027
OPAL	90-91 publ.	0.285±0.050	S<0.12	0.2321±0.0017±0.0028
Average				0.2320±0.0011±0.0011

Table 2.8: Summary of the determination of $\sin^2\theta^{\rm lept}_{eff}$ from inclusive hadronic charge asymmetries at LEP.

The effective electroweak mixing angle $\sin^2\theta^{\rm lept}_{eff}$

The effective electroweak mixing angle $\sin^2\theta^{\rm lept}_{eff}$ defined in the first part of this section can be determined from the combined LEP measurements for the various asymmetries. For the case of the lepton asymmetry only the assumption of universality is used for the combination. This holds in practice also for the quark asymmetries due to the reduced sensitivity to the hadronic vertex. The results of the determinations of $\sin^2\theta^{\rm lept}_{eff}$ and their combination are shown in Table 2.9.

Standard Model Constraints

The precision measurements collected in the preceeding sections can be used to check the validity of the Standard Model and to infer valuable information about its basic parameters. Their accuracy makes them sensitive to the top quark mass, $M_{\rm top}$, and the mass of the Higgs boson, $M_{\rm H}$, through the loop corrections. The leading top quark dependence is quadratic and allows a determination of $M_{\rm top}$. The main dependence on $M_{\rm H}$ is logarithmic and, with the present data accuracy, it is not expected to allow a meaningful determination of $M_{\rm H}$. The measurements collected above, are summarized in Table 2.10.

Table 2.11 shows the constraints obtained on $M_{\rm top}$ and $\alpha_S(M_{\rm Z}^2)$ when fitting all the above measurements to the most up to date Standard Model calculations [43].

Since the data is not expected to have sensitivity with respect to $M_{\rm H}$, the fits have been repeated for $M_{\rm H} = 60,\ 300$ and 1000 GeV and the difference in the fitted param-

	$\sin^2\theta^{lept}_{eff}$
$A^{0,\ell}_{FB}$	0.2315 ± 0.0012
$\mathcal{A}_\tau$	0.2327 ± 0.0018
$\mathcal{A}_e$	0.2338 ± 0.0031
$A^{0,b}_{FB}$	0.2322 ± 0.0011
$A^{0,c}_{FB}$	0.2313 ± 0.0036
$\langle Q_{FB} \rangle$	0.2320 ± 0.0016
LEP Average	0.2321 ± 0.0006

Table 2.9: Comparison among different determinations of $\sin^2\theta^{lept}_{eff}$. The LEP average is obtained as a weighted average assuming no correlations. The χ^2 of the average is $\chi^2/(\text{d.o.f.}) = 0.7/5$.

eters is quoted as the uncertainty. Two different cases are presented for comparison purposes: the results obtained using only the LEP data, with $\alpha_S(M_Z^2)$ constrained by the LEP event shape measurements ($\alpha_S(M_Z^2) = 0.123 \pm 0.006$ [42]) and the results obtained using in addition the measurements of M_W and M_W/M_Z from CDF [44] and UA2 [45], and the measurements of the neutrino neutral to charged current ratios from CDHS [46], CHARM [47] and CCFR [48] also with the $\alpha_S(M_Z^2)$ constraint. The χ^2 of the fits shows that the agreement of the data with their Standard Model predictions is excellent.

The fact that the $\Gamma_{b\bar{b}}/\Gamma_{had}$ measurement has an accuracy of the order of one per cent should allow the estimation of the top mass entering the $Z^0 b\bar{b}$ vertex correction in a way which is largely free from assumptions on the Higgs sector structure (in contrast to other measurements for which the M_{top} determination is strictly valid only in the Standard Model framework). Unfortunately, there is no M_{top} value which in the Standard Model would lead to the measured $\Gamma_{b\bar{b}}/\Gamma_{had}$. This is due to the fact that the measurement would prefer an M^2_{top} correction of different sign than the one predicted by the Standard Model. Therefore, the fast increase of χ^2 as a function of M_{top} is somewhat 'artificial' and its interpretation has to be taken with care.

Figure 2.4 shows, for the fit in Table 2.11 column 5, the χ^2 value as a function of M_{top} for the three values of M_H considered in Table 2.11. The increase in χ^2 when the Higgs mass is changed between the two extreme values is of about 1.7. The bulk of this increase is traced back basically to the contribution of the $\Gamma_{b\bar{b}}/\Gamma_{had}$ measurement. Since this measurement constrains 'artificially' the top mass and, given the fact that the rest of data gives a determination of the top mass which is strongly correlated with the Higgs mass, it constrains also the Higgs mass. Our conclusion is that this sensitivity to the Higgs mass also might be just 'artificial' and hence its interpretation has to be taken with extreme care.

measurement	result
a) LEP	
line-shape and lepton asymmetries:	
M_Z	91.187 ± 0.007 GeV
Γ_Z	2.489 ± 0.007 GeV
σ_{had}^{pole}	41.55 ± 0.14 nb
R_ℓ	20.766 ± 0.049
$A_{FB}^{0,\ell}$	0.0161 ± 0.0019
+ correlation matrix	
τ polarization asymmetries:	
$\mathcal{A}_\tau$	0.138 ± 0.014
$\mathcal{A}_e$	0.130 ± 0.025
b and c quark results:	
$A_{FB}^{0,b}$	0.098 ± 0.006
$A_{FB}^{0,c}$	0.075 ± 0.015
$\Gamma_{b\bar{b}}/\Gamma_{had}$	0.2200 ± 0.0027
$q\bar{q}$ charge asymmetry:	
$\sin^2\theta_{eff}^{lept}$	0.2320 ± 0.0016
topology of hadronic events:	
$\alpha_S(M_Z^2)$ [42]	0.123 ± 0.006
b) $p\bar{p}$ and νN	
M_W/M_Z (UA2)	0.8813 ± 0.0041
M_W (CDF)	79.91 ± 0.39
$\sin^2\theta_W(\nu N)$	0.2256 ± 0.0047

Table 2.10: Summary of measurements included in the combined analysis of Standard Model parameters. Section a) summarizes LEP averages, section b) electroweak precision tests from hadron colliders and νN-scattering.

	α_S constrained	α_S constrained + Collider and ν data
$M_{\rm top}$ (GeV)	$164^{+18\ +19}_{-20\ -22}$	$162^{+16\ +18}_{-17\ -21}$
α_S	$0.123 \pm 0.004 \pm 0.001$	$0.122 \pm 0.004 \pm 0.001$
χ^2/ d.o.f.	3.6/9	4.5/12
$\sin^2\theta^{\rm lept}_{eff}$	$0.2325 \pm 0.0005\ ^{+0.0001}_{-0.0002}$	$0.2325 \pm 0.0005\ ^{+0.0001}_{-0.0002}$
$\sin^2\theta_{\rm W}$	$0.2257 \pm 0.0019\ ^{+0.0005}_{-0.0003}$	$0.2259 \pm 0.0017\ ^{+0.0004}_{-0.0003}$
$M_{\rm W}$ (GeV)	$80.24 \pm 0.10\ ^{+0.02}_{-0.03}$	$80.23 \pm 0.09\ ^{+0.01}_{-0.02}$

Table 2.11: Results of fits to LEP and other data for $M_{\rm top}$ and α_S. In the second and third columns α_S is constrained to the value 0.123 ± 0.006. In the third column data are included from the $\rm p\bar{p}$ experiments UA2 [45]: $M_{\rm W}/M_{\rm Z} = 0.8813 \pm 0.0041$, and CDF [44]: $M_{\rm W} = 79.91 \pm 0.39$ GeV and from the neutrino experiments, CDHS [46], CHARM [47] and CCFR [48]: $\sin^2\theta_{\rm W} = 0.2256 \pm 0.0047$. The first error is experimental while the second error corresponds to 60 GeV $< M_{\rm H} <$ 1000 GeV.

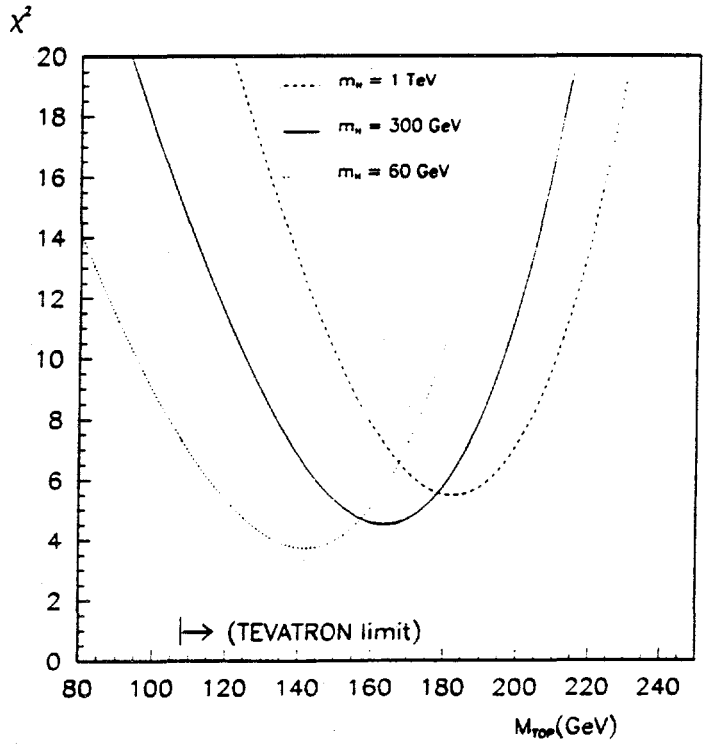

Figure 2.4: The χ^2 curves for the Standard Model fit in Table 2.11, column 3 to the electroweak precision measurements listed in Table 2.10 as a function of $M_{\rm top}$ for three different Higgs mass values spanning the interval $60 < M_{\rm H}\,({\rm GeV}) < 1000$. The strong coupling constant has been constrained to $\alpha_S(M_{\rm Z}^2) = 0.123 \pm 0.006$.

2.2.4 QCD and Hadronic Final States

Large data statistics and excellent detector capabilities have made the subjects QCD and hadronization important and prolific areas of study for OPAL. Within OPAL, UCR plays a leading role in organization, infrastructure and data analysis for these studies. UCR installed and operates a cluster of ten HP-PA workstations at CERN which form the RSF, or "Riverside Snake Farm," the main OPAL facility for generating large samples of simulated multihadron Z^0 decays. This cluster constitutes a major contribution of UCR to the OPAL data analysis program. Amongst UCR personnel, Gary serves as coordinator of OPAL QCD activities. He also continues his role as a central coordinator of OPAL Monte Carlo work. Jui and Schenk manage the RSF cluster. Beyond its use for general OPAL multihadron simulation work, the cluster is an essential resource for the UCR based QCD analyses. Summaries of the UCR projects are given below.

Quark-Gluon Jet Differences

The UCR group in OPAL pioneered work at LEP on the subject of quark and gluon jet structure. New techniques were introduced to tag quark and gluon jets and to compare their properties. A follow-up analysis to the original work [49] was completed and published this past year [50]. As with the original work, this new publication is entirely a UCR effort. The new publication is the first from a single experiment to be based on more than one million hadronic Z^0 decays. It is also the first analysis to employ secondary vertex reconstruction to separate quark and gluon jets in a multi-jet environment. The new publication contains a comprehensive study of quark and gluon jet differences and a presentation of the innovative quark and gluon tagging techniques. The OPAL method for observing quark and gluon jet differences is now being repeated by other LEP experiments, who obtain preliminary results very similar to the published OPAL ones [51].

In QCD, the gluon is associated with a color charge $C_A = 3$ and the quark with a charge $C_F = 4/3$ and one naïvely expects a ratio of $(C_A/C_F) = 9/4$ for the multiplicity of soft gluons produced from the two jet types [52]. For equal quark and gluon jet energies, the larger multiplicity of the gluon jet means that its particle energy spectrum is softer. This in turn implies that the angles of particles relative to the jet axis should be larger in gluon than in quark jets of equal energy, because the mean transverse energy value of the particles is expected to be about the same: thus that gluon jets are spread over a larger angular interval than quark jets and in this sense are broader. Much experimental effort has been spent to observe these differences, but without much success. The situation for the earlier analyses was confused because of the use of quark and gluon jets with different energies or else because the quark jets were sometimes taken from two-jet events in e^+e^- annihilations while the gluon jets were taken from three-jet events, whereas model calculations imply that the jet

energy and environment substantially influence quark and gluon jet properties. As a consequence, the experimental results have been contradictory and inconclusive, being dependent on QCD Monte Carlos for interpretation.

In the OPAL-invented analysis, a new technique for identifying quark and gluon jets and comparing their properties was introduced. Rare, symmetric three-jet events were employed, in which the angles between the highest energy jet and each of the two lower energy jets were essentially the same, namely $150 \pm 10°$: therefore the jet energies and environments of the two lowest energy jets were identical. For this configuration, the highest energy jet is known to be a quark or an antiquark jet with high probability, because of the bremsstrahlung nature of gluon radiation. In the original OPAL work [49], a high energy lepton, assumed to originate from charm or bottom quark semi-leptonic decay, was required to be present in one of the two lower energy jets. Since heavy quarks in e^+e^- annihilation are produced predominantly at the electro-weak vertex, the observation of such a lepton identified the jet as being a quark jet, with high probability. The lower energy jet without the lepton was thus "anti-tagged" as the gluon jet. To obtain an unbiased sample of quark jets with which to compare these gluon jets, the same symmetric event sample was employed, but without the lepton tag requirement. In this case, the two lower energy jets were known to be an equal mixture of quark and gluon jets and were presumed to have normal properties: comparing these jets to the anti-tagged gluon jets from the tagged events allowed a comparison of quark and gluon jet properties because the latter sample had a much larger gluon jet component. Since the quark and gluon jets being compared had the same energy, event environment and selection criteria, they could be compared directly, with no need for Monte Carlo calculations to establish the results. This study yielded direct and model independent observations of quark and gluon jet differences which were in qualitative agreement with the expectations of QCD, as discussed above, and which avoided the systematic pitfalls of the previous experimental analyses.

In the new publication [50], the previous OPAL study is updated using a data sample which is about seven times larger. A new technique to anti-tag the gluon jet is introduced, based on reconstructed secondary vertices to identify bottom quark jets instead of high energy leptons. This is the first time that secondary vertices have been used in a three-jet analysis. Furthermore, this is the first paper from OPAL making use of the silicon microvertex detector, installed in 1990. Because of their relatively long lifetime ($\tau \sim 10^{-12}$s), bottom hadrons travel a considerable distance from their point of creation before they decay. They thus lead to "secondary vertices" displaced from the primary e^+e^- collision point, from which the bottom hadron decay products emanate. Reconstruction of secondary vertices in jets therefore permits bottom quark jets to be identified and the methods we developed in our earlier study of symmetric three jet events to be applied. Additionally, the tagged event sample from secondary vertices has little overlap with the lepton tagged one and so provides a consistency check on our previous results. In our previous study, the quark and

gluon jets were not corrected for residual quark and gluon jet misidentification. In the new study, the purities of the identified quark and gluon jets are evaluated using Monte Carlo. After presenting the data directly in a model independent manner, as in the first publication, the measurements are corrected for the residual quark-gluon jet impurities and are then compared to QCD models containing different assumptions about the perturbative phase and the hadronization process.

As examples of the new results, Figures 2.5 (a) and (b) show the particle mul-

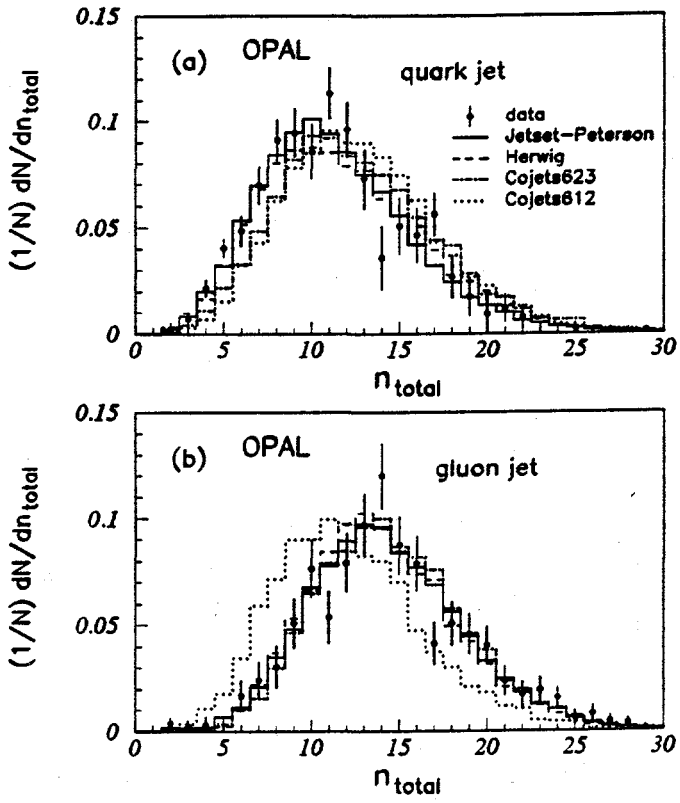

Figure 2.5: (a) and (b): Multiplicity distributions of the quark and gluon jets, corrected for quark and gluon jet misidentification. The Monte Carlo results include detector simulation and the same selection criteria as the data, except the quark and gluon jets are identified using Monte Carlo information.

tiplicity distributions for the separated quark and gluon jet samples. The energies of the jets in the study are about 24.5 GeV: the jets being compared are essentially monochromatic because of the analysis technique. The data in Figure 2.5 have been corrected for the residual quark-gluon jet impurities. The mean values are $\langle n \rangle_{\mathbf{quark}} = 11.37 \pm 0.13$ for the quark jet distribution (Figure 2.5 (a)) and

$\langle n \rangle_{\mathbf{gluon}} = 14.41 \pm 0.13$ for the gluon jet distribution (Figure 2.5 (b)). This leads to a ratio of

$$\frac{\langle n \rangle_{\mathbf{gluon}}}{\langle n \rangle_{\mathbf{quark}}} = 1.267 \pm 0.043\,(\text{stat.}) \pm 0.055\,(\text{syst.}) \quad ; \tag{2.1}$$

for the multiplicity of gluon relative to quark jets, which represents the first significant measurement of this quantity.[1] Thus the gluon jets yield a mean particle multiplicity which is approximately 1.3 times larger than the corresponding value for the quark jets. We note that this value, although significantly different from unity, is substantially smaller than the naïve value of 9/4 mentioned above. This is not entirely unexpected, however, because the analytic result is valid only for so-called "asymptotic energies" which may not correspond to the experimental conditions, because the analytic result is performed for partons whereas the experimental measurements are based on hadrons, and because the jet definitions used in the calculation and in the experiment are not entirely the same. We are currently studying methods of testing the analytic result more directly. At the same time, we are working with theorists to obtain a calculation which corresponds more closely to the experimental conditions.

In Figure 2.5 are also shown the predictions of several QCD parton shower Monte Carlos including hadronization. The Jetset-Peterson model [54], which employs string fragmentation, and the Herwig [55] model, which employs cluster hadronization, yield good descriptions of both the quark and gluon jet multiplicity. This establishes that the difference we observe between the quark and gluon jets is indeed consistent with QCD. The model Cojets623 [56], which employs independent hadronization, also provides a reasonable description of the data. The model Cojets612 [56] likewise employs independent hadronization, but unlike the other models implements no difference between quark and gluon jet properties: Cojets612 does not describe the measurements, as is most clearly seen for the gluon jet in Figure 2.5 (b), which emphasizes the sensitivity of our analysis to differences between quark and gluon jet structure.

In Figure 2.6 (a) are shown the measured distributions of the inclusive particle energy spectra for the quark and gluon jets. The ratio of the gluon to the quark jet data is shown in Figure 2.6 (b). The softer particle energy spectrum of gluon jets relative to quark jets, as expected from QCD, is very clear. Again, the model predictions are in good agreement with the data except for Cojets612.

In Figure 2.7 the widths of the quark and gluon jets are compared. Figure 2.7 (a) shows the differential distribution of the visible jet energy with respect to the polar angle around the jet axis for the two jet types. The distributions are normalized event-by-event by the total visible jet energies: therefore the integral of each curve from $\theta = 0°$ to $\theta = 180°$ is unity. It is seen that gluon jets have a larger fraction of their energy at large angles relative to the jet axis compared to quark jets and in this sense are broader, conforming with the QCD expectation. Figure 2.7 (b) shows the

[1] Previous to the OPAL study, the only published measurement of this ratio was $1.29^{+0.21}_{-0.41} \pm 0.20$ from the HRS Collaboration [53].

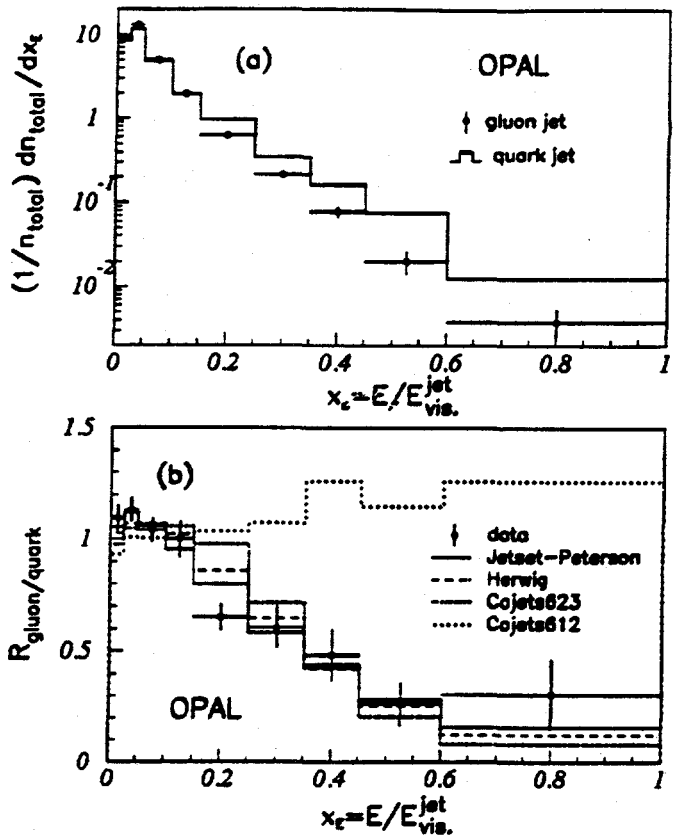

Figure 2.6: (a) Inclusive scaled particle energy distributions of the quark and gluon jets, corrected for quark and gluon jet misidentification. (b) Ratio of the two curves in (a).

ratio of the gluon to the quark jet data compared to the Monte Carlo calculations. Again, it is seen that the QCD models are consistent with the measurements, with the exception of Cojets612.

The Electric Charge of Quark and Gluon Jets

The UCR-OPAL technique to identify quark and gluon jets in three-jet events [49, 50, 57] can also be used to study the *electric* charge distributions of quark and gluon jets in a model independent manner. Such an analysis has been published this past year by OPAL [58] as an extension of the analysis based on *color* charge discussed in the previous section. This publication is the first study of the gluon's electric charge to appear from an e^+e^- experiment.

The technique is largely the same as presented above. Three jet $q\bar{q}g$ events are

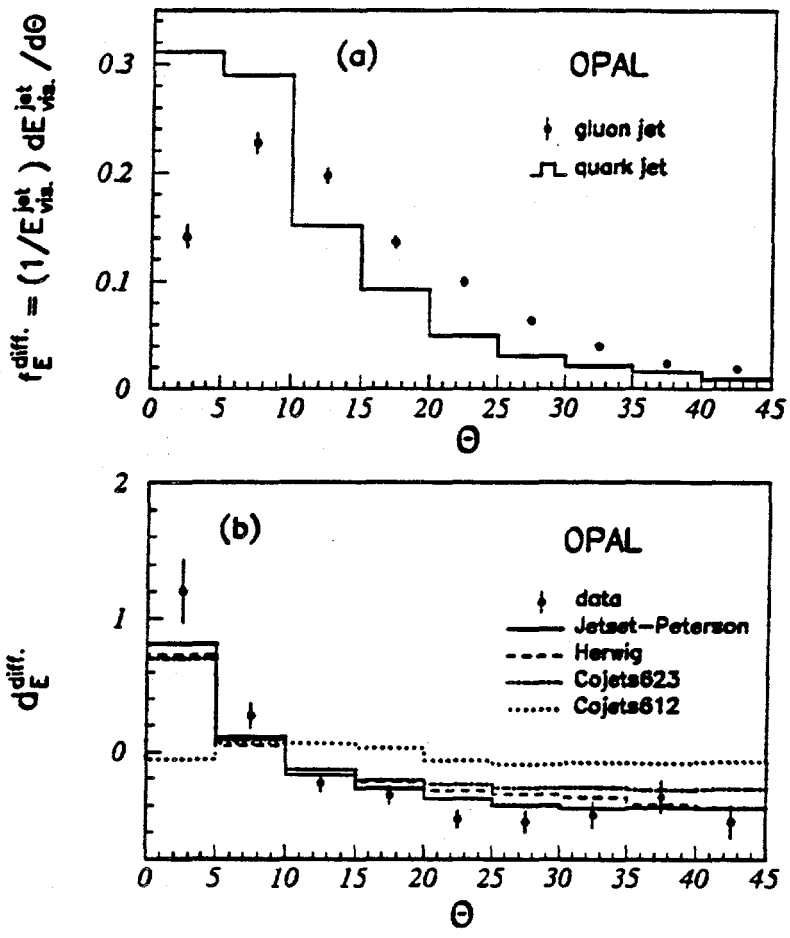

Figure 2.7: (a) Differential polar angle distribution of a jet's visible energy around the jet axis for the quark and gluon jets, corrected for quark and gluon jet misidentification. (b) Ratio of the two curves in (a).

selected using a jet finder and retained only if one of the lower energy jets contains a high energy lepton associated with heavy quark decay. The highest energy jet and the jet with the lepton are assumed to be the quark jets, while the lower energy jet without the lepton is assumed to be the gluon jet.

The quark jet samples thus obtained are a mixture of jets from both positively and negatively charged primary quarks and antiquarks. To be sensitive to the sign of the quark charge, subsamples enriched with jets from positive and negative quarks are selected. The selection is based on the semi-leptonic decay $b^{-1/3} \rightarrow c^{+2/3} \ell^- \nu_\ell$, where the sign of the lepton is the same as that of the primary quark. Thus the jet with the lepton is considered to originate from a negative primary quark if the sign of the lepton is negative, and *vice versa*. Correspondingly, the highest energy jet (i.e. the quark jet without the lepton) is considered to originate from a negative primary quark if the lepton is *positive*, and *vice versa*. The number of cascade decays

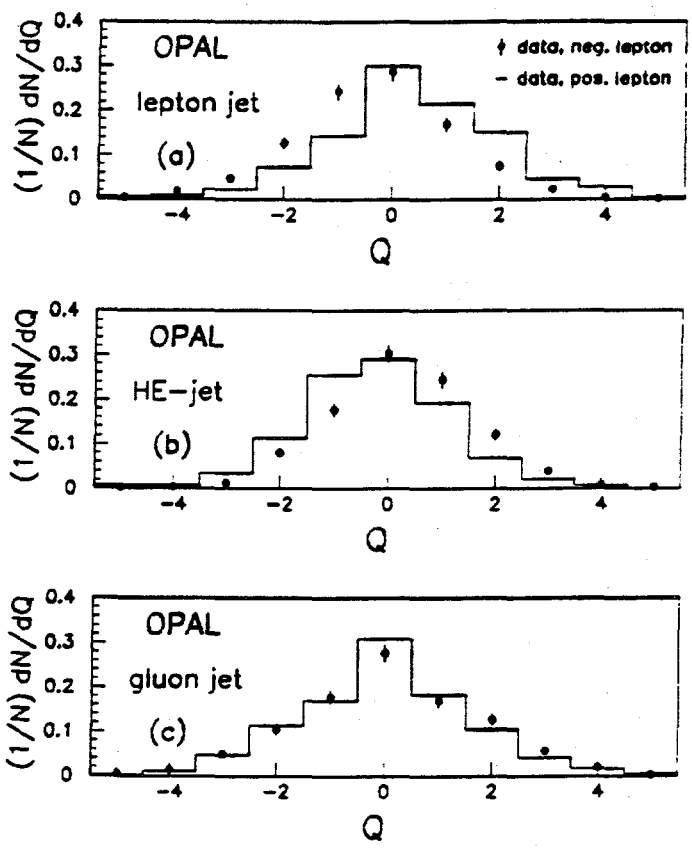

Figure 2.8: The measured jet charge distributions Q in tagged three-jet events for (a) the jets with a lepton, (b) the highest energy jets and (c) the gluon jets.

$b^{-1/3} \rightarrow c^{+2/3} \rightarrow \ell^+\nu_\ell$, where the lepton and primary quarks have opposite sign, is reduced by requiring the transverse momentum of the lepton with respect to the jet axis to exceed 0.8 GeV/c if the lepton is an electron or 1.0 GeV/c if it is a muon. Therefore, this study of quark and gluon jet electric charges compares b quark jets to gluon jets. The estimated purity of the b quark selection is estimated to be about 80%.

The jet charge Q is defined by the arithmetic sum of the electric charges of the particles assigned to the jet by the jet finder:

$$Q = \sum_{i=1}^{n_{ch.}} q_i \tag{2.2}$$

with $n_{ch.}$ the charged multiplicity and q_i the electric charge of the ith particle. The measured distributions for Q are shown in Figure 2.8. The data are uncorrected and the errors the statistical ones. In Figure 2.8 (a) are shown the results for the quark jets with the lepton. The points with errors show the jets with a negatively charged

lepton while the histogram shows the jets with a positively charged lepton. The distributions are not centered at zero but instead are distinctly shifted to negative values if the lepton is negative and to positive values if the lepton is positive. Thus the charge of the jet is observed to be incompatible with zero while its sign corresponds to that of the presumed primary quark.

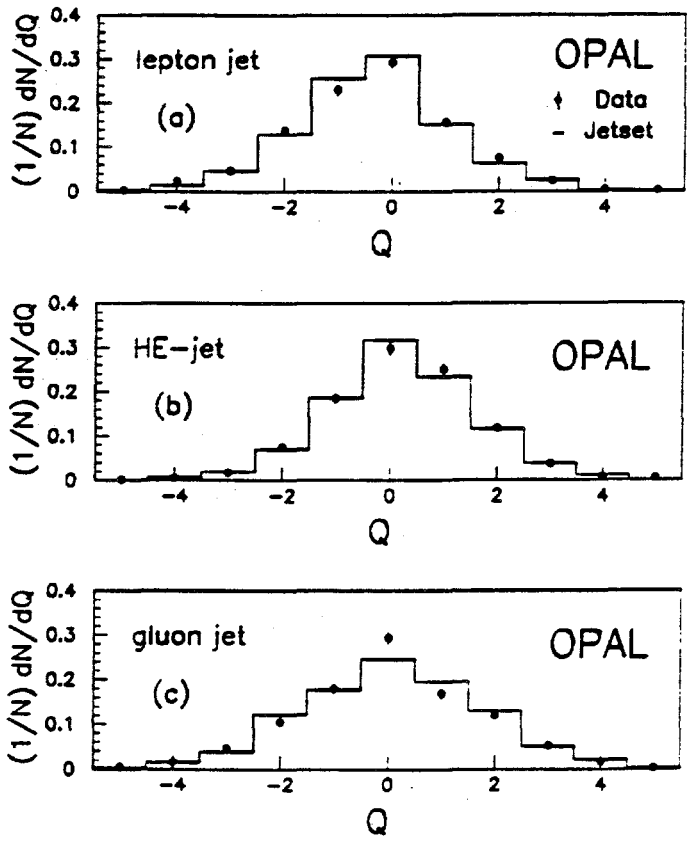

Figure 2.9: The combined jet charges for (a) the jets with a lepton, (b) the highest energy jets and (c) the gluon jets, compared to the predictions of the Jetset Monte Carlo.

The jet charge distribution of the jet with the lepton might be biased because of the presence of the identified lepton, which enters the jet charge Q. Therefore our main result for quark jets is based on the results for the highest energy jets, presented in Figure 2.8 (b), which have no such bias. Again the distributions are not centered at zero, but are shifted to positive values for events with a negative lepton and to negative values for events with a positive lepton: the mean values are $\langle Q \rangle = +0.25 \pm 0.05$ and $\langle Q \rangle = -0.23 \pm 0.05$ for the two cases, respectively. Thus, again, the measured charge of the jet is incompatible with zero and has a sign which

corresponds to that of the presumed primary quark. This indicates that the jet charge is indeed a sensitive indicator of the primary jet charge.

Finally, we show the result for the gluon jet in Figure 2.8 (c). Within the statistics, the distributions are compatible with being centered at zero irrespective of the sign of the lepton charge in the event: the mean values are $\langle Q \rangle = +0.07 \pm 0.06$ and $\langle Q \rangle = +0.02 \pm 0.06$ for events with a negative and positive lepton, respectively.

Since the results for the samples with negative and positive leptons are consistent with each other, we combine them by reflecting the distributions for events with a positive lepton around zero and adding them to the distributions for events with a negative lepton. These combined distributions are shown in Figure 2.9. The mean charges of the highest energy jets and the gluon jets are $\langle Q \rangle = +0.24 \pm 0.04$ and $\langle Q \rangle = +0.03 \pm 0.04$, respectively. In Figure 2.9, we also show the corresponding distributions from the Jetset Monte Carlo, which agrees well with the data.

Thus we conclude that a significant difference in the jet charge distributions of quarks and gluons is observed, which arises from their different electric charges.

Strange Baryon Correlations

Another UCR-led analysis published this past year is on strange baryon correlations in the Z^0 hadronic decay data.

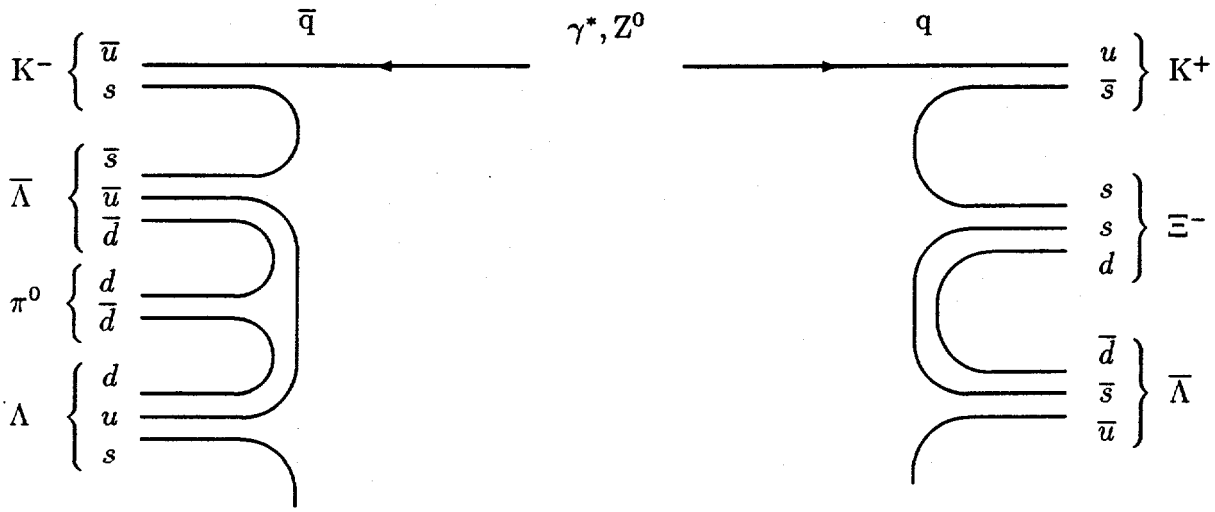

Figure 2.10: Schematic diagrams which show the chain-like diquark production of baryon-antibaryon pairs (right side) and the popcorn mechanism with its chain of antibaryon-meson-baryon (left side).

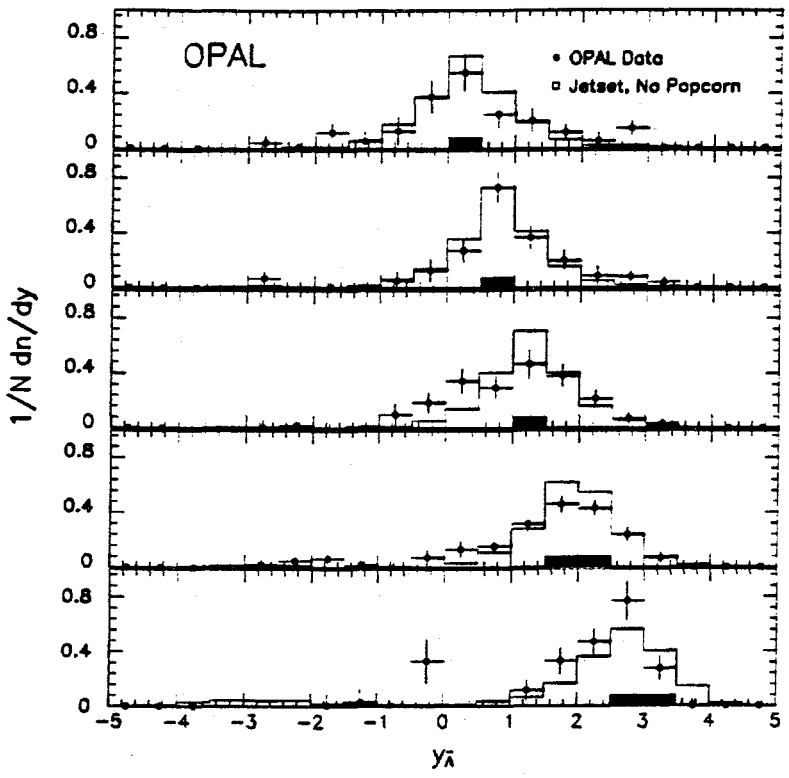

Figure 2.11: Rapidity distribution of $\overline{\Lambda}$ for various tagging intervals of Λ (shown as solid bars).

A very general assumption of jet hadronization is chain-like particle creation with local conservation of quantum numbers, as indicated in Figure 2.10. Correlations between particle pairs with compensating strangeness or baryon quantum numbers can be used to test this assumption. Studies of baryon and strangeness correlations were undertaken at PEP and PETRA but with only limited success because of the small statistics. In particular, it was not possible to distinguish between the popcorn and diquark models for baryon production illustrated in Figure 2.10. In the diquark model, the baryon is always produced next to the antibaryon, leading to strong correlations in rapidity space. In the popcorn model, a meson lies between the baryon and antibaryon, leading to weaker correlations.

The new OPAL study [59] is based on observed correlations between strange baryons Λ and Ξ^- and their anti-particles in hadronic Z^0 decays. The selection of Λ and Ξ^- hadrons is similar to that published in our earlier work on inclusive strange baryon production [60], also a UCR-led analysis. Having required that either a Λ ($\overline{\Lambda}$) or Ξ^- ($\overline{\Xi}^+$) be found in an event, identical criteria are used to identify additional Λ or Ξ^- baryons or their anti-particles in the same event. Identified baryon pairs are then used to measure the correlation strength in rapidity space. As an example, Figure 2.11 shows the rapidity distribution of $\overline{\Lambda}$ (Λ) hadrons when a Λ ($\overline{\Lambda}$) has been

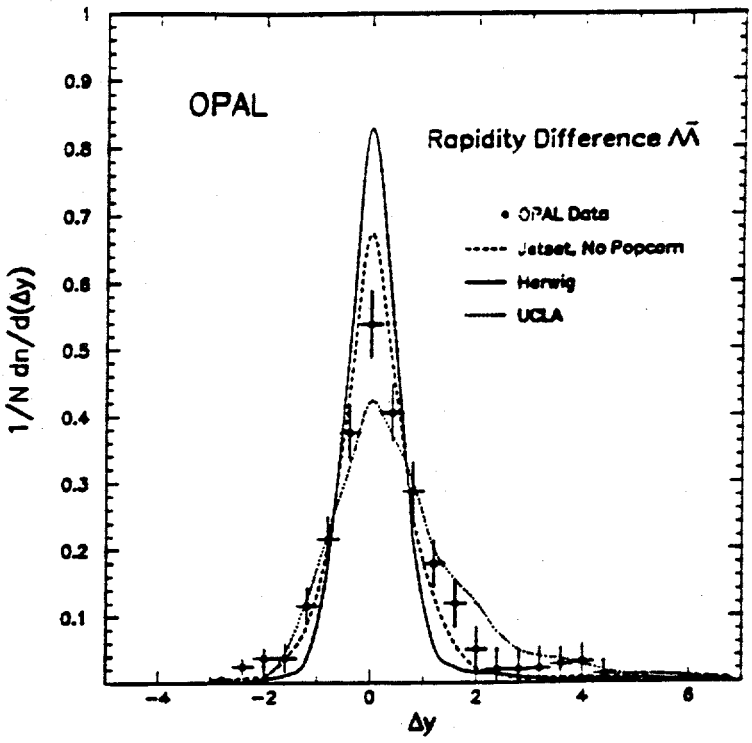

Figure 2.12: Rapidity difference of $\overline{\Lambda}\Lambda$ pairs. The predictions of Herwig, Jetset with 0% popcorn probability and the UCLA model are also shown.

identified in the rapidity range indicated by the solid dark bar along the rapidity axis. The data have been corrected for background and efficiency. The background is determined from the distribution of same baryon number $\Lambda\Lambda$ pairs in the events. As the baryon rapidity increases, so does the rapidity of the antibaryon, indicating strong, simultaneous and local compensation of strangeness and baryon numbers. The observed rapidity correlations are described qualitatively by the Jetset and Herwig Monte Carlos, both of which implement a chain-like mechanism for baryon production. The result for Jetset, using a pure diquark mechanism for baryon production ("no popcorn") is included in Figure 2.11.

To obtain a more quantitative measurement of the rapidity correlation strength and to discriminate between different baryon production models, the rapidity difference of $\Lambda\overline{\Lambda}$ pairs is used. The distribution of this rapidity difference, $(1/N_{pairs})$ $dn/d\Delta y$, is shown in Figure 2.12. The $\overline{\Lambda}$ is found to have a 53% probability to lie within ± 0.6 units of the Λ's rapidity. The predictions from Herwig and Jetset, both with a pure diquark mechanism, are shown in Figure 2.12. Both models exhibit stronger $\Lambda\overline{\Lambda}$ rapidity correlations than are found in the data. The prediction of the

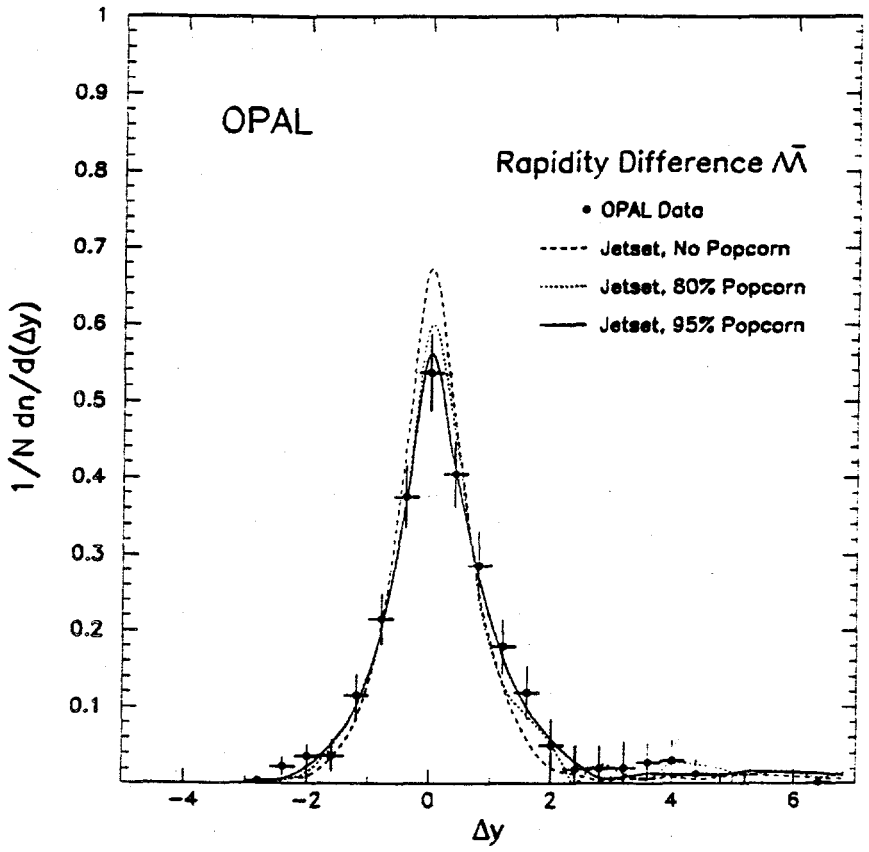

Figure 2.13: Rapidity difference of $\overline{\Lambda}\Lambda$ pairs. The predictions of Jetset with a popcorn probability of 0%, 80% and 95% are also shown.

UCLA model [61] is also shown in Figure 2.12. It predicts weaker correlations than are present in the data.

In Jetset, both the popcorn and diquark mechanisms are available. Figure 2.13 shows the measured $\Lambda\overline{\Lambda}$ rapidity difference in comparison to Jetset with 0%, 80% and 95% probability for the popcorn mechanism. Agreement with the data is best when more than 80% of the baryons are produced through the popcorn mechanism rather than through the diquark one.

In Table 2.12, we summarize the results of our strangeness and baryon number compensation study. The values in this table give the measured probability for a baryon Λ or Ξ^- to be compensated by an antibaryon $\overline{\Lambda}$ or $\overline{\Xi}^+$. The uncorrelated background rate of like baryon number pairs $\Lambda\Lambda$ and $\overline{\Lambda\Lambda}$ is also given. Included in Table 2.12 are the predictions of the Herwig, Jetset and UCLA models. The Jetset results are given for the diquark mechanism (i.e. 0% popcorn) and for the popcorn mechanism with 95% probability. None of the models yield a particularly good description of the data. For example, Jetset with 95% popcorn probability, which was found to provide an optimal description of the $\Lambda\overline{\Lambda}$ rapidity correlations

		probability				
first baryon	second baryon	OPAL data	Jetset no popcorn	Jetset 95% popcorn	UCLA	Herwig 55 tuned
Λ	$\overline{\Lambda}$	0.354± 0.034	0.291	0.235	0.398	0.374
$\Xi^-(\overline{\Xi}^+)$	$\overline{\Lambda}(\Lambda)$	0.463± 0.099	0.589	0.412	0.580	0.860
Ξ^-	$\overline{\Xi}^+$	0.037 ± 0.065	0.172	0.071	0.082	0.225
$\Lambda(\overline{\Lambda})$	$\Lambda(\overline{\Lambda})$	0.117± 0.024	0.151	0.129	0.117	0.144

Table 2.12: Probabilities to find an additional strange baryon or antibaryon in events which already contain a Λ or a Ξ^-. The errors are the combined statistical and systematic errors.

(Figure 2.13), predicts $\Lambda\overline{\Lambda}$ and $\Xi^-\overline{\Xi}^+$ event rates which are 30% lower and 90% higher than the measurements, respectively.

Therefore, we observe strong rapidity correlations between identified Λ and $\overline{\Lambda}$ baryons in an event, which supports the assumption of a chain-like mechanism for particle production in hadronic final-states. Furthermore, in a detailed test to discriminate between different chain-like models, we observe a correlated production of $\Lambda\overline{\Lambda}$ pairs which supports the baryon-meson-antibaryon popcorn mechanism rather than the baryon-antibaryon diquark one. This result is the most accurate and conclusive to be published to date on this question. We find in addition, however, that no model provides a satisfactory description of the event rates for simultaneous strangeness and baryon number compensation. This implies that baryon production is still inadequately understood and that new ideas may be required to accurately model this sector.

Measurement of the QCD Color Factors Using Four-Jet Events

A new UCR analysis which we expect to publish later this year is on angular correlations between jets in four-jet events, leading to a measurement of the QCD color factors and a direct observation of the gluon self coupling. This study is the principal Ph.D. thesis subject for Shun-Lung Chu.

The dynamics of a gauge theory, such as QCD, are completely defined by the commutation relations between its group generators T^i:

$$\left[T^i\ ,\ T^j\right] = if^{ijk}\cdot T^k \quad , \tag{2.3}$$

where the coefficients f^{ijk} are the group structure constants. In terms of Feynman graphs, the generators and structure constants appear in the vertex functions, shown in Figure 2.14 for QCD. Squaring the vertex functions, averaging over initial states and summing over final states leads to the combinatoric factors C_F, C_A and T_F, where

$$T^k_{\alpha\eta}T^k_{\eta\beta} \ = \ \delta_{\alpha\beta}C_F \tag{2.4}$$

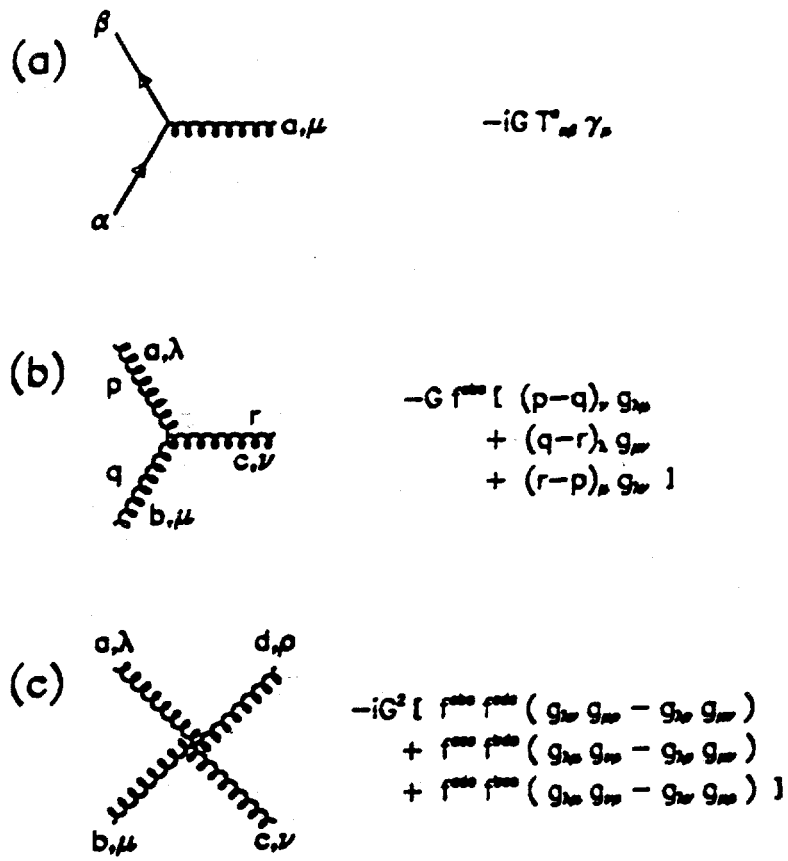

Figure 2.14: Vertex functions of QCD.

$$f^{jkm} f^{jkn} = \delta^{mn} C_A \tag{2.5}$$

$$T^m_{\alpha\beta} T^n_{\beta\alpha} = \delta^{mn} T_F \quad . \tag{2.6}$$

These quantities, known as the color factors, are physical manifestations of the underlying group structure. For the case of strong interactions, they represent the relative strengths of the processes (a) $q \rightarrow qg$, (b) $g \rightarrow gg$, and (c) $g \rightarrow q\overline{q}$, respectively. For a theory based on $SU(3)$, like QCD, the color factors are $C_F = 4/3$, $C_A = 3$ and $T_F = 1/2$. For the Abelian "gluon" theory $SU(1)_3$, from which the gluon self-couplings of Figures 2.14 (b) and 2.14 (c) are absent, they are $C_F = 1$, $C_A = 0$, and $T_F = 3$. The ratios between the color factors, for instance C_A/C_F and T_F/C_F, are therefore sufficient to distinguish between different gauge groups and thus, for example, to demonstrate the non-Abelian character of QCD.

A measurement of the ratios C_A/C_F and T_F/C_F at e^+e^- colliders is possible only through the study of processes at order α_S^2 or higher. The simplest case is the study of angular correlations between jets in four-jet events. Four jet production in

e^+e^- annihilations occurs through three processes, shown in Figure 2.15: (1) double

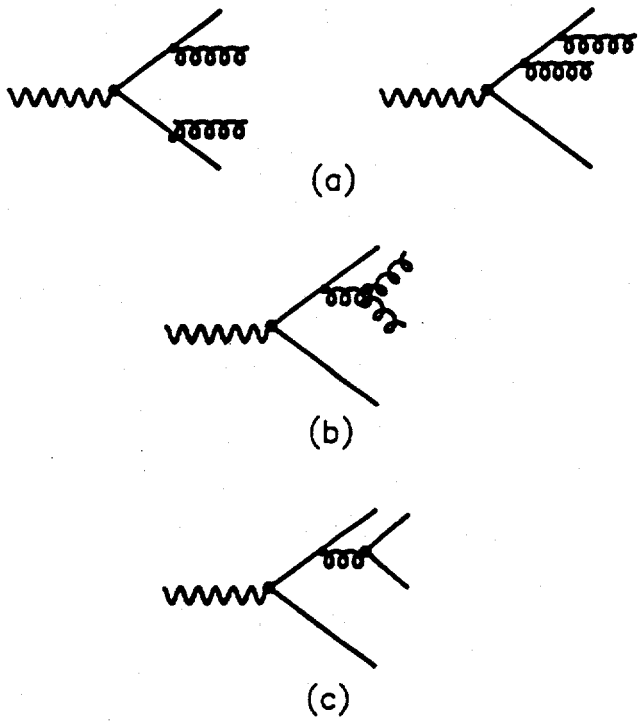

Figure 2.15: Four-jet production to order α_S^2 in QCD.

gluon bremsstrahlung (Figure 2.15 (a)), (2) the triple gluon vertex (Figure 2.15 (b)) and (3) four quark production (Figure 2.15 (c)). Since double gluon bremsstrahlung and the triple gluon vertex yield the same final state, their contributions to the four jet cross section do not factorize; the two processes lead to different angular correlations between the four jets in the final state and therefore their contributions can be separated, however.

To order α_S^2, the differential cross section for $e^+e^- \rightarrow$ 4 jets can be expressed as:

$$d\sigma_4(y_{ij}) = d\sigma_{q\bar{q}gg}(y_{ij}) + d\sigma_{q\bar{q}q\bar{q}}(y_{ij}) \tag{2.7}$$

where the quantities $y_{ij} = (p_i + p_j)^\mu (p_i + p_j)_\mu / s$ denote the normalized two-body invariant masses, with the indices i, j running over the four partons or jets. The first term on the right side of (2.7) is the sum of the double gluon bremsstrahlung and triple vertex processes, while the second term is the contribution of the four quark final-states. The two distinct terms in (2.7) are:

$$\frac{1}{\sigma_0} d\sigma_{q\bar{q}gg}(y_{ij}) = \left(\frac{\alpha_S C_F}{\pi}\right)^2 \left[A(y_{ij}) + \left(1 - \frac{1}{2}\frac{C_A}{C_F}\right) B(y_{ij}) + \frac{C_A}{C_F} C(y_{ij})\right] \tag{2.8}$$

$$\frac{1}{\sigma_0} d\sigma_{q\bar{q}q\bar{q}}(y_{ij}) = \left(\frac{\alpha_S C_F}{\pi}\right)^2 \left[N_F \frac{T_F}{C_F} D(y_{ij}) + \left(1 - \frac{1}{2}\frac{C_A}{C_F}\right) E(y_{ij})\right] \quad , \tag{2.9}$$

where N_F is the number of active flavors. Thus the four jet cross section depends on five kinematic functions, $A(y_{ij}) \ldots E(y_{ij})$, whose relative weights are determined by the ratios of color factors. These five kinematic functions are independent of the gauge group: it is solely the coefficients of these functions, namely C_A/C_F and T_F/C_F, that differentiates QCD from theories based on other gauge groups.

We choose three experimental variables for our analysis, each of which has a different dependence on the kinematical factors $A(y_{ij}) \ldots E(y_{ij})$. These experimental variables are constructed from the angles between jets in reconstructed four-jet events. The energies of the four jets in an event are ordered such that jet 1 has the highest energy and jet 4 the lowest energy. The three variables are:

(I) the Bengtsson-Zerwas angle, χ_{BZ} [62], the angle between the plane subtended by jets 1,2 and that by jets 3,4:

$$\chi_{BZ} = \cos^{-1} \left| \frac{(\vec{p}_1 \times \vec{p}_2) \cdot (\vec{p}_3 \times \vec{p}_4)}{|\vec{p}_1 \times \vec{p}_2| \, |\vec{p}_3 \times \vec{p}_4|} \right| \quad , \tag{2.10}$$

(II) the modified Nachtman-Rieter variable, $|\cos\theta^*_{NR}|$ [63], the absolute value of the cosine of the angle between the vectors $\vec{p}_1 - \vec{p}_2$ and $\vec{p}_3 - \vec{p}_4$:

$$|\cos\theta^*_{NR}| = \left| \frac{(\vec{p}_1 - \vec{p}_2) \cdot (\vec{p}_3 - \vec{p}_4)}{|\vec{p}_1 - \vec{p}_2| \, |\vec{p}_3 - \vec{p}_4|} \right| \quad , \tag{2.11}$$

(III) and $\cos\alpha_{34}$, the cosine of the angle between the two lowest energy jets:

$$\cos\alpha_{34} = \frac{\vec{p}_3 \cdot \vec{p}_4}{|\vec{p}_3| \, |\vec{p}_4|} \quad . \tag{2.12}$$

We find these three variables to be largely independent of each other.

The analysis is based upon a simultaneous fit of the theoretical predictions for χ_{BZ}, $|\cos\theta^*_{NR}|$ and $\cos\alpha_{34}$ to the measured distributions, after correcting the latter for detector and hadronization effects and for background from two- and three-jet events. The theoretical predictions are obtained from linear combinations of the five kinematic functions $A(y_{ij}) \ldots E(y_{ij})$, with their coefficients constrained to have the same form as in equations (2.7)-(2.9). The color factor ratios C_A/C_F and T_F/C_F and the overall normalization are used as the fit parameters. This analysis strategy is similar to one first introduced by the DELPHI Collaboration [64], but instead of restricting our fit to two experimental variables, as do they, we use three variables as discussed above. This yields a better constraint on the fit parameters and smaller errors on the final results.

An innovative aspect of our study is the use of calculated jet energies. All three observables used in our analysis rely on energy ordering of the jets, as noted above. By using the jet energies calculated from the directions of the jets, we achieve superior jet energy resolution and hence more reliable results than are attainable using visible jet energies. Use of calculated jet energies is a standard technique in three-jet analyses, but ours is the first study to introduce this to four-jet kinematics.

Currently, our analysis is well advanced. All of the necessary machinery, as outlined above, has been implemented and tested. Preliminary results for C_A/C_F and T_F/C_F have been presented at internal OPAL general meetings. These results are consistent with the SU(3) color factor values of QCD. In particular, we obtain a non-zero value for C_A/C_F, which constitutes direct evidence for the triple gluon vertex (Figure 2.15 (b)) and for the non-Abelian character of QCD. We expect to have results to show at conferences soon, with a publication following afterwards. A new theoretical calculation is expected soon, which contains the next-to-leading order α_S^3 corrections to the differential four-jet cross section. If this calculation becomes available on a timely basis, we intend to incorporate this into our study before publication.

Δ^{++} Baryons

Another UCR analysis in progress is a study of Δ^{++} baryons in e^+e^- annihilations. The principal motivation for this study is to continue our program to test the baryon production mechanism. In addition, the Δ^{++} has never been observed in e^+e^- annihilations above the $\Upsilon(1S)$, making a measurement of its cross section important. The Δ^{++} is interesting because it is a spin 3/2 particle. A measurement of its production rate would allow the suppression factor for spin 1 diquarks, relative to spin 0 diquarks, to be determined: this would be the first such measurement for non-strange baryons. Such a suppression factor exists in certain models like Jetset. Furthermore, a measurement of the Δ^{++} production properties allows the predictions of other models like Herwig and UCLA to be tested. Our first goal is to measure and publish the total production rate and differential energy spectrum of the Δ^{++} and its anti-particle. Following this, we intend to investigate multi-particle correlations involving the Δ^{++} such as those presented above for $\Lambda\overline{\Lambda}$ pairs. This investigation is expected to yield further, detailed information about the mechanism of quark and gluon confinement.

Figure 2.16 shows some first, preliminary results from this study. The points with errors show the experimental data for proton-pion p-π^+ mass combinations for which the proton has been identified using energy loss dE/dx information. The baryon state Δ^{++} is shown in Figure 2.16 (a) while the antibaryon state $\overline{\Delta}^{--}$ is shown in Figure 2.16 (b). The p and π^+ are both required to emanate from the beam constrained primary event vertex point since the Δ^{++} decays strongly. The histogram in Figure 2.16 shows the Monte Carlo prediction from Jetset after the Δ^{++} signal has been removed. Away from the region of the Δ^{++} mass ($m_{p\pi^+} > 1.25$ GeV/c^2), the Monte Carlo and data are in good agreement, which demonstrates that the combinatoric

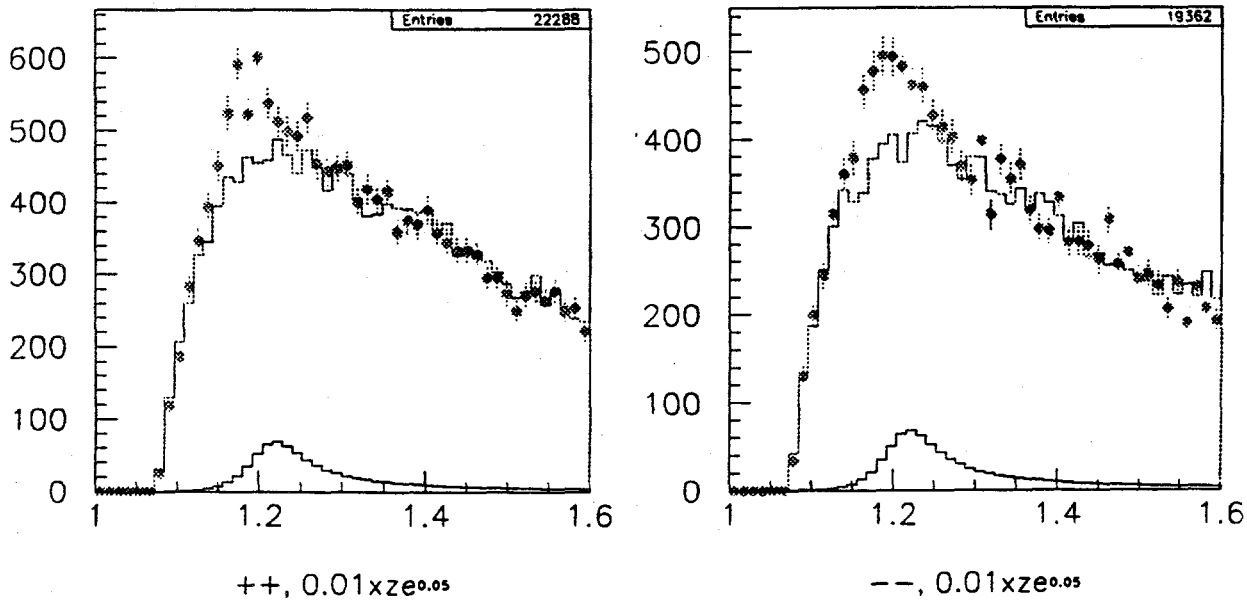

Figure 2.16: (a) and (b): Δ^{++} and $\overline{\Delta}^{--}$ mass peaks.

background is well modeled. In the region of the Δ^{++} mass ($m_{p\pi^+} \approx 1.23$ GeV/c^2), the data are in excess of the Monte Carlo. We interpret this excess to be the first signal for Δ^{++} production ever observed in e^+e^- annihilations above the $\Upsilon(1S)$. Using the Monte Carlo to estimate the background and fitting the Δ^{++} region above background to a relativistic Breit-Wigner resonance shape leads to the extracted Δ^{++} signals shown by the histograms inserted into the lower portions of Figures 2.16 (a) and (b).

2.2.5 Studies of Events with Photons

The OPAL detector, with its lead glass electromagnetic calorimeter, is well suited to the study of events with photons. Members of the Collaboration have carried out several such studies, two of which are described here.

- The announcement by the L3 Collaboration of the observation of four events of the type $\ell^+\ell^-\gamma\gamma$ with an invariant mass of the two photons clustering around 60 GeV caused considerable interest and led the OPAL group to attempt to verify the observation. No similar clustering of events was seen.
- An accurate measurement of the single photon cross-section can provide a measurement of the effective number of light-mass neutrino generations. OPAL published the first paper on this subject and is currently working to update this measurement.

High Mass Photon Pairs

The L3 collaboration has observed four $\ell^+\ell^-\gamma\gamma$ events [67] (three $\mu^+\mu^-\gamma\gamma$ and one $e^+e^-\gamma\gamma$), where the two energetic photons have a mass $m_{\gamma\gamma}$ near 60 GeV, within a data sample of about 0.95 million produced Z^0s. The invariant masses of the two photon system for the four events are 58.8, 59.0, 62.0 and 60.0 GeV with a mass resolution of 0.6 GeV. The QED background was estimated using the YFS3 Monte Carlo [68] and a probability of order 10^{-3} was calculated for the observation of four or more events in any 5 GeV mass interval above 50 GeV. L3 has also searched for events of the type $q\bar{q}\gamma\gamma$ and $\nu\bar{\nu}\gamma\gamma$, but no event with a high mass photon pair was found. Recently, L3 has updated the result with a larger data sample of 1.6 million produced Z^0's [69]: no additional $\ell^+\ell^-\gamma\gamma$ event near 60 GeV was found and the probability of a QED fluctuation as calculated above is of order 10^{-2}. Several authors have recently repeated or calculated independently the QED expectation [70]. The L3 publication has motivated the other LEP experiments to look for such events [71], and experiments at TRISTAN to scan in the 60 GeV energy region. The results from TRISTAN [72] exclude a large coupling to electrons of a possible new particle.

If the photon pairs are produced in association with a virtual Z^0 decaying to a lepton pair, they should also be observable in events where the virtual Z^0 decays to $q\bar{q}$ or $\nu\nu$. Events of the type $q\bar{q}\gamma\gamma$ could also be produced with a comparable production rate if the lepton pair comes from a virtual photon. Motivated by the possible production in association with a real photon, we also search for high mass photon pairs in $e^+e^- \rightarrow \gamma\gamma\gamma$ events, and for the production via two-photon collisions of a resonant state decaying to two photons in the no charged particle topology. Finally, we search for events with an isolated high momentum charged lepton pair in the $\ell^+\ell^-q\bar{q}$, $\ell^+\ell^-\ell^+\ell^-$ or $\ell^+\ell^-\nu\nu$ topologies. The motivation for this study is to search for a resonance state X with a mass of about 60 GeV that can be produced

together with a lepton pair in e^+e^- annihilation and has decay modes other than $X \to \gamma\gamma$.

We have analysed a data sample, collected between 1990 and 1992, to search for events with a pair of photons with a high mass. The data sample corresponds to a total integrated luminosity of 43 pb^{-1} or to roughly 1.8 million produced Z^0's.

Two independent but similar searches for $\ell^+\ell^-\gamma\gamma$ events have been performed. The lepton selection is based on low charged multiplicity jets. Starting from energetic tracks, geometric cones, with opening angles between 10–35° depending on the specific analysis goals, are used to combine close by tracks and clusters into jets. The events of interest are identified as having exactly two such charged jets and at least two isolated energetic electromagnetic clusters without associated charged particles. These clusters are considered to be photons.

The second analysis has a somewhat larger acceptance for charged leptons and a slightly reduced acceptance for photons. The analysis starts from a sample with a charged multiplicity between 2 and 6, and a minimum visible energy (scalar sum of the charged particle momenta and electromagnetic cluster energies) of 10% of the centre-of-mass energy. Low multiplicity charged jets are defined by a cone of 10° half-angle. The jets and photons are each required to have an energy of more than 2 GeV and be detected within $|\cos\theta| < 0.9$. Photon pairings are considered if the photons are separated by more than 10° from each other and each jet.

The same four events with a two-photon invariant mass above 40 GeV are found by both selections: two $\mu^+\mu^-\gamma\gamma$ and two $e^+ e^-\gamma\gamma$ events. In order to compare with the YFS3 Monte Carlo which is currently only available for muon pair production with multiple hard photons, we selected events with $\mu^+\mu^-$ from the above sample. The $m_{\gamma\gamma}$ distribution for events with $\mu^+\mu^-$ is shown in Figure 2.17, together with the YFS3 MC expectation with full detector simulation. We observe 29 events with $m_{\gamma\gamma}$ above 10 GeV which is consistent with the YFS3 MC prediction of 22.6 ± 1.2. Two events are seen with $m_{\gamma\gamma}$ above 40 GeV compared with the Monte Carlo prediction of 1.2 ± 0.3.

Four $\ell^+\ell^-\gamma\gamma$ events with a photon pair mass above 40 GeV are found. No clustering of $m_{\gamma\gamma}$ is observed at large masses. No events are directly measured to be consistent with a mass of around 60 GeV. It should be noted that one event which is not fully reconstructed may be consistent with such a mass but that the interpretation of this event is ambiguous.

Three hadronic events with two isolated photon candidates are found with mass above 40 GeV with no obvious resonance structure. No event without tracks and two or more acoplanar photons with missing transverse energy and a mass of more than 5 GeV is found. The search for high mass photon pairs near 60 GeV in the neutrino and hadronic channel limits the branching ratio $B(Z^0 \to Z^*\gamma\gamma)$ to 6.0×10^{-6} at 95% C.L. Therefore, any anomalous production of $\ell^+\ell^-\gamma\gamma(\ell = e, \mu, \tau)$ events where the lepton pair originates from a virtual Z^0 occurs with $B(Z^0 \to Z^*\gamma\gamma \to \ell^+\ell^-\gamma\gamma) < 6.0 \times 10^{-7}$.

Thirty-eight events of the type $e^+e^- \to \gamma\gamma\gamma$ have been detected. The overall

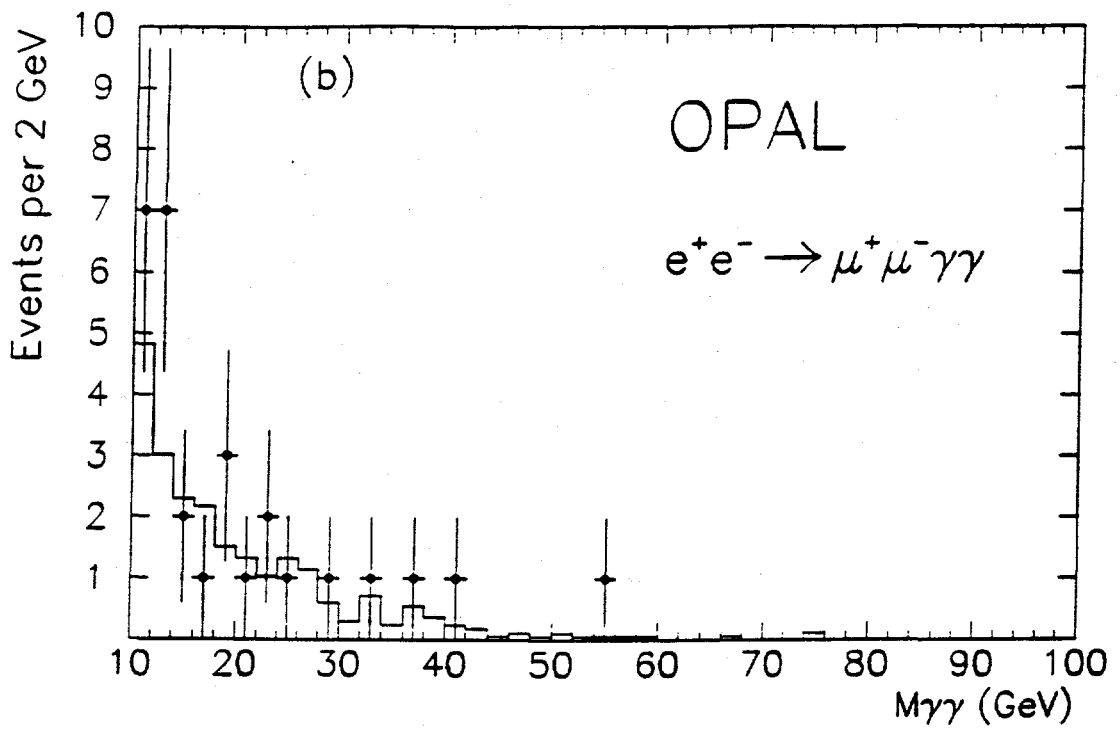

Figure 2.17: Invariant mass $m_{\gamma\gamma}$ of isolated photon pairs in muon pair events (points with error bars) together with the expectation of the YFS3 Monte Carlo (histogram). The direct mass measurement from the calorimeter is shown.

production rate is in good agreement with the expectation from QED (36.5 ± 4.0). In a search for γX production, with X decaying to $\gamma\gamma$, seven events are found with at least one photon pairing with a mass within ± 2.5 GeV of 60 GeV. The expectation from QED is 2.7 ± 0.4. The probability of seven or more events originating from a QED background fluctuation is 2%. Four of these events are measured within a bin of ± 1 GeV centred on 59.25 GeV : the corresponding probability of a background fluctuation is 2.5%.

In a search for the production in two-photon collisions of a 60 GeV resonance X decaying to two photons, we set an upper limit on $\Gamma_X B^2(X \rightarrow \gamma\gamma)$ of 2.6 MeV at 95% CL, assuming a spin 0 resonance. We also looked for $\ell^+\ell^-X(\ell = e, \mu)$ events, where X decays into either $q\bar{q}$, $\ell^+\ell^-(\ell = e, \mu, \tau)$ or $\nu\nu$. No indication of a 60 GeV resonance is seen in these modes.

Neutrino counting

The observation of single photon events can be used to measure the cross-section for the production of weakly interacting particles. This method, first suggested by Ma and Okada [73], uses a photon radiated from the initial state to tag the otherwise invisible final state. At LEP energies, this topology is expected to be dominated by Z^0 decays to invisible particles. Within the Standard Model these particles can only

Z^0 decays to invisible particles. Within the Standard Model these particles can only be light-mass neutrinos.

The first measurement of the Z^0 invisible width by single photon counting was published by OPAL in 1990 based on 5.3 pb^{-1} integrated luminosity [74]. The result was $\Gamma_{inv} = 0.50 \pm 0.07 \pm 0.03$ GeV corresponding to $N_\nu = 3.0 \pm 0.4 \pm 0.2$ light neutrino generations. The analysis of the 1991 data has been carried through by UCR graduate student Edward Heflin. The combined 1990-1991 data set contains 18.3 pb^{-1} in scans around the Z^0. Further work and the increased statistics have led to a better understanding of the background sources and to much reduced systematic errors on the acceptance. An example of this is shown in Figure 2.18 comparing momentum and angular distributions of barrel electrons with Monte Carlo predictions for signal and background.

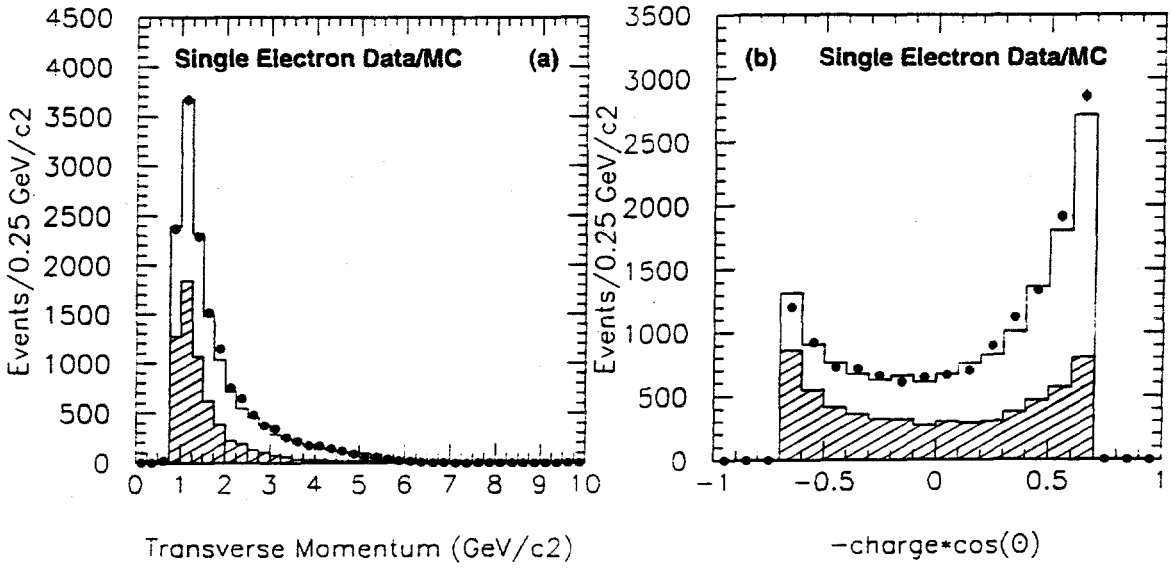

Figure 2.18: *Left:* The observed momentum spectrum and *Right:* the angular distribution of single electron events compared with Monte Carlo expectations. The shaded histograms show the contribution from two photon reactions, while the open histograms are from radiative Bhabha events. The points with error bars are the data.

The method developed by Heflin uses the photon energy corrected for energy loss in the material before the lead glass as the basis of all selection. The earlier paper used the observed energy for the selection and then made adjustments the numbers of events in each energy bin. The current method exhibits greater stability with respect to cuts on the energy. In the 1991 data sample, 204 events with corrected energy

greater than 1.5 GeV are observed. The number of light neutrino species determined by a maximum-likelihood fit to the number of observed events is $3.04 \pm 0.26 \pm 0.15$, where the first error is statistical and the second systematic. The fit is shown in Figure 2.19. When combined with the 1990 result, the number of neutrino species is $3.03 \pm 0.22 \pm 0.16$

A paper including the 1992 data was to have appeared before the end of last year, but the project was delayed when Dr. Graham Wilson of UCR, leader of the neutrino counting working group, was asked to take charge of the working group studying high mass photon pairs, a subject deemed more urgent by the Collaboration. Now that the high mass photon pair paper is completed, it is expected that a paper on single photon counting including 1992 data will be completed by the end of the summer. This will conclude UCR's work on this topic.

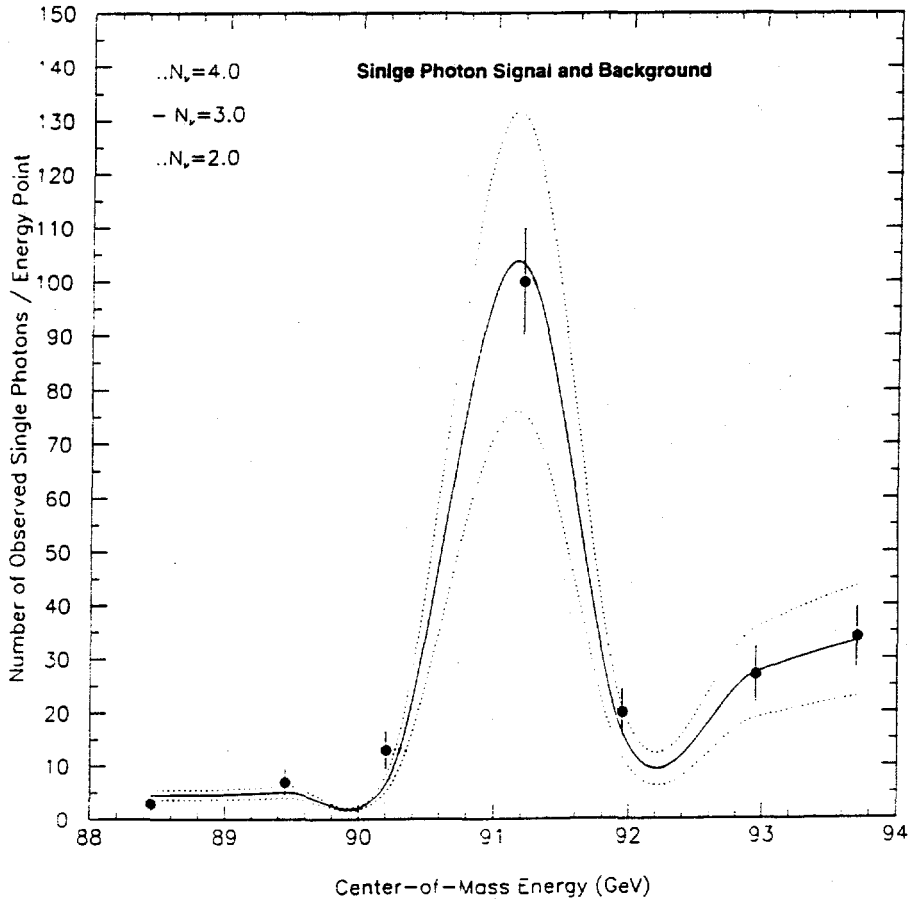

Figure 2.19: Fit to the number of observed single photon events at each center of mass energy point. The data are shown with solid points. The number of events expected for $N_\nu = 3$ is shown with the solid line, while the dotted lines are the expectation for $N_\nu = 2$ and 4.

2.2.6 Two-Photon Physics

The reaction $e^+e^- \rightarrow e^+e^-\mu^+\mu^-$ is a pure QED reaction and is in principle well understood. Consequently it was one of the first τ pairreactions studied in the PEP-PETRA era [75], and this is the case as well at LEP. On the contrary, τ pairtau pair production was never observed at lower energies since the $\gamma\gamma$ mass range was too low. The OPAL Collaboration has made the first observation of tau pair production at LEP.

The F_2 structure function of the photon has been measured in the reaction $e^+e^- \rightarrow$ *hadrons* at lower energy colliders for values of Q^2 from 0.1 to over 100 GeV^2 [76]. LEP offers the possibility of testing QCD over a wider range of Q^2 if sufficient luminosity becomes available. At the present time sufficient statistics are available in the region $4 < Q^2 < 31$ GeV^2 to provide a meaningful check of earlier results.

Muon Pair and Tau Pair Production

The cross section for deep inelastic scattering of an electron (or positron) from a nearly real virtual photon associated with the opposing positron (or electron) can be written in terms of the structure functions F_1 and F_2 as

$$\frac{d^2\sigma}{dxdy} = \frac{16\pi\alpha^2 EE'}{Q^4}[(1-y)F_2(x,Q^2) + xy^2F_1(x,Q^2)]$$

The structure functions F_1 and F_2 are functions of the variables x and Q^2, where Q^2 is the momentum transfer squared of the photon, as determined by the measurement of the scattered lepton. The kinematic variable x is defined as

$$x = Q^2/(Q^2 + W^2)$$

where W is the invariant mass of the muon pair. The variable y is defined as

$$y = 1 - \frac{E'}{E}\cos^2(\frac{\theta'}{2})$$

For sufficiently small values of y, the τ paircross section can be written as a function of F_2 only. In contrast to the hadronic structure functions, the leptonic structure functions can in principle by calculated in QED.

Interesting high Q^2 events, with $\theta_{tag} > 200$ mrad and $Q^2 > 100$ GeV^2, would be tagged in the OPAL Barrel or End Cap lead glass arrays, but at current LEP luminosities, these are unfortunately few in number. The events considered here are tagged in the OPAL Forward Detector and have Q^2 between 4 and 30 GeV^2 with an average value of 8.0 GeV^2. In the remainder of the event, there can be two and only two charged tracks of opposite sign, well contained in the central detector and with certain minimum momenta.

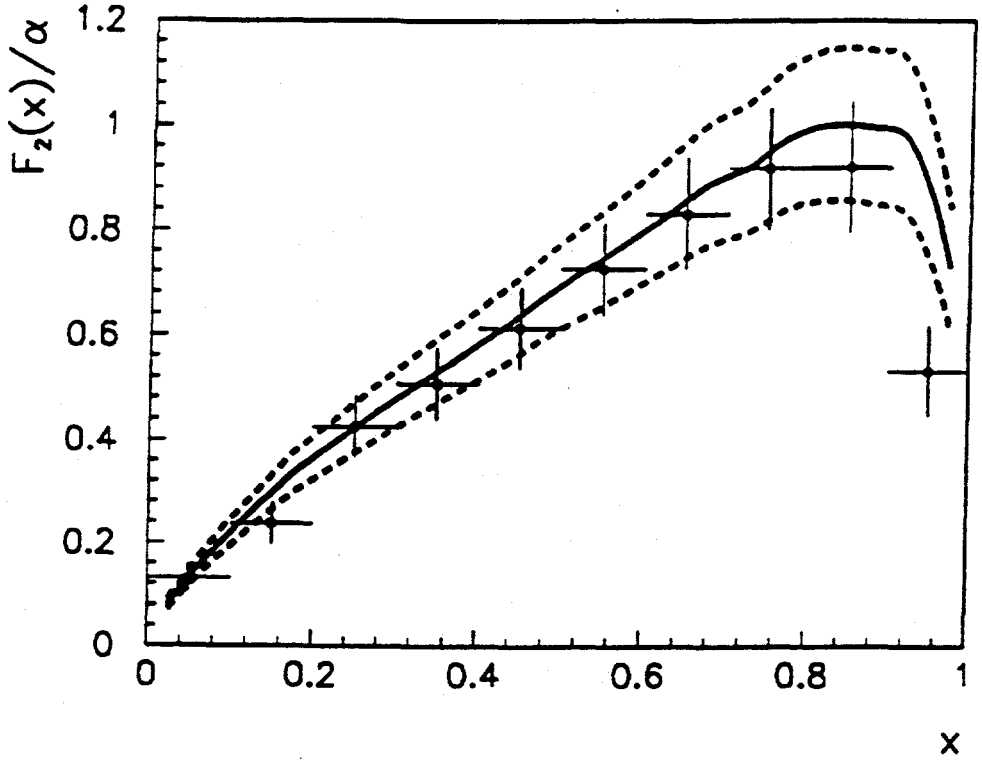

Figure 2.20: The measured values of the structure function F_2 as a function of x. The solid line is the QED expectation; the dashed lines are one-sigma deviations of the systematic error due to the selection efficiency.

The $e^+e^- \rightarrow e^+e^-\mu^+\mu^-$ final state is identified by requiring the presence of one identified muon, as determined by standard muon chamber algorithms or allowed hit patterns in the instrumented iron hadron calorimeter. The event is rejected if the central detector track is identified as an electron by its E/p ratio or dE/dx value.

The QED structure function is extracted from the data using the following procedure: *i*) Events are generated according to the theoretical luminosity function, but with a constant $F_2 = 1/\alpha$. The distribution of the production angle of the muon with respect to the photon direction in the $\gamma\gamma$ center of mass is generated according to the QED prediction. *ii*) These events are passed through the detector simulation and the analysis cuts. *iii*) The x-distribution of the data is divided by the corresponding Monte Carlo distribution, thus eliminating the effects of the detector and of the photon flux factor. The resulting F_2 distribution, shown in Figure 2.20can be compared directly with the QED calculation. The measurement of F_2 agrees well with an analytical form of the structure function [77] incorporated in a simple Monte Carlo generator [78]. There is no indication of an excess over the QED expectation, as had been reported in some preliminary KEK results [79].

Tau pair candidates are triggered with either of two independent triggers involving the forward detector. The overall trigger efficiency was found to be $97.5 \pm 0.7\%$. The data sample for this study corresponds to 17.1 pb^{-1} from 1990 and 1991 running. In

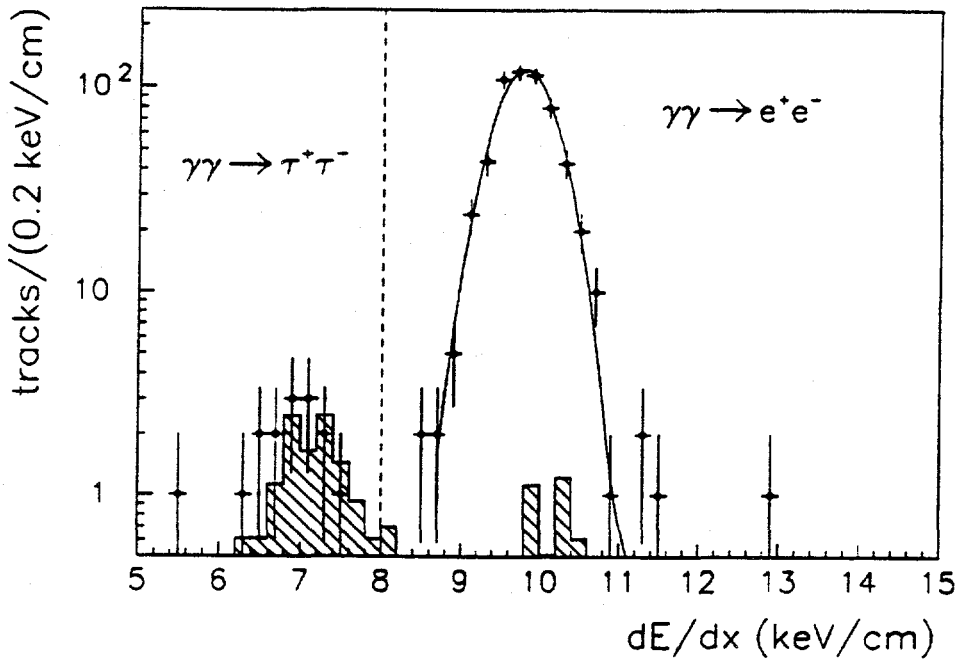

Figure 2.21: Projection of the energy loss spectrum for tracks in events in which the other track is identified as an electron. The shaded histogram corresponds to a Vermaseren Monte Carlo tau pair simulation normalized to the integrated luminosity of the data sample. The dashed line indicates where the cut was applied

the subsequent selection, the requirements for the tagging electron are the same as described above for the case of the muon pairs. Furthermore, events were required to have two and only two good tracks of opposite charge, within certain angular regions and with certain minimum momenta.

For the identification of the $\tau^+\tau^-$ final state, only those events were considered in which one tau decayed into an electron and the other into a muon or a hadron with possible additional neutral particles. Both electron identification and non-electron (π, μ, K) identification was carried out by cuts on the dE/dx signal. The resulting sample of 40 events is shown in Figure 2.21. A simple addition of all conceivable background sources leads to an estimated background of 5.1 ± 2.7 events. The $\tau^+\tau^-$ sample is thus 34.9 ± 6.7 events, in good agreement with the Monte Carlo estimate, made with the Vermaseren program, of 32.7 ± 4.8 events.

The Photon Structure Function

The appropriate kinematic variables for the determination of the F_2 structure function have been discussed above. In contrast to the leptonic case, the hadrons present both theoretical and experimental problems. The theoretical problem [81] revolves around the separation of the "point-like" part of F_2, calculable in QCD, from the "hadronic"

part, for which there is no clearcut calculational prescription. The experimental problem arises from the fact that not all of a hadronic event can be seen because of detector limitations. Hence the visible energy of the event W_{vis} is less than the true energy W_{true}, and x_{vis} is greater than x_{true}. This difficulty can be dealt with by "unfolding" [80] the data to recover the true values, but the efficacy of this step depends on having a good Monte Carlo description of the data.

The TPC/2γ experiment [83] demonstrated that at low Q^2 (¡1.5 GeV^2) the target photon behaves like a vector meson. A number of experiments [84] with data at a mean Q^2 of about 5 GeV^2 show that F_2 begins to grow for $x > 0.3$, as predicted by QCD, but the tranformation from $Q^2 \sim 1$ GeV^2 to $Q^2 \sim 5$ GeV^2 is so abrupt that it has been difficult to devise a model which fits both regions. This OPAL result confirms previous results obtained at the upper end of the region.

The hadronic event trigger is essentially the same as that for the tau pairs. In the central detector, there must be three or more charged tracks, at least one of which must have a momentum greater than 1 GeV/c. The tracks must satisfy certain quality cuts, and their invariant mass W_{track} must be greater than 2 GeV/c^2. Cuts on transverse momentum in and out of the tag plane are used to remove residual backgrounds. In the 1990-1991 data sample there are 582 events with $Q^2 < 8$ GeV^2, and 799 with $Q^2 > 8$ GeV^2.

A Monte Carlo program F2GEN has been developed which generates events according to given F_2 structure functions. For the hard contribution the AMY parametrization [85] of F_2 as given by Kapusta's "all order QCD" approach [86] is used, with a cutoff parameter p_t^0 which represents the lowest allowed transverse momentum of the virtual quark at the target photon vertex. It is assumed that the contribution with $p_t < p_t^0$ comes entirely from VMD (Vector Meson Dominance) of the hadronic part of the photon, with $F_2/\alpha = 0.2(1-x)$. In this case, it is found that the decay of the $q\bar{q}$ system is peripheral, with the mean transverse momentum of the outgoing quark jet $\langle p_t \rangle = 300$ MeV/c. Additionally $c\bar{c}$ and $\tau^+\tau^-$ events are generated with the Vermaseren Monte Carlo [80], and fragmentation is effected with the LUND string fragmentation model.

Events from all four samples (QCD, VMD peripheral, $c\bar{c}$, and $\tau^+\tau^-$) are generated according to the measured experimental luminosity, processed through standard OPAL simulation and reconstruction programs, and analyzed with the same selection criteria as the real data. The parameter p_t^0 is then varied to make the combined sample agree with the experimental x_{track} distribution. Unfolding of the data using this Monte Carlo is done with the Blobel scheme mentioned above for the two Q^2 regions $4 < Q^2 < 8$ ($\langle Q^2 \rangle = 5.9$ GeV^2) and $8 < Q^2 < 31$ GeV^2/c^2 ($\langle Q^2 \rangle = 14.7$ GeV^2). The results are shown in Figure 2.22, which includes data from PLUTO [84] and TPC/2γ [83]. The OPAL result confirms that a significant pointlike component of the photon is present when the probing photon has $Q^2 > 4$ GeV^2.

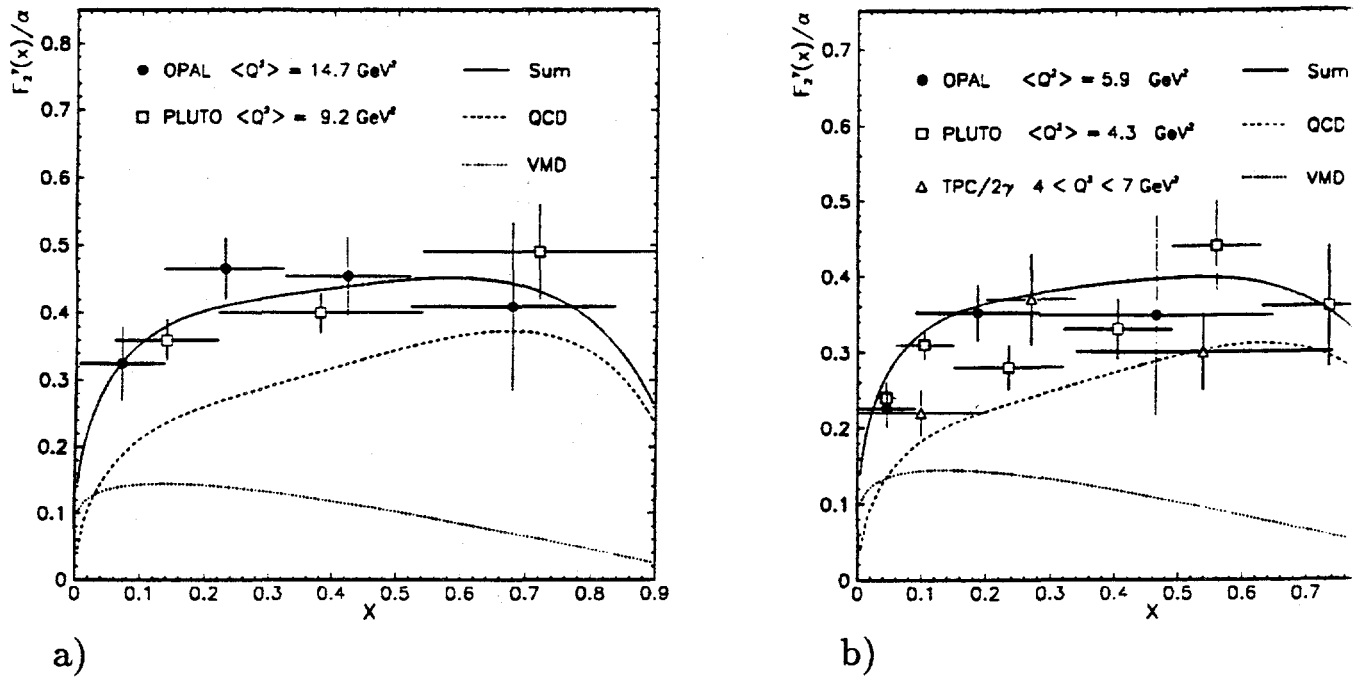

Figure 2.22: Unfolded F_2 with other measurements at similar mean Q^2 shown for comparison: a) ($\langle Q^2 \rangle = 14.7$ GeV^2), and b) ($\langle Q^2 \rangle = 5.9$ GeV^2). The curves show the predictions of the QCD-based model described in the text. The errors are statistical only.

2.2.7 Plans for the Future

From now until the end of 1994, or the end of the first phase of LEP running at or near the Z^0 peak, the continued operation of OPAL and the physics analysis of data taken with the OPAL detector will be the central part of our program.

In the hardware area, our group will continue to share the major responsibility for the operation and maintenance of the OPAL hadron calorimeter and the time-of-flight system. We will fulfill our responsibilities in various areas of on-line and off-line data analysis. Members of our group continue to lead the OPAL efforts in the generation of Monte Carlo events and in the management of the Riverside Snake Farm - the cluster of HP 9000 series workstations.

We will particularly focus our efforts on the physics analysis. While we will continue to participate in the precision measurements of the electroweak parameters, we will concentrate more on the detailed study of hadronic events and try to achieve a better understanding of the effects of QCD. The study of b physics with secondary vertex and lepton tagging will also be an area in which we will contribute. The physics analysis efforts will continue even after LEP200 begins running for experiments in 1996.

2.3 OPAL at LEP200

One of the longterm objectives of the LEP program is the study of e^+e^- collisions at center of mass energies above the W^+W^- production threshold [87]. It is anticipated that operating LEP at around 200 GeV will take place after a few million Z^0s has been accumulated by each of the four LEP experiments. At the end of the 1992 running period, a total of about five million Z^0 events have been recorded by the four detectors. LEP has been operating very efficiently with 8 bunches on 8 bunches and delivering record luminosities during 1993. It is expected that by 1994, at the end of the first phase of LEP operation at the Z^0 peak, each experiment will have accumulated about four million Z^0 events.

The present plan calls for the the installation of 192 NbCu SC cavities by the end of 1994. Machine Development (MD) will begin after October 1994 to increase beam energy. The year 1995 will be devoted mostly to the commissioning of LEP200 to reach energies above the W boson pair threshold. Some amount of luminosity will be provided for the experiments during 1995, and from 1996 onward there will be full operation for physics at the highest energy available and with a peak luminosity of approximately 5×10^{31} cm^{-2}sec^{-1}. Therefore, the rich and unique physics of LEP200 will become the central part of our program for the second half of this decade.

The physics interests and capabilities of LEP200 have been thoroughly studied in the past [88]. However, new motivation and emphasis emerge as more results from LEP and the Tevatron become available. We will concentrate our discussion here on the most important physics topics.

2.3.1 The Measurement of M_W

The mass of the W boson is one of the most important parameters in the Standard Model. Although the W boson was first observed a decade ago, its mass is still poorly measured relative to that of the Z boson. Up to now, the experiments at CERN and Fermilab have measured the mass of W to a precision in the neighborhood of $\pm$400 MeV. This is expected to improve significantly as the experiments at the Tevatron accumulate more data during the next few years.

The precision measurement of M_W is very important for a critical test of the radiative corrections to the electroweak theory. The mass of the W^+W^- and Z^0 are related by the formula

$$M_W^2 = \frac{\pi\alpha}{\sqrt{2}G(1 - M_W^2/M_Z^2)(1 - \Delta r)}$$

where Δr is the radiative correction to the boson mass arising from loop diagrams due to virtual boson and fermion exchanges. From precision measurments of the Z^0 decay at LEP, we have already been able to predict, albeit with relatively large errors, the mass of the top quark within the full range of the Higgs mass of 60 GeV to 1 TeV.

The precision measurements of the mass of the W boson can place very tight limits on the mass of the top quark. And if the mass of the top quark is experimentally measured at Fermilab, one can obtain reasonably tight limits on the Higgs mass.

The pair production of W bosons in the process $e^+e^- \rightarrow W^+W^-$ has a cross section which rises sharply from threshold to a peak of about 17 pb at E_b of 100 GeV, as shown in Figure 2.23.

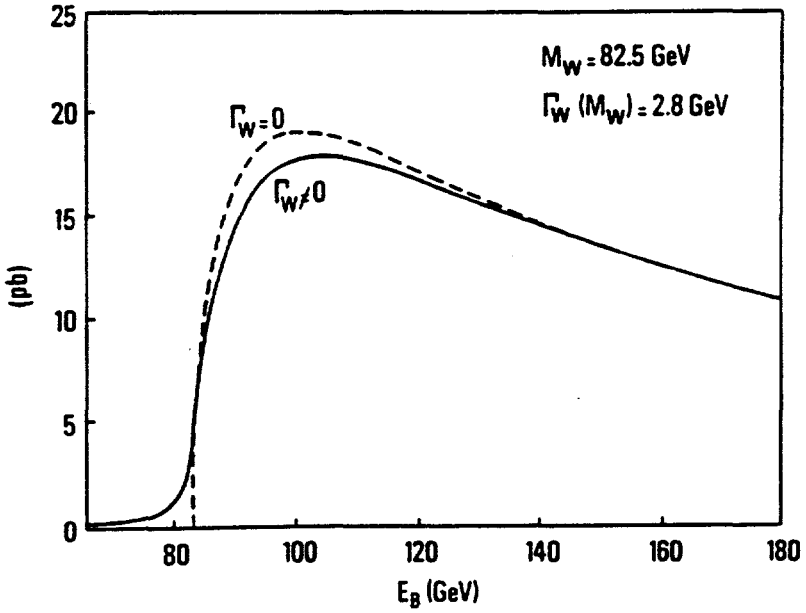

Figure 2.23: Cross section of $e^+e^- \rightarrow W^+W^-$

For an integrated luminosity of 500 pb^{-1} and running at the cross section peak, one expects about 10000 events for each experiment. There are several methods [89] to measure the W mass: (1) measuring directly the invariant mass in hadronic and hadronic-leptonic final states, (2) measuring the excitation function of the cross section near threshold, and (3) measuring the end point of the electron spectrum in $W \rightarrow e\nu_e$.

From the Monte Carlo studies carried out by ALEPH, DELPHI, L3, and OPAL, we have the following results [90]. After reconstructing the four jets from hadronic final states, the jet-jet invariant mass distribution can be compared with the input mass of the W. The statistical error is ± 70 MeV for a sample corresponding to 500 pb^{-1}. In the hadronic-leptonic final state, the mass of $\ell\nu_\ell$ can be calculated by defining the neutrino momentum to be that of the missing momentum and requiring energy conservation. The statistical error on the mass from fitting the mass spectrum of $e\nu_e$ and $\mu\nu_\mu$ is about ± 90 MeV. Combining both hadronic and hadronic-leptonic events, one can reach a statistical precision on M_W of about ± 55 MeV for 500 pb^{-1}

of data at c.m. energy of 175 GeV (Figure 2.24). The statistical error does not vary significantly with respect to the c.m. energy.

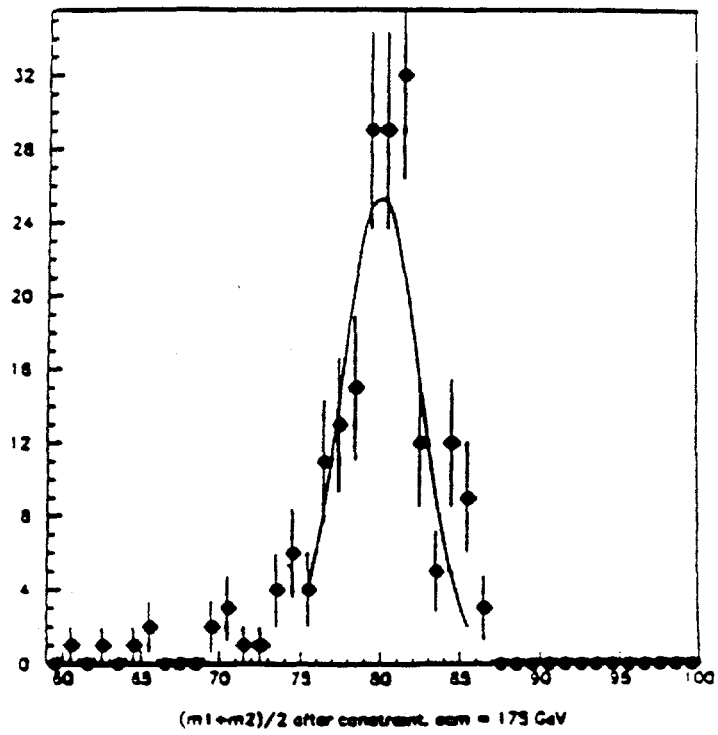

Figure 2.24: The average of hadronic and leptonic masses for mixed decay events

The sensitivity of the W pair production cross section as a function of M_W has been examined. A difference of 100 MeV in M_W gives a 2% difference in cross section at the production threshold and decreases rapidly with increasing energy. Since the statistical precision for 500 pb^{-1} of data will be 1% at best, measuring the excitation curve of the cross section is not a very sensitive method for determining M_W. Furthermore, any running near the threshold reduces the number of events in the total data sample which will be used for the study of many physics topics.

The spectra of the electron energy corresponding to different values of M_W become different only above 65 GeV. The sensitivity on M_W is poor because of the low statistics and the uncertainty associated with the absolute energy calibration of the detector.

A combination of the above mentioned methods will eventually be used in the measurement of M_W. The estimated statistical error is around ± 50 MeV. Systematic errors come from the determination of the beam energy, the calculation of the radiative corrections, detection performance and reconstruction methods. It is estimated that the uncertainty on the beam energy contributes ± 17 MeV, and the

uncertainty associated with each of the others is ±10 MeV. The overall systematic error is estimated to be ±24 MeV.

2.3.2 $e^+e^- \rightarrow W^+W^-$ and the 3-boson coupling

The principal mechanisms responsible for W-pair production in high energy e^+e^- collisions are the t-channel exchange of a fermion and the s-channel exchange of a vector boson, as depicted in Figure 2.25. In the Standard Model, the large cancellations be-

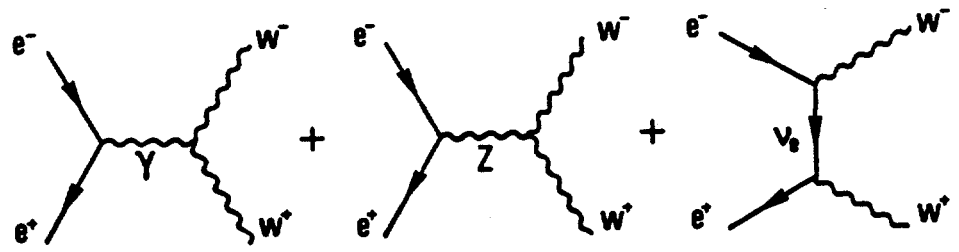

Figure 2.25: t- and s-channel diagrams contributing to $e^+e^- \rightarrow W^+W^-$ in the Standard Model

tween the amplitudes from these processes keep the cross section well behaved as the energy increases and prevent it from violating the unitarity bound at high energies.

At LEP 200, it will be possible for the first time to determine experimentally the couplings of the three gauge bosons WWγ and WWZ. This will be a crucial test of the Standard Model and should point to "new physics."

The most general WWV vertex $\Gamma_V^{\alpha\beta\mu}$ is described in terms of 2×7 independent form factors f_i^V [91]

$$\begin{aligned}\Gamma_V^{\alpha\beta\mu}(q,\bar{q},P) = \quad & f_1^V(q-\bar{q})^\mu g^{\alpha\beta} - (f_2^V/m_W^2)(q-\bar{q})^\mu P^\alpha P^\beta \\ & + f_3^V(P^\alpha g^{\mu\beta} - P^\beta g^{\mu\alpha}) + i f_4^V(P^\alpha g^{\mu\beta} + P^\beta g^{\mu\alpha}) \\ & + i f_5^V \epsilon^{\mu\alpha\beta\rho}(q-\bar{q})_\rho - f_6^V \epsilon^{\mu\alpha\beta\rho} P_\rho \\ & - (f_7^V/m_W^2)(q-\bar{q})^\mu \epsilon^{\alpha\beta\rho\sigma} P_\rho (q-\bar{q})_\sigma,\end{aligned}$$

for V = γ,Z and $g_{WW\gamma} = -e$, $g_{WWZ} = -e\cot\theta_W$. While the form factors f_i^V for $i = 1,2,3$ characterize couplings which are separately P and C conserving, for $i = 4,6,7$ they correspond to CP-violating ones, and for $i = 5$ to couplings separately violating P and C. For $i = 1,2,3$ they may be expressed in terms of the more familiar quantities κ_V and λ_V (for $g_1^Z = G_1^\gamma = 1$):

$$
\begin{aligned}
f_1^V &= 1 + (s/2m_W^2)\lambda_V, \\
f_2^V &= \lambda_V, \qquad V = \gamma, Z, \\
f_3^V &= 1 + \kappa_V + \lambda_V,
\end{aligned}
$$

which in turn are directly related to the W magnetic dipole and electric quadrupole moments

$$
\begin{aligned}
\mu_W &= e(1 + \kappa_\gamma + \lambda_\gamma)/2m_W \\
Q_W &= -e(\kappa_\gamma - \lambda_\gamma)/m_W^2.
\end{aligned}
$$

In the Standard Model all the form factors f_i^V vanish at tree level except for $f_1^V = 1$ or $\lambda_V = 0$, and $f_3^V = 2$ or $\kappa_V = 1$. Once the Standard Model constraints have been relaxed, there are a large number of free parameters to be tested for. The present limits from hadron colliders are $-3.1 < \kappa_V < 4.2$ and $-3.6 < \lambda_V < 3.5$ (at 95% CL). The limits from neutrino scattering and LEP, through loop effects, are $0.9 < \kappa_V < 2.3$ (at 68% CL) and $-1.7 < \lambda_V < 1.6$ (at 95% CL).

The cross section of $e^+e^- \rightarrow W^+W^-$, assuming Standard Model couplings, is shown in the previous section. It peaks at $\sqrt{s} \approx 200$ GeV with a cross section of approximately 17 pb. A total integrated luminosity of 500 pb^{-1} can be accumulated during the running of LEP 200, producing about 8500 events [92]. This sample will be divided into three different final state configurations depending on the decay of the W:

2 leptons + missing $\vec{p}$	700 events
1 lepton + hadrons + missing $\vec{p}$	3400 events
hadrons	4400 events

From the analysis of this sample of events, we will be able to determine λ_V or κ_V to an accuracy of about 30% [93].

2.3.3 The Search for the Higgs Boson

While the Standard Model has been very successful in describing experimental results at energies available in laboratories today, there is as yet no experimental information on the mechanism for electroweak symmetry breaking which gives masses to particles. In the Standard Model, the simplest system of Higgs fields consists of a doublet and its conjugate. Three of the four real fields in this complex doublet are "eaten up" by the $W^\pm$ and Z^0, and only one real neutral Higgs boson H^0 remains to be observed. There is however no theoretical prediction of the mass of H^0. OPAL has set a mass limit of 57.5 GeV on H^0 using a partial sample of data obtained so far. The limit is approaching 63 GeV if all LEP experiments are considered, as Figure 2.26 shows [94].

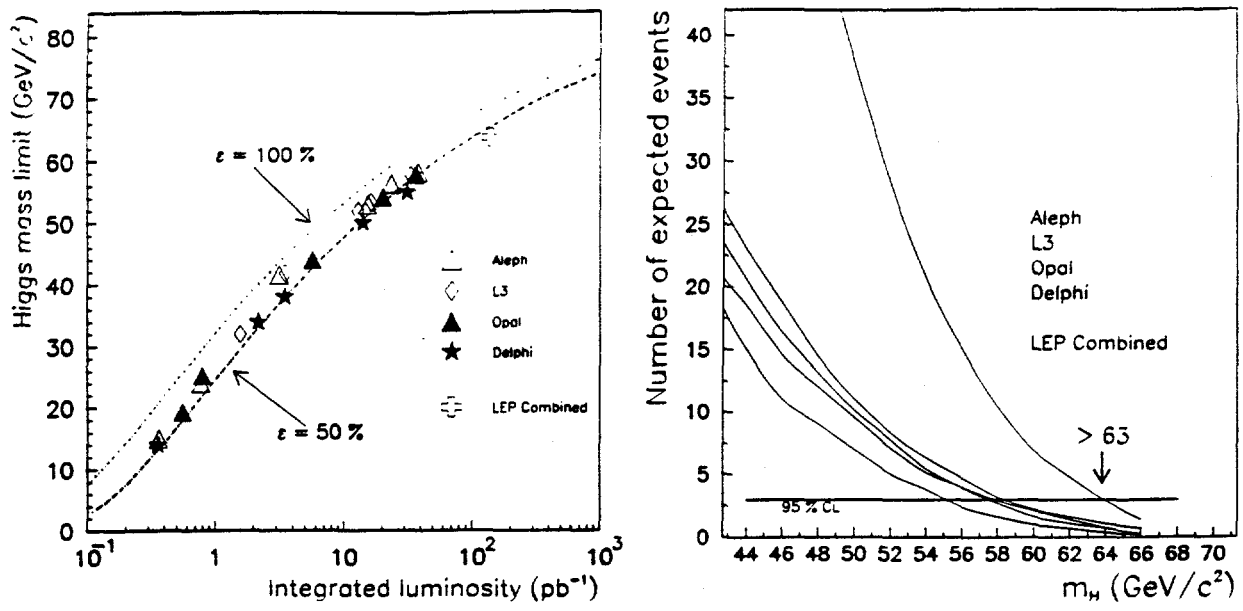

Figure 2.26: *(left)* Published limits on the Higgs boson mass as a function of integrated luminosity. *(right)* The current limit reached by the four LEP experiments.

The dominant process for the Standard Model neutral Higgs boson production at LEP 200 energies is

$$e^+e^- \rightarrow Z^* \rightarrow H^0Z^0$$

The cross sections for this process for various masses of H^0 are shown as a function of the beam energy in Figure 2.27 a), and the cross section as a function of Higgs boson mass is shown in Figure 2.27 b) [95]. They range from 1 pb to 0.2 pb for H^0 mass between 60 and 100 GeV at a beam energy of 100 GeV. Backgrounds to the Higgs signal come from $e^+e^- \rightarrow \gamma Z^0$, W^+W^-, and Z^0Z^0.

OPAL has carried out a Monte Carlo analysis of a data sample corresponding to a luminosity of 500 pb^{-1} at a center of mass energy of 200 GeV. If we tag the events with $Z^0 \rightarrow l^+l^-$, we expect about 35 events for 50 GeV Higgs and 20 events for 80 GeV Higgs. Figures 2.28 show the jet-jet mass distributions recoiling against the Z^0 for 50 GeV and 80 GeV Higgs bosons respectively. As can be seen, it is relatively straightforward to identify the Higgs signal up to 80 GeV in mass with appropriate cuts.

To search for the neutral Higgs of masses up to the beam energy is much more difficult. The process $e^+e^- \rightarrow Z^0Z^0$ has a cross section several times that of the signal, and the Z^0 peak dominates the invariant jet-jet mass distribution in the vicinity of 90 GeV. W boson pair production also produces copious background unless special selections are applied to the data.

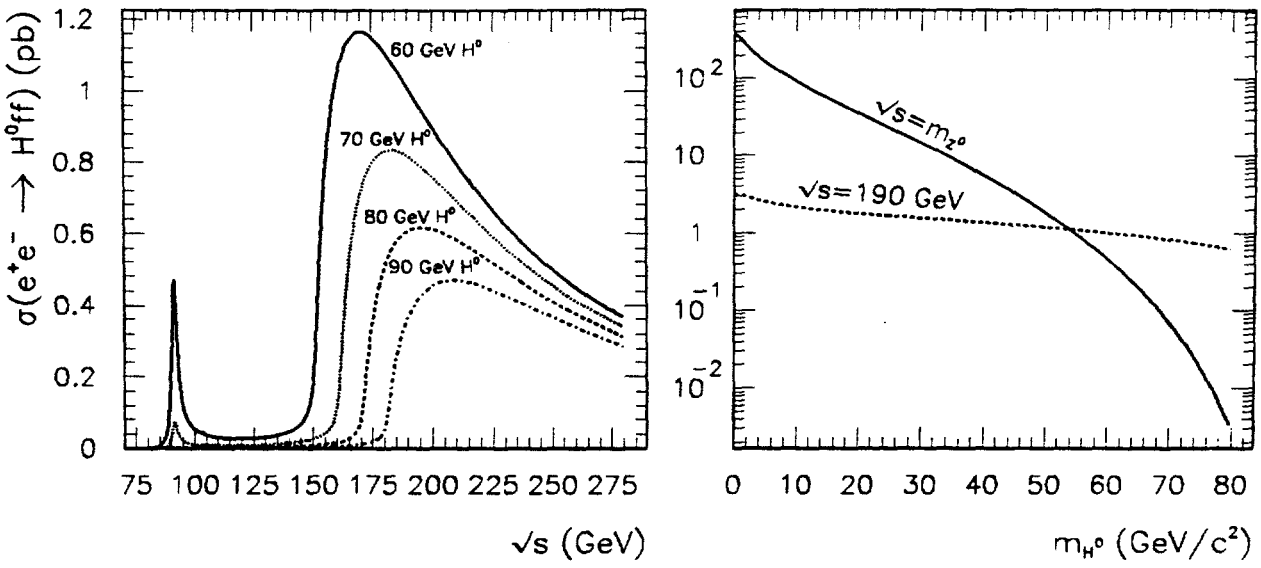

Figure 2.27: Cross sections for the process $e^+e^- \rightarrow Z^* \rightarrow H^0Z^0$ as a function of a) beam energy, and b) Higgs boson mass

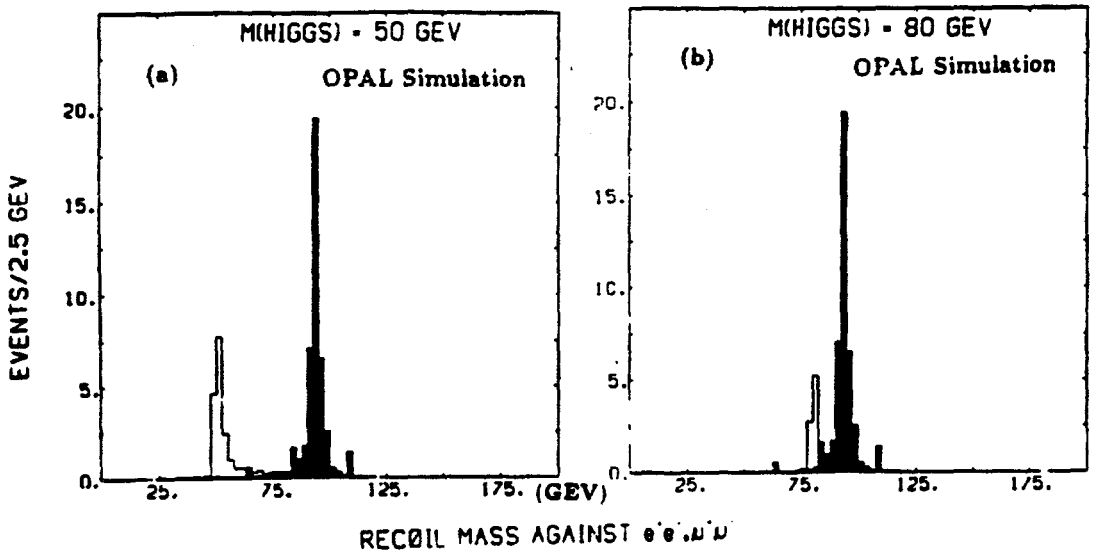

Figure 2.28: Jet-jet Mass Distributions recoiling against the Z: a) m_H of 50 GeV and b) m_H of 80 GeV

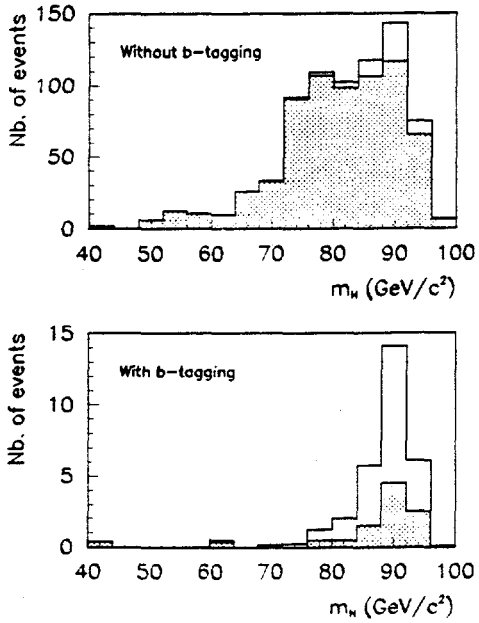

Figure 2.29: The mass distribution of the Higgs candidates for the various backgrounds and for the sum of signal and background: a) before b-tagging, and b) after b-tagging.

The coupling of the Higgs boson to fermion-pair is proportional to the fermion mass. Consequently, one expects the $b\bar{b}$ channel to be the dominant decay mode and constitute about 85% of the Higgs decay. On the other hand, $Z^0 \rightarrow b\bar{b}$ is only 15% and W does not decay into $b\bar{b}$. Thus, by applying b-tagging using secondary vertex and/or lepton identification, the background from Z^0Z^0 and W^+W^- processes can be greatly suppressed. This is demonstrated in the Monte Carlo analysis as shown in Figures 2.29 a) and b) [96].

One can estimate the discovery limit of the Higgs boson based on the production cross section and assuming an effect of 5 σ with at least 5 events observed. Figures 2.30 a) and b) show such limits for the luminosity required versus the mass of the Higgs for the center of mass energies of 175 GeV and 190 GeV respectively. As can be seen, a limit of 93 GeV can be achieved in a single experiment with 500 pb^{-1} at the center of mass energy of 190 GeV. And if it should be possible for LEP to operate at higher energies, one can reach even higher mass limits according to the approximate relation

$$M_H \approx \sqrt{s} - 100 \quad \text{GeV}$$

2.3.4 Plans for the Future

According to the present schedule, LEP200 commisioning will take place in 1995, and there will be some luminosity for the experiments toward the end of that year. The

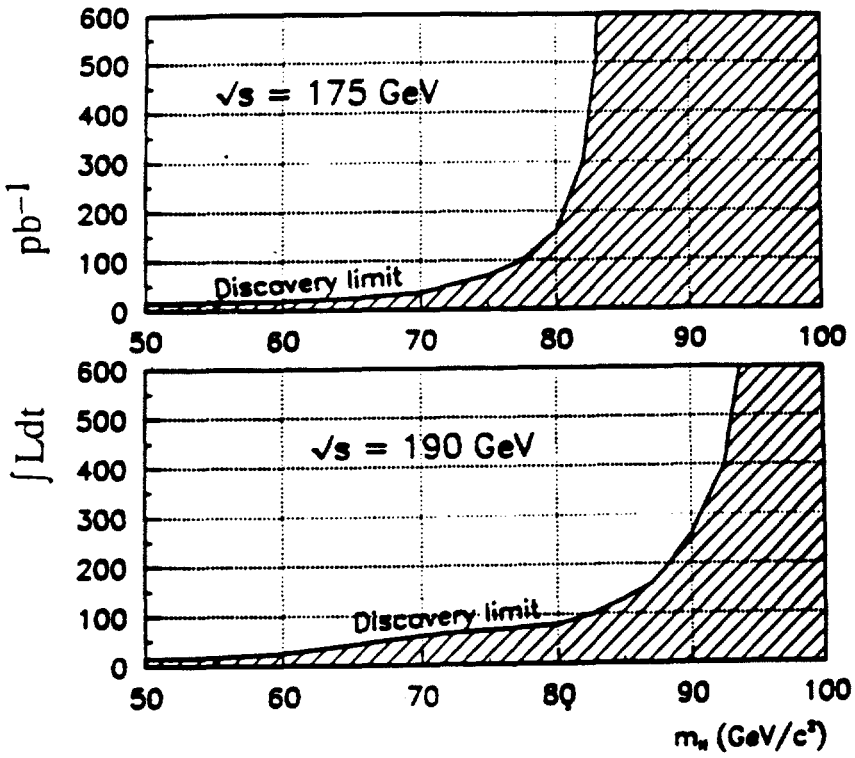

Figure 2.30: Discovery limits (integrated luminosity needed versus M_H) for two center of mass energies.

first full-year physics run is expected to be in 1996, and the present understanding is that LEP200 will operate for at least four years.

Before the turn-on of LEP200, some of the efforts of our group will be devoted to the preparation for any hardware upgrade required for the higher energy operation, as well as for LEP running with possibly higher numbers of bunches. We will also prepare the analysis programs for the physics topics mentioned earlier using Monte Carlo events. During the four or five years of LEP200 running, we will participate in the data acquisition efforts of OPAL and concentrate on the physics analysis on the topics mentioned above.

2.4 The Compact Muon Solenoid (CMS) at LHC

One of the most fundamental questions to be answered in the next decade is the physics origin of the electroweak symmetry breaking and how the particles acquire their masses. Within the minimum version of the Standard Model, spontaneous symmetry breaking through the Higgs mechanism leads to the existence of a spin zero particle, the Higgs boson H^0. More than one Higgs boson can be accomodated in various extensions of the Standard Model. The searches carried out at LEP so far have set a 95% confidence level lower limit of 63 GeV for the Higgs boson mass. The limit on the mass is expected to approach 70 GeV with further running of LEP at the Z^0 peak. As discussed earlier, with LEP200 the search will have a sensitive range up to the mass of the Z^0. Recent work involving members of the UCR theory group indicates that, on the basis of very general arguments, there may exist an upper bound in the neighborhood of 800 GeV for the Higgs boson mass. Therefore, the search for the Higgs boson will be the most important physics goal of the next generation of colliders.

As part of our continuing effort in the systematic study of the physics of the Standard model, the UCR group began participating in 1990 in the RD5 experiment at the CERN-SPS to study how muons can be used in the search of the Higgs boson at a high energy hadron collider. The work on RD5 has formed the basis of a proposal for the construction of the Compact Muon Solenoid to exploit the full range of physics potential of the Large Hadron Collider at CERN.

We do this with the understanding that

- our major physics program beyond LEP will be at a future high energy hadron collider,
- the LHC, because it will be constructed in the LEP tunnel at a much lower cost than SSC, will almost inevitably enjoy a several year window of exclusivity in the search for the Higgs boson,
- it is natural and logical for us, being already at CERN on OPAL, to participate in the design and construction of CMS, and
- it is incumbent on American groups that have the possibility of doing so to participate in the CERN endeavor so that American physicists have a significant involvement in this important next step.

2.4.1 The Detector Design

The Compact Muon Solenoid detector is designed to exploit the full range of physics of proton proton collisions st the Large Hadron Collider with a design luminosity of $1.7 \times 10^{34}\,\mathrm{cm}^{-2}\mathrm{sec}^{-1}$ at the c.m. energy of 15.4 TeV. The detector will be built

around a high-field superconducting solenoid leading to a compact design for a muon spectrometer. Identification and precise measuremment of muons, photons, and electrons are emphasized in the design considerations. Details of the CMS detector are available in the CMS Letter of Intent [98]. We will describe some of the components very briefly.

The Muon System

The muon spectrometer consists of a single solenoidal magnet, with a radius of 2.9m and a length of 14m, producing a uniform magnetic field of 4 T. The favorable aspect ratio of the solenoid allows efficient muon detection and measurement up to rapidities of 2.5, making forward toroids unnecessary. The inner radius is large enough to accomodate the inner tracker and the calorimeters. The magnetic flux is returned via a 1.8m thick saturated iron yoke (1.8 T) instrumented with muon chambers. The overall dimensions of the CMS detector are shown in Figure 2.31.

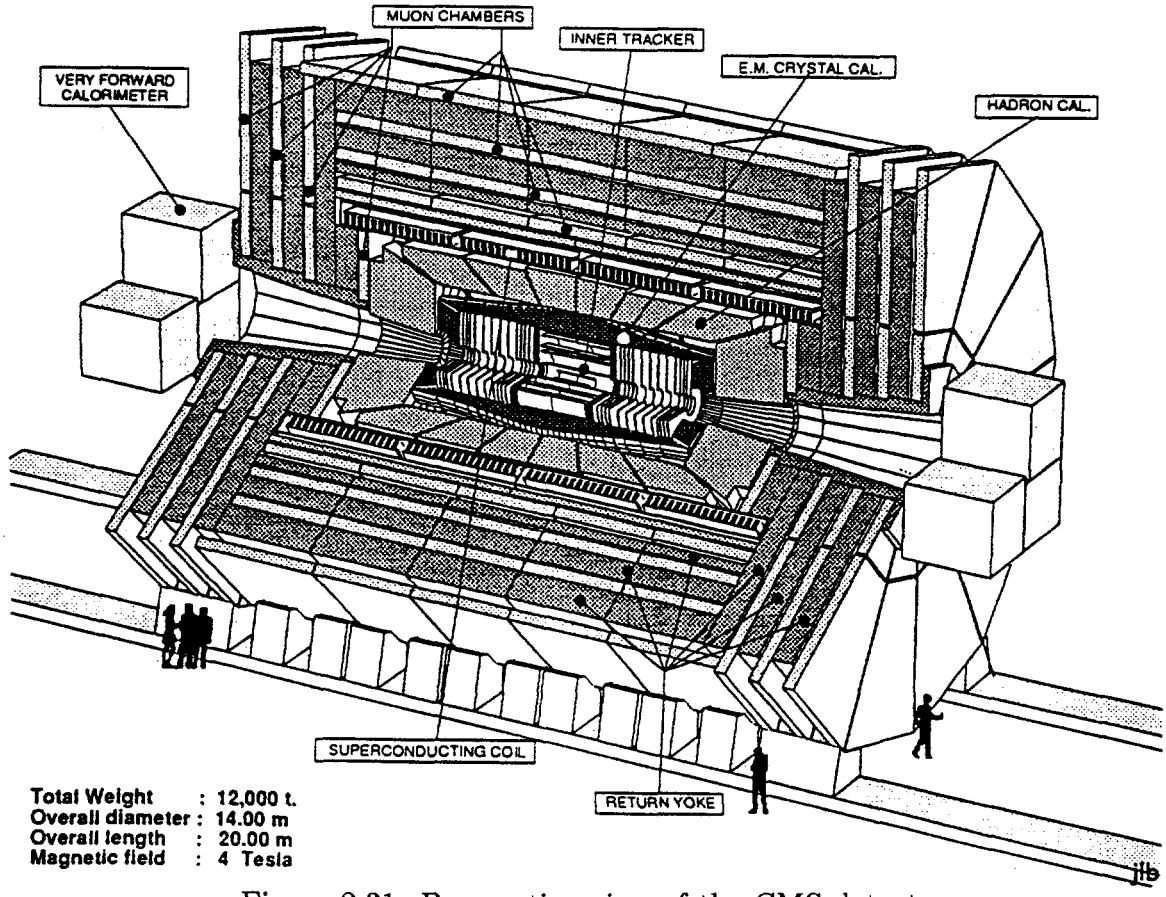

Figure 2.31: Perspective view of the CMS detector

The 4 T central field together with a powerful tracking system leads to excellent momentum resolution. The momentum is measured three times: inside the inner

tracking volume, just after the coil, and in the flux return. These almost independent measurements make the muon identification system very robust. Furthermore, the two measurements outside the coil are guaranteed at any luminosity. The muons are identified in four separate muon stations (MS1 to MS4) inserted in the return yoke. Each muon station consists of several planes of drift chambers designed to give a muon vector in space with 100 μ precision in position and better than 1 mrad in direction. The four muon stations also contain triggering planes.

The combined muon momentum resolution is better than 3% at 0.4 TeV in the central rapidity region ($|\eta| < 2.5$), degrading to 5% at 2 TeV. Low momentum ($p <$ 100 GeV) muons are measured before the absorber with a precision of about 1% up to a rapidity of 2.5.

Tracking

The primary goal of the tracking system is to reconstruct all high p_t muons and isolated electrons produced in the central rapidity region with a momentum precision of $\Delta p/p \sim 0.1 p_t$ (p_t in TeV). A second goal of the tracking system is to recognize all tracks with $p_t > 2$ GeV. This capability plays an important role in electron identification. In order to detect inclusive isolated electrons with a contamination of less than 10% from QCD jets a rejection of 10^6 per jet must be achieved. At high luminosities pile-up effects limit the power of the calorimeter isolation cuts. With magnetic tracking, one can base the isolation cuts on the absence of high $p_t (p_t > 2$ GeV) charged tracks in a cone around the electron.

To solve the problem of pattern recognition at high luminosities, the tracking detector must be highly segmented with small cell sizes. Solid state and gas microstrip detectors can provide the required granularity and precision. Strip length of the order of 10 cm will be necessary to maintain the cell occupancy below 1%. This leads to a system of 10^7 channels. The reconstruction efficiency of isolated high p_t tracks is better than 95%, and for high p_t tracks within jets better than 90%, in the rapidity range $|\eta| < 2.5$.

Calorimeter

In order to identify narrow signals in the gamma-gamma mass spectrum from a low mass Higgs boson decay or from a possible toponium bound state, the electromagnetic calorimeter must have the best possible mass resolution. At high luminosities, there will be an average of 10 to 15 vertices for the origin of the photon. The calorimeter must be able to measure the photon direction with sufficient precision so as not to degrade the di-photon mass resolution. Powerful isolation cuts and two-shower separation capability are required to eliminate background from jets of moderate E_t (20–50 GeV) faking single photons. Rejection of 10^4 or better per jet is necessary. To fulfill these requirements, CMS has chosen, as the preferred design, a high resolution

cerium floride (CeF_3) crystal calorimeter with good lateral granularity ($\Delta\eta \times \Delta\phi = 0.02 \times 0.02$) surrounding the inner tracking volume inside the coil. The crystals start at 1.4m. They will be split into two longitudinal segments. An energy resolution of better than 1% at 50 GeV can be achieved in a homogeneous crystal calorimeter. The strong magnetic field of the CMS reduces the pile-up from charged particles in the crystals and allows, by energy-momentum conservation, a precise *in situ* calibration using electrons from W and Z decays. As an alternative solution, a Pb–scintillator sampling calorimeter, the so-called "Shashlik" or "Shish-Kebab" design, is also being considered.

A hadron calorimeter with copper absorber is installed between the e.m. calorimeter and the coil. It begins at the radius of 2.95m for a total of 7 interaction lengths at $\eta = 0$ (10λ at $\eta \geq 1$). Scintillator tiles equipped with wavelength-shifter fibers are used as detecting elements. A "tailcatcher" is installed after the coil in the rapidity region $|\eta| \leq 0.6$. The use of low cost silicon pads as alternative detecting elements is being considered for the end-caps.

Owing to the high radiation levels in the very forward direction ($2.6 \leq |\eta| \leq 4.7$), a calorimeter employing an exchangeable active medium (gas) is being considered. It is a sampling calorimeter consisting of iron sandwiching Parallel Plate Chambers (PPC). Together with the very forward calorimeter, the central hadron calorimeter system is designed for the measurement of large missing transverse energies and of high p_t jets up to $|\eta| = 4.7$.

2.4.2 Physics Potential of CMS

There have been exhaustive studies at the SSC and LHC workshops on the physics at very high energy hadron colliders, [97] and there is no reason to repeat them here. We will, however, briefly describe how we can exploit some of these physics topics using the CMS. More detailed discussions are contained in the Letter of Intent of the CMS.

For the mass range between the LEP limit and about 140 GeV, the search for the Higgs boson will concentrate on the channel $H \rightarrow \gamma\gamma$. The capability of the CMS in detection the Higgs is studied using Monte Carlo simulation of both the signal and background [99] [100]. The key input parameters and results of the study are shown in Table 2.13. An efficiency of 85% was assumed for reconstruction of each photon, leading to a 28% loss of signal and background. A further loss of 8% is due to pile-up in the isolation cut region. The crystal calorimeter is assumed to have an energy resolution given by $\Delta E/E = 2\%/\sqrt{E} \oplus 0.5\% \oplus 0.150/E$ and an ability to measure the photon direction with a resolution $\Delta\alpha = 40(\text{mrad})/\sqrt{E}$.

Figure 2.32 a) shows a background subtracted two-photon effective mass plot for an integrated luminosity of 10^5 pb^{-1}, with signals at $m_H = 110$ and 130 GeV, in the CMS crystal calorimeter, while Figure 2.32 b) show the same plot for the backup lead-scintillator calorimeter (Shashlik).

Signal	m_H	
	110 GeV	130 Gev
$\sigma \cdot B(H^0 \to \gamma\gamma)$ (fb)	87.7	86.5
Acceptance	53%	60%
σ_m (MeV)	640	720
$N_S/\sqrt{N_B}$	17.2	23.5

Table 2.13: Signal cross section, acceptance, mass resolution, and statistical significance at $m_H = 110$ and 130 GeV.

The Higgs decay channel of $H^0 \to ZZ^*$ with the Z boson decaying into two leptons provides a clear signal in the search for the Higgs in the intermediate mass range from about 120 GeV to $2M_Z$. The main background comes from $t\bar{t}$ and $Zb\bar{b}$ production.

Electron and muon identification down to low transverse momenta and over a large rapidity range is required to keep the acceptance for the signal high. Appropriate kinematical cuts are applied to reduce the background. Figure 2.33 a) shows the four lepton signals for a Higgs mass of 120, 130, 150, 170 GeV, together with the background from $t\bar{t}$ and $Zb\bar{b}$ before any isolation cuts. With isolation cuts on the two lowest p_t leptons the background is greatly suppressed as shown in Figure 2.33 b). Key parameters and results are summarized in Table 2.14

		m_H (GeV)			
		120	130	150	170
$\sigma \cdot B(H^0 \to ZZ^* \to 4e)$	(fb)	0.35	0.91	2.01	0.57
Acceptance $\times$ efficiency	$4e$	5.9%	12.6%	22.2%	27.0%
	4μ	17.5%	23.4%	28.7%	31.6%
	4ℓ	12.1%	19.6%	27.1%	31.3%
Signal width σ_m (GeV)	$4e$	0.63	0.64	0.72	0.92
	4μ	0.66	0.66	0.75	0.95
$N_S/\sqrt{N_B}$ (before isolation)		2.7	7.1	25.8	12.6
$N_S/\sqrt{N_B}$ (after isolation)		4.1	13.2	52.8	24.4

Table 2.14: Key parameters in the $H^0 \to ZZ^*$ study

The search for a Higgs boson above the $2M_Z$ threshold but below about 600 GeV is less demanding. The signal stands out clearly in the four-lepton effective mass spectrum. Using the mass constraint of the Z^0 further sharpens the signal. For the mass region above 700 GeV, the search can be effectively conducted in two different channels as discussed below.

In the channel $H^0 \rightarrow ZZ \rightarrow \ell^+\ell^-\nu\nu$, the signal appears as a broad Jacobian peak in the $p_t(Z)$ distribution. Figure 2.34 a) shows the expected signal for a 800 GeV Higgs above the ZZ background for an integrated luminosity of 10^5 pb^{-1} after using various cuts. By tagging forward jets with energy above 700 GeV in the rapidity range of 2.5 to 4.5, the background is further reduced as shown in Figure 2.34 b).

In the channel $H^0 \rightarrow ZZ \rightarrow \ell^+\ell^- jj$ it is possible to extract the Higgs signal since there is no $t\bar{t}$ background. However, because of the low branching ratio more integrated luminosity is needed to make definitive identification. Figure 2.35 shows the $\ell^+\ell^- jj$ effective mass distribution of the production of a 1 TeV Higgs together with background after various kinematical cuts for an integrated luminosity of 3×10^5 pb^{-1}.

2.4.3 UCR Participation

The Large Hadron Collider is the next accelerator to be constructed at CERN, even though it has not yet been officially approved by the CERN Council. The CERN Research Board has accepted the recommendation of the LHCC that the CMS Collaboration be approved to proceed with a Technical Proposal based on the CMS Letter of Intent for the construction of one of the two general purpose detectors at the LHC. The Technical Proposal in due in May 1994.

We will be working with other members of the CMS Collaboration on the writing of the Technical Proposal. In addition to UCR, there are presently three other American institutions participating in CMS: UC Davis, UCLA, and University of Texas, Dallas. These groups have been meeting regularly and working together on the design of the forward muon detector. We are preparing a joint proposal to DOE for our participation in CMS and for the construction of this detector component. We expect to submit this proposal in the near future.

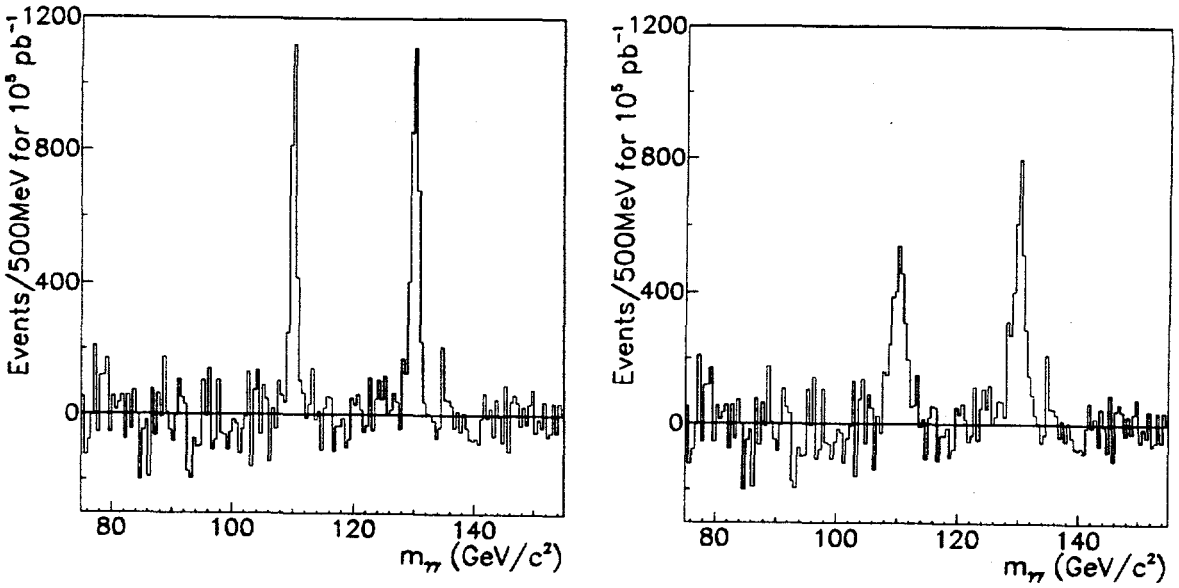

Figure 2.32: Background-subtracted $\gamma\gamma$ effective mass plot for 10^5 pb^{-1} with signals at $m_H = 110$ and 130 GeV in a) the CMS crystal calorimeter and b) the backup lead-scintillator calorimeter.

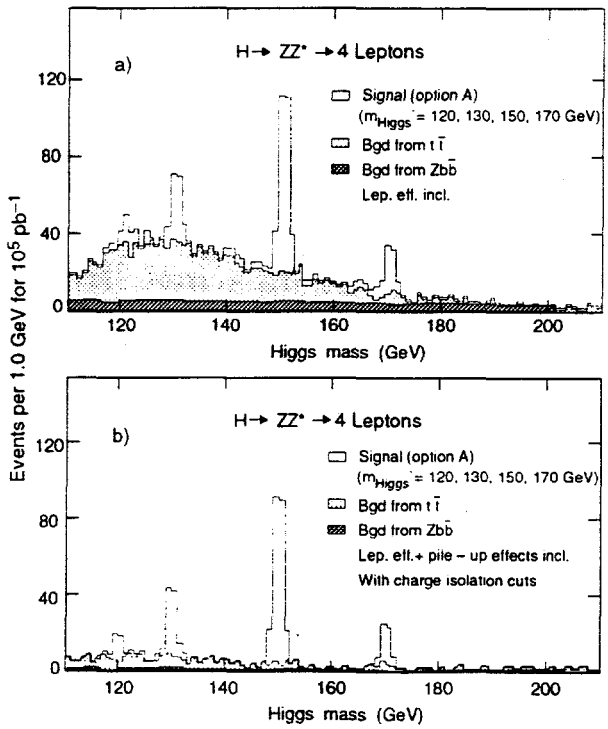

Figure 2.33: The four-lepton signal in $H^0 \rightarrow ZZ^*$ a) before isolation, and b) after track isolation cut.

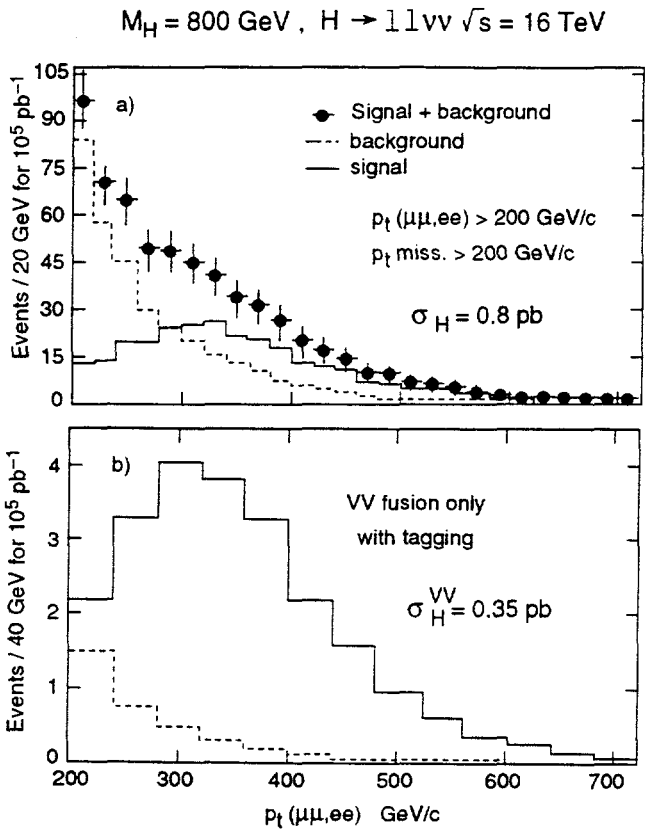

Figure 2.34: Jacobian peak from $m_H = 800$ GeV with background: a) no forward jet tagging, b) forward jet tagging.

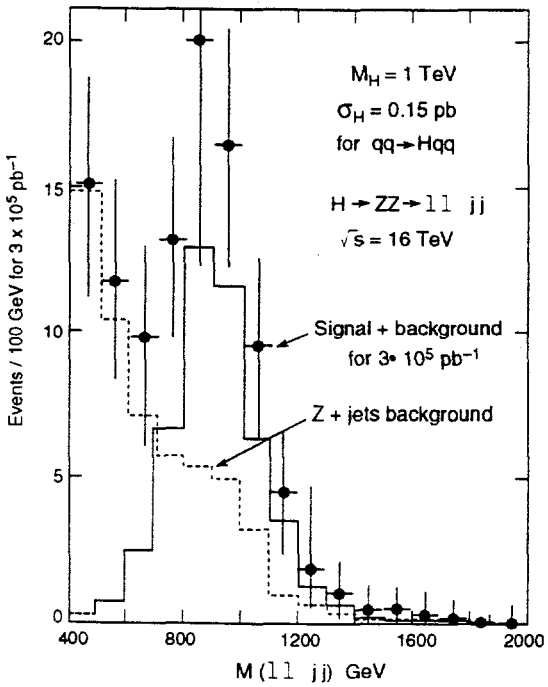

Figure 2.35: A 1 TeV mass peak seen in the $H^0 \to ZZ \to \ell^+\ell^- jj$ channel for 3×10^5 pb^{-1}.

2.5 The RD5 Experiment

The RD5 experiment, with which UCR has been associated since 1990, is one of a series of detector R&D experiments sponsored under the auspices of CERN's Detector Research and Development Committee (DRDC) to study various detector and electronics concepts for possible use in eventual collaborations at the Large Hadron Collider (LHC). The RD5 experiment in particular studies a number of questions which are crucial for the successful use of muon triggers in a detector such as CMS: the rate of muons from hadron punchthrough and decays, the efficiency of triggering using transverse momentum cuts, and the precision in momentum reconstruction required for identifying the Higgs. In addition RD5 serves as a test bed for a number of candidate detector technologies. The original RD5 program was expected to be carried out in two or three years, ending with this year's running. However with the selection of CMS as one of the two detectors for LHC exploitation, RD5 will now evolve into a dedicated vehicle for detailed prototyping of CMS detector elements. The apparatus used for the experiment, located in the P2 test beam at the CERN SPS, is illustrated schematically in Figure 2.36.

2.5.1 Punchthrough and Trigger Studies

One of the aims of RD5 is to study the hadron punchthrough and the behavior of muons produced in hadron showers from secondary pion or kaon decays in an absorber, with and without magnetic field. Reliable punchthrough data are necessary for the construction of muon triggers which allow a fast and efficient cut on the transverse momentum of muons produced at the LHC. RD5 first obtained beam time during the summer of 1991. However the cryogenic system for the M1 magnet was not available during that summer, so the experiment did not fully mimic a section of the CMS detector. Consequently that year's running period was largely a shakedown of the various detector elements and the combined readout system. Nevertheless, valuable information on hadronic punchthrough was obtained from the runs, and a paper on this subject has recently been completed and submitted for publication [101].

Two methods were used to evaluate the punchthrough from the data. The first, more simple-minded method defined the punchthrough probability at a given depth as the ratio of the number of events with at least one hit in a detector element at that depth to the total number of incoming beam particles. The second, more sophisticated method used information from all possible detector elements to define the punchthrough probability in terms of the probability that a given configuration of detector hits would be realized at a given depth. This method allowed information on chamber noise and efficiency to be incorporated in a natural way. Surprisingly, the two methods give nearly identical answers, as shown in Figure 2.37 where the punchthrough probabilities obtained for various beam momenta are presented. Similar results from the CCFR Collaboration [102] are also shown on the figure.

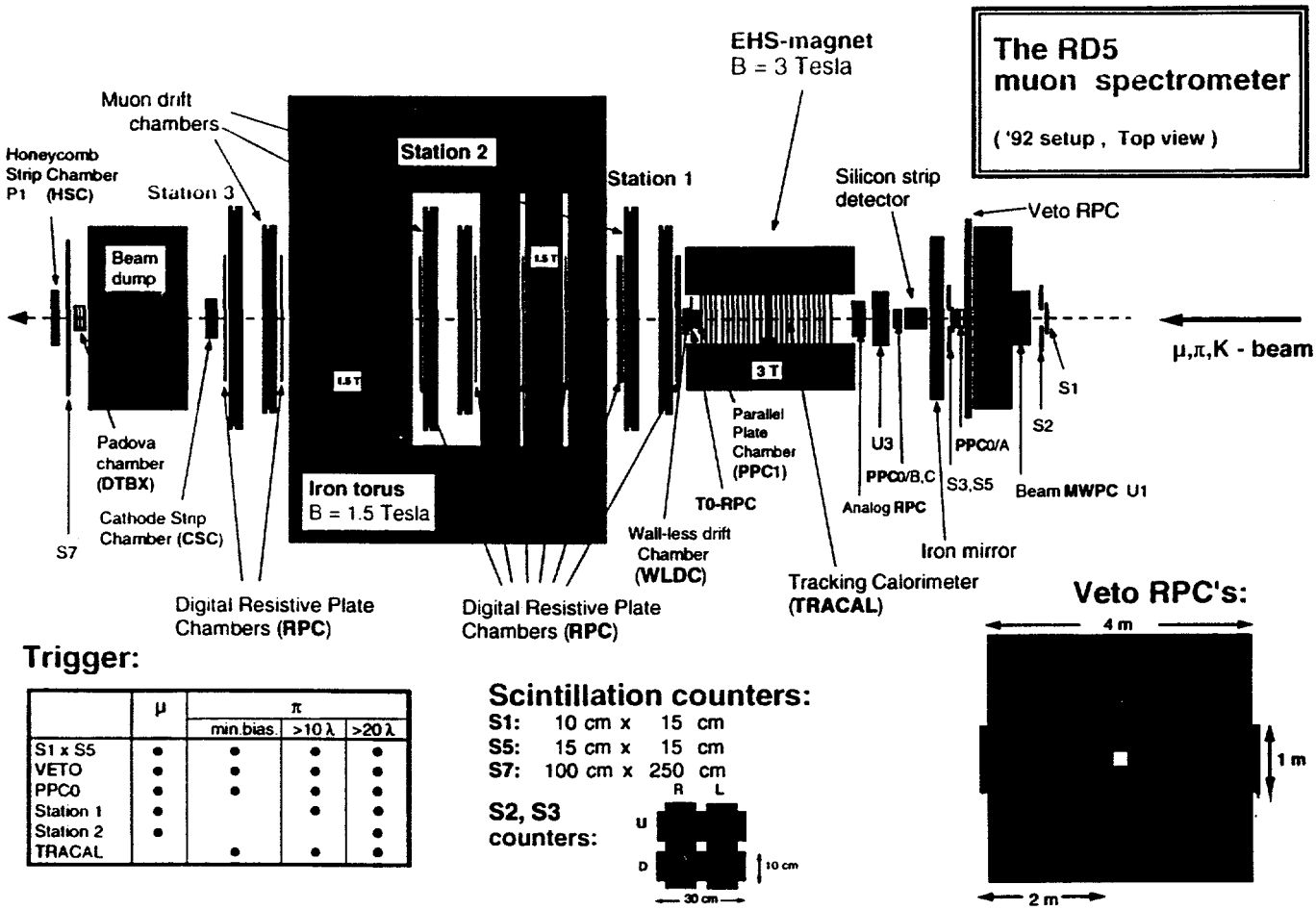

	μ	π		
		min.bias	>10 λ	>20 λ
S1 x S5	●	●	●	●
VETO	●	●	●	●
PPC0	●	●	●	●
Station 1	●		●	●
Station 2	●			●
TRACAL		●	●	●

Figure 2.36: Plan view of the experimental setup of the RD5 project.

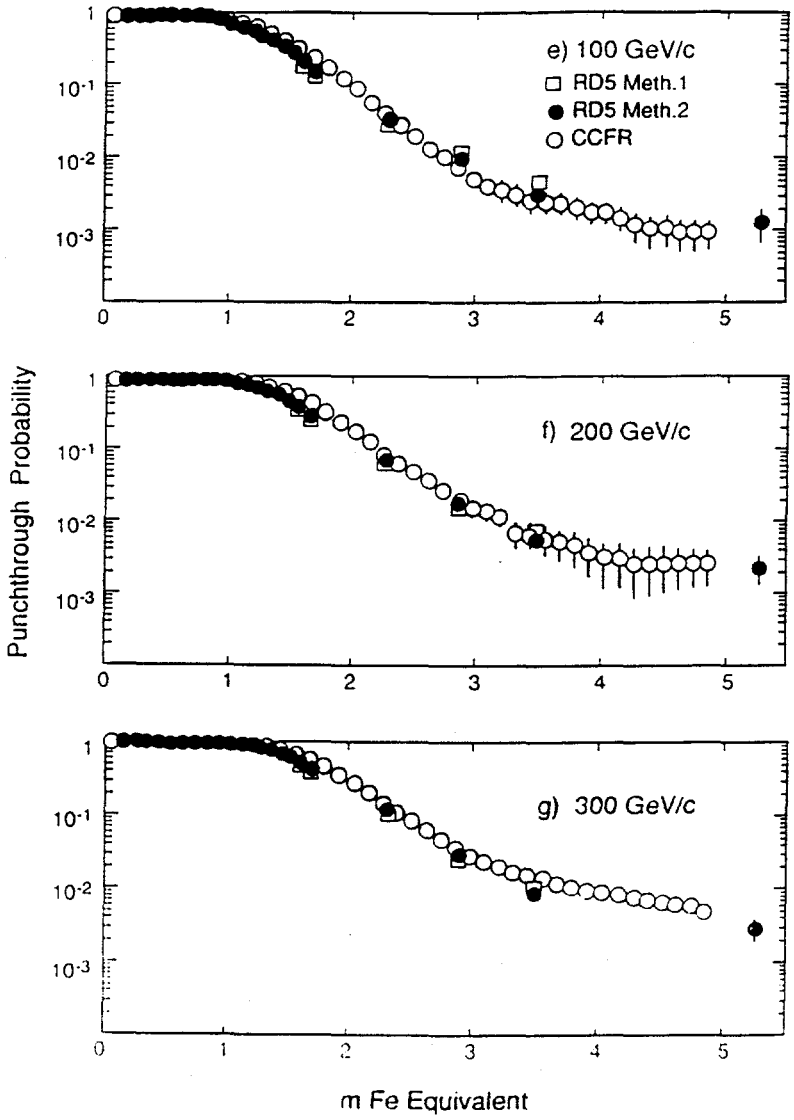

Figure 2.37: Punchthrough probability for various beam momenta.

An accurate punchthrough measurement at large absorber depths requires the elimination of any muon contamination in the pion beam. The two methods use various combinations of information from the detectors to separate beam muons from shower muons. Even so, the residual muon contamination begins to be dominant at about 20 λ, corresponding to distances greater than 330 cm in Figure 2.37. Upstream veto counters installed in 1992 help control this contamination, and an update to the punchthrough results will be available soon. Further papers are in preparation on the subjects of muon-induced electromagnetic showers and on muon brehmsstrahlung, as well as instrumentation papers on individual detectors.

2.5.2 Detector Studies

Many detectors have been placed in the RD5 experiment to test their suitability for further development. Among the candidates for muon chambers for CMS are

- Wall-Less Drift Chambers (WLDC) proposed by the Aachen group,
- DTBX chambers from the Padua group,
- Honeycomb Strip Chambers (HSC) from NIKHEF in Amsterdam,
- Cathode Strip Chambers (CSC) from the American GEM groups.

Candidates for triggering chambers are

- Parallel Plate Chambers (PPC) from the Moscow groups,
- Resistive Plate Chambers (RPC) and Analog RPCs (ARPC) from the Rome groups and an alternate RPC from the Warsaw group.
- Fire Fly Chambers (FFC) proposed by the Zurich group.

In addition silicon strip detector technologies have been explored by the Finnish groups, and several calorimeter possibilities such as the Shashlik or Shish-Kebab detector will be tested as possible cheap alternatives to crystals for the CMS electromagnetic calorimeter.

Since all of these technologies have been discussed in some detail in the CMS Letter of Intent, we will not present them here. As CMS moves to the stage of a Technical Proposal, the RD5 program will focus less on general questions such as punchthrough and more on the ability of the proposed detectors to deliver their advertized performance in the CMS context.

2.5.3 UCR Participation

UCR's initial participation in RD5 consisted in the installation and preparation of the reference muon chambers, originally built for the UA1 experiment by the Aachen group, and in developing the system for monitoring and control of the high voltage supplies for the chambers. This system has been maintained for the 1992 and 1993 running.

Riverside is also supervising the construction and installation of a prototype cathode strip chamber (CSC) to investigate its suitability for use in the forward muon stations of CMS. The device is being constructed to our specifications at Dubna and will use electronics loaned by the the GEM group at Brookhaven. Chambers in the forward muon stations operate in a high magnetic field perpendicular to the cathode planes. Since the field direction in the M1 magnet is transverse to the beam axis and the magnet is not readily movable, the only way to test the chambers at RD5 is with horizontal cosmic rays. We are scheduled to carry out these tests after the RD5 beam running is completed. In parallel with this effort, members of the UCR group are working to develop a suitable simulation package for CSC chambers. A detailed modeling program written by Tcherniatine of Moscow and BNL has been adapted and incorporated into the RD5 and CMS GEANT descriptions. Comparison of program and test results will provide valuable information on this chamber technology. The members of the Riverside group who are involved are W. Gorn, J.G. Layter, B.C. Shen, G.W. Wilson, J.R. Letts and P. Giacomelli.

2.6 LSND at LAMPF

Neutrino interactions have been used throughout the development of particle physics to study a wide range of fundamental questions including the nature of the electroweak interaction, lepton number conservation, and as a probe of cosmology. Low energy neutrinos, such as those available at LAMPF, offer significant advantages in testing the fundamental properties of the neutrinos themselves. In the decade of the 80's as series of experiments at LAMPF have measured neutrino interactions at low energies. Since 1982 several members of our group, notably William Gorn and Gordon VanDalen, have participated in an experiment at LAMPF which established significant limits in the search for neutrino oscillations [103] and measured neutrino scattering cross sections [104] and [105].

We are now collaborating in a new program which is a natural successor to the previous experiment, and serves as a logical next step in the entire LAMPF neutrino program. The primary goal of the experiment is to search for neutrino oscillations to the levels of 10^{-2} eV^2 in mass difference and 2×10^{-4} in mixing. This greatly extends the range explored by accelerator based searches.

The new experiment, called the Large Scintillation Neutrino Detector, or LSND, will consist of 200 tons of dilute mineral oil–liquid scintillator located near the LAMPF beam stop neutrino source. The primary focus of LSND is neutrino oscillations, although a range of related neutrino interactions will also be investigated. The collaboration of 33 physicists from LAMPF and 5 universities prepared a proposal which has been approved with the highest ranking by the Los Alamos PAC [111]. An expanded collaboration began construction in 1990-91, and data acquisition with the complete detector began in July of 1993.

The future of this program looks toward two proposed experiments that have been highly rated in review. The original Large Cerenkov Detector (LCD) proposal [106] pre-dates the LSND experiment. We propose to a larger detector at a beam stop for the Proton Storage Ring (PSR) also located at LAMPF. The time structure of the PSR spill, less than 300ns in length, allows time separation of the ν_μ produced in π^+ decay from the later $\overline{\nu_\mu}$ and ν_e produced μ^+ decay. Precision measurements of the Weinberg angle, and better limits on neutrino oscillation are possible.

The E889 proposal [107] would push Δm^2 sensitivity to well below 10^{-2} eV^2 using detectors similar to the LSND located at 1km, 3km and 20km from the AGS neutrino source at Brookhaven. The proposal received preliminary approval by the AGS PAC this winter, and we are preparing a detailed technical proposal for further review.

2.6.1 The Detector

The detector is similar to a large water Cerenkov device but with better angular, position, and energy resolution due to more light collected from scintillation, and the improvements in Cerenkov imaging from higher index of refraction, longer radiation

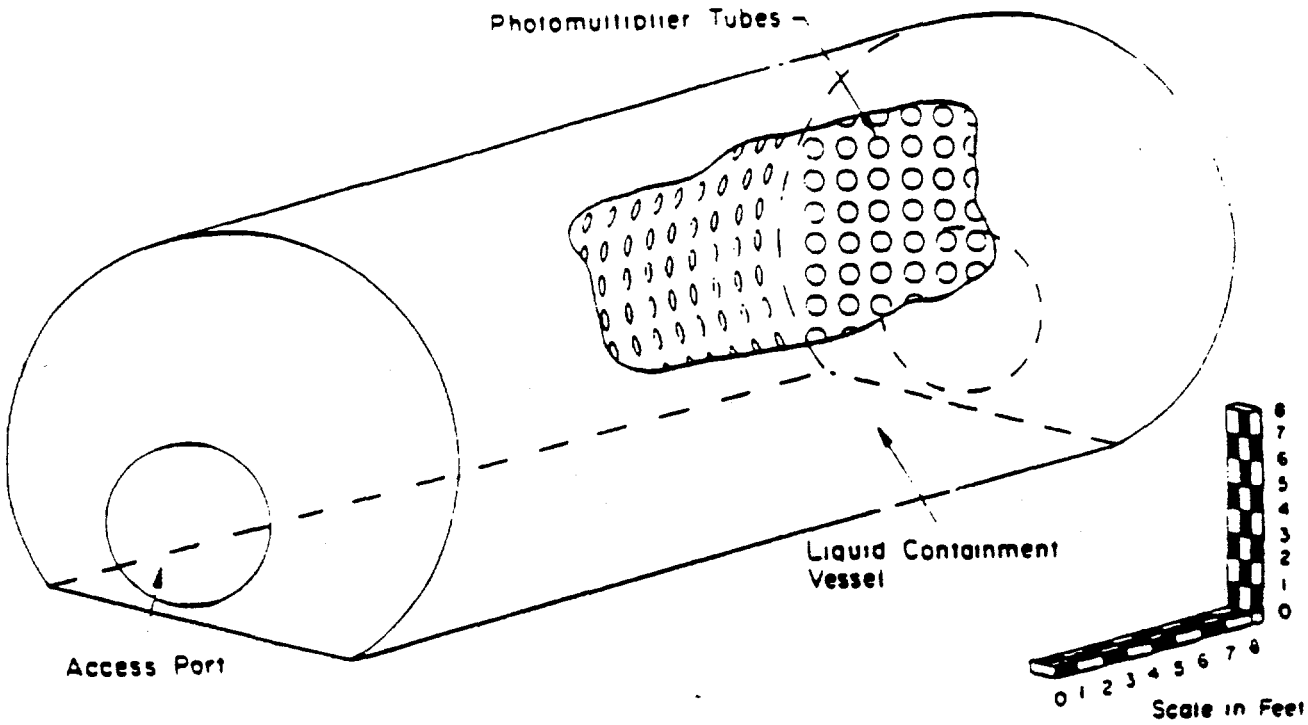

Figure 2.38: Schematic view of the LSND detector

length, and lower density of mineral oil compared to water. The expected energy, position and angular resolutions for a 45 MeV electron are $< 5\%$, < 25 cm, and $< 15°$ respectively. Protons are identified by the absence of a Cerenkov cone, and neutrons will be tagged by the 2.2 MeV photon from neutron absorption on a free proton. The superb event timing and vertex reconstruction allows us to separate neutrino induced events from pion decay in flight, decay at rest, and cosmic ray backgrounds using the 200 MHz fine structure in the LAMPF beam.

The proposed detector is shown in Figure 2.38. It consists of a cylindrical tank of dilute mineral-oil-based liquid scintillator approximately 6 m in diameter by 9 m long with an active mass of 200 tons. The 1224 8" photomultiplier tubes cover 28% of the surface area of the tank with sensitive photocathode.

The current data acquisition system was described at the 1992 Computing in High Energy Physics Conference [109]. The overall data acquisition control, through online event reconstruction will be supervised by the CODA data acquisition environment being developed at CEBAF [108].

The basic readout card design has been described at the 1990 Computing in High Energy Physics Conference [110]. Essentially deadtime free operation is achieved by having each tube digitized continuously by a pair of flash ADC's into dual-ported memory. One flash ADC records the raw charge in 100 nsec bins, and the other records the pulse time from the decay of a charge initiated by a tube trigger. The trigger system reflects the relative simplicity of the detector. Each crate will provide

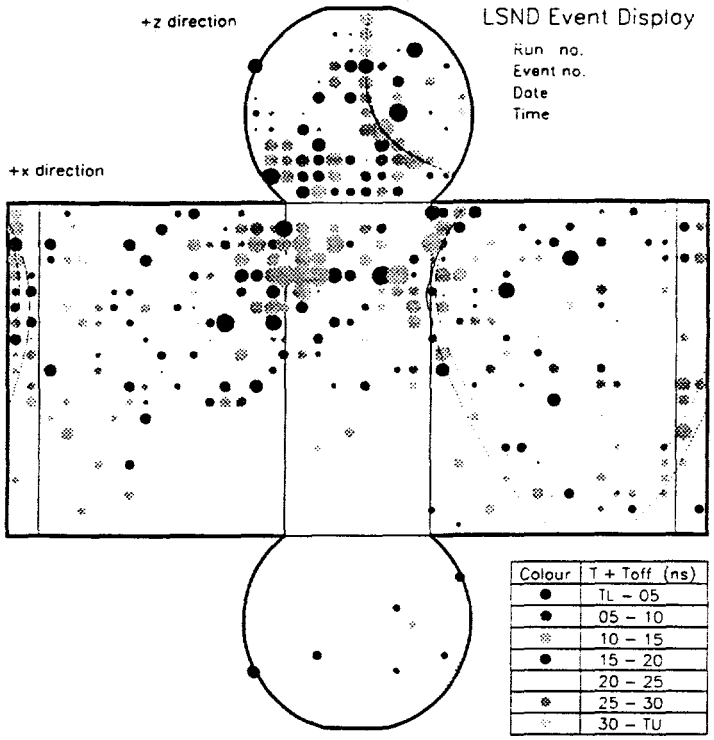

Figure 2.39: Monte Carlo event seen in the detector.

a sum of the number of phototubes active, and a second analog sum of total charge in each 100 nsec digitization interval. The global trigger sums the signals from each crate and uses fast digital comparators to establish several energy thresholds.

Figure 2.39 shows a typical 40 MeV electron event generated by the Monte Carlo. Each hit photomultiplier tube is represented by a disk with diameter proportional to the number of photoelectrons. The time recorded by each phototube is indicated by the shading color. The detector cylinder has been unrolled to clearly show the phototube hit pattern. Note that the location of the Cerenkov ring can be seen by eye.

2.6.2 The Physics

LSND does two largely independent neutrino oscillation experiments with similar sensitivities that can be performed concurrently. Simply stated, one experiment looks for high-energy ν_e ($80 < E_\nu < 200$ MeV) produced by conversion of the ν_μ from the decay-in-flight component of the beam-dump neutrino beam. Simultaneously, another experiment looks for low-energy $\bar{\nu}_e$ produced by conversion of $\bar{\nu}_\mu$ ($40 < E_\nu < 53$ MeV) from the decay-at-rest component of the same beam. In each experiment the incident beam, the event signature, and the backgrounds are different. Consequently, with similar sensitivities as shown in Figure 2.40, the two experiments (plus the PSR experiment) provide important redundancy in addition to significantly wider coverage

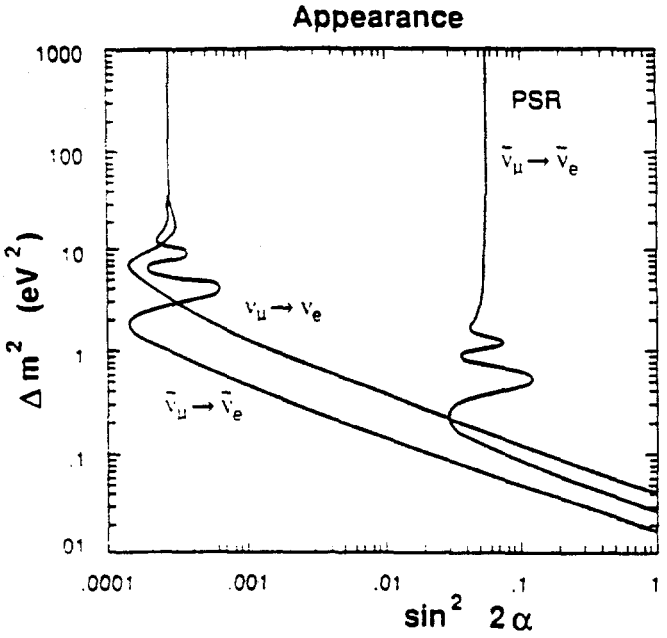

Figure 2.40: Limiting oscillation curve in the Δm^2 versus $\sin^2 2\theta$ parameter space for accelerator experiments.

of the $\Delta m^2 - \sin^2 2\theta$ space than all previous accelerator searches for $\nu_\mu \rightarrow \nu_e$ ($\bar{\nu}_\mu \rightarrow \bar{\nu}_e$) oscillations combined.

There are many other physics objectives that can be pursued with the liquid scintillator detector. Searching for $\bar{\nu}_\mu \rightarrow \bar{\nu}_e$ oscillations is equivalent to searching for the lepton number violating decay $\mu^+ \rightarrow e^+ \nu_\mu \bar{\nu}_e$. The $\nu C \rightarrow \nu C^*$ (15.11 MeV γ) neutral-current reaction, one of the only neutrino-nuclear neutral-current reactions that can be easily observed, will be measured to approximately 10% accuracy. The rare decays $\pi^o \rightarrow \nu\bar{\nu}$ and $\eta \rightarrow \nu\bar{\nu}$, followed by $\nu_e C \rightarrow e^- N$, can be searched to sensitivities of about 10^{-8} and 10^{-4}, respectively, with very little background because the neutrinos from these decays are extremely energetic. These decays are forbidden for massless Weyl neutrinos and can proceed only if neutrino states of both chiralities exist or if lepton number is not conserved. We shall also measure the $\nu_e C$ and $\nu_\mu C$ charged-current scattering cross sections and the νe elastic scattering cross section to approximately $10 - 15\%$ accuracy. These measurements would test present theories of neutrino-nucleus scattering and provide an estimate of $\sin^2\theta_W$.

Finally, we will obtain a large sample of neutrino-proton elastic-scattering events, where the neutrinos are from pion decay in flight. The cross section for $\nu p \rightarrow \nu p$ is proportional to $G_A^2 + F_1^2 + Q^2/4m_p^2 F_2^2$ at low Q^2. The term involving G_A is dominant, and a measurement of the cross section at low Q^2 affords a method of measuring G_A directly. The principal component of G_A is isovector, which is known from neutron decay at low Q^2. Any additional contribution (an isoscalar term, for example) would affect the total cross section. We expect to make a preliminary search for recoil protons from neutrino-proton elastic scattering in the 20 to 60 MeV range. These

protons will be coherent with the beam spill from LAMPF in contrast to proton recoil from cosmic-ray or beam neutrons. A preliminary estimate of this background gives a signal to noise as evidenced by the 200 MHz RF time structure of about 1.

2.6.3 Schedule

Construction of the LSND began in 1990, and completed in summer of 1993. Data acquisition with the LAMPF beam should began in July of 1993. UC Riverside is heavily involved in the data acquisition computing hardware and software, drawing heavily on the very successful OPAL data acquisition system.

G. VanDalen will devote a fraction of his research time to the LSND project. A grant from DOE Medium Energy Physics, now in its second year, partially supports the research students and the expenses associated with UCR participation in LSND for 1992-94. A post-doc was hired with university funds in February of 1993, and is now supported by the DOE Medium Energy grant. W. Strossman, who is supported by task A2, is working on a thesis based on the $\nu_\mu \rightarrow \nu_e$ oscillation search, while K. McIlhany will study νp elastic scattering.

2.7 Personnel and Budget Discussion

The OPAL experiment at LEP is the major project of our group, and our responsibilities include operation of the Hadron Calorimeter strip system, operation of the time-of-flight electronics, maintenance and development of online data acquisition, offline reconstruction software, Monte Carlo event simulation, and physics analysis.

In 1990 our group began participating actively on the RD5 experiment, since we felt this was the only way we could play a role in eventual hadron collider physics at a time when most of the group was stationed at CERN. RD5 is the main research and development vehicle for the Compact Muon Solenoid Collaboration, and our involvement has been in the area of muon detector development for the specific needs of CMS. We have taken an active role in the preparation of the CMS Letter of Intent, and are involved in the management structure of the Collaboration.

2.7.1 Personnel

The physicists participating in OPAL are J.W. Gary, P. Giacomelli, W. Gorn, C.C.H. Jui, J.G. Layter, P. Schenk, B.C. Shen, G.J. VanDalen, and G.W. Wilson. Paolo Giacomelli replaces Michael Dittmar who has taken a permanent position at ETH, Zurich. Paolo was previously a CERN Fellow on the DELPHI experiment at LEP. He has worked on the data acquisition software and participated in the search for the Higgs boson. Paul Schenk joined us at the end of 1992. He has recently completed his Ph.D. work at the University of Victoria on a measurement of b-asymmetry using OPAL data.

Four graduate students W.J. Larson, C. Ho, H. Oh, and B.P. O'Neill, completed their Ph.D. research since our group began working on the OPAL experiment. Among the current students, Edward Heflin will finish during this summer, and James Letts during the following academic year. Shun-Lung Chu has already made significant progress in his research project since he moved to CERN in the Fall of 1992. A second-year graduate student Charles Ju, who is in his second year at UCR, has recently joined our group and will participate in the OPAL experiment at CERN during 1994. A new student Leslie Weaver, currently supported by a University Fellowship, will begin her research on OPAL during 1995–96. We anticipate other new students joining our group as some of the more senior students receive their degrees and leave UCR.

William Gorn, John Layter and Benjamin Shen were responsible for setting up the reference muon chambers for the RD5 experiment in the North Area of the SPS, and they continue to take part in running the experiment. Graham Wilson joined the team and has participated in the data taking and analysis. John Layter was a member of the editorial board for the Letter of Intent and continues his involvement on the CMS "Management Board." He, William Gorn, and other American CMS collaborators are constructing prototype chambers for the CMS forward muon stations.

Paolo Giacomelli and James Letts are working on the Monte Carlo simulation of these chambers. The physicists participating in the CMS experiment are J.W. Gary, P. Giacomelli, W. Gorn, C.C.H. Jui, J.G. Layter, P. Schenk, B.C. Shen, G.J. VanDalen, and G.W. Wilson.

Our group also has a modest participation in the neutrino oscillation experiment LSND at LAMPF. Gordon VanDalen and graduate student William Strossman are involved in this effort.

2.7.2 Budget Discussion

The proposed budget of Task A2 for the 94-97 grant period is designed to maintain and continue the research activities at the current level. The research personnel is kept at the present level on the assumption that the increased level of hardware activity in RD-5 and CMS will be compensated by the decrease in our hardware commitment to OPAL. The budget for the two-year period between February 1, 1995 and January 31, 1997 includes the portion of the program of J.W. Gary which has been supported under his three-year Outstanding Junior Investigator grant for the three-year period ending January 31, 1995.

Our share of the common operations cost of OPAL is estimated at 73,000 SwF for 1994. This is equivalent to $48,500, at the exchange rate of 1.51 SwF to the dollar. In addition, we anticipate that, as the detector enters into its fifth year of operation, we will need to replace some of the detector components and associated electronics that our group built. We have estimated an amount of $11,500 for this purpose, and have included a total amount of $60,000 for both of these items under the heading "OPAL Operational Upgrades." The amounts requested for the subsequent years include nominal increases due to inflation.

Similarly, most of our general electronics equipment and workstations are getting old and obsolete after many years of operation. Some have even stopped working and cannot be repaired in a manner which is cost effective. We have included a request of funds for this under the item "Equipment Replacement." The $20,000 requested for 1994-95 will be used to replace a Tektronics digital scope and an Apple PC which are using in our detector design and testing work. The funds requested for the subsequent years will be used to replace other electronic equipment and workstations. Funds under the item "Fabrication of Particle Detector" are used to cover the cost of both the fabrication and maintenance of the detector, as well as detector research and development.

We have not requested funds within this budget for any equipment support associated with RD5 or CMS. A separate proposal will be submitted jointly by the US groups in CMS in the near future for the construction of the detector component that the US groups will be responsible for.

The personnel at the Ph.D. level for the 1994–97 contract period will remain basically at the same level as for the current period. Beginning in 1994 we will

need funds for two months of summer salary for Professor Shen since he will no longer receive summer salary from the University when he stops being Chairman of Physics. We also include one month of summer salary for Professor VanDalen, who has returned to the Physics Department from his administrative appointment as Associate Dean, assuming that one other month will be supported by a grant from DOE Medium Energy Physics for his participation in the LSND experiment. During the 1994–95 period the two-month summer salary of Professor Gary will be shared equally between Task A2 and his OJI grant. The summer salary support for Professor Gary for the subsequent years is included in our request. Approximately one-fourth the salary support for Adjunct Professor Layter will come from the University for his contribution to the instructional program of the Physics Department. During 1994-1995, Dr. Paul Schenk's salary will be supported jointly by Gary's OJI grant and our Task A2; in the subsequent two years support will be entirely by Task A2.

The 1993–94 contract year has been very difficult for us financially because of the increase in OPAL running costs and increased cost of living in working in the Geneva area. We would not have been able to manage if we did not receive generous support from the University. The University provided part of the summer salaries of VanDalen and Shen in consideration of their services respectively as Associate Dean and Chairman during the academic year. The University also provided some salary support for research personnel for our group. In the area of computing, the University provided computer hardware which makes up the HP UNIX cluster of workstations for the OPAL Monte Carlo work, as part of the startup support for Gary. It also provided one HP workstation for the analysis of RD5 data and for the design of the CMS detector through Monte Carlo simulation.

The budget requested for the 1994-97 grant period represents the very bare minimum. While there is practically no change in personnel, both at the Ph.D. level and in graduate students, our salary burden has increased because of the decreased support from the University. In addition, both Shen and VanDalen will not receive summer salary support from the University when they complete their terms of administrative services on June 30, 1993. The continuation of the program supported by Gary's OJI grant is incorporated in our Task beginning 1995.

Bibliography

[1] Lyndon Evans, *"Plans for LEP"* presented at the Europhysics Conference, Marseilles, July 23, 1993.

[2] CERN-PPE/93-48, submitted to Nucl. Instr. and Meth. in Phys. Res.

[3] Nucl. Instr. and Meth. in Phys. Res. **A323** (1992) 169-177.

[4] Nucl. Instr. and Meth. in Phys. Res. **A325** (1993) 271-293.

[5] Nucl. Instr. and Meth. in Phys. Res. **A325** (1993) 129-141.

[6] Comp. Phys. Comm., **67** (1992) 407-411.

[7] Nucl. Instr. and Meth. in Phys. Res. **A320** (1992) 183-200.

[8] Nucl. Instr. and Meth. in Phys. Res. **A324** (1993) 34.

[9] The LEP Collaborations; Phys. Lett. **B199** (1992) 224.

[10] *Parameters of the Z^0 Resonance from Combined Preliminary Data of the LEP Experiments*, The LEP Electroweak Working Group, informal note, August 1992.

[11] ALEPH Collaboration, D.Buskulic, *et al.*, *Update of Electroweak Parameters from Z decays*, CERN-PPE/93-40 (1993).
Update of Electroweak Parameters from Z decays. Preliminary. Contribution to the EPS Conference on HEP in Marseille, July 1993, and to the Lepton-Photon Conference in Cornell, August 1993., ALEPH Collaboration, ALEPH-note 93-123.

[12] DELPHI Collaboration, P. Aarnio, *et al.*, Nucl. Phys. **B367** (1991) 511.
DELPHI data on electroweak parameters for the Marseille and Cornell Conferences 1993, DELPHI Collaboration, DELPHI 93-101 PHYS 328.

[13] L3 Collaboration, O. Adriani, *et al.*, *Results from the L3 Experiment at LEP,* CERN-PPE/93-31 (1993).

Results on Electroweak Parameters from L3, L3 Collaboration, prepared for the EPS conference, Marseille, July 1993, L3 note 1444.

[14] OPAL Collaboration, G. Alexander, *et al.*, Z. Phys. **C52** (1991) 175.
OPAL Collaboration, P. Acton, *et al.*, Z. Phys. **C58** (1993) 219.
Precision Measurements of the Neutral Current from Hadron and Lepton Production at LEP. A Preliminary Update including the 1992 data, OPAL Physics Note PN-093, 5 March 1993.

[15] *The Energy Calibration of LEP in 1991*, L. Arnaudon, *et al.*, CERN-PPE/92-125 and CERN-SL/92-37(DI).
The Energy Calibration of LEP in 1992, L. Arnaudon, *et al.*, CERN SL/93-21 (DI), April 1993.
Measurement of the Mass of the Z^0 Boson and the Energy Calibration of LEP, LEP Energy Group, ALEPH, DELPHI, L3 and OPAL Collaborations, CERN-PPE/93-53 (16th March 1993), CERN-SL/93-17 (16th March 1993).

[16] ALEPH Collaboration, D.Buskulic, *et al.*, *Measurement of the τ Polarization at the Z Resonance*, CERN-PPE/93-39 (1993).

[17] DELPHI Collaboration, P. Abreu, *et al.*, Z. Phys. **C55**, 555, (1992).
Measurement of the 1992 tau-lepton cross-section and charge asymmetry, DELPHI Collaboration, DELPHI 93-103 PHYS 330.

[18] L3 Collaboration, O. Adriani, *et al.*, Results from the L3 Experiment at LEP, CERN-PPE/93-31 (1993).
An Updated Measurement of Tau Polarisation from L3, L3 Collaboration, L3 Note 1447, July 15, 1993.

[19] OPAL Collaboration, G. Alexander, *et al.*, Phys. Lett. **B266** (1991) 201.
Measurement of Branching ratios and τ Polarization from $\tau \to e\nu\overline{\nu}$, $\tau \to \mu\nu\overline{\nu}$ and $\tau \to \pi(K)\nu$, OPAL Physics Note PN-072, 24 July 1992.
An Update to the $\tau \to \rho\nu$ Analysis, OPAL Physics Note PN-073, 24 July 1992.
Measurement of the Forward-Backward τ Polarization Asymmetry from $\tau \to e\nu\overline{\nu}$, $\tau \to \mu\nu\overline{\nu}$ and $\tau \to \pi(K)\nu$ using the 1991 OPAL data, OPAL Physics Note PN-099, 29 March 1993.

[20] D. Decamp, *et al.*, (ALEPH Collab.), *Heavy Flavour Quark Production and Decay using Prompt Leptons in the Aleph detector*, Paper in preparation;
M. Pepe, Proceedings of La Thuile Conference, LNF - 93/019 ;
P. Perret, Proceedings of La Thuile Conference, PCCF RI/9313 ;
R. Tenchini, Proceedings of Moriond Conference, INFN PI/AE 93/14.

[21] DELPHI Collaboration, *Determination of $\Gamma_{b\overline{b}}$ and BR($b \to \ell$) using semi-leptonic decays*, DELPHI 93-74 PHYS 301.

[22] L3 Collaboration, *Measurement of* $R_{b\bar{b}}$ *and* Br(b $\rightarrow \ell\nu$X) *from b-quark Semileptonic Decays*, L3 Note 1449, July 1993, Contributed to the International Europhysics Conference, Marseille, July 22-28, 1993.

[23] OPAL Collaboration, CERN-PPE/93-46, to be published in Z. Phys. C;
OPAL Collaboration, *A Measurement of* $\Gamma_{b\bar{b}}/\Gamma_{had}$ *Using Single and Double Lepton events*, OPAL Physics Note PN091.

[24] D. Decamp, *et al.*, (ALEPH Collab.), *Measurement of the ratio* $\Gamma_{b\bar{b}}/\Gamma_{had}$ *using Event Shapes Variables*, CERN-PPE/93-113.

[25] DELPHI Collaboration, Phys. Lett. **B295** (1992) 383.

[26] L3 Collaboration, Phys. Lett. **B307** (1993) 237.

[27] D. Decamp, *et al.*, (ALEPH Collab.), *A Precise Measurement of* $\Gamma_{b\bar{b}}/\Gamma_{had}$, CERN-PPE/93-108.

[28] DELPHI Collaboration, *Direct measurement of the* $b\bar{b}$ *branching ratio at the* Z^0 *by hemisphere double tagging*, DELPHI 93-75 PHYS 302;
DELPHI Collaboration, *Measurement of* $\Gamma_{b\bar{b}}/\Gamma_{had}$ *using micro vertex and lepton double tags*, DELPHI 93-93 PHYS 320.

[29] OPAL Collaboration, CERN-PPE/93-79, Submitted to Z. Phys. C;
OPAL Collaboration, *An Updated Measurement of* $\Gamma_{b\bar{b}}/\Gamma_{had}$ *Using Double Lifetime Tagging*, OPAL Physics Note PN104.

[30] D. Brown, Presented at the 5th International Symposium on Heavy Flavour Physics, Montreal, July 1993.

[31] DELPHI Collaboration, Phys. Lett. **B295** (1992) 383;
DELPHI Collaboration, Phys. Lett. **B252** (1990) 140;
DELPHI Collaboration, CERN-PPE/93-70, submitted to Z. Phys. C.

[32] OPAL Collaboration, *Update of a Study of* D^* *Production in Z Decays*, OPAL Physics Note PN064.

[33] C. Matteuzzi, Presented at the International Europhysics Conference, Marseille, France, 22nd - 28th July 1993 ;

[34] D. Decamp, *et al.*, (ALEPH Collab.), $B\overline{B}$ *mixing and* $b\bar{b}$ *asymmetry from high* p_t *leptons (update)*, Contributed paper to the International Europhysics Conference, Marseille, France, 22nd - 28th July 1993 ;
D. Decamp, *et al.*, (ALEPH Collab.), *A Preliminary Measurement of* $\sin^2(\theta)^{eff}$ *from* $A_{FB}^{b\bar{b}}$ *in the 1992 lifetime tagged Heavy-Flavour sample*, Contributed paper to the International Europhysics Conference, Marseille, France, 22nd - 28th

July 1993 ;
D. Decamp, *et al.*, (ALEPH Collab.), *Production of Charmed Mesons in Z Decays*, Paper in preparation;
M. Pepe, Proceedings of La Thuile Conference, LNF - 93/019;
P. Perret, Proceedings of La Thuile Conference, PCCF RI/9313;
R. Tenchini, Proceedings of Moriond Conference, INFN PI/AE 93/14.

[35] DELPHI Collaboration, *Measurement of the forward-backward asymmetry of* $b\bar{b}$ *using prompt muons*, DELPHI 93-77 PHYS 304;
Inclusive measurement of the forward-backward asymmetry in $b\bar{b}$ *events at LEP*, DELPHI 93-78 PHYS 305;
Forward-backward asymmetry of $c\bar{c}$ *from* D^*, DELPHI 92-161 PHYS 247

[36] L3 Collaboration, *An Updated Measurement of* χ_B, $A_{FB}^{b\bar{b}}$ *and* $A_{FB}^{c\bar{c}}$, L3 Note 1448, July 1993, Contributed to the International Europhysics Conference, Marseille, July 22-28, 1993.

[37] OPAL Collaboration, CERN-PPE/93-78, To be published in Z. Phys. C;
OPAL Collaboration, *A Measurement of the Forward-Backward Asymmetry of* $c\bar{c}$ *and* $b\bar{b}$ *using* D^* *Mesons*, OPAL Physics Note PN103.

[38] D. Decamp, *et al.*, (ALEPH Collab.), Phys. Lett. **B259** (1991) 377.

[39] P. Abreu, *et al.*, (DELPHI Collab.), Phys. Lett. **B277** (1992) 371.

[40] P. D. Acton, *et al.*, (OPAL Collab.), Phys. Lett. **B294** (1992) 436.

[41] A. Blondel, *et al.*, (ALEPH Collab.), ALEPH-Note 93-041 PHYSIC 93-032 (1993);
ibid., ALEPH-Note 93-042 PHYSIC 93-034 (1993);
ibid., ALEPH-Note 93-044 PHYSIC 93-036 (1993).

[42] S.Bethke, Proceedings of the Linear Collider Workshop in Waikoloa/Hawaii, April 1993.
S. Catani, presented at the International Europhysics Conference, Marseille, France, 22nd - 28th July 1993.

[43] Electroweak libraries:
ZFITTER: D. Bardin, *et al.*, Z. Phys. **C44** (1989)493, Nucl. Phys. **B351**(1991)1, Phys. Lett. **B255** (1991)290 and CERN-TH 6443/92 (May 1992).
BHM: G. Burgers, W. Hollik and M. Martinez; M. Consoli, W. Hollik and F. Jegerlehner: Proceedings of the Workshop of Z physics at LEP, CERN Report 89-08 Vol.I,7 and G. Burgers, F. Jegerlehner, B. Kniehl and J. Kühn: the same proceedings, CERN Report 89-08 Vol.I,55
These computer codes have recently been upgraded by including the results of:

B. A. Kniehl and A. Sirlin DESY 92-102
S. Fanchiotti,B. A. Kniehl and A. Sirlin CERN-TH.6449/92
R. Barbieri, *et al.*, Phys. Lett. **B288** (1992)95
K. G. Chetyrkin, J. H. Kühn, Phys. Lett. **B248** (1990)359
K. G. Chetyrkin, J. H. Kühn and A. Kwiatkowski, Phys. Lett. **B282** (1992)221
J. Fleischer,O. V. Tarasov and F. Jegerlehner, Phys. Lett. **B293** (1992) 437.

[44] F. Abe, *et al.*, (CDF Collab.), Phys. Rev. **D43** (1991) 2070.

[45] J. Alitti, *et al.*, (UA2 Collab.), Phys. Lett. **B276** (1992) 354.

[46] H. Abramowicz, *et al.*, (CDHS Collab.), Phys. Rev. Lett. **57** (1986) 298 and A. Blondel, *et al.*, Z.Phys. **C45** (1990) 361.

[47] J.V. Allaby, *et al.*, (CHARM Collab.), Phys. Lett. **B177** (1986) 446, and Z. Phys.**C36** (1987) 611.

[48] M. Shaevitz (CCFR Collab.), Proceeding of the La Thuile '93 Conference.

[49] G. Alexander, *et al.*, (OPAL Collab.), Phys. Lett. **B265** (1991) 462.

[50] P. D. Acton, *et al.*, (OPAL Collab.), Z. Phys. **C58** (1993) 387.

[51] ALEPH Collab., private communication.

[52] S. J. Brodsky and J. Gunion, Phys. Rev. Lett. **37** (1976) 402.

[53] HRS Collab., Phys. Lett. **B165** (1985) 449.

[54] T. Sjöstrand, Comput. Phys. Commun. **39** (1986) 347;
T. Sjöstrand, CERN-TH.6488/92.

[55] B. R. Webber, *et al.*, Comput. Phys. Commun. **67** (1992) 465.

[56] R. Odorico, Comput. Phys. Commun. **59** (1990) 527.

[57] M. Z. Akrawy, *et al.*, (OPAL Collab.), Phys. Lett. **B261** (1991) 334.

[58] P. D. Acton, *et al.*, (OPAL Collab.), Phys. Lett. **B302** (1993) 523.

[59] P. D. Acton, *et al.*, (OPAL Collab.), Phys. Lett. **B305** (1993) 415.

[60] P. D. Acton, *et al.*, (OPAL Collab.),Phys. Lett. **B291** (1992) 503.

[61] C. D. Buchanan and S. B. Chun, UCLA-HEP-92-008.

[62] M. Bengtsson, and P. Zerwas, Phys. Lett. **B208** (1988) 306.

[63] O. Nachtmann and A. Reiter, Z. Phys. **C16** (1982) 306;
M. Bengtsson, Z. Phys. **C42** (1989) 75.

[64] P. Abreu, *et al.*, (DELPHI Collab.), Phys. Lett. **B255** (1991) 49;

[65] T. Sjöstrand, Comp. Phys. Comm. **39** (1986) 347 and CERN-TH.6488/92.

[66] L3 Collaboration, B. Adeva *et al*, Phys. Lett. **B259** (1991) 119.

[67] O. Adriani, *et al.*, (L3 Collab.), Phys. Lett. **B295** (1992) 337.

[68] S. Jadach and B.F.L. Ward, Phys. Lett. **B274** (1992) 470.

[69] O. Adriani, *et al.*, (L3 Collab.), CERN-PPE/93-31, submitted to Phys. Rep.

[70] M. Martinez and R. Miquel, CERN-PPE/92-211, submitted to Phys. Lett. **B** ;
K. Kolodziej, F. Jegerlehner and G.J van Oldenborgh, PSI Report No. PSI-PR-93-01 Jan. 1993;
J. Fujimoto, *et al.*, KEK Report No. P 92-195. Feb. 1993;
A. Ballestrero, E. Maina, and S. Moretti, Univ. of Turin Report No. DFTT 4/93, Feb. 1993.

[71] Y.-H. Chang, Proceedings of the XXVIIIth Rencontre de Moriond, March 1993. In preparation.

[72] K. Abe, *et al.*, (VENUS Collab.), Phys. Lett. **B302** (1993) 119;
K. Abe, *et al.*, (TOPAZ Collab.), KEK Report No. P 92-205. Feb. 1993;
K.L. Sterner, *et al.*, (AMY Collab.), Virginia Polytechnic Institute, Report No. VPI-IHEP-93-2.

[73] E. Ma and J. Okada, Phys. Rev. Letters **41** (1978) 287.

[74] M.Z. Akrawy, *et al.*, (OPAL Collab.), Z. Phys. **C50** (1991) 373-384.

[75] M.P. Cain, *et al.*, (PEP-9 Collab.), Phys. Lett. **B147** (1984) 232-6.

[76] Ch. Berger, *et al.*, (PLUTO Collab.), Z. Phys. **C27** (1985) 249.
W. Bartel, *et al.*, (JADE Collab.), Z. Phys. **C30** (1986) 545.
B. Adeva, *et al.*, (MARK-J Collab.), Phys. Rev. **D38** (1988) 2665.
H.-J. Behrend, *et al.*, Z. Phys. **C43** (1989) 1.

[77] V.M. Budnev, *et al.*, Phys. Rep. **15** (1975) 181.

[78] W.J.G. Langeveld, Ph.D. Thesis (unpublished), Rijksuniversiteit Utrecht (1985) 63-8.

[79] Y.H. Yo, *et al.*, (AMY Collab.), Phys. Lett. **B244** (1990) 573.

[80] J.A.M. Vermaseren, Nucl. Phys. **B229** (1983) 347.

[81] W.A. Bardeen and A.J. Buras, Phys. Rev. **D20** (1979) 166,
D.W. Duke and J.F. Owens, Phys. Rev **D22** (1980) 2280,
J.H. Field, F. Kapusta, and L. Poggioli, Phys. Lett **181B** (1986) 362,
J.H. Field, F. Kapusta, and L. Poggioli, Z. Phys. **C36** (1987) 121-9,
W.R. Frazer, Phys. Lett. **B194** (1987) 287.

[82] V. Blobel, CERN Report 85-09.

[83] H. Aihara, *et al.*, (TPC/2γ Collab.), Z. Phys. **C34** (1987) 1.

[84] H. Aihara, *et al.*, (TPC/2γ Collab.), Phys. Rev. Lett. **58** (1987) 97,
Ch. Berger, *et al.*, (PLUTO Collab.), Phys. Lett. **142** (1984) 111.

[85] T. Sasaki, *et al.*, (AMY Collab.), Phys. Lett. **B252** (1990) 491-8.

[86] F. Kapusta, Z. Phys. **C42** (1989) 225-9.

[87] LEP Design Report, CERN/LEP 84-01 (1984).

[88] See for example, Proceedings of the ECFA Workshop on LEP 200, CERN 87-08. Eds. A. Böhm and W. Hoogland.

[89] J. Bijnens, *et al.*, Proceedings of the ECFA Workshop on LEP 200, Vol. I, (1987) 49.

[90] Summarized by D. Treille, CERN-PPE 93-54, and in *Precision Tests of theStandard Electroweak Model,* Ed. P. Langacker, World Scientific, 1993.

[91] K. Hagiwara, R. Peccei, D. Zeppenfeld, and K. Hikasa, DESY86-058 (1986).

[92] A. Blondel, *et al.*, Proceedings of the ECFA Workshop on LEP 200, CERN 87-08. Vol. I (1987) 120.

[93] F. Olness and W.K. Tung, Phys. Letters **179** (1986) 269.

[94] P. Giacomelli, CERN-PPE/93-18, and Proceedings of the 2^{nd} Trieste Conference on Recent Developments in the Phonomenology of Particle Physics, Trieste, October 19–23, 1992.

[95] E. Gross and P. Yepes, Intl. Journal of Mod. Phys **A**, Vol. 8, No. 3 (1993) 407.

[96] P. Janot, LAL92-27, and in Proceedings of the 27^{th} Rencontres de Moriond (1992).

[97] See for example, Proceedings of the Large Hadron Collider Workshop, Aachen, 1990, Eds. G. Jarlskog and D. Rein, CERN 90-10.

[98] *"CMS The Compact Muon Solenoid,"* Letter of Intent, CERN/LHCC 92-3, LHCC/I1, October 1, 1992.

[99] C. Seez, *et al.*, Proceedings of the Large Hadron Collider Workshop, Aachen, 1990, Eds. G. Jarlskog and D. Rein, CERN 90-10, Vol II, 474.

[100] M. Della Negra, *et al.*, Proceedings of the Large Hadron Collider Workshop, Aachen, 1990, Eds. G. Jarlskog and D. Rein, CERN 90-10, Vol II, 509.

[101] M. Aalste, *et al.*, CERN-PPE/93-71.

[102] F.S. Merritt, *et al.*, Nucl. Instr. and Meth in Phys. Res. **A245** (1986) 27.
P.H. Sandler, *et al.*, Phys. Rev. **D42** (1990) 759.

[103] T. Dombeck, *et al.*, Phys. lett. **B194** (1987) 591.

[104] D. Koetke, *et al.*, submitted to Phys. Rev. C.

[105] D.D. Koetke, *et al.*, *"Muon-neutrino carbon charged current interaction near the muon threshold,"* Phys. Rev. C46 (1992) 2554–2566.

[106] *"A Proposal for a Precision Test of the Standard Model by Neutrino-Electron Scattering (Large Čerenkov Detector Project),"* LA-11300-P, UC-410, April 1988.

[107] *"Proposal for a Long Baseline Neutrino Experiment at the AGS,"* E889, January 26, 1993.

[108] CODA: CEBAF On-Line Data Acquisition, developed at the Continuous Electron Beam Accelerator Facility lab.

[109] *"Data Acquisition System for the Large Scintillating Neutrino Detector at Los Alamos,"* G. Anderson, *et al.*, LA-UR-92-315 to appear in the proceedings of the 1992 Conference on Computing in High Energy Physics, September 21-25, Annecy, France.

[110] *"Delayed Time Triggering and Data Acquisition,"*, V.Sandberg, A.Band, T.N.Thompson, Eighth Conference on Computing in High Energy Physics, Santa Fe, New Mexico, April 1990.

[111] X. Q. Lu, *et al.*, LSND Proposal, Los Alamos Meson Physics Facility, 1989.

Task B

Task B: Theory

a) Introduction

The High Energy Physics Theory Program at UC Riverside has continued to be active and productive in the past year. Since July 1992, there have been 14 completed research papers (UCRHEP-T100 to UCRHEP-T113). They are listed under **Publications** (Section c) together with 14 other papers which were listed in last year's report as yet to be published but are now published.

The Theory Group has consisted mainly of E. Ma (Professor), J. Wudka (Assistant Professor), H. Kikuchi (Postgraduate Researcher), T. V. Duong, J. Pérez de Muniain, and M. Roy (Graduate Student Research Assistants).

In Section b) the research activities of the Theory Group since July 1992 are discussed. In Section c) there is a list of completed or published papers since July 1992. In Section d) travel activities of the group are described and visitors to Riverside noted. In Section e) there is a list of personnel and there are statements concerning their needs. In Section f) the future research plans of Ma and Wudka are outlined.

b) Research Program

Since July 1992, **E. Ma** has completed 8 papers for publication. They are described briefly below.

In Papers 15 and 17, E. Ma shows that it is possible for the one-loop renormalization of the Higgs-boson mass to be finite in the standard model provided that $m_t^2 \simeq m_H^2 = (2M_W^2 + M_Z^2)/3$. This work was motivated by speculations in the recent literature [P. Osland and T. T. Wu, Phys. Lett. B291, 315 (1992); Z. Phys. C55, 569, 585, 593 (1992); A. Blumhofer and B. Stech, Phys. Lett. B293, 137 (1992); R. Decker and J. Pestieau, Mod. Phys. Lett. A4, 2733 (1989); 5, 2579(E) (1990)] on the desirability for certain renormalization factors to be set equal to zero, but these were all chosen rather arbitrarily. It is pointed out that if any choice is to be made, the most natural one is for m_H to be finite. However, that would imply $m_t \simeq 84$ GeV + higher-order radiative corrections, which may be already ruled out by the present CDF and D0 data that m_t is greater than about 100 GeV.

In Paper 18, E. Ma and D. Ng (TRIUMF, Vancouver, Canada) suggest that there is a good reason why the standard electroweak SU(2) × U(1) gauge model may be supplemented by two Higgs scalar doublets. They may be remnants of the spontaneous breaking of an

$SU(2) \times SU(2) \times U(1)$ gauge symmetry at a much higher energy scale. In one case, the two-doublet Higgs potential has a custodial SU(2) symmetry and implies an observable scalar triplet. In another, a light neutral scalar becomes possible because of a softly broken U(1) global symmetry.

In Paper 20, E. Ma points out an interesting possible relationship in the MSSM (Minimal Supersymmetric Standard Model.) By minimizing the minimum V_0 of the Higgs potential as a function of $\tan\beta \equiv v_2/v_1$, holding m_1^2, m_2^2, and $v_1^2 + v_2^2$ fixed, it is shown that $m_A = M_Z$ + radiative correction, where A is the one pseudoscalar boson of the theory. If one further plausible assumption is made, then $\tan\beta > \sqrt{3}$. This scenario follows if V_0 is indeed minimized by some underlying dynamics which can be represented by a certain combination of parameters of the effective theory.

In Paper 22, E. Ma and D. Ng show that the existence of supersymmetry and two Higgs doublets at the electroweak energy scale does not necessarily result in the MSSM. The reason is that under $SU(2) \times U(1)$, there can be no cubic invariant in the superpotential involving two Higgs doublets, but if the gauge symmetry is enlarged, such a coupling can exist. At the electroweak energy scale, there may be only two Higgs doublets, but their self-couplings will not be those of the MSSM. It is shown in this paper that for a particularly interesting $SU(2)_L \times SU(2)_R \times U(1)$ model, first considered as coming from an E_6 superstring model [E. Ma, Phys. Rev. D36, 274 (1987)], a very different mass spectrum is obtained for the Higgs bosons. Instead of the MSSM conditions

$$\lambda_1 = \lambda_2 = \frac{1}{4}(g_1^2 + g_2^2), \quad \lambda_3 = -\frac{1}{4}g_1^2 + \frac{1}{4}g_2^2, \quad \lambda_4 = -\frac{1}{2}g_2^2, \quad \lambda_5 = 0,$$

the following now hold for the respective quartic scalar couplings:

$$\begin{aligned}
\lambda_1 &= \frac{1}{4}\left(1 + \frac{4f^2}{g_2^2}\right)\left[g_1^2 + g_2^2 - 4f^2\left(1 - \frac{g_1^2}{g_2^2}\right)\right], \\
\lambda_2 &= \frac{1}{2}g_2^2 + \frac{1}{4}(g_1^2 - g_2^2)\left(1 - \frac{4f^2}{g_2^2}\right)^2, \\
\lambda_3 &= \frac{1}{4}g_2^2 - \frac{1}{4}\left(1 - \frac{4f^2}{g_2^2}\right)\left[g_1^2 - 4f^2\left(1 - \frac{g_1^2}{g_2^2}\right)\right], \\
\lambda_4 &= -\frac{1}{2}g_2^2 + f^2, \quad \lambda_5 = 0,
\end{aligned}$$

where f is the new cubic coupling in the superpotential. This demonstrated nonuniqueness of the MSSM has very important phenomenological implications because an enormous amount of numerical work has gone into the Higgs sector of the MSSM. One should bear in mind

that in the event of finding two Higgs doublets in the future, even if supersymmetry exists, the MSSM is not the only possibility. This work was also summarized in Paper 27.

In Paper 26, T. V. Duong (Graduate Student Research Assistant) and E. Ma work out a supersymmetric extension of the recently proposed SU(3) $\times$ U(1) [F. Pisano and V. Pleitez, Phys. Rev. D46, 410 (1992); P. Frampton, Phys. Rev. Lett. 69, 2889 (1992)] and show that it is possible to have only two Higgs doublets at the SU(2) $\times$ U(1) energy scale but they are not those of the MSSM or the abovementioned left-right model. It is shown in particular that the upper bound on the lightest scalar boson of this model is $4M_Z \sin\theta_W$ at tree level and goes up to about 189 GeV after radiative corrections. Another example of the nonuniqueness of the MSSM is thus provided.

Finally, E. Ma participated in Paper 24 on CP violation in a model of leptogenesis together with H. Kikuchi and two visitors (A. Acker and U. Sarkar.) This will be described later by Kikuchi.

In the past year **J. Wudka** has been interested in several aspects of theoretical physics which will be summarized below.

Effective lagrangians. There has been a resurgence of interest in effective lagrangians in the area of electroweak physics. The new input is based on the realization that the methods deviced for the strong interactions can be applied directly for the electroweak case as well; similar results can also be obtained for the case where the underlying physics is weakly coupled. Advantages of this approach are: *i*) that all the symmetries of the model are automatically respected; and *ii*) only a minimal set of assumptions regarding the underlying physics (such as its being strongly or weakly coupled) is required.

By its very nature this method cannot give quantitative predictions, but can certainly provide reliable estimates of the contributions from new physics to various processes, and can therefore determine the sensitivity of a given experiment to the scale of the physics underlying the standard model. Perhaps more importantly, the approach will clarify a large number of misconceptions regarding the sensitivity of future and present experiments to physics beyond the standard model. These results are based on a mis-interpretation of the divergences in loop calculations (leading to erroneous conclusions regarding the sensitivity of high precision measurements to the scale of new physics); or to untenable assumptions regarding the coefficients of the effective lagrangian. In fact these coefficients are often taken to be 10^4 times larger than expected, and would lead to strong interactions amongst the standard model particles in the electroweak sector.

The philosophy of this approach was originally spelled out in the talks by H. Georgi and J. Wudka in the Topical conference on Precise Electroweak Measurements, Santa Barbara, California, Feb. 21-23, 1991 (unpublished); by M.B. Einhorn and J. Wudka in [Paper 3] and [Yale Workshop on future Colliders, Yale University, Oct. 2-3, 1992]; and by J. Wudka in [Annual Meeting of the SSC Fellows, SSC Laboratory, Nov. 19-21, 1992], [V Mexican School of Particles and Fields, Guanajuato, México, Dec. 1992], [Aspen Winter Conference, Jan. 1993] and [Paper 23]. The results of these investigations are varied and important. The main issue is that most colliders will be far less sensitive radiative effects induced by new physics than previously claimed. In fact, most precision experiments claiming to probe the "compositeness scale" will give weaker constraints than those obtained, for example, from direct production cross section restrictions at LEP and Fermilab. The positive side of these results is that new physics can be right around the corner and still our present sensitivity be too small to detect it [Paper 28].

The effective lagrangians are, contrary to standard lore, renormalizable: all divergences can be absorbed in the coefficients of the effective operators. It follows that all divergences are unobservable and no physical consequences can be derived from them (a fact regularly ignored in the literature). The power divergences are important when considering the naturalness of a given theory, but this is a separate issue from renormalizability. The renormalizability of electroweak effective lagrangians was studied by J. Wudka in a collaboration with C. Arzt and M. Einhorn [Paper 14] where the effective operator contributions to the anomalous magnetic moment of the muon were calculated. This quantity will soon be measured very precisely at the Brookhaven experiment AGS821. It is concluded that this experiment will be sensitive to new physics up to a scale of $\sim$ 700 GeV. This limit is based solely on the anomalous magnetic moment of the muon induced by new physics and has *nothing* to do with the electromagnetic structure of the W, since these contributions to $g-2$ stemming from possible anomalous moments of the vector bosons are at best marginally observable.

Radiative corrections and oblique parameters. In a collaboration with M. Einhorn, J. Wudka studied the effects of heavy scalars on the ρ parameter. This problem was first studied by Veltman [Acta Phys. Pol. **B8**, 475 (1977)] in the context of the Standard Model where he discovered that when the Higgs is very heavy the W and Z masses depend only logarithmically its mass (to one loop); this phenomenon is known as "screening". This result was further investigated by Einhorn and Wudka in [Phys. Rev. **D39**, 2758 (1989)] where it was demonstrated that it was no accident, but a direct consequence of the custodial symmetry and the renormalizability of the model. In [Paper 13] the conditions for screening in a general gauge theory are derived (assuming no fine tuning). It is found that the presence

or absence of screening can be determined by a simple counting procedure: if the number of available wave function renormalizations in the Goldstone-boson sector is larger or equal than the number of quadratic invariants that can be formed using the Goldsonte fields, then screening is present. This result was verified in several known examples by explicit calculation; it is also shown that a natural left-right model cannot accommodate known data without the presence of light scalars (with masses of the same order as that of the right-handed W and Z). A side benefit of these investigations was the development of a new gauge fixing condition which preserves both the qualities of the R_ξ and background field gauges.

In collaboration with M. Velkovsky, a former student at UCR, J. Wudka studied a large N extension of the standard model [Paper 2] where N corresponds to the dimension of the scalar multiplet (the gauge group is still $SU(2)_L \times U(1)$). The Higgs propagator was obtained to leading order in $1/N$, and it was shown that, for large scalar self couplings the scale of the physical mass of the Higgs is determined by the vacuum expectation value; these results agree with those obtained using simpler models. We also calculated the leading contributions to the S, T and U parameters; we found that T vanishes while that S and U are non-zero and uncorrelated. Finally we showed that scalar exchange will generate a strong attractive force which will pair-up scalars of opposite charge into almost neutral composites.

Strong CP problem. H. Kikuchi, J. Wudka have an ongoing investigation into the physics of the strong CP problem. The motivation for this investigation is based on the old controversy between the Crewther and t'Hooft point of view on the problem. The first results [Paper 6] back t'Hooft's and clarified the origin of the non-perturbative contribution to the η' mass as an effect produced by the screening of a gas of interacting instantons: the bare η' mass is dressed by instanton effects (in the same way as the electron mass is dressed by phonons) resulting in $m_{\eta'} \gg m_\pi$; and we related this shift to the interacting instanton density.

In [Paper 16] a Lorentz covariant sum rule for the correlator $\langle T\nu(x)\nu\rangle$ (where ν is the instanton number density) is derived. This correlator is used to determine the θ dependence of the vacuum energy in QCD and the expressions obtained resolve an apparent violation of Lorentz invariance by providing explicit expressions for certain contact terms in terms of various vacuum condensates. These results are consistent with the value for $m_{\eta'}$ obtained from the Cheshire-Cat bag picture.

Other aspects of this investigation are described by H. Kikuchi below.

Cosmological neutrinos. J. Wudka has studied the propagation of neutrinos in the pres-

ence of strong gravitational fields, such as those generated by massive black holes of $\sim 10^8 M_\odot$; these objects are believed to be the power sources of active galactic nuclei (AGN). The possible situations under which neutrinos can undergo resonant transitions generated by these strong gravitational fields are derived [Mod. Phys. Lett. A6, 3291 (1991),Paper 4.]. The results are of relevance for experiments such as DUMAND which purport to determine the neutrino flux from AGN. The results depend not only on the neutrino mass spectrum, but also on their magnetic moments as it is expected that the AGN environment will contain large magnetic fields.

Since July 1992, **Hisashi Kikuchi** has completed four papers for publication. They are described below.

The strong CP problem is one of the most puzzling issues in the well-established standard model. The problem can be understood in two steps: first, the chiral phase of the quark mass matrix (the argument of the determinant of the mass matrix) contributes to the vacuum angle θ, which characterizes the vacuum state of QCD under the influence of instanton effects; second, physical predictions are believed to depend nontrivially on θ and they are expected to violate CP invariance for nonzero θ. No experimental evidence of CP violation in the strong interaction looks unnatural once one recognizes that there is no symmetry principle to restrict the mass matrix to zero chiral phase.

The theoretical calculations which deduce the above two steps require highly nonperturbative techniques and are not necessarily clear so far. Kikuchi's standing point to the strong CP problem is to refine these nonperturbative techniques and to make the problem clearer.

The Papers 16 and 19 are dedicated to the second point.

The two-point function of the pseudoscalar gluon density, $F_{\mu\nu}\tilde{F}^{\mu\nu}$, is the most commonly used quantity to study the θ-dependence of physical observables. Its zero momentum limit reflects the θ-dependence of vacuum energy density. The Lagrangian path integral can be used to evaluate this quantity directly, taking into account instanton effects. In a previous work with J. Wudka (Phys. Lett. B248 (1992) 111, Paper 6), H. Kikuchi evaluated it by the path integral paying a special attention to instanton interactions. The result gives a clear insight for the U(1) problem. On the other hand, to connect this two-point function to the θ-dependence of the vacuum energy density, one has to evaluate it using the Hamiltonian canonical quantization; for this, the most useful gauge for maintaining all the concepts of instanton effects is the temporal gauge, which is, however, not Lorentz covariant and is difficult to connect the Lorentz covariant result in the path integral.

In the collaboration with J. Wudka (Paper 16), H. Kikuchi figured out the exact corre-

spondence between these two different quantization languages. This correspondence enables one to pick up all the contact terms in the two-point function, which was not specified in the literature, and to get a better insight over the problem by means of the Lorentz covariance.

H. Kikuchi further pursued the Lorentz covariance, or more generally the Poincare covariance of the temporal gauge canonical quantization (Paper 19). He examined the algebra of energy momentum vector and angular momentum tensor to verify the Poincare invariance of the noncovariant quantization scheme. He also showed that the Gauss law constraint is insufficient to calculate the θ-dependence, and argued that the explicit construction of large gauge transformations is indispensable in order to restrict the physical space, and to evaluate the θ-dependence of the vacuum.

The way to examine the first step, contributions of the chiral phase to the vacuum angle, is to investigate the chiral phase dependence of the free energy of fermions in a given background gauge field. The well-cited result is that the free energy density contains the CP violating term $F_{\mu\nu}\tilde{F}^{\mu\nu}$ with the chiral phase as the coefficient.

In a previous work (Phys. Rev. D46 (1992) 4704, Paper 9), H. Kikuchi verified this result by explicitly calculating the free energy by the path integral. The functional space for the path integral is defined by providing eigenstates of the Dirac operator. An asymmetry of the zero eigenstates between different chiralities was identified as the source of the CP violation. In the calculation, it was assumed that there is an one-to-one correspondence between nonzero eigenstates for different chiralities. Although this correspondence is based on a symmetry of the Dirac operator, it is known to be violated for some Dirac operators in certain background configurations, e.g., for fermion in the monopole background in three dimensions. If it were true also for four dimensional fermions, there may be extra CP violating terms in the free energy.

H. Kikuchi examined this point carefully (Paper 25). He used a two dimensional fermion as an example, since it has the similar chiral anomaly to the four dimensional one. Applying two dimensional scattering theory, he verified the one-to-one correspondence is still exact and the well-cited result is correct.

One interesting possibility to incorporate the inflation and the baryon number asymmetry of our universe was proposed recently by H. Murayama.et.al (Phys. Rev. Lett. 70 (1993) 1912). An essential ingredient in their scenario is CP violation in the decay of the inflaton which is identified with the superpartner of the electron-type heavy gauge-singlet neutrino. Once this CP violating process generates an asymmetry in the lepton number, it will be converted to the baryon number asymmetry through electroweak anomalous processes.

In a collaboration with A. Acker, E. Ma and U. Sarkar, H. Kikuchi investigated the problem of CP violation in the inflaton decay (Paper 24); in particular, they counted the number of the independent CP violating phases in the above mentioned decay process.

c) Publications

The following list contains work published or completed by the Riverside Theory Group since July 1992.

1. UCRHEP-T84: "Dirac Neutrinos in Dense Matter," J. Pantaleone, Phys. Rev. D46, 510 (1992).

2. UCRHEP-T87: "A Large N Standard Model," M. Velkovsky and J. Wudka, Nucl. Phys. B (1993).

3. UCRHEP-T88: "Effective Lagrangian Description of Precision Measurements or How to Parametrize Ignorance," M. B. Einhorn and J. Wudka, in Proc. of Workshop on Electroweak Symmetry Breaking, Hiroshima, Japan, November (1991).

4. UCRHEP-T89: "Neutrinos in the Mist", J. Wudka, in Proc. of the Workshop of High Energy Neutrino Astrophysics, Univ. of Hawaii, Manoa, March 23–26, 1992, ed. by V. J. Stenger et al. (World Scientific, Singapore, 1992), p.17.

5. UCRHEP-T90: "Generation Nonuniversality and Precision Electroweak Measurements," X. Li and E. Ma, Phys. Rev. D46, R1905 (1992).

6. UCRHEP-T91: "Screening in the QCD Instanton Gas and the U(1) Problem," H. Kikuchi and J. Wudka, Phys. Lett. B284, 111 (1992).

7. UCRHEP-T92: "Longer Tau Lifetime and Negative T," E. Ma, in Proc. of XXVII Rencontres de Moriond: Electroweak Interactions, Les Arcs, France, March (1992), ed. by J. Tran Thanh Van (Editions Frontieres, Gif-sur-Yvette, France, 1992) p.475.

8. UCRHEP-T93: "Accidental Approximate Generation Universality and its Possible Verification," E. Ma, in Proc. of Beyond the Standard Model III, Ottawa, Canada, June (1992), ed. by S. Godfrey and P. Kalyniak (World Scientific, Singapore, 1993), p.485.

9. UCRHEP-T94: "Chiral Phase Dependence of the Massive Fermionic Path Integral," H. Kikuchi, Phys. Rev. D46, 4704 (1992).

10. UCRHEP-T95: "Fixing the Top-Quark and Higgs-Boson Masses," E. Ma, Mod. Phys. Lett. A7, 2741 (1992).

11. UCRHEP-T96: "Decay of the Z Boson into Scalar Particles," T. V. Duong and E.

Ma, Phys. Rev. D47, 2020 (1993).

12. UCRHEP-T97: "Gauge Model of Generation Nonuniversality Reexamined," X. Li and E. Ma, J. Phys. G (1993).

13. UCRHEP-T98: "Screening of Heavy Scalars beyond the Standard Model," M.B. Einhorn and J. Wudka, Phys. Rev. D47, 5029 (1993).

14. UCRHEP-T99: "Effective Lagrangian approach to precision measurements: the anomalous magnetic moment of the muon," C. Arzt, M. B. Einhorn, and J. Wudka, submitted to Phys. Rev. D.

15. UCRHEP-T100: "Possible Finiteness of the Higgs-Boson Mass Renormalization," E. Ma, Phys. Rev. D47, 2143 (1993).

16. UCRHEP-T101: "A Lorentz Invariant Sum Rule for the Theta Dependence in QCD," H. Kikuchi and J. Wudka, submitted to Phys. Rev. D.

17. UCRHEP-T102: "Hints Within the Standard Model on the Top-Quark and Higgs-Boson Masses," The Fermilab Meeting, ed. by C. H. Albright et al. (World Scientific, Singapore, 1993), p.474.

18. UCRHEP-T103: "Symmetry Remnants: Rationale for Having Two Higgs Doublets," E. Ma and D. Ng, submitted to Phys. Rev. D.

19. UCRHEP-T104: "Poincare Invariance in Temporal Gauge Canonical Quantization and Theta Vacua," H. Kikuchi, submitted to Int. J. Mod. Phys. A.

20. UCRHEP-T105: "Derivation of $m_A \simeq M_Z$ and $\tan\beta > \sqrt{3}$ in the Minimal Supersymmetric Standard Model," E. Ma, submitted to Phys. Rev. D.

21. UCRHEP-T106: "Statistical Origin of Classical Mechanics and Quantum Mechanics," S.-Y. Chu.

22. UCRHEP-T107: "New Supersymmetric Option for Two Higgs Doublets," E. Ma and D. Ng, submitted to Phys. Rev. Lett.

23. UCRHEP-T108: "Effective Lagrangian and Triple Boson Coupling," J. Wudka, to appear in the proceedings on "Electroweak Interactions and Unified Theories", *XXVIII* Recontres de Moriond, Les Arcs, Savoie, France, March 13-20, 1993.

24. UCRHEP-T109: "CP Violation and Leptogenesis," A. Acker, H. Kikuchi, E. Ma, and U. Sarkar, submitted to Phys. Rev. D.

25. UCRHEP-T110: "Chiral Phase Dependence of Fermion Partition Function in Two

Dimensions," H. Kikuchi, submitted to Nucl. Phys. B.

26. UCRHEP-T111: "Supersymmetric SU(3) $\times$ U(1) Gauge Model: Higgs Structure at the Electroweak Energy Scale," T. V. Duong and E. Ma, submitted to Phys. Lett. B.

27. UCRHEP-T112: "New Supersymmetric Two-Higgs-Doublet Structure at the Electroweak Energy Scale," E. Ma, to appear in Proc. of "New Directions in the Application of Symmetry Principles to Elementary Particle Theory."

28. UCRHEP-T113: "Anomalous neutrino reactions at HERA", J. Wudka, submitted to Phys. Rev. D.

d) Travel and Consultants

E. Ma attended the Second Trieste (Italy) Conference on Recent Developments in the Phenomenology of Particle Physics in October 1992 and gave a talk. In November 1992, he attended the APS-DPF Meeting at Fermilab, Batavia, Illinois and gave a talk. In March 1993, he gave a review talk on "Electroweak Extensions at the TeV Energy Scale" at the SSC Symposium in Madison, Wisconsin. In May 1993, he talked about his new work on supersymmetry and two Higgs doublets at the electroweak energy scale at a special Montreal-Rochester-Syracuse-Toronto Meeting in Syracuse, New York. Finally in June 1993, he attended the Workshop on B Physics at Hadron Accelerators in Snowmass Village, Colorado.

J. Wudka participated in the 1992 Aspen Summer Institute. He presented a talk at the Annual Meeting of the SSC Fellows, SSC Laboratory, Nov. 19-21, 1992, and at the *V* Mexican School of Particles and Fields, Guanajuato, México, Dec. 1992. He attended the conference on "Electroweak Symmetry Breaking at Colliding-Beam Facilities, Univ. of California, Santa Cruz, Dec. 11-12 1992. He gave a talk at the Aspen Winter Physics Conference, Jan. 1993 He presented a talk at the conference on "Electroweak Interactions and Unified Theories", Moriond 1993. Finally, in June 1993, he participated in the 1993 Aspen summer institute. All the above talks were on the subject of electroweak effective lagrangians.

Visitors who gave high-energy theory seminars/colloquia include M. Pérez (CINVESTAV-IPN, Mexico), D. Choudhury (TIFR, Bombay), M. G. Olsson (Wisconsin), S. Pakvasa (Hawaii), G. Bhattarcharyya (Calcutta), L. Orr (UC Davis), M. Dine (UC Santa Cruz), R. C. Hwa (Oregon), V. Khoze (Durham, UK & St. Petersburg, Russia), D. Ng (TRIUMF, Canada), U. Sarkar (Ahmedabad, India), A. Acker (Hawaii), U. Baur (Florida State), Y. S. Tsai (SLAC), and B. Haeri (Purdue). Two visitors (A. Acker and U. Sarkar) spent 2 months

and 1 month respectively at Riverside collaborating on research with H. Kikuchi and E. Ma. M.A. Pérez (CINVESTAV-IPN, México) visited UCR for one week and collaborated with J. Wudka on a forthcoming paper.

e) Personnel and Needs

Two faculty members are covered by this proposal: E. Ma (Professor) and J. Wudka (Assistant Professor), for whom 2 months of summer salary are requested. H. Kikuchi will continue to be Postgraduate Researcher (100%). Graduate Research Assistants will be T. V. Duong, J. Pérez de Muniain, and M. Roy.

Two foreign trips are planned, at about $3,000 each, to conferences such as Neutrino '94 in Israel and the International Conference on High Energy Physics in Scotland. Four domestic trips are planned, at about $1,500 each, to conferences such as APS meetings and various other workshops and summer institutes yet to be announced. About $2,000 is requested for visitors. A total of $7,000 is needed for supplies and expenses.

f) Future Research Plans

E. Ma plans to continue his work on the possible supersymmetric two-Higgs-doublet structures based on extended gauge models he initiated in Papers 22 and 26. The key observation is that if two Higgs doublets are found at the 100 GeV energy scale but they are not those of the Minimal Supersymmetric Standard Model (MSSM), it does not necessarily mean that there is no supersymmetry. There may well be supersymmetry but the electroweak $SU(2) \times U(1)$ gauge group is enlarged, so that although the reduced Higgs potential has only two doublets, their interactions are not those of the MSSM. This means that the mass spectrum of the 5 physical Higgs bosons, $H^\pm, H^0, h$, and A, can be very different. In particular, the upper bound on the lighter of the two scalar bosons H^0 and h, which is by definition h, is changed from 115 GeV in the MSSM to 120 GeV in the E_6-inspired left-right model and to 189 GeV in the new $SU(3) \times U(1)$ model. A very large body of phenomenology now exists for the study of two Higgs doublets in the MSSM. With the realization that supersymmetry by itself does not uniquely determine the two-Higgs-doublet structure, we should generalize previous studies first to the two specific models we have discussed and then to other possible models as well. We need to ascertain whether future experimental capabilities at higher energies will be able to test for the existence of supersymmetry in all these different guises.

E. Ma and D. Ng are in the process of analyzing phenomenologically the two-Higgs-doublet structure of the supersymmetric E_6-inspired left-right model. This model was first

proposed by E. Ma (Phys. Rev. D36, 274 (1987)) and is very interesting on its own right. Recall that the conventional left-right model has an unavoidable problem with flavor-changing neutral currents in the scalar sector. This means that except for the one neutral Higgs boson corresponding to that of the standard model, all the other Higgs bosons have to be much heavier than, say, a few TeV. As a result, although there can be in principle two Higgs doublets at the electroweak energy scale, our present knowledge of weak-interaction phenomenology already forbids them. In contrast, in this alternative left-right model, because the right-handed quark doublet is $(u,h)_R$ where h is a new quark, instead of the conventional $(u,d)_R$, only one scalar field contributes to the mass of a given type of quark. The Glashow-Weinberg theorem is satisfied and the suppression of flavor-changing neutral currents is ensured. This allows us to consider two Higgs doublets at the electroweak energy scale whose interactions are different from those of the MSSM. The goal of this work is to compare the details of the MSSM in all accessible experimental tests against the proposed new scenario.

E. Ma and T. V. Duong will continue their work on Paper 26 which proposed a supersymmetric version of the new SU(3) $\times$ U(1) model. In addition to imposing supersymmetry, a new mechanism of mass generation for leptons was proposed and will be investigated in detail. Since both the charged lepton and its charge conjugate appear together as members of an antitriplet under SU(3), a Higgs sextet was considered by other authors as the means of giving mass to the electron, etc. A simpler alternative is not to have a Higgs sextet at all, but to introduce a heavy singlet charged lepton and use the existing Higgs triplets to connect it to the usual charged leptons in a see-saw manner. Three such singlets can be used to obtain see-saw masses for the three charged leptons, in analogy to what is often proposed for the neutrinos. However, it may also be possible to have only one such singlet in which case only the tau gets a see-saw mass whereas the muon and electron will obtain radiative masses. Such a mechanism in the neutrino sector has been discussed by K. S. Babu and E. Ma (Phys. Rev. Lett. 61, 674 (1988)).

Because of supersymmetry, instead of only three Higgs triplets, there must also be three antitriplets to cancel the anomalies generated by the superfields. They are also needed for the Yukawa couplings to the quarks which result in masses as the neutral scalar fields acquire vacuum expectation values. This means that four Higgs doublets can appear at the electroweak energy scale. The details of this scenario will be investigated. (In Paper 26, it is assumed that a radiative mechanism can be used for the light quark masses so that only two Higgs doublets are present at the electroweak energy scale. Details of this alternative will be investigated further.) There are of course also a lot of phenomenology to be worked

out here. This entire project will be the substance of Duong's Ph.D. dissertation.

Suppose the fundamental theory of particle interactions is a supersymmetric gauge theory at some very high energy scale. As we come down in energy, the gauge symmetry may be broken down to a smaller group or the supersymmetry may be broken, but they need not be at the same scale. The MSSM is based on the specific assumption that the gauge symmetry is broken down to SU(2) $\times$ U(1) at some high scale but the supersymmetry is not broken. Then at a few TeV the supersymmetry is broken and at 100 GeV, SU(2) $\times$ U(1) is also broken. However, we can also envision that the fundamental gauge symmetry is broken down to something larger than SU(2) $\times$ U(1) at some high scale. Then at a few TeV the supersymmetry is broken as well as this intermediate gauge group down to SU(2) $\times$ U(1). This alternative will then lead to possible two-Higgs-doublet structures different from that of the MSSM.

A different project that E. Ma is thinking of has to do with rare decays of B mesons and possible observable CP-violating asymmetries. A lot of theoretical and phenomenological work has gone into the identification of suitable decay modes. The new idea here is to consider radiative decays. In particular, the decay $B_s \to J/\psi\gamma$ is an unambiguous indication of an exchange diagram (as opposed to the usual spectator diagram) and can have a CP asymmetry as a function of time through $B_s - \overline{B}_s$ mixing. The rate is undoubtedly small but some detailed work is needed to ascertain its feasibility. This is under discussion with J. Soares who will be at TRIUMF beginning in September, 1993.

In the near future **J. Wudka** will pursue several research projects which are summarized below.

Effective lagrangians In a collaboration with M.A. Pérez and J. Toscano, J. Wudka is in the process of completing an investigation into the effects of new physics in the two scalar doublet extension of the standard model. In particular the coupling of CP odd scalar excitation A to two photons is studied in detail as a probe for new physics in future colliders. Partial results of this calculations have been reported in [V Mexican School of Particles and Fields, Guanajuato, México, Dec. 1992], [Aspen Winter Conference, Jan. 1993] and [Paper 23] where it is shown that for large $\tan\beta$ (which is the ratio of the vacuum expectation values of the scalar fields) this coupling is dominated by the new physics contributions. This vertex can also be probed in photon colliders where the availability of polarization can be used to suppress the standard contributions in A production, and to enhance possible anomalous effects. The results of this project are currently being written-up.

J. Wudka will also participate in a collaboration with M. Einhorn and C. Arzt whose purpose will be the determination of the quantitative estimates of new physics effects using effective operators. It is known that effective operators are often suppressed by "loop factors" of order $1/16\pi^2$ (multiplied by the number of particles in the loop). This investigation will determine which operators do not suffer this suppression and are therefore better suited for observation. Several issues regarding the use of the equations of motion and the presence of "blind directions" will be discussed.

In the next few months J. Wudka will finish a review paper on the subject of electroweak effective lagrangians for the Int. Journal of Modern Physics. This material will also be presented in a series of invited lectures to be given at the *IV Workshop on Particles and Fields* of the Mexican Physical Society to be held in Mérida, Yucatán, México Oct. 25-29, 1993.

Oblique parameters. In another study of radiative corrections J. Wudka has evaluated the general form of the gauge boson vacuum polarization tensor in a general spontaneously broken gauge theory without fermions. The aim is to determine the contributions from a set of heavy gauge bosons to the S, T and U oblique parameters. The effects are bound to be less dramatic than the ones obtained from a set of heavy scalars since, by decoupling arguments, there can be no power mass dependence of S, T and U on the masses of the heavy bosons. This calculation is currently being completed.

Strong CP problem. J. Wudka, in collaboration with H. Kikuchi and J. Pérez de Muniain (the latter a student at UCR) will study the effects of anomalous commutators in the evaluation of various sum rules related to CP violation in QCD. This has more than academic interest, for example, Crewther has criticised t'Hooft's solution of the $U(1)_A$ problem on the basis that the commutators obtained using the effective six-quark lagrangian derived by 't Hooft differ from those derived using QCD. These commutators are, however, ill defined and require careful consideration; in this investigation the BJL limit will be used.

Cosmological neutrinos. J. Wudka will extend his previous results to the most general case where the neutrinos can be either Dirac or Majorana. The oscillation effects will be calculated with a reasonable model of the AGN's matter density and magnetic field profiles.

Tree level unitarity. In a previous collaboration with H. Haber and J. Gunion [Phys. Rev. **D43**, 904 (1991)] J. Wudka re-examined the implications of tree level unitarity along the lines of Cornwall *et. al.* [Phys. Rev. Lett. **30**, 1268 (1973), Phys. Rev. **D** 10, 1145 (1974)] and Llewellyn-Smith [Phys. Lett. **46B**, 233 (1973)] with the purpose of providing a user-friendly set of sum rules which summarize the tree level unitarity conditions. These

sum rules are expected to be of relevance in future experiments: if they are not satisfied then new particles (or other effects) can be expected to be present. It was also found that there is an allowed term in the lagrangian which was ignored by Cornwall *et. al.* . This term was considered by Llewellyn-Smith who found it inconsistent with tree level unitarity in some simple models.

J. Wudka has used the above loose end as a first project for M. Roy, a graduate student at UCR. The idea is to determine the general conditions under which these "extra" terms are allowed by tree level unitarity. Preliminary results show that these terms are consistent with tree level unitarity in some models, but are not consistent with spontaneously broken theories. A general set of conditions under which such terms are inconsistent with tree level unitarity have also been derived.

Thomas Fermi model of QCD. In collaboration with P. Kaus and D. Dixon, J. Wudka has been involved in a project where the ideas of the Thomas-Fermi atom are applied to QCD. The aim is to obtain the equation of state of the system within this approximation. This project is nearing completion

The idea is to consider the most general spherically symmetric expression for the gauge fields (which, in contrast to other approaches, does make use of the possibility of mixing spin with isospin), interacting with a gas of fermions (quarks); the fermions are quantum-mechanical while the gauge fields are purely classical. Local stability is imposed by requiring that the non-Abelian forces cancel the Fermi pressure and this leads too a closed set of equations for the gauge fields. The remaining ingredient is the determination of the boundary conditions, these are determined by coupling the system to a pseudoscalar field, in the same manner as in the Cheshire-Cat bag model; the resulting conditions ensure that color does not leak out of the system. We also require that the color charge, obtained from the Thomas-Fermi approach matches the one obtained at the boundary of the system where the bag boundary conditions are imposed. The equations are integrated numerically with these boundary conditions. The results, determine the pressure at the boundary as a function of the particle density the temperature and the volume.

In a future project the same approach will be applied to study heavy quark systems. The information that can be obtained is by necessity rather limited: the quark distribution functions in such a system can be derived and the splitting between the ground state and several radial excitations can be found.